Aston University
Birmingham

DOCTORAL THESIS

QUANTITATIVE RISK ASSESSMENT OF GROUNDWATER QUALITY UTILIZING GIS TECHNOLOGY AND COUPLED GROUNDWATER MODELS

Olayinka Oladeji

QUANTITATIVE RISK ASSESSMENT OF GROUNDWATER QUALITY UTILIZING GIS TECHNOLOGY AND COUPLED GROUNDWATER MODELS

OLAYINKA SIMEON OLADEJI

Doctor of Philosophy

ASTON UNIVERSITY
May 2011

ASTON UNIVERSITY, BIRMINGHAM

QUANTITATIVE RISK ASSESSMENT OF GROUNDWATER QUALITY UTILIZING GIS TECHNOLOGY AND COUPLED GROUNDWATER MODELS

OLAYINKA SIMEON OLADEJI (Doctor of Philosophy)
Aston University, 2011

ABSTRACT

The thesis presents a two-dimensional Risk Assessment Method (RAM) where the assessment of risk to the groundwater resources incorporates both the quantification of the probability of the occurrence of contaminant source terms, as well as the assessment of the resultant impacts. The approach emphasizes the need for a greater dependency on the potential pollution sources, rather than the traditional approach where assessment is based mainly on the intrinsic geo-hydrologic parameters. The risk is calculated using Monte Carlo simulation methods whereby random pollution events were generated to the same distribution as historically occurring events or a priori potential probability distribution. Integrated mathematical models then simulate contaminant concentrations at the pre-defined monitoring points within the aquifer. The spatial and temporal distributions of the concentrations were calculated from repeated realisations, and the number of times when a user defined concentration magnitude was exceeded is quantified as a risk.

The method was setup by integrating MODFLOW-2000, MT3DMS and a FORTRAN coded risk model, and automated, using a DOS batch processing file. GIS software was employed in producing the input files and for the presentation of the results. The functionalities of the method, as well as its sensitivities to the model grid sizes, contaminant loading rates, length of stress periods, and the historical frequencies of occurrence of pollution events were evaluated using hypothetical scenarios and a case study. Chloride-related pollution sources were compiled and used as indicative potential contaminant sources for the case study. At any active model cell, if a random generated number is less than the probability of pollution occurrence, then the risk model will generate synthetic contaminant source term as an input into the transport model.

The results of the applications of the method are presented in the form of tables, graphs and spatial maps. Varying the model grid sizes indicates no significant effects on the simulated groundwater head. The simulated frequency of daily occurrence of pollution incidents is also independent of the model dimensions. However, the simulated total contaminant mass generated within the aquifer, and the associated volumetric numerical error appear to increase with the increasing grid sizes. Also, the migration of contaminant plume advances faster with the coarse grid sizes as compared to the finer grid sizes. The number of daily contaminant source terms generated and consequently the total mass of contaminant within the aquifer increases in a non linear proportion to the increasing frequency of occurrence of pollution events. The risk of pollution from a number of sources all occurring by chance together was evaluated, and quantitatively presented as risk maps. This capability to combine the risk to a groundwater feature from numerous potential sources of pollution proved to be a great asset to the method, and a large benefit over the contemporary risk and vulnerability methods.

KEYWORDS: Groundwater, Pollution, Monte Carlo, vulnerability, risk assessment

DEDICATION

This thesis is dedicated to my wife, Oyenike Teminikan, and to my three daughters, Biola, Bimbola and Boluwatife, who had to endure the commitments which the successful completion of this work demanded.

ACKNOWLEDGEMENTS

The study was conducted under the direct supervision of Dr John Elgy. The author is very grateful for his support and encouragement. Faiz Parker and Rob Poole provided the necessary computing support. The author also acknowledges the assistance from Dr. and Mrs A. Adeloye, as well as Dr. Michael Kehinde in various aspects during the course of this work. Data used in the thesis were provided in part by the Environment Agency, England and Wales. Finally, of particular importance is The God Almighty, who enabled the author to carry this work this far.

TABLE OF CONTENTS

LIST OF FIGURES

LIST OF TABLES

GLOSSARY OF TERMS

AVI:	Aquifer Vulnerability Index
BNG:	British National Grid
ConSim:	Contamination Impact on Groundwater: Simulation by Monte Carlo Method
DEM:	Digital Elevation Model
DRASTIC:	Depth to water, net Recharge, Aquifer media, Soil media, Topography, Impact of vadose zone, and hydraulic Conductivity of the aquifer
EACD:	Environment Agency Controlled Document
EPA:	Environment Protection Agency
ESRI:	Environmental Systems Research Institute
FAO:	Food and Agricultural Organisation
GCG:	Generalized Conjugate Gradient
GIS:	Geographical Information System
GOD Index:	Groundwater occurrence, Overall aquifer class, and Depth to groundwater
GRASS:	Geographic Resources Analysis Support System
GUS Index:	Groundwater Uniquity Score
IGWMC:	International Groundwater Modelling Centre
LTA:	Long Term Average
m OD:	Metres Ordinance Datum
MORECS:	Meteorological Office Rainfall and Evaporation Calculation System
MT3DMS:	Modular 3-D Transport model [where MS denotes the Multi-Species]
NIRS:	National Incidence Recording System
PM:	Probable Mass
PPO:	Probability of Pollution Occurrence
PRA:	Probabilistic Risk Assessment
RAM:	Risk Assessment Method
RN:	Random Number
S-P-R:	Source-Pathway-Receptor
SPZ:	Source Protection Zones
SSSI:	Sites of Special Scientific Interest
STG:	Source Term Generation
USEPA:	United State Environmental Protection Agency
WFD:	Water Framework Directive

Chapter 1: Introduction

1.1 Background

The need to balance the dependence of groundwater utilization against the increasing global pollution threats from industrialization, urbanization and agricultural activities, facilitated this research work.

Generally, groundwater possesses some inherent valuable properties compared with surface water, and compromising these properties has implications for human health (Lee *et al.* 2002; Clark *et. al.* 2003; Aiuppa *et al.* 2003). Also, approximately 97% of the earth's useable fresh water is stored as groundwater (Delleur, 1999), though with much higher resident time within the water cycle as compared to the more readily available surface waters. In many parts of the world, the groundwater component of the water cycle maintains soil moisture, stream flow and wetlands, as well as being the source of drinking water, agricultural and industrial supplies. Groundwater is relatively more reliable during drought, especially because of its large storage, wide spread occurrence and protection from evapotranspiration and these good qualities makes its development relatively inexpensive.

Further to this, industrialization has become the nucleus of global economic development and has in addition, greatly improved the prospects of human well being. However, the resultant industrial growth is accompanied with environmental degradation problems, which impose pressures on the environment. Generally, industrial developments can constitute locations where pollution incidents can potentially be triggered. This is because the associated generated wastes are becoming more varied in composition, more toxic and more difficult to dispose and degrade, as well as increasing in quantity, greater than that which the environment will ordinarily absorb. Consequently, preferred waste disposal methods have become a case of selecting the least objectionable methods from a set of objectionable alternatives.

Pollution has therefore become one of the major environmental concerns with the potential for depleting the values of groundwater resources, and the effects had become widespread and pronounced globally. Cases of these have been reported in Hong Kong (Parsons, 1998), Beijing in China (Marilyn, 2001), South and East Asia (Usaid, 2004), Taejon area in Korea (Jeong, 2001), as well as in the developing countries (Egbu, 2004; Olokesusi, 2005).

Chemicals that are anthropogenically introduced into the water environment may have serious effects on human health (Lee *et al.* 2002). Untreated/treated sewage, industrial effluents and agricultural wastes are often discharged into the water bodies (Kurt *et al.* 2006; Grover and Kaur, 1999), thus limiting their use for recreational purposes, and causing adverse effects on aquatic eco-systems. These may also find their way into the groundwater system. Petrochemical leaks into groundwater from underground petroleum storage tanks (Li *et al.* 2000), heavy metals escape from mining wastes and tailings (Ali, *et al.* 2006a; Ali, *et al.* 2006b), leachates from landfills (Wichmann *et al.* 2006; Dimitra and Carmela, 2006), also pollute groundwater. The scale of impacted groundwater bodies is becoming more widespread and the persistence of groundwater pollutants is increasing, making the cost of aquifer restoration to be excessive in many cases. Therefore, pollution prevention rather than pollution management proffers the basis for a truly sustainable approach to groundwater protection.

Generally, risk and vulnerability are two relevant terminologies that describe methodological approaches for assessing threats posed to groundwater resources (Al-Adamat *et al.,* 2003; Aller *et al.* 1985; Connell and Dale, 2003). The existing methods employed to assess these parameters can be broadly grouped into three, namely, ranking index, process-based computer simulation and post-pollution assessment methods.

The most commonly applied group are the ranking index methods, an example includes DRASTIC which is an acronym for **D**epth to water, net **R**echarge, **A**quifer media, **S**oil media, **T**opography, **I**mpact of vadose zone, and hydraulic **C**onductivity of the aquifer (Aller *et al.* 1985). Other index based methods include GOD Index (Foster, 1987), which stands for **G**roundwater occurrence, **O**verall aquifer class, and **D**epth to groundwater; GUS Index (Gustafson, 1989), which is the acronym for **G**roundwater **U**niquity **S**core; and AVI (Van Stempvoort *et.al.* 1992), which stands for **A**quifer **V**ulnerability **I**ndex.

The process-based computer simulation method, as the name implies, uses mathematical models which are based on the physics of the solute transport within the porous media. Examples of these methods are those presented by Khan and Liang, 1989 and Rao *et al.* 1985. The post-pollution assessment methods (USEPA, 1989) carry out exposure assessment, dosimetry and risk characterisation in order to evaluate the post impacts of a pollution event on human health and ecology. All these methods have their merits and de-merits.

Potential pollution sources can be defined as locations where there is high probability of pollution incidents to occur due to prevailing ground surface anthropogenic activities. The fact that potential sources are often locations of pollution incidents necessitates the need to incorporate their occurrence and distribution in the prediction of risk posed to the underlying groundwater resources, and the subsequent assessment of such effects.

Generally, risk is defined as the probability of occurrence of loss, as well as the effects of such loss. The concept of risk therefore comprises of two-dimensional components. From the point of view of the water resources, the first component is the probability of contaminant source terms being generated from potential pollution sources at the ground surface while the second component is the assessment of impact of such occurrence. Existing contemporary methods in the assessment of risk to groundwater resources have only been concerned with the assessment of impact of pollution occurrence on water features, and no consideration is given to the probability of generation of source terms to cause such impacts. Therefore, this work is set to achieve a development of a two-dimensional risk assessment methodological approach, where assessment of risk to groundwater resource incorporates both the quantification of the probability of occurrence of source terms, as well as the impact of such pollution event.

1.2 Aim and Objectives

The aim of this research work is to develop and demonstrate the applicability of a generic modelling approach that will provide a wholesome assessment of the quantitative risk to groundwater quality.

The specific objectives are:

1. To carry out review of relevant literature.
2. To develop a Risk Assessment Method (RAM) utilizing coupled models and algorithms for the assessment of risk. This involves the generation of random pollution events at potential sources and determining spatial and temporal distributions of contaminants at pre-defined monitoring locations within the aquifer, using coupled flow, transport and risk models.
3. To assess the utilities of the method using hypothetical data. This involves varying the model grid sizes, contaminant loading rates, number of stress periods and the historical frequency of pollution occurrence or probability distribution model.

4. To demonstrate the applicability of the method using a case study.
5. To employ a GIS capability for the preparation of the model input data and the presentation of the model outputs in support of the RAM development.

1.3 Outline of the thesis

This thesis is divided into seven Chapters. The first Chapter presents the background to the research work. The aim and specific objectives are also listed. The second Chapter presents a review of the relevant published literature including previously developed flow models, as well as the Environment Agency's vulnerability map, the distribution of source protection zones, and the concept of the source-pathway-receptor model. A review of the definition of 'vulnerability' and 'risk' terms are also presented, as well as the existing risk assessment methods.

Chapter three presents an overview of the development of the concepts and methods of the risk assessment approach. The assessment of the functionalities of the method using hypothetical data is demonstrated in Chapter four, while Chapter five presents a case study showing the field application of the method. This involves the development of a three-dimensional flow and transport model for the area of study.

The discussions of the results of the hypothetical and field applications are presented in Chapter six, while the summary of the thesis, limitations, conclusions and the recommendations are presented in Chapter seven.

Chapter 2: Literature Review

2.1 Background

The terms 'risk' and 'vulnerability', have been inter-changeably used in the literature to describe existing approaches for assessing risk to, and vulnerability of the groundwater resources. This Chapter reviews some of the existing risk and vulnerability methods as well as their applications. Two existing groundwater flow models and overview of the various levels of integration between the groundwater models and the GIS technologies are also presented.

2.2 Definition of vulnerability and risk terms

Some literature definitions of vulnerability and risk are presented below.

2.2.1 Definition of vulnerability

Margat (1968) defined aquifer vulnerability as the possibility of percolation and diffusion of contaminants from the ground surface into natural water table reservoirs, under natural conditions. According to Olmer and Rezac (1974), vulnerability is the degree of endangerment determined by natural conditions and independent of present sources of pollution. Bachmat and Collin (1987) define groundwater vulnerability as the sensitivity of groundwater quality to anthropogenic activities, which may prove detrimental to the present or intended usage value of the resource, while Sotornikova and Vrba (1987) defined vulnerability of a hydrogeological system as the ability of the system to cope with external, natural and anthropogenic impacts that affects its state and character in time and space. Also, according to the International Association of Hydrogeologists, (Vrba and Zoporozec, 1994), vulnerability is an intrinsic property of a groundwater system that depends on the sensitivity of that system to human and/or natural impacts. Furthermore, Villumsen *et. al.,* (1983) defined vulnerability as the risk of chemical substances, used or disposed of on or near the ground surface, to influence groundwater quality. Palmquist (1991) defined vulnerability as the measure of the risk place upon the groundwater by human activities and the presence of contaminants. In the same trend, the U.S. National Research Council (1993) defined vulnerability as the tendency of, or likelihood for, contaminants to reach a specified position in the groundwater system after introduction at some location above the uppermost aquifer.

2.2.2 Definition of risk

Definition of the term 'risk' in the literature appears to vary with different fields of application. Risk has been described by Brugnot (1998) as a more or less possible predictable danger; the hazard to incur harm; probability of damage; and the crossing between vulnerability and unforeseen (probability). Lowrance (1976) defined risk as a measure of the probability and severity of adverse effects. According to the International Organisation for standardization (ISO, 2002), risk is defined as the effects of uncertainty on objectives. The Project Management Institute (PMI, 2000) defined risk as an uncertain event or condition that, if it occurs, has a positive or negative effect on a project's objectives.

Haimes (2006) defines risk in terms of vulnerability, intent, capability and threat:

- **Vulnerability** is the manifestation of the inherent states of the system (e.g., physical, technical, organizational, cultural) that can be exploited to adversely affect (cause harm or damage to) that system.
- **Intent** is the desire or motivation to attack a target and cause adverse effects.
- **Capability** is the ability and capacity to attack a target and cause adverse effects.
- **Threat** is the **intent** and **capability** to adversely affect (cause harm or damage to) the system by adversely changing its states.
- **Risk** is the result of a **threat** with adverse effects to a **vulnerable** system.

Other common definitions of risk in the literature include the following:

Risk is the expected loss or the probability of an adverse outcome (Graham and Weiner, 1995); a set of scenarios each of which has a probability and a consequence (Kaplan, 1991). Other definitions include two-dimensional combination of events/consequences and associated uncertainties (Aven, 2007); uncertainty of outcome, of actions and events (Cabinet Office, 2002); a situation or event where something of human value (including humans themselves) is at stake and where the outcome is uncertain (Rosa, 1998); an uncertain consequence of an event or an activity with respect to something that has human value (IRGC, 2005). Aven and Renn (2009) reviewed the literature definitions of 'risk' and categorized them into two, namely expression by means of probabilities and expected

values, as well as expression through events/consequences and uncertainties. Palmquist (1991) concluded that the most susceptible groundwater is not at risk without the presence of contaminant.

Following the literature definitions as presented above, groundwater vulnerability can be defined as a one dimensional concept that measures the ease with which a contaminant at the ground surface reaches an aquifer. This represents the degree to which an aquifer is naturally insulated from above ground activities. Vulnerability can either be of specific type, where a particular contaminant is being considered or intrinsic which does not consider attributes or behaviour of any specific contaminant, but that of the aquifer materials. Conversely, risk is defined as the measure of the likelihood that contaminants at the ground surface will result in the degradation of groundwater resources. Risk is a two dimensional concept, consisting of the likelihood of an event occurring, and the consequence of such event. These two dimensions are descriptively referred to as probability and impact.

2.3 Contemporary risk and vulnerability assessment techniques

Some commonly applied contemporary techniques for assessing risk and vulnerability to groundwater resources are discussed below.

2.3.1 Risk indices

Risk index based vulnerability methods are usually designed to indicate areas of greatest potential for groundwater pollution on the basis of geo-hydrological properties. It usually involves a process of assigning point ratings to the individual parameter and then summing the points together. The commonly applied index based methods are discussed below.

The DRASTIC (Aller *et al.,* 1985) method is probably the most widely used groundwater vulnerability mapping method. DRASTIC was designed for the systematic evaluation of the potential for groundwater pollution in any hydrogeological setting. Each DRASTIC parameter is assigned a relative weight between 1 and 5, with 5 being considered most significant in regard to contamination potential and 1 being considered least significant. The final result for the hydrogeological setting is a numerical value, where a high numerical index is assumed to be indicative of a geographic area that is likely to be susceptible to groundwater pollution. Other index based vulnerability methods include

GOD Index (Foster, 1987), GUS Index (Gustafson, 1989), and AVI (Van Stempvoort *et.al.,* 1992).

Thirumalaivasam and Karmegam (2001) assessed the aquifer vulnerability of the upper Palar Watershed in India, using a DRASTIC model. An analytical hierarchy process which involves Microsoft Access database, interfaced by ArcView GIS, using avenue codes was used to determine respective weights and rank the geo-hydrological parameters. The results include the development of user friendly Visual Basic software for the estimation of weights used in the aquifer vulnerability assessment. Leal and Castillo (2003) applied AVI to the Turbo river valley in Guanajuato State, Mexico. The aim of the authors was to calibrate the vulnerability output maps through verification with field data. The results demonstrate the importance of employing validation alternatives in the application of risk indexed based assessment. Al-Adamat *et al.,* (2003) integrated the DRASTIC index and a Geographical Information System to delineate vulnerability zones that were caused by the increased use of agrochemicals in the Northern Badia region of Jordan. The DRASTIC model adopted incorporates major geological and hydrogeological factors that affected and controlled the groundwater movement. The potential risk to pollution was qualitatively assessed, by integrating the resulted vulnerability map with a land use map. After testing the DRASTIC model with hydrochemical data, the vulnerability classification was such that, approximately 84 % of the area was designated as moderate risk, while 16 % was classified as low risk areas.

According to Aller *et al.* (1987), the DRASTIC Index provides only a relative evaluation tool and is not designed to provide absolute answers, but a reconnaissance tool, indicator of areas deserving a detailed hydrogeological evaluation.

2.3.2 Process-based computer simulation

The process-based computer simulation method uses flow and solute transport mathematical models to simulate contaminant transport through the porous media and assesses its impact at the point of interest. This is a mathematically based process which can be implemented using either a probabilistic or deterministic approach. The Probabilistic Risk Assessment (PRA) approach involves a technique where a range of values is being used as input for each parameter to a risk equation. This makes it possible for a range of risks to be calculated based on various combinations of the input values.

The PRA can be viewed as an approach to evaluate multiple 'what if' scenarios. It allows the same calculations to be performed several times, with various combinations of input values for each parameter. These values are randomly selected to fit a selected probability density function. The method also requires extensive application of statistics. The PRA differs from the traditional deterministic approach where a single numerical value is used for each input variable. Thus, PRA approach incorporates computation of associated uncertainties by incorporating Monte Carlo analysis.

Monte Carlo methods are a class of computational algorithms that rely on repeated random sampling to compute their outputs. The algorithms incorporate uncertainty considerations and use probability distributions to characterise risk. Monte Carlo methods are often used in simulating physical and mathematical systems. Typical stages involved in the application of the Monte Carlo analysis include the following:

1. Selection of the model input parameters on which the analysis will be performed.
2. Assigning ranges and distributions to each of the selected input parameter.
3. Generating random samples from each distribution of the input parameter.
4. Running of the model for each set of elements sampled from the distribution of the input parameter.
5. Assessing the model output in statistical terms such as mean, variance, cumulative distribution chart etc.

Some of the setbacks identified with the PRA methods include immense time investment and the need for additional data collection, especially because of the multi-variant nature of the input distributions. PRA is also more complex than the deterministic methods and the results may be misleading and difficult to communicate and validate.

2.3.2.1 @RISK software

An example of proprietary software that utilizes the PRA approach is @RISK (Pallasade, 2008). Risk analysis in @RISK is a quantitative method that seeks to determine the outcomes of a decision as a probability distribution. The @RISK software uses Monte Carlo simulation to allow for multi-variant outcomes and replaces the input uncertain parameters with @RISK functions, in order to represent a range of possible risk values.

2.3.2.2 The Source-Pathway-Receptor Model

The Source-Pathway-Receptor (S-P-R) is a management concept tool that utilizes the PRA approach and underlines the process of Environmental Impact Assessment (EIA). The concept helps to identify how best to manage unacceptable risks to environmental features. It requires an understanding of the sources of pollution, the potential receptors, and the various means by which the receptor may be adversely affected. The source-pathway-receptor relationship is applicable in the assessment of the impact of pollutant sources on, for instance the quality of water abstracted from groundwater sources, as well as in determining local protection needs and investment decisions. This implies that there must be source of pollutants, potential receptors and pathway that the pollutant can utilise to reach the source. Where either no pathway exists or that the pathway can be blocked or modified such that contamination will not occur, then it will be considered that no risk exist or rather negligible.

There are many tools that are available to aid the implementation of the source-pathway-receptor concept. This includes simple spread sheet to complex numerical models. An example of the numerical model is ConSim (Golder Associates, 2008), which is designed to provide tools for the management of land contamination with a means of assessing the risk that is posed to groundwater by leaching contaminants. ConSim (Contamination Impact on Groundwater: Simulation by Monte Carlo Method) has been developed on behalf of the Environment Agency by Golder Associates, to use commonly available site investigation data for simulating contaminant mobilisation and transport. Its probabilistic approach allows for full incorporation of data uncertainty, where input data is repetitively sampled from a user defined probability distribution.

ConSim can be applied in the estimation of spatial and temporal distributions of the contaminant concentration, which in turn can be used to deduce existence of pollutant linkages with respect to its potential to cause pollution of controlled waters. Other applications of ConSim include determination of the extent of remediation required to reduce the risk of contamination of controlled waters to an acceptable level, comparison of viability of various remedial techniques to successfully reduce the risks of pollution to controlled waters and assessment of whether a discharge to land or soakaway will meet the legal requirements. However, ConSim is not designed to be used to assess the level of exposure or risk from soil contamination to any receptor other than controlled waters.

2.3.2.3 Other examples of process-based risk assessment methods

Connell and Daele (2003) presented an example of process-based quantitative approach to aquifer vulnerability mapping. The authors adopted an analytical approach and presented procedures for calculating the transport of ground surface-released contaminants to groundwater. According to the authors, a means of efficient computation of contaminant concentration at the water table was provided by the steady state form of the advection-dispersion equation, and hence its application for vulnerability mapping.

Mackay and Morakinyo (2006) developed an inverse stochastic modelling approach to determine the pattern of contamination release in the assessment of a contamination site. The aim is to provide an approach that can potentially improve the methods for the assessment of pattern of contaminant releases in a site over a period of time. The model simulates the duration, extent and timing of the contaminant releases based on the knowledge of the pattern and duration of the operations, activities on the site, as well as perceived probability of discharges from each site activity. The methods associate specific site activity or group of activities to a defined geographical area called zone within the site, with capability to handle scenarios where the defined zones are overlapping.

The method was applied to a site in the West Midlands, UK, which has been used for power generation for over 50 years. The site was divided into 5 overlapping zones, and characterised to provide the required input data for the model setup. The results were presented in terms of spatial distribution of the modelled spills, and the simulated pattern of spills was found to be independent of the observed contaminant distribution at the site. Although, the method incorporates considerable simplified assumptions, the authors concluded from the simulations that the approach could potentially have wider applications.

2.3.3 Post-pollution assessment methods

The risk assessment method adopted by USEPA (1989) is a post-pollution approach that provides guidance on the evaluation activities of human health. The method examines potential adverse health effects caused by hazardous substances released from a contaminated site. The approach involves data collection and analysis, exposure and toxicity assessment, as well as risk characterization. The outcomes of the assessment are used to evaluate need for additional response action, modify preliminary remediation

goals, and to document the occurrence, causes and magnitude of the risk. This method is site-specific based and therefore may vary in approach depending on the complexity of the risk.

2.4 Groundwater models

There are several groundwater models which have been developed over time. The degrees to which the models have been validated vary widely. While some are empirically based, others have enjoyed wide spread field applications. Some of the databases that maintain information on the capabilities of models, system requirements and previous applications include:

1. Environment Protection Agency (EPA)'s Integrated Model Evaluation System, documented in EPA/600/C-92/002 (USEPA, 1996a)
2. International Groundwater Modelling Centre (IGWMC)'s Model Annotation Search and Retrieval System, documented in EPA/600/SR-96/009 (USEPA, 1996b)

Also, a list of some of the commonly available groundwater and transport models is presented in appendix A1.1 (Kumar, 2005; HSSW, 2008).

2.4.1 Description of some existing groundwater flow models

Two examples of existing groundwater models developed for the Birmingham area are presented below.

2.4.1.1 Groundwater model for Birmingham area

One of the earliest existing groundwater models for the Birmingham area is the work of Knipe *et al.,* (1993). The authors reported on the pressure of abstraction on groundwater resources between 1860 – 1930 due to the prevailing needs for industrial development and urbanisation. This subsequently led to scenario where abstraction rates exceed recharge flux. However from the early 1950s, declining fortunes and changing practice of many industrial consumers caused appreciable reduction in the abstraction rates, which has consequently caused rapid rise in groundwater levels.

The objective of their work was to evaluate the effects of the rising groundwater on the physical structures. Specific objectives include the following:

1. Representation of the prevailing groundwater systems and prediction of future groundwater levels in response to the prevailing pumping rates.
2. Evaluation of the engineering implications of the rising groundwater levels on buildings, structures, foundations, and basements.
3. Evaluation of the effects of the rising groundwater levels on its quality as well as that of the surface water and drainage.
4. Evaluation of the effectiveness of local groundwater control schemes and the need for further future regional control.

The study area covers the extent of water bearing sandstone around the city of Birmingham. In their work, Triassic sandstone was treated as a single model layer. A finite difference model MODFLOW-88 (McDonald and Harbaugh, 1988), was adopted for the study. The adoption of a single model layer with constant hydraulic conductivity value was due to the extremely limited available data, which restricted further sub-division of the aquifer into constituent lithological formations.

The geographical area covered by the model is 110 km^2, and discretized into 48 rows and 40 columns of varying rectangular shaped grid cells. The model boundaries include no flow at perimeters where no groundwater flow occurs, and leaky head control boundaries were assigned to perimeters along perennial river sections where groundwater levels were at or above river surface. The Birmingham fault was modelled by a reduction in aquifer thickness, which caused a reduction in the computed transmissivity values along the fault boundaries. A pre-abstraction condition with no urbanisation was set up to represent a steady state model for the area. Thereafter, stress periods which represent various stages of development were used to represent the transient conditions of the model. The input values for the transmissivity and storage coefficients, as well as the specific yield were 65 – 370 m^2/d, 0.0005 and 0.15, respectively. The value used for the recharge parameter was computed using a written pre-processing program, which is based on the relationship presented in Equation 2.1.

$$Recharge = (Effective\ rainfall \times F_{drift} \times F_{urbanisation}) + (Urban\ return\ flows \times F_{drift}) \quad 2.1$$

where

Effective rainfall = Precipitation – Evapotranspiration

F_{drift}: Recharge modification factor for superficial deposits

$F_{urbanisation}$: Recharge modification factor for housing density and industry
Urban return flows: Recharge from public water supply mains and sewer losses

Knipe *et al.,* (1993) found the value of the effective rainfall of 251 mm/yr to be appropriate from the steady state modelling. The authors obtained final hydraulic conductivity and transmissivity coefficient values of 1 - 1.5 m/d and 20 - 330 m^2/d, respectively. The interactions between the river and the aquifer were based on the head difference between the water levels in the river and aquifer, as well as the conductance of the river bed, and this was computed using Equation 2.2.

$$Conductnce(m^2/d) = \frac{K\ x\ length\ of\ river\ x\ width\ of\ river}{Thickness\ of\ bed\ deposit} \qquad 2.2$$

where *K* is the hydraulic conductivity of the river bed.

Three input parameters namely, transmissivity, recharge and river bed conductance were selected for specific sensitivity analyses, and the results showed that the model was most sensitive to the river bed conductance, least sensitive to the transmissivity coefficient and moderately sensitive to the overall recharge value. The model was used to make predictions of future groundwater levels and the implications of the rising groundwater levels for the underlying geological materials, structures and services were discussed.

2.4.1.2 Lichfield Permo-Triassic sandstone aquifer investigation

This project was undertaken by the Environment Agency, British Geological Survey (BGS) and Environmental Simulations International (ESI) Ltd. The purpose of the project was to develop a numerical 3-D groundwater model for the Lichfield Permo-Triassic sandstone aquifer, to be used as a regulatory tool for decision making on issues related to water resources abstraction licensing. The final report (Buss *et. al.,* 2008) synthesizes previous field investigations, development of the conceptual understanding of the site, and the options appraisal.

The groundwater model was developed and calibrated as a transient model, using integrated MODFLOW and 'Adit code', which is a modified version of MODBRANCH (Swain and Wexler, 1996). The model temporal discretization spans over two periods, namely 'warm-up' (January 1930 – December 1969), and recent actual (January 1970 to

March 2006). The model was divided into 435 monthly stress periods with daily time steps, and consists of three layers, covering approximately 1,700 km^2, and extending 92.25 km towards the north and 18.5 km towards the east. The area was divided into 117 rows and 74 columns, with squared grid cells of 250x250 m.

The values of the hydraulic properties used in the model are presented in Table 5.5. Surface water features were represented within the groundwater model using head-dependent flux boundary conditions, while groundwater abstractions were modelled using the constant flux boundary condition. Numerous faults are present within the area and these structures were represented by the Horizontal Flow Barrier (HFB) of the MODFLOW package. Interaction between the underlying Permo-Triassic sandstone aquifer and the overlying confining Mercia mudstone Group was represented by the General Head Boundary of the MODFLOW package. Daily recharge to the aquifer was calculated using the Environment Agency Water Framework Directive recharge calculator spreadsheet (Environment Agency, 2007).

The results were presented as a series of cross plots of simulated groundwater heads versus observed groundwater levels at selected target locations throughout the model area. The spatial pattern of groundwater heads, as well as the comparison between the gauged and simulated baseflow were also presented and discussed. The flow volumetric balance for the entire groundwater model was reviewed, and the numerical error did not exceed 0.005% throughout the entire model period which indicated that the groundwater model was converging with only a small numerical error.

2.5 Water resources management tools

In order to protect groundwater resources, the Environment Agency provides risk-based management tools for assessing the risks posed to the groundwater regime, as well as for planning and supporting decisions relating to regulatory duties and powers. These tools are executed through groundwater vulnerability maps and delineation of source protection zones.

2.5.1 Vulnerability map

Groundwater vulnerability maps show areas that can potentially be polluted based on their intrinsic lithological properties. The Environment Agency's groundwater vulnerability

maps are based on the local hydrogeological factors and therefore, the same formation may be classified differently across the entire country. The groundwater vulnerability maps also only relate to the geological strata that are present at or near the land surface. Where a significant thickness of a low permeability material overlies a permeable aquifer, the groundwater vulnerability map will only show the vulnerability of the groundwater in the near-surface deposits.

The maps provide information on how significant the groundwater is likely to be impacted by pollution occurring at the ground surface. The Environment Agency has been able to classify how vulnerable the aquifers in England and Wales are, to pollution, and these maps are published as a series of 53 maps. The map that covers Birmingham area is the Sheet 22 (Environment Agency, 1997), and the relevant part is presented in Figure 2.1. The vulnerability maps present the classification of the aquifers using descriptive terms such as major and minor, with further sub-division of the vulnerability as high, intermediate and low vulnerability. The aquifers that are classified as major are known to have strategic importance in water resources because of their support for public water supply. Minor aquifers have a more localised significance in their applications, while non-aquifers do not store significant amounts of groundwater. Therefore, the vulnerability of groundwater is classified to be high if the host aquifer is overlain by a relatively high permeable material. The intermediate and low vulnerability are essentially a function of the lesser degrees of permeability to which the host aquifers are covered.

2.5.2 Source Protection Zones

The Environment Agency has also defined Groundwater Source Protection Zones (SPZs), mostly for the groundwater features that are being used for public water supply (Environment Agency, 2008a). The zones, which are based on the travel times of pollutants and the entire recharge extent, provide an indication of the risk to groundwater supplies that may result from potentially polluting activities and accidental release of pollutants. The shape and extent of the zones were determined by mathematical modelling. The purpose of the zones is to protect abstractions used for public water supply. Generally, three zones namely inner, outer and total catchments are usually defined, although a fourth zone to represent zone of special interest may also be defined. The SPZ map for part of Birmingham area is presented in Figure 2.2.

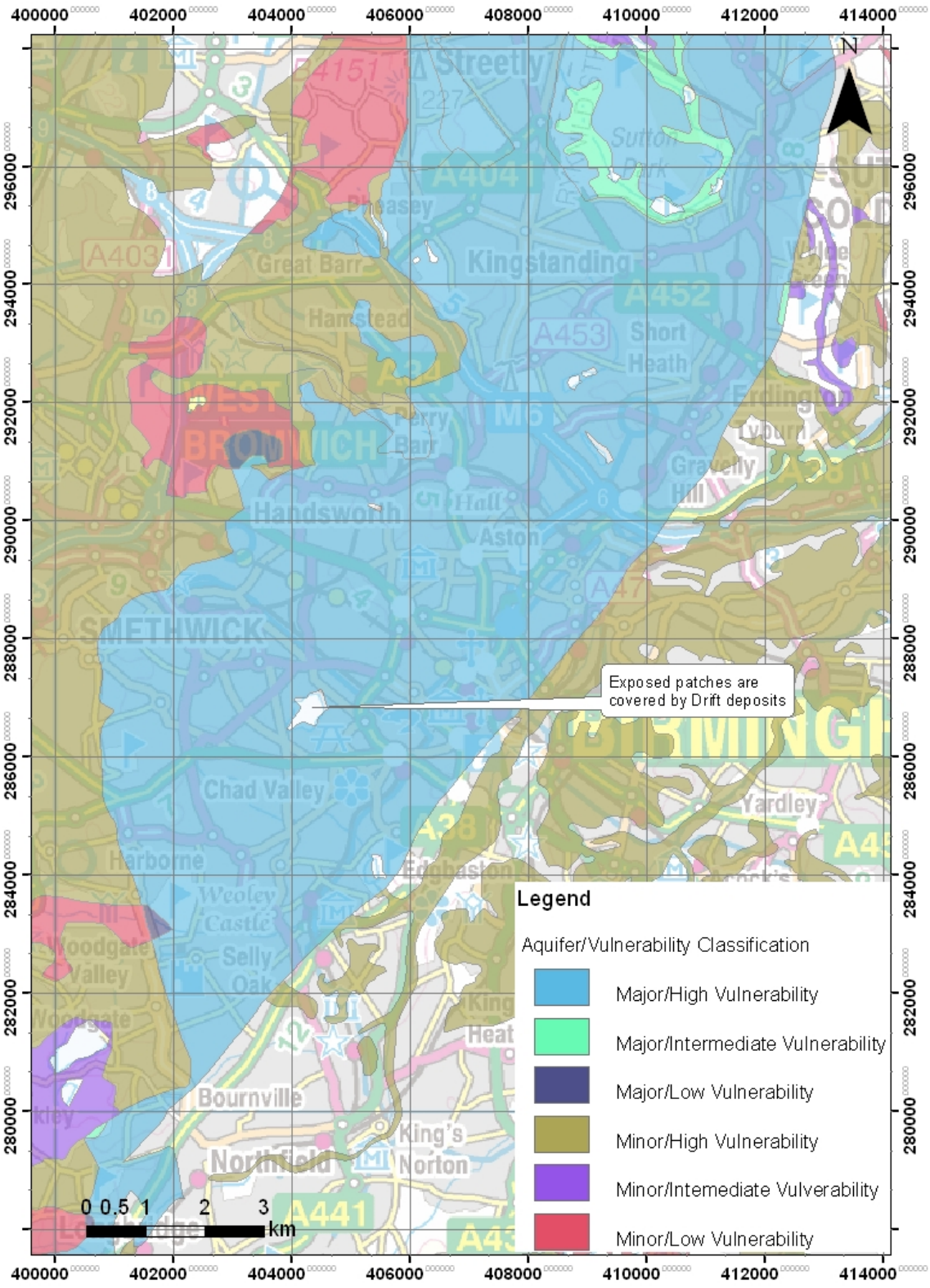

Figure 2.1: Vulnerability map for part of Birmingham area

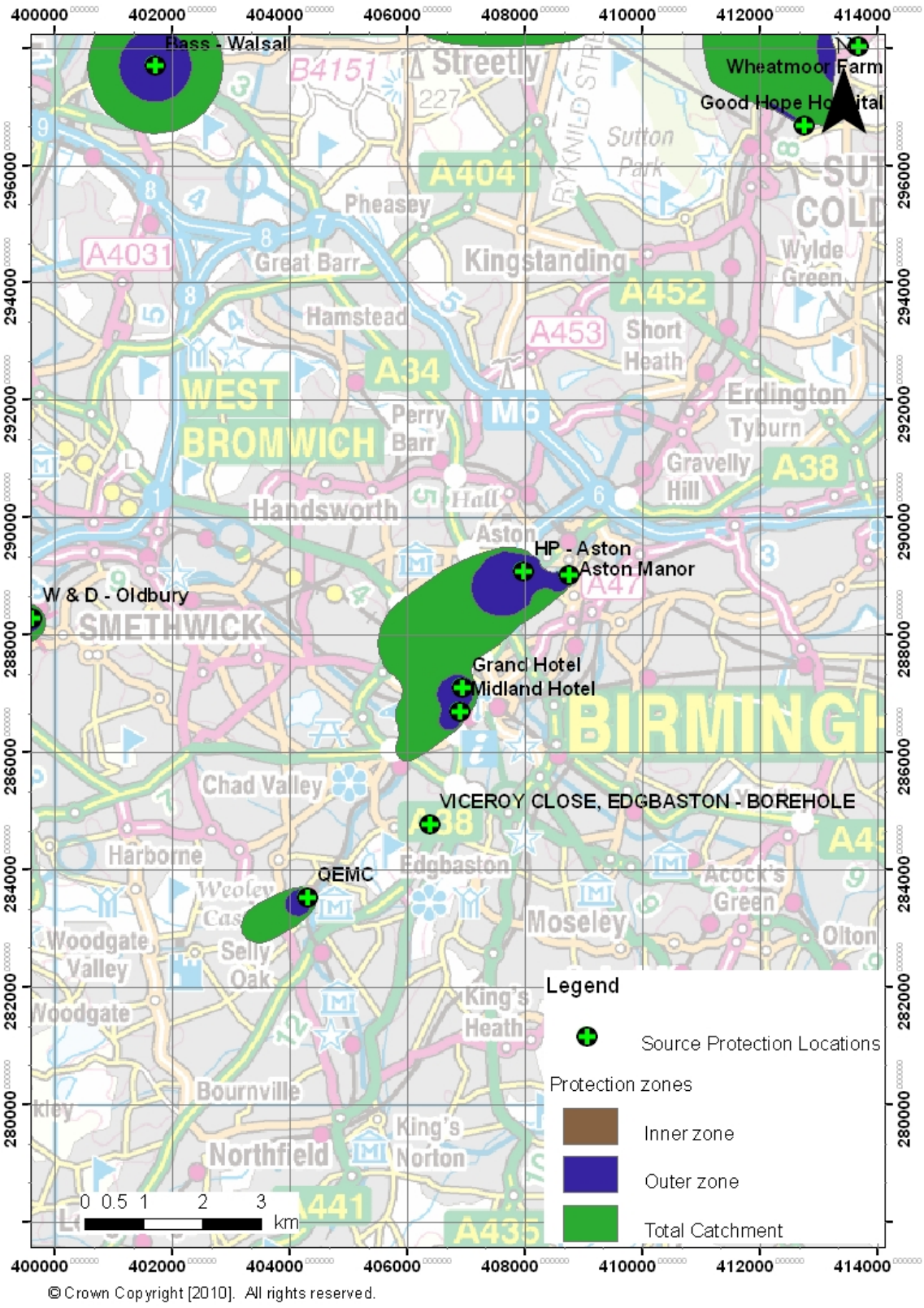

Figure 2.2: Distribution of source protection zones for part of Birmingham area

2.6 Integration of groundwater models and GIS technologies

A Geographical Information System (GIS) is defined as an organised collection of computer hardware, software, geographic data, and personnel designed to efficiently capture, store, update, manipulate and display all forms of geographically referenced information (ESRI 1995a). The volume of data involved in the development of groundwater models is enormous, and GIS technology has been introduced to facilitate the management of such data. This is achieved by integration of groundwater models and the Geographical Information System. The popularity of this concept has become phenomena in recent years, especially with its applications to various fields of science and engineering. The increased popularity is partly due to the ability of GIS technologies to enable representations of the spatial and temporal data that are commonly employed in the groundwater modelling, by means of geographically referenced database.

The level of integration between groundwater models and GIS technology has been generally classified into three categories by different authors. According to Maidment (1993), these are: data exchange, GIS interface, and integrated GIS model. Tim and Jolly (1994) also presented an overview of three types of model interface with GIS as ad-hoc integration, partial integration and complete integration. Also, Watkins *et al.* (1996) classified the various levels of integration that exists between GIS and hydrological models into three namely, linked, integrated and embedded. There are similarities in the classifications presented by the three authors, and the three levels of integration are diagrammatically presented in Figure 2.3.

The first level is the lowest level of integration, where both the GIS program and the groundwater model are developed independently, and therefore do not have direct linkage. A large number of GIS and modelling integration falls into this group. The GIS program is employed for pre- and post- processing of the model data. The communication between the GIS and the model is by import and export capabilities of the individual programs. However, the format requirements for the two programs usually differ, and pre-processing techniques are employed using a third party software package. This level of integration places little demand on both the GIS and the model, and the potential for error is high. It is however the most flexible and least expensive method of integrating GIS and groundwater models, and for this reason, it is the approach used in this thesis.

The second form of integration may involve two approaches. Firstly, a GIS database is developed around an existing model while the second approach may involve developing a model on top of an existing GIS database and input data are structured according to the data in the GIS. However, in both cases, both the GIS and the model are executed separately, but the GIS supplies input data for modelling and also accept modelling output for further processing and presentation, without any need for file interchange interface.

The third level of integration is the highest level of integration and it is usually referred to as modelling within GIS environment. It involves complete integration of the two technologies, where the GIS and model are developed within a single operating system. The data stored in the GIS is structured to meet the demands of the model and vice versa. This level of integration requires a modular modelling structure that is robust enough to provide framework for linkage with the unique data structures of the GIS. Also, the data structure of the GIS should be compatible with the spatial discretization of the modelled system. This level of integration is difficult and limited in terms of the required efforts for the development, as well as proprietary rights posed by the commercial GIS software and the models. Hence, the first two levels are the only ones that are of practical solution.

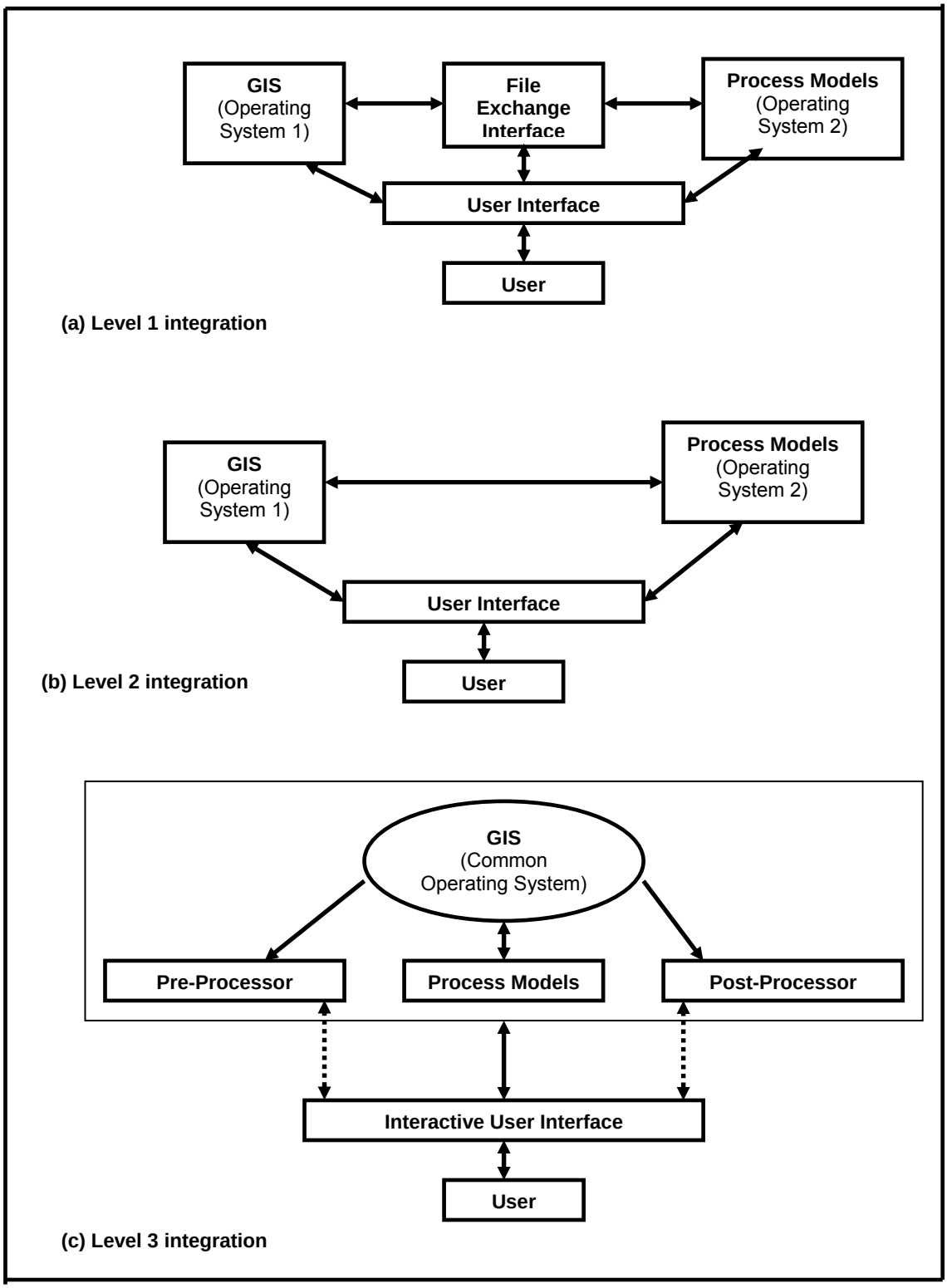

Figure 2.3: Levels of integration of GIS and groundwater models

2.7 Summary of the Chapter

In this Chapter, the meanings of the terms 'risk' and 'vulnerability' as defined in the literature as well as two existing groundwater flow models developed for Birmingham area are presented. Some management tools used in assessing risk to groundwater resources in England and Wales, namely vulnerability map and source protection zones, are also presented. In addition, contemporary vulnerability assessment techniques are discussed, including the dependency of these techniques on the intrinsic geo-hydrologic parameters as well as the observed underplay of the occurrence and distribution of potential pollution sources in the assessment of risk to groundwater resources. The Chapter is concluded by the review and presentation of the three possible levels of integration between groundwater models and the GIS technologies

The definition of the vulnerability indicates that it is a one dimensional approach assessment where the impact of the occurrence of contaminant generated at the ground surface on the water resources is assessed. Conversely, risk has a dual dimensionality in its assessment approach, and these include probability of occurrence of pollution incident and the assessment of the impact of such occurrence. The review of the literature shows that the contemporary methods have not incorporated this dual dimensionality concept of the definition of risk term in their implementation approach of assessing risk to groundwater resources. All the existing methods have only been concerned with the second dimension where the impact of occurrence of pollution incident on the groundwater resources is assessed. No consideration is given to the probability of the occurrence of the contaminant in the first instance, and this could lead to overly conservative approach in the assessment of risk to water resources. Therefore, there is a need for development of a two dimensional approach where assessment of risk to the groundwater resources involves quantification of the probability of occurrence of pollution incidents, as well as the assessment of the impact of such occurrence.

Chapter 3: Methodology

3.1 Conceptual approach of the risk assessment method

If risk is defined as the product of the probability of an event occurring and the consequences of that event, that is:

$$Risk = probability\ of\ pollution\ occurrence\ (PPO) \times consequence \quad 3.1$$

where PPO is expressed as $\left[\frac{Event}{Time}\right]$ and consequence is expressed as $\left[\frac{Amount}{Event}\right]$

Then, it is possible to take the probability of a pollution event of a specific magnitude occurring at the surface and then numerically calculate the probability of obtaining a specific concentration in a borehole of interest or point in the aquifer. This tracing of probabilities through a complex system such as a groundwater system with multiple potential sources is difficult to perform. However, it is not an uncommon problem in risk analysis of complex systems and techniques have been developed to assist in their analysis. These techniques have largely revolved around techniques known as Monte Carlo simulation.

Monte Carlo simulation involves the generation of random inputs to a system following a prescribed statistical distribution, and then simulating the behaviour of the generated inputs using a numerical model and observing the outputs. Typically, after thousands of simulations the probability distribution of the outputs can be built up and the risk evaluated. General purpose computation packages such as @RISK (Pallasade, 2008), have been written to assist in this process, but the packages lack the complex modelling processes required for groundwater risk assessment.

The Risk Assessment Method (RAM) developed in this work involves the generation of random inputs into a groundwater system, and then simulating the behaviour of the input using integrated numerical models and observing the outputs at pre-defined monitoring points. The method is used as a tool to assess the risk to groundwater quality by observing spatial and temporal distributions of the output of transport model at monitoring boreholes, as well as by observing the number of times at which a user defined contaminant concentration magnitudes are exceeded over a period of time.

The method incorporates a mechanism for generating synthetic pollution events from potential sources as a function of the frequency of historical pollution incidents of a given contaminant of interest or a priori knowledge of the distribution. The mechanism is achieved through integrated coupled flow and transport models, as well as the risk model. The risk model generates synthetic pollution events to a defined distribution for a period of time, and the generated events are subsequently introduced into a transport model in order to assess the concentrations that appeared at pre-defined monitoring points.

The principle of the generation of the synthetic pollution source terms is similar to the computational techniques for a randomly generated number such as dice, coin flipping, and the shuffling of playing cards, where sequence of numbers are generated to a specific probability distribution. In the case of this RAM, a synthetic pollution event is generated if a random number generated by the RAM algorithm is less than a computed parameter called Probability of Pollution Occurrence (PPO). This parameter is computed as the ratio of the number of historical pollution incidents to the period of time over which the incidents occurred. It follows that the probability distribution of the resulting events will be Poisson distribution.

A Poisson distribution expresses the probability of a number of events occurring in a fixed period of time if these events occur with a known average rate and independent of the time since the last event. If the expected number of occurrence in an interval of time is given as λ, then the probability that there are exactly *k* occurrences (where *k* being a non-negative integer) is given as:

$$f\ (k:\lambda) = \frac{\lambda^k e^{-\lambda}}{k!} \qquad 3.2$$

where e is the base of the natural logarithm, and k! is the factorial of k.

Previous applications of random number generators include gambling, statistical sampling, computer simulation and cryptography (Wegenkittl, 2001; Szczepanski *et. al.* 2004; Hu *et. al.* 2009). This work represents the application of random generated numbers in the assessment of risks to groundwater quality. The principle of random number generator is utilized to represent the unpredictability associated with a pollution occurrence. Generally, there are two major approaches to generate random numbers. The first is to measure some physical phenomenon such as the decay of a nucleus of an atom that is expected to be

random and then compensates for possible biases in the measurement process, by using randomness extractor algorithm that converts a weak source of randomness into an almost uniform distribution (Nissan, 1996). The other uses computational algorithms that produce long sequences of apparently random results, which are in fact completely determined by a shorter initial value, called the seed. The latter method which is also referred to as pseudorandom number generators has a greater ease of incorporation into mathematical algorithm, and therefore it is the method used in this work.

Assuming an aquifer with a recharge area where discharge pipes from industrial processes and plants are located, and each represents a single, identifiable and localized source with risk of discharging pollutants that may infiltrate into the aquifer. This risk of pollution consists of the probability of an event occurring as well as consideration of its magnitude. In a simple case, these events have average return periods which are independent of the time of the year or previous occurrence at the same site, or events occurring at other sites. In this case, the probability of an event is represented by a Poisson distribution. The probability of the occurrence of a pollution incident at any of the potential pollution sources is equal and the event of this type is considered to be of short duration. Although, this simple event scenario is considered in this thesis, the methodology is not restricted to this simple probabilistic structure, but can be extended to include pollution incidents with temporal and/or spatial correlation.

Incidents with a temporal correlation involve scenarios where a pollution event occurring may go on for a very long time before detection. This could be caused by several reasons including ageing of plant, leakages from underground storage tanks etc. Conversely, spatial correlation incidents involve scenarios where the occurrence of an event is dependent on other potential sources over a large area. There could be generation of source terms at the primary source, which in turn can consequently cause other potential pollution sources (secondary) to generate source terms by virtue of the primary event. However, the probability of generating secondary source terms is weighted by the separating distance and reduces with the increasing distance from the primary source. An example of spatial correlation is the railway stations which are potential pollution sources of spillages from train fuelling and other maintenance activities. However, the potential for pollution from spillages decreases as the train moves away from the station. Scenarios involving combinations of both the spatial and temporal correlations could also be

considered. The modelling of these stochastic relationships is complex and perhaps outside the remit of this thesis. However, the structure of the method allows the scenarios to be incorporated within the model if required.

3.2 The structure of the risk assessment method

The algorithm of the risk assessment method (RAM) is implemented by a flow chart presented in Figure 3.1. The main components of the flow chart are the parametization of the risk model, generation of the source terms, implementation of the coupled flow and transport models, as well as assessment of the impact of the simulated source terms on the groundwater resources and collation of the model output for the entire iterated simulation. The batch file that controls the implementation of the risk assessment method is presented in appendix A1.2. The risk model components of the RAM structure are implemented by a computer program written in a standard FORTRAN 90, and presented in appendix A1.3. The order in which the RAM is executed in a typical simulation run is also shown in Figure 3.1. The detailed descriptions of the risk model are presented in Section 3.3.

The risk model is run over the same period of time as the flow and transport models. Source terms are generated for each stress period of the simulation, which are then transported within the subsurface environment using the transport model. The effects of the generated source terms are assessed by observing the spatial and temporal concentrations of the contaminant at pre-determined monitoring boreholes or points within the aquifer, as well as by counting the number of times the concentration exceeds a user defined concentration magnitude.

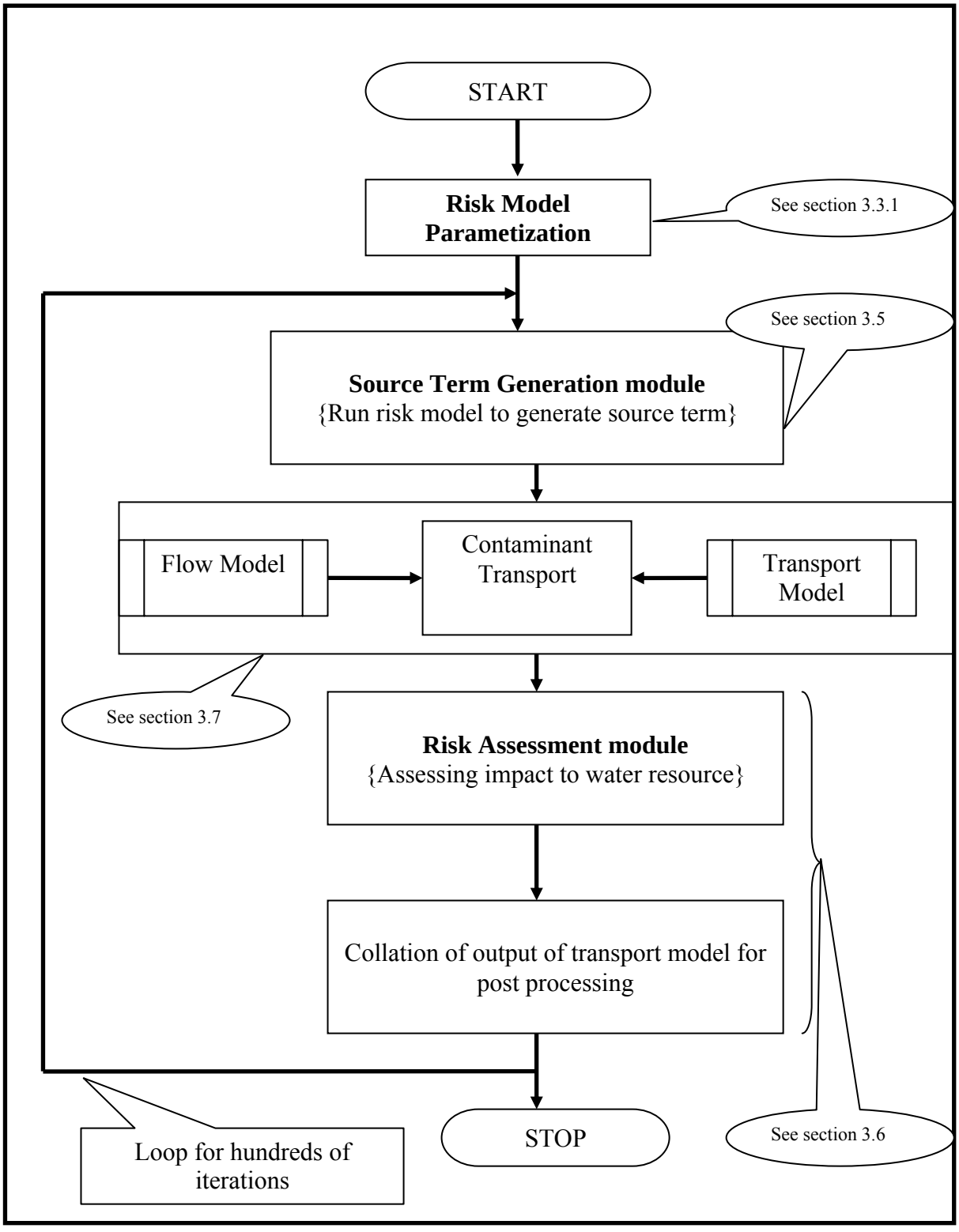

Figure 3.1: Conceptual algorithm of the risk assessment method

3.3 Description of the risk model

The risk model generates source terms from a multiple of single identifiable localized potential pollution source, where the probability of the occurrence of a pollution incident at any of the potential pollution sources is equal for a given stress period. The generic description of the risk model has already been presented in Figure 3.1, while the FORTRAN code for the execution of the RAM is presented in appendix A1.3. The risk algorithm consists of two modules, namely Source Term Generation and Risk Assessment modules (see Figure 3.1). The Risk Assessment module is activated after the execution of both the Source Term Generation module as well as the flow and transport models.

3.3.1 The parametization of the risk model

This section involves the processes of defining the parameters required in the setting up and running of the risk model.

3.3.1.1 Pre-processing of the potential pollution sources

This task is required for the preparation of the input data. The objective is to obtain locations of potential pollution sources defined in terms of layer, row and column. This is achieved by identifying existing potential sources of pollution within the area of interest or proposed developments within the study area. They can be found by various methods available to the investigator such as field investigation, planning applications, internet searches, desk studies etc.

The National Grid Reference of the locations of potential sources are initially obtained using global positioning equipment, geospatial information systems or software or from archives, and then posted on the base map. The National Grid References are subsequently transformed into the appropriate layer, row and column numbers of the model grid using GIS utilities.

3.3.1.2 Quantification of qualitative chemical data

This section is required if previous pollution incidents are recorded using descriptive terms. Otherwise the task will not be necessary if previous occurrences of pollution incidents are recorded as the loading rate of the mass of contaminant released during historical pollution incidents. This work utilises the qualitative descriptive terms presented

by EACD (2006), which describes the occurrence of pollution incidents using qualitative terms such as major, significant and minor. The scenarios that define each of these terms are presented below.

1. Major: A pollution incident is classified as major if the incident causes major damage to fish population, habitat, Sites of Special Scientific Interest (SSSI), invertebrate populations, watercourse or potable abstraction point, amenity value, agriculture, commerce or community.

2. Significant: A pollution incident is classified as significant if the incident is less severe.

3. Minor: Incidents falling within this category must be where pollution has been confirmed but the effects are very limited and localised.

The next stage is to estimate the quantitative loading rate of mass of the contaminant of interest that is capable of causing the corresponding effects as presented by EACD (2006). This can be empirically determined or obtained from literature. For instance, USEPA (1988) and Suciu and Wikoff (1982) presented the effects of chloride related pollution on plants and some alloys. USEPA (1988) empirically determines chloride concentrations (in mg/l) that are considered to be of acute and chronic toxicity to plants and animal. Also, Suciu and Wikoff (1982) published empirical results of corrosion characteristics of a number of alloys that may be used in cooling system components. Suciu and Wikoff (1982) carried out corrosion tests by exposing metals to chloride concentrations of 10,000 – 200,000 mg/l, in order to determine the resistant factor for the metals.

The case study carried out in this work to demonstrate the applicability of the method (see Chapters 4 and 5) considers chloride as the contaminant. This is because of the conservative and non reactive nature of chloride within the natural subsurface environment. Considering the range of concentrations used in the empirical reports (USEPA, 1988; Suciu and Wikoff, 1982), and coupled with personal communications with the Environment Agency, equivalence between the descriptive qualitative terms (EACD, 2006), and quantitative values is estimated, and presented in Table 3.1. It is important to reiterate that the classification presented in Table 3.1 will be dependent on the contaminant under consideration.

Table 3.1: Quantitative equivalence of the qualitative chloride chemical data

Qualitative description	Proposed Quantitative Description (kg)
Major Pollution	>25,000
Significant Pollution	25,000 – 5,000
Minor Pollution	5,000 - 250
Contamination (No Pollution)	< 250

Worthington and Smart (2005) presented a review of 203 sites where tracer tests were carried out using Sodium Chloride (salt). The maximum quantity of salt used was 50,000 kg, over a range of distance of 30 m – 30 km. The values in Table 3.1 are within similar range of values to those presented by Worthington and Smart (2005).

Also, the adopted method in the classification presented in Table 3.1 and the introduction of additional parameters are not uncommon approaches. For instance, Al-Adamat *et al.,* (2003) subjectively assigned values to parameters such as built-up area, uncultivated land and irrigated field in the development of a risk assessment method. Seconda *et al.,* (2001) incorporated additional extensive agricultural land-use data in the modification of DRASTIC method. Piscopo (2001) replaced the recharge term in DRASTIC with rainfall amount, slope and soil permeability, while Evans and Mayers (1990) replaced DRASTIC parameters, namely recharge, impact of vadose zone and aquifer media, with landuse, land cover and septic tank system density.

The product of this section is the list of actual and potential pollution sources located within the area of interest, and their associated National Grid References. Also if no quantitative contaminant data are available, an equivalent table establishing the qualitative and quantitative data, similar to Table 3.1, but with reference to the specific contaminant of interest for the study area is prepared.

3.3.2 Data interpolation method

The field data available in the development of groundwater related models are general insufficient compared to the actual required data. Therefore, few data points are often interpolated to generate additional data in the development of a model, though this procedure tends to create a degree of uncertainty in the model output. Data interpolation carried out in this work uses the geostatistical kriging interpolation technique capability in-built into ArcGIS (Ormsby *et al.,* 2001). Other common examples of interpolation methods incorporated into the ArcGIS are Inverse Distance Weighted and Spline methods.

Kriging interpolation techniques consider both the distance and the degree of variation between known data points when estimating values in unknown areas. An estimated value represents a weighted linear combination of the known sample values around the point to be estimated. It attempts to minimize the error variance and sets the mean of the prediction errors to zero so that there are on average no over- or under-estimates. The kriging routine includes the ability to construct a semivariogram of the data which is used to weight nearby sample points when interpolating. Therefore, when properly applied, kriging allows the user to derive weights that result in optimal and unbiased estimates. Estimation of the errors at each interpolated point are also generated which further provides measure of confidence in the generated data.

There are two approaches to kriging methods, and they include ordinary and universal. Ordinary kriging assumes that the data set has a stationary variance but also a non-stationary mean value within the search radius. It is highly reliable and most widely used of the kriging methods and it is the approach used in this work. Universal kriging assumes that there is an overriding trend in the data.

3.3.3 The grid systems of the risk model

The risk assessment method uses two grid systems namely a local system and a global system (Figure 3.2). Generally, flow and transport models tend to take advantage of natural boundaries in defining the extent of the model domain. This is not a requirement for the implementation of the risk model. Therefore, the use of the dual grid system allows the risk model to be run independently of flow and transport models. The local grid may be equal to or smaller than the global grid system used in groundwater flow and contaminant transport models. The use of the local grid system also increases the

efficiency in the implementation of the risk model in terms of the time and memory requirements for the simulation.

Generally, the risk model uses the local grid system in the generation of the source terms. The row and column numbers of the potential sources that are initially specified in the risk model are the local grid system. However, these numbers are transformed into the global grid system in the final output of the simulation of risk model, using the row and column numbers of the global grid, that correspond to the first row and first column of the local grid. This concept is demonstrated in Figure 3.2, which shows the global system (blue lines) of 11 x 13 grids and the local system (black lines) of 6 x 7 grids. The row and column numbers of the global system that correspond to the first row and first column of the local grid are 4:4. The equivalent local and global grid systems are also presented in Figure 3.2.

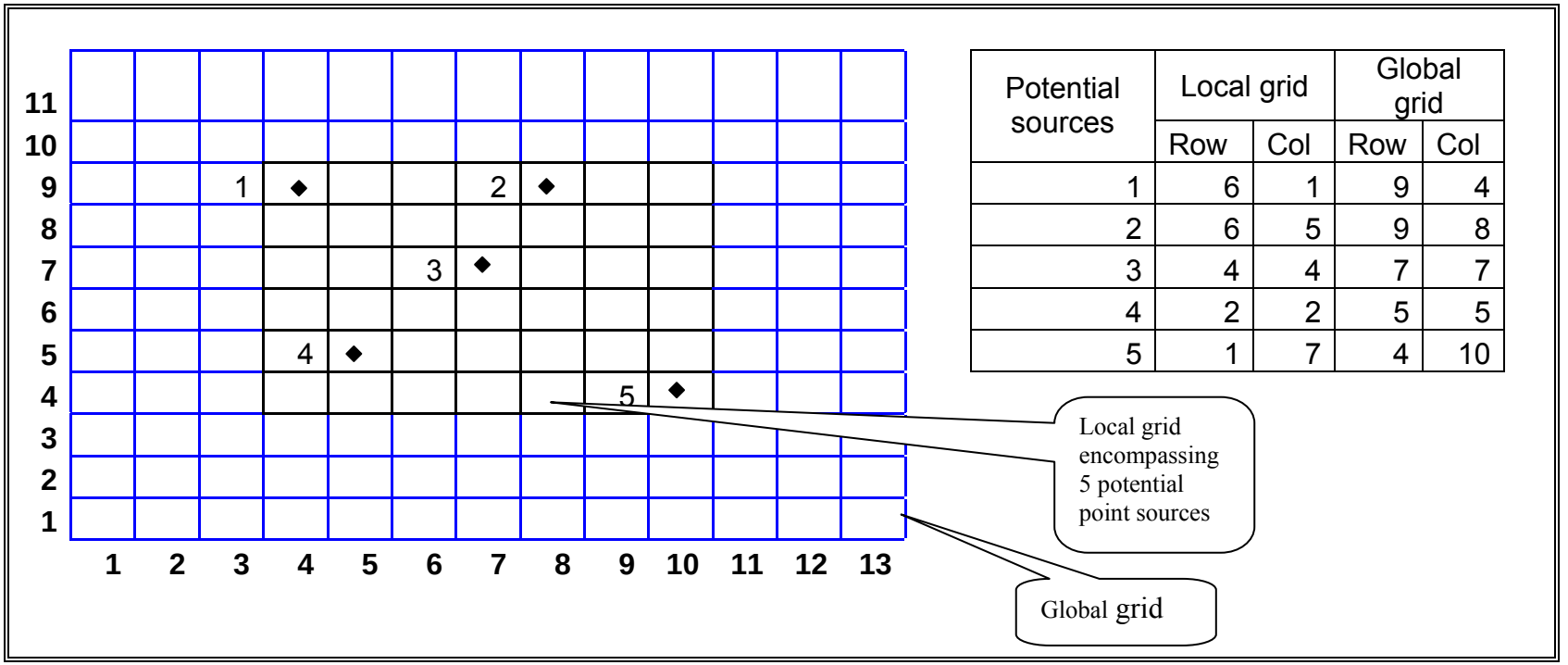

Potential sources	Local grid		Global grid	
	Row	Col	Row	Col
1	6	1	9	4
2	6	5	9	8
3	4	4	7	7
4	2	2	5	5
5	1	7	4	10

Figure 3.2: Demonstration of the global and local grid systems

3.3.4 The consideration of the unsaturated zone

The unsaturated zone (which is also referred to as zone of aeration or vadose zone) is the zone between the ground surface and the deepest water table. This zone includes the capillary fringe, and the pore spaces are occupied by combinations of air and water, with the pressure head within the zone generally less than the atmospheric pressure. The water table represents the demarcation between the overlying unsaturated zone and the underlying saturated zone (Figure 3.3a). There are numerous processes within the unsaturated zone that can potentially affect the mass, toxicity and the concentration of a contaminant travelling through this zone. Also, the rate and pattern at which groundwater resource is replenished is largely dependent on both the thickness of the unsaturated zone, the active processes within this zone, as well as the rainfall. Therefore adequate understanding, characterisation and incorporation of these attenuating zone and processes are required in the development of a risk assessment methodology to water resources. Traditionally, borehole drilling is used as intrusive means of interrogation to characterise the subsurface environment. However this approach yields little success in its application to the study of unsaturated zone, and non-convectional methods such as geophysical methods are favoured (Vereecken, *et al*., 2006).

The risk assessment method developed in this work uses modelling techniques to incorporate a delay factor caused by the processes operating within the unsaturated zone. Generally, the groundwater flow model consists of two parts namely a recharge model and a flow model. Most of the recharge modelling approaches incorporates capabilities to represent the dominant processes operating within the unsaturated zone. The method adopted in this work involves the Food and Agricultural Organisation (FAO) based FORTRAN recharge model jointly developed by the Environment Agency and the Scotland and Northern Ireland Forum for Environmental Research (SNIFFER). In this RAM, the thickness of the unsaturated zone is estimated as the difference between the surface elevation and the initial groundwater level. This recharge tool accounts for the rainfall, evapotranspiration, soil types, land use, and crop properties (Figures 3.3b and 5.14) in the estimation of the recharge value.

Further to this, the approach also involves the development of a simple distribution of unsaturated zone delays based on the thickness of the unsaturated zone, as well as the

analysis of the lag in the groundwater level responses to the rainfall. The required spatial variability component of the output from the recharge model for use in the groundwater flow model is implemented by using the zonation and multiplier factor capability of the MODFLOW model. This allows the total recharge value to be re-distributed across the model domain based on the thickness and the properties of the overlying drift deposits or soil types. The output of the recharge model is shifted in time (i.e. temporally) when applied to the flow model, and this shift is assumed to accounts for the delay caused by the unsaturated zone. The degree of shift is determined as a function of both the thickness of the unsaturated zone, and the analysis of the lag in the response of the groundwater level to the rainfall events.

It is acknowledged that this is a rather simplistic model of the recharge process and a more sophisticated model based upon Richard's equation for unsaturated flow or the Green and Ampt (1911) model of a progressive wetting front could improve the estimation of contaminant travel time from the source to the aquifer. However, such a model would require much greater knowledge of the superficial deposits over the area. This knowledge would be extremely difficult to acquire in an area of drift deposits that overlay the aquifer and require excessive field work. The combination of the data acquisition problem and the writing of a new module for the Modflow suite are beyond the scope of this work and the simple time shift of recharge adopted.

A conservative non-reactive contaminant is used in the demonstration of the applicability of the method, and therefore the contaminant is assumed to travel along with the groundwater velocity without any significant interaction with the subsurface environment. A more detailed demonstration of this approach using the actual field data is presented in Section 5.2.

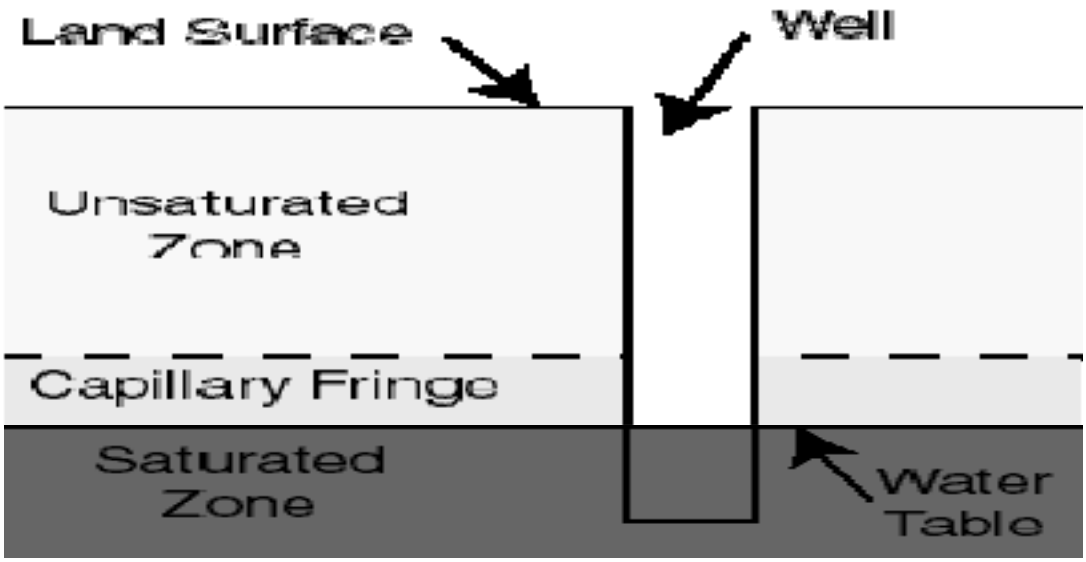

(a) The unsaturated zone

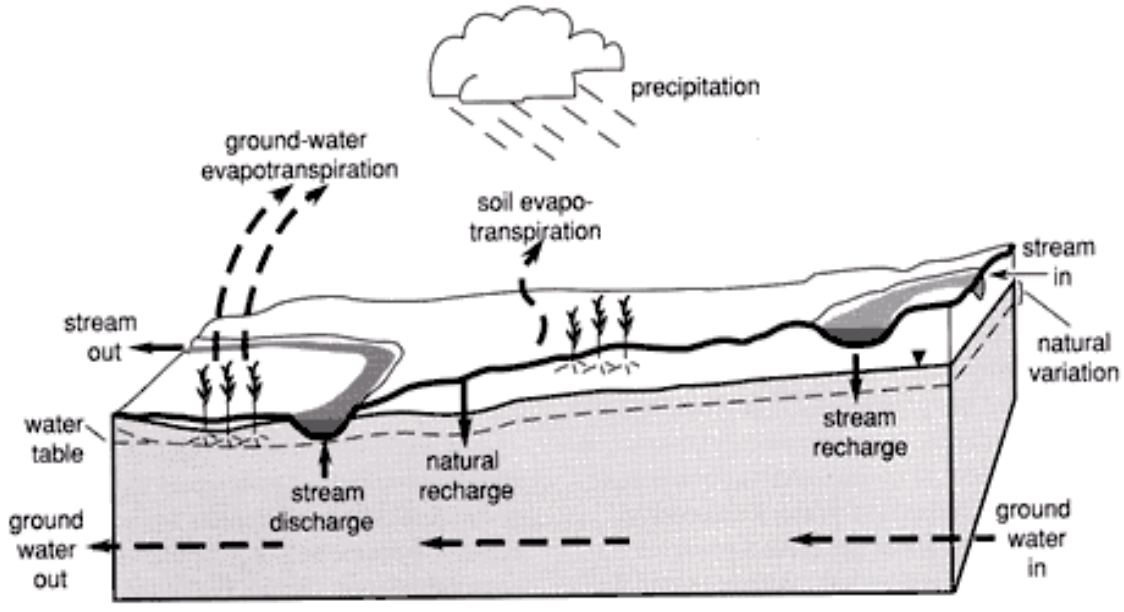

(b) Natural recharge process

Figure 3.3: The unsaturated zone and recharge processes

3.4 Descriptions of the risk model input data

The description of the input data for the risk model is presented below. All the file names are written in ***bold lower case italics***, and the input data (record) are written in *lower case italics*. The risk model reads input data from three files namely ***ram_input_file.dat***, ***advance_flag.dat***, and ***ram_files.dat.*** Examples of these files are presented in Figures 3.4 – 3.6, respectively. The detailed descriptions of the file records, as well as the required format for input into the risk model are presented below.

A. File Name:***ram_input_file.dat***

(Note: Records A1 to A7 are for each simulation)

A1. Record: *title_1*
Format: A80
title_1: This is the first line of comment for the current simulation run. It is a character value and should not be longer than 80 columns.

A2. Record: *title _2*
Format: A80
title_2: This is the second line of comment for the current simulation run. It is a character value and should not be longer than 80 columns.

A3. Record: *layer, nrow, ncol*
Format: 3I10
layer: This is an integer value that defines the layer number to which the generated source terms are applied
nrow: This is an integer value that defines the total number of rows in the local grid
ncol: This is an integer value that defines the total number of columns in the local grid

A4. Record: *tspnumber, itype, previousmult, min_mult, max_mult*

Format: 3I10, 2F10.1

tspnumber: This is an integer value that defines the total number of stress periods in a simulation

itype: This is an integer value that specifies the type of source concentration in the MT3DMS model. A default value of 15 sets the source terms as mass loading rate.

previousmult: This is a user defined multiplier. It is an integer value for varying the number of historic frequency of occurrence of pollution incidents (*nprevious* in Record A9). The default value is 1.

min_mult & max_mult: These are user defined multipliers. They are real values for varying minimum and maximum values of probable contaminant mass loading rate (*min_mass, max_mass* in Record A11) at a potential pollution source. Further details are presented in Section 3.5.1 (iv). The default value for both parameters is 1.0.

A5. Record: *fwel, fdrain, frch, fevt, friv, fghb*

Format: 6A2

Fwel: This is a character value which must be either 'F' or 'T'. The 'F' indicates that no source terms are generated from well option, while the 'T' states otherwise.

Fdrain: As above for Drain option.

Frch: As above for recharge option.

Fevt: As above for evapotranspiration option.

Friv: As above for river option.

Fghb: As above for General-Head-Dependent Boundary option.

Note: The risk model is currently setup to incorporate contaminant concentration only from the infiltrating recharge, and not from other sources. Therefore, the default value for *Frch* is 'T', while others are 'F'. The input parameters in A6 are then used to define the concentration rate in the recharge.

A6. Record: *Incrch, rarray1, buffer*

Format: 2I10, F10.0

Incrch: This is an integer value that indicates whether an array containing the concentration of recharge flux for the contaminant will be read for the current stress period. If *Incrch* ≥ 0, an array containing the concentration of recharge flux for the contaminant will be read from unit number represented by that value. If *Incrch* < 0, the concentration of recharge flux will be reused from the last stress period.

rarray1: This is an integer value that defines the array control that assigns values to the elements in the recharge flux array. The integer value 0 sets every element in array to be equal to the value *buffer*. (See Zheng and Wang (1999), Pg 97 – 99, for alternative values that can be used to define the array control).

buffer: This is a real value that is equal to concentration of contaminant in the recharge flux.

Note: The risk model is currently setup to incorporate a single contaminant species in a simulation. The contaminant concentration in the recharge defined by *buffer* is assumed to be constant in all the stress periods.

A7. Record: *global_row, global_col*

Format: 2I10

global_row: This is an integer value that defines the row number of the flow/transport model that corresponds to the first row of the local grid system.

global_col: This is an integer value that defines the column number of the flow/transport model that corresponds to the first column of the local grid system.

(Note: Records A8 to A9 are repeated for each stress periods in the simulation)

A8. Record: *spnumber, splength*

Format: 2I10

spnumber: This is an integer value that defines the number of the current stress period

splength: This is an integer value that defines the length of the current stress period [T].

A9. Record: *npsource, nprevious*

Format: 2I10

npsource: This is an integer value that defines the number of potential pollution sources in the current stress period.

nprevious: This is an integer value that defines the frequency of historical incidents aggregated for all the potential sources (*npsource)* for each stress period. In order to obtain the historical frequency for each potential source, the *nprevious* is divided by *npsource* (see Equation 3.3).

(Note: Records A10 to A11 are repeated for each potential source in each stress period)

A10. Record: *sorrow, sorcol*

Format: 2I10

sorrow: This is an integer value that defines local grid row number of the location of a pollution incident

sorcol: This is an integer value that defines local grid column number of the location of a pollution incident

A11. Record: *min_mass, max_mass*

Format: 2F10.0

min_mass & max_mass: These are real values that define minimum and maximum loading rates of probable contaminant mass associated with a potential pollution source.

Examples of ***ram_input_file.dat*** that show two possible approaches of representing the stress period and the mass loading rates are presented in Figure 3.4 (a and b), respectively. A detailed description of these approaches is presented in Section 4.3.1.

B. File Name: ***advance_flag.dat***

B1. Record: A 2-dimensional array with integer values between 0 and 5. The numbers of the rows and columns in the 2 D array must be equal to the local grid.

Format: 10I2

Note: This is a 2-D array that dynamically controls the actual proportion of generated contaminant source terms infiltrating the subsurface at any active model cell. Additional information is presented in Section 3.5.1 (v).

Example of ***advance_flag.dat*** file is presented in Figure 3.5.

C. File Name: ***ram_files.dat***

C1. Record: *funit, fname, fstatu*

Format: I4, A21, A3

funit: This is an integer value the defines unit file number for saving generated source terms for each stress period.

fname: This is a character value the defines unit file name for saving generated source terms for each stress period.

fstatu: This is a character value the defines unit file status for saving generated source terms for each stress period.

Note: The file (i.e. ***ram_files.dat)*** contains names of files that stores generated source terms for the current simulation. Each line of the file contains records for the file number (I4), file name (A21), and the file status (A3). The number of lines in the file equals the number of stress periods in the simulation. The files status is designated as 'old' therefore the files need to be created prior to executing the program. Example of ***ram_files.dat*** file is presented in Figure 3.6.

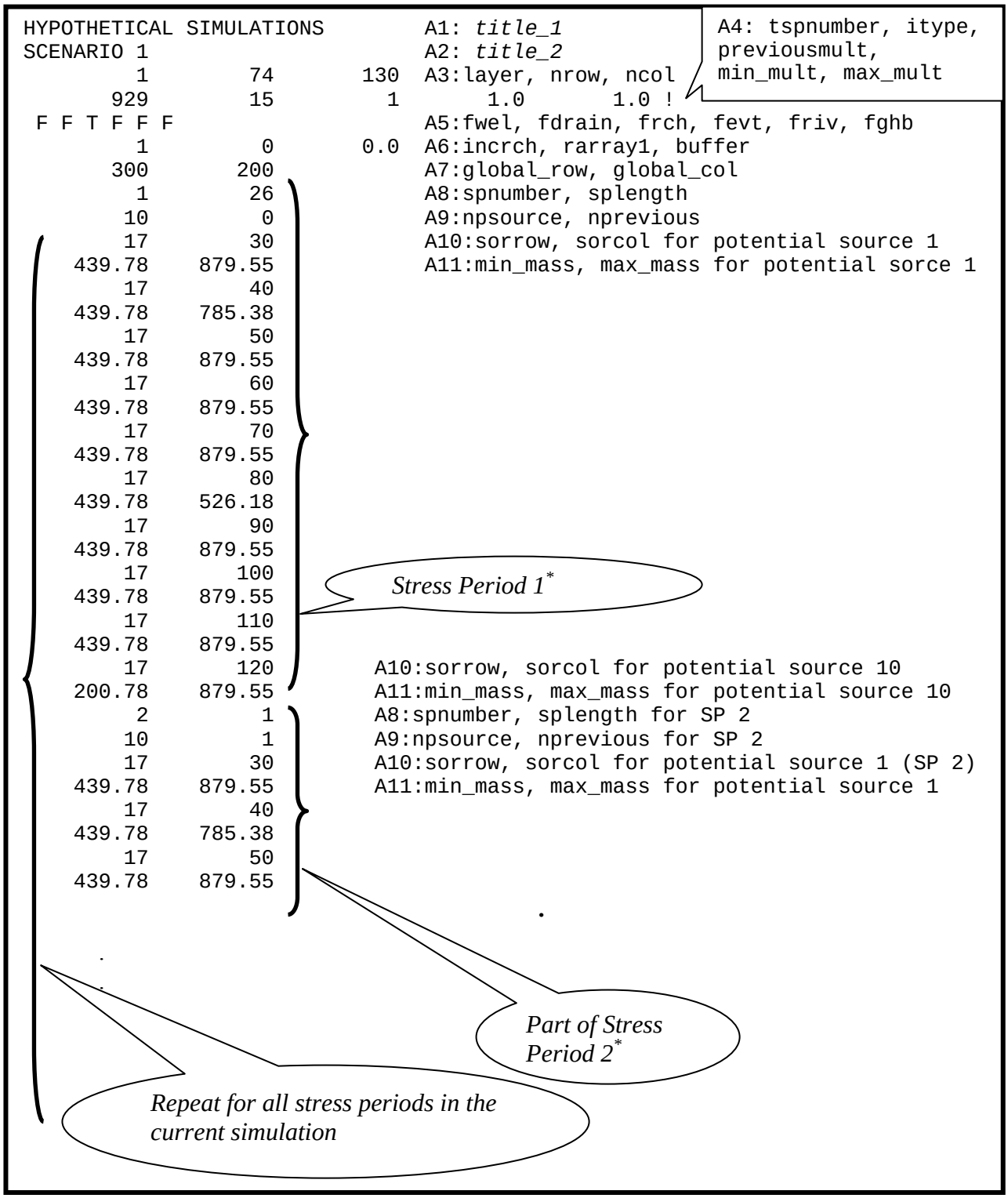

*The unit for the mass loading rate is kg/day

Figure 3.4a: Example of ram_input_file.dat input file (Approach 1)

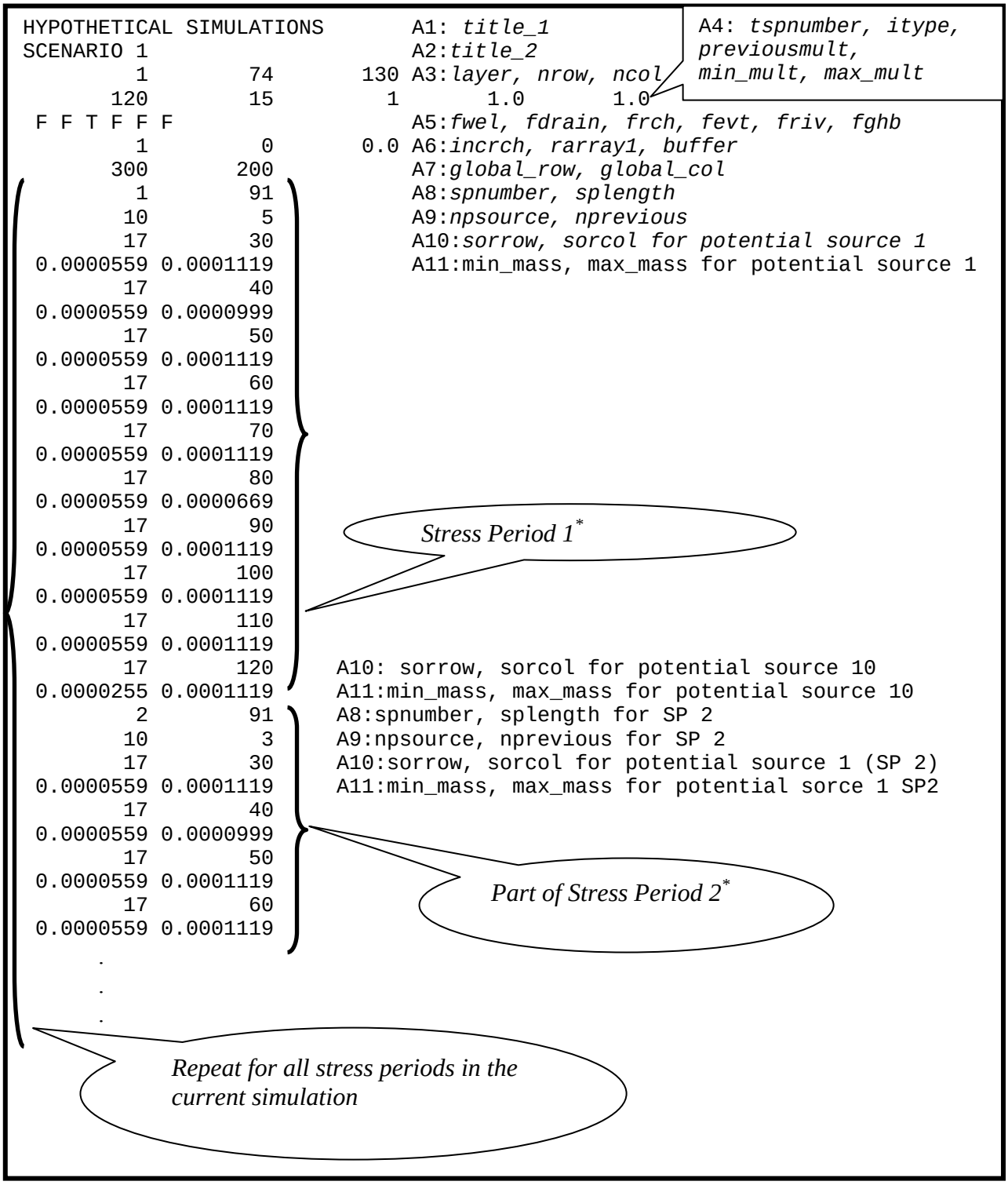

*The unit for the mass loading rate is kg/sec

Figure 3.4b: Example of ram_input_file.dat input file (Approach 2)

```
0 0 0 0 0 0 0 0 0 0    B1: 2D array with integer values between  0 & 5
0 0 0 0 0 0 0 0 0 0
0 0 0 0 0 5 0 0 0 0
0 0 0 0 0 0 0 0 0 0
0 0 1 1 0 0 0 0 0 0
0 0 1 1 0 0 0 0 0 0
0 0 0 0 0 0 0 0 0 0
0 0 0 0 0 0 0 0 0 0
0 0 0 0 1 1 0 0 0 0
0 0 0 0 1 1 0 0 0 0
0 0 0 0 0 0 0 0 0 0
0 0 0 0 0 0 0 0 0 0
0 0 0 0 0 0 0 0 0 0
0 0 0 0 0 0 4 4 0 0
1 1 0 0 0 0 0 0 0 0
1 1 0 0 0 0 0 0 0 0
0 0 0 0 0 0 0 0 0 0
```

Figure 3.5: Example of advance_flag.dat input file

```
1001acute_indepe\dis.1001old          C1:funit, fname, fstatu
1002acute_indepe\dis.1002old
1003acute_indepe\dis.1003old
1004acute_indepe\dis.1004old
1005acute_indepe\dis.1005old

.
.
1354acute_indepe\dis.1354old
1355acute_indepe\dis.1355old
1356acute_indepe\dis.1356old
1357acute_indepe\dis.1357old
1358acute_indepe\dis.1358old
1359acute_indepe\dis.1359old
1360acute_indepe\dis.1360old
1361acute_indepe\dis.1361old
1362acute_indepe\dis.1362old
1363acute_indepe\dis.1363old
1364acute_indepe\dis.1364old
1365acute_indepe\dis.1365old
```

Figure 3.6: Example of ram_files.dat input file

3.5 Source Term Generation (STG) module

The generation of synthetic source terms as well as the output of the STG module are presented in this section, and summarised in Figure 3.7.

3.5.1 Generation of a synthetic pollution incident

This involves synthetic generation of source terms that can potentially cause pollution and derogatory impacts that could be observed at pre-defined monitoring boreholes. The specific tasks of the STG module include the following:

i. The STG module computes the total number of cells in the local model grid (see Figure 3.2). The local grid describes the points where potential pollution sources will be located. The STG module then displays the results of the computation on the screen, as well as writing them into the output file ***ram_output_file.dat*** (see Figure 3.8). Also, a unique identity number is assigned to each of the local model grid cells.

ii. The STG module reads from the input file ***ram_input_file.dat***, the locations (in terms of the layer, row, and column) of the model grid cells where potential sources are located. These locations are then activated using a one dimensional logical variable array, by flagging them to be 'active'. All other model cells without a potential pollution source are flagged as 'passive'.

iii. For each stress period, the STG module computes the Probability of Pollution Occurrence (PPO) for each of the active model cells using Equation 3.3. By definition, PPO is an integral part of the risk calculation presented in Equation 3.1.

$$PPO = \frac{No\ of\ previously\ occurred\ pollution\ events \Big/ No\ of\ sources}{Period\ over\ which\ such\ events\ occurred} \qquad 3.3$$

Since the PPO is calculated for each stress period, the denominator in equation 3.3 is taken to be the length (in days) of the current stress period. Note that equation 3.3 is implemented when the PPO has to be evaluated during the execution of the risk model. If PPO is already known by priori knowledge then the values can be entered appropriately, for example multiply the known PPO by 100 and enter the time period as 100 days and number of sources as 1.

iv. For each day in the stress period, and for each active model cell, the STG module reads from ***ram_input_file.dat***, the minimum and maximum values of contaminant mass loading rates that have previously occurred based on historical records or other priori sources. The loading rate of the source term that will be generated from that potential source is randomly sampled (inclusively) between the two extreme minimum and maximum values as probable mass per event (PM), using the algorithm presented in Equation 3.4. This value represents the 'consequence' component described in Equation 3.1.

$$Probable\ mass = minima + (maxima - minima)\ x\ harvest \qquad 3.4$$

where

minima and maxima: minimum and maximum values of probable contaminant mass loading rate at a potential pollution source.

harvest: real random number generated between 0.0 and 1.0.

Similarly, the minimum and maximum magnitudes of the probable mass loading rate may be obtained from other sources such as knowledge of the processes involved.

v. The STG module reads a two-dimensional array 'advance_flag' from ***advance_flag.dat*** input file (see Figure 3.5). The array has an integer value of between 0 and 5 for each model cell of the local grid. These values dynamically control the actual proportion of infiltrating contaminant mass per unit time at every active node. A value of 0 indicates that all the synthetically generated probable mass loading rate of contaminant at a particular active node are transported from that source, while a value of 5 indicates that, although synthetic pollution is generated at the source, no pollutant is assumed to be

transported from that source. This utility is used to incorporate source control capability as mitigating measures.

vi. Next, for each day in the current stress period and for each active node, the STG module generates a Random Number (RN) between 0.0 and 1.0, and compares the random generated number (RN) with the PPO value computed (using Equation 3.3) for the current stress period. If PPO > RN, then a pollution incident with associated sampled probable mass loading rate (PM) (see (iv) above) is assumed to have occurred at that source. However, the actual loading rate of contaminant mass transported from the source will be scaled by the corresponding value of *advanced_flag* (see (v) above) for that active source.

vii. The spatial and temporal contaminant concentration (source term) simulated by the risk model based on the loading rate described in (vi) above, will be accumulated for the current stress period, and automatically collated into a two-dimensional spatial array, with each array value representing the accumulated contaminant mass discharged at that point into the environment during the length of the stress period. The names (including path) to which the two dimensional arrays are saved, are read from ***ram_files.dat*** input file (see Figure 3.6).

viii. Finally, the STG module extracts the generated source terms for all the stress periods where values are greater than zero, and presents the source terms in a format that is compatible with the transport model input data. In addition, STG module transforms the row and column numbers from local grid system into that of the global grid system used for flow/transport model, as previously described in Section 3.3.3.

The above steps (i – viii) made up the first realisation of the risk assessment method. These steps are iterated and the source terms are generated in each realisation such that the frequency distribution of the observed contaminant concentration at points of interest in the aquifer is developed by observing the number of times that the user defined concentration magnitude is exceeded.

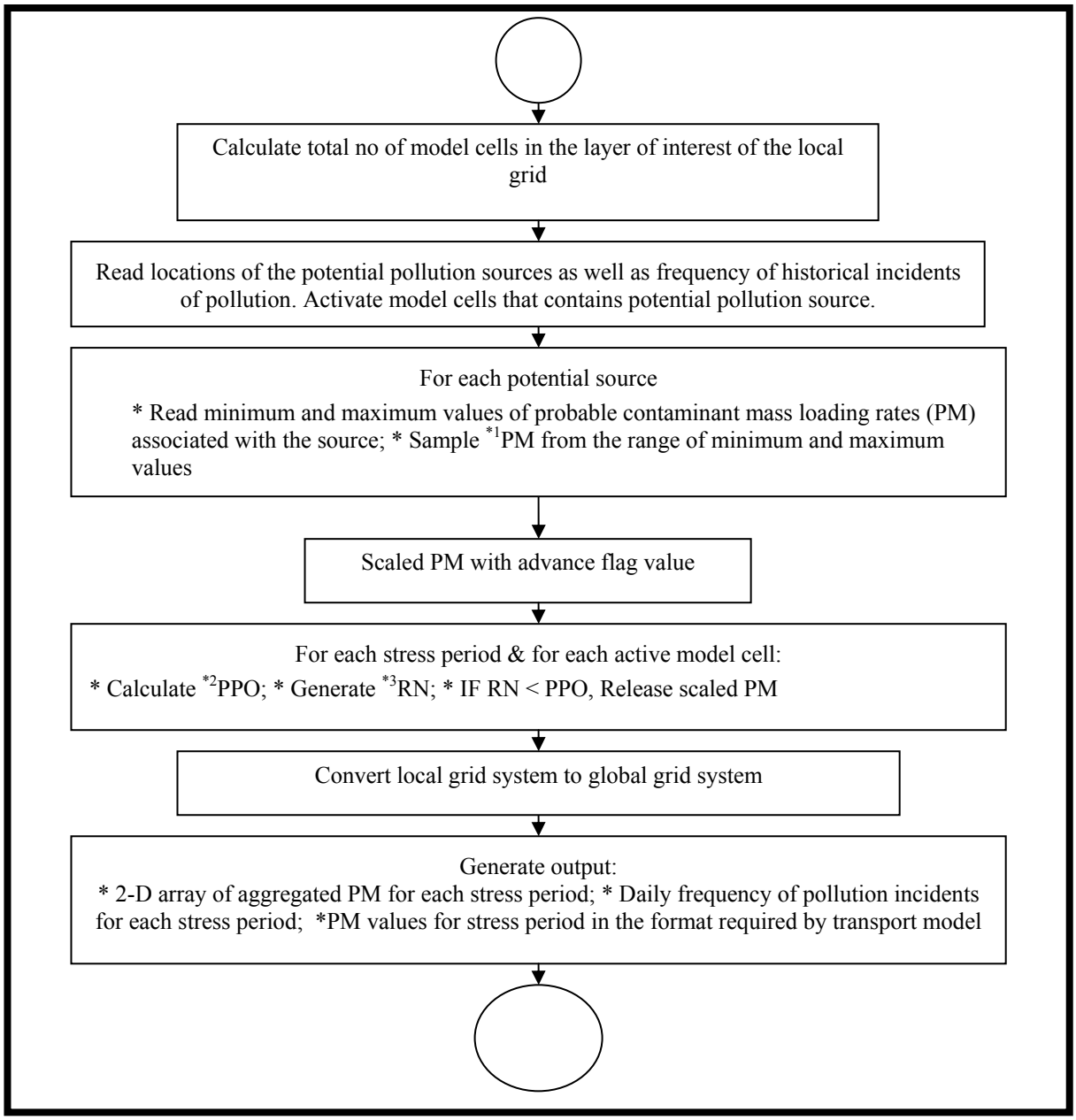

*1: Probable mass loading rate; *2: Probability of pollution occurrence; *3: Random number

Figure 3.7: Flow chart for Source Term Generation module

3.5.2 Output of the Source Term Generation module

The following files are generated as output from the execution of STG module. The file status used in the Fortran programs to define the output files is set to 'old', therefore all files must be created in the folder prior to the execution of the program.

i. ***ram_output_file.dat***: The file consists of the echo of the input data for the simulation, as well as the locations and number of synthetic pollution sources for each of the stress period. Depending on how the stress period and loading rates are defined, examples of the output file are presented in Figure 3.8.

ii. ***ram_distribution.dat***: This file contains generated daily frequency of pollution incidents for all the stress periods of the simulation. Example of the file is presented in Figure 3.9.

iii. ***ram.ssm***: The file contains source terms for all the stress periods, in a format that feeds directly into the transport model. Also, depending on how the stress period and loading rates are defined, examples of ***ram.ssm*** are presented in Figure 3.10.

```
HYPOTHETICAL SIMULATIONS
SCENARIO 1
 No of Row(s) =    74


 No of  Column(s) =   130


 Total no of nodes =  9620


 SOURCE TERM: CELL NO, ROW, COL, CONC, PREVIOUS INCIDENTS
 STRESS PERIOD             1

 THE LENGTH OF THE CURRENT STRESS PERIOD IS             26  DAYS

       2110        17        30    735.7761230         0
       2120        17        40    554.1683960         0
       2130        17        50    504.6393433         0
       2140        17        60    765.8464966         0
       2150        17        70    591.1317749         0
       2160        17        80    447.5439148         0
       2170        17        90    763.6478882         0
       2180        17       100    669.9603271         0
       2190        17       110    710.0283813         0
       2200        17       120    656.0779419         0


 No of Potential Pollution Sources is           10


 SOURCE TERM: CELL NO, ROW, COL, CONC, PREVIOUS INCIDENTS
 STRESS PERIOD             2

 THE LENGTH OF THE CURRENT STRESS PERIOD IS              1  DAYS

       2110        17        30    503.7561035         1
       2120        17        40    661.0507813         1
       2130        17        50    440.9072571         1
       2140        17        60    643.4888916         1
       2150        17        70    752.7261353         1
       2160        17        80    448.0473022         1
       2170        17        90    535.1425171         1
       2180        17       100    771.0029297         1
       2190        17       110    761.1729126         1
       2200        17       120    329.3972168         1


 No of Potential Pollution Sources are           10
```

Repeated for all the stress periods

Note: The unit for the mass loading rate is kg/day

Figure 3.8a: Example of ram_output_file.dat output file (Approach 1)

```
HYPOTHETICAL SIMULATIONS
SCENARIO 1
 No of Row(s) =    74


 No of  Column(s) =   130


 Total no of nodes =  9620


 SOURCE TERM: CELL NO, ROW, COL, CONC, PREVIOUS INCIDENTS
 STRESS PERIOD             1

 THE LENGTH OF THE CURRENT STRESS PERIOD IS             91  DAYS

       2110        17         30      0.0000936         5
       2120        17         40      0.0000705         5
       2130        17         50      0.0000642         5
       2140        17         60      0.0000974         5
       2150        17         70      0.0000752         5
       2160        17         80      0.0000569         5
       2170        17         90      0.0000971         5
       2180        17        100      0.0000852         5
       2190        17        110      0.0000903         5
       2200        17        120      0.0000835         5


 No of Potential Pollution Sources is           10


 SOURCE TERM: CELL NO, ROW, COL, CONC, PREVIOUS INCIDENTS
 STRESS PERIOD             2

 THE LENGTH OF THE CURRENT STRESS PERIOD IS             91  DAYS

       2110        17         30      0.0000668         3
       2120        17         40      0.0000957         3
       2130        17         50      0.0000870         3
       2140        17         60      0.0001067         3
       2150        17         70      0.0001049         3
       2160        17         80      0.0000606         3
       2170        17         90      0.0000866         3
       2180        17        100      0.0000848         3
       2190        17        110      0.0000923         3
       2200        17        120      0.0000785         3


 No of Potential Pollution Sources are           10


 Repeated for all the stress periods
```

Note: The unit for the mass loading rate is kg/sec

Figure 3.8b: Example of ram_output_file.dat output file (Approach 2)

STRESS PERIOD 1

There are 0 active sources in SP 1 day 1
There are 0 active sources in SP 1 day 2
There are 0 active sources in SP 1 day 3
There are 0 active sources in SP 1 day 4
.
.
There are 0 active sources in SP 1 day 26
There are 1 active sources in SP 1 day 27
There are 0 active sources in SP 1 day 28
.
.
There are 0 active sources in SP 1 day 40
There are 0 active sources in SP 1 day 41
There are 0 active sources in SP 1 day 42
.
There are 0 active sources in SP 1 day 77
.
There are 0 active sources in SP 1 day 87
There are 1 active sources in SP 1 day 88
.
There are 0 active sources in SP 1 day 91

STRESS PERIOD 2

There are 0 active sources in SP 2 day 1
.
.
There are 0 active sources in SP 2 day 42
There are 0 active sources in SP 2 day 43
There are 1 active sources in SP 2 day 44
There are 0 active sources in SP 2 day 45
.
There are 0 active sources in SP 2 day 50
There are 1 active sources in SP 2 day 51
There are 0 active sources in SP 2 day 52
.
There are 0 active sources in SP 2 day 86
There are 0 active sources in SP 2 day 87
There are 0 active sources in SP 2 day 88
.
There are 0 active sources in SP 2 day 91

STRESS PERIOD 3
.
.

Repeated for all the stress periods

Figure 3.9: Example of ram_distribution.dat output file

```
F F T F F F
     10490
         1
         0       0.0
         0
         1
         0       0.0
         1
         1       316       229    801.60        15
         1
         0       0.0
         0
         1
         0       0.0
         1
         1       316       279    469.40        15
         1
         0       0.0
         0
         1
         0       0.0
         2
         1       316       299    734.80        15
         1       316       309    758.60        15
         1
         0       0.0
         0
         1
         0       0.0
         1
         1       316       299    797.60        15
         1
         0       0.0
         0
         1
         1       316       269    484.30        15
         1
         0       0.0
         0
         1
         0       0.0
         2
         1       316       299    747.60        15
         1       316       309    524.60        15
         1
         0       0.0
         2
         1       316       269    461.60        15
         1       316       309    833.80        15
```

Repeated for all the stress periods

Note: The unit for the mass loading rate is kg/day

Figure 3.10a: Example of ram.ssm output file (Approach 1)

```
F F T F F F
      9434
         1
         0       0.0
         4
         1       316       229 0.0000936       15
         1       316       249 0.0000642       15
         1       316       269 0.0000752       15
         1       316       299 0.0000852       15
         1
         0       0.0
         1
         1       316       259 0.0001067       15
         1
         0       0.0
         2
         1       316       289 0.0000588       15
         1       316       319 0.0000755       15
         1
         0       0.0
         4
         1       316       229 0.0000598       15
         1       316       269 0.0000756       15
         1       316       279 0.0000616       15
         1       316       319 0.0000389       15
         1
         0       0.0
         2
         1       316       269 0.0000567       15
         1       316       299 0.0001069       15
         1
         0       0.0
         4
         1       316       239 0.0000715       15
         1       316       259 0.0001441       15
         1       316       289 0.0000577       15
         1       316       319 0.0000529       15
         1
         0       0.0
         3
         1       316       259 0.0000580       15
         1       316       279 0.0000658       15
         1       316       309 0.0001056       15
         1
         0       0.0
         4
         1       316       249 0.0000953       15
         1       316       259 0.0000573       15
         1       316       269 0.0001523       15
         1       316       309 0.0000904       15
```

Repeated for all the stress periods

Note: The unit for the mass loading rate is kg/sec

Figure 3.10b: Example of ram.ssm output file (Approach 2)

3.6 Risk Assessment module

After the running of one iteration of the transport model, the Risk Assessment (RA) module counts the number of times at which the contaminant concentrations exceeds the user defined concentration magnitudes. The simulated contaminant concentration data at monitoring points serve as input into the risk assessment module. This process is repeated several times. The output file of the risk assessment module, ***risk_outfile.dat***, contains the ranges of user defined concentration magnitudes and exceedance frequency. An example of the output file is presented in Figure 3.11. This result is saved into an output file at the end of each completed realisation. The FORTRAN code for the risk assessment module is presented in appendix A.13. All other flow and transport model outputs are over-written by the next realisation. Subsequent outputs of the risk assessment module are appended onto the same output file as the simulation progresses. When the total number of iteration set by the user is complete, the saved output for all the realisations will be exported into Microsoft Excel spreadsheet for collation and post-processing.

The transport model (MT3DMS) has an internal capability to adjust the length of the time step during a simulation in order to ensure numerical stability. This therefore limits the control of the user in defining the exact number of transport time steps for the simulations under different scenarios. Hence, in order remove the effects of the variability in the time steps across different scenarios, the number of exceedances for each contaminant concentration magnitude is normalised during the post-processing stage of the model output by dividing the number of exceedances by the total number of time steps in that simulation, and express the result as a percentage.

```
BH_7
      <  0.10E-08     489
0.10E-08  -  0.10E-06       0
0.10E-06  -  0.10E-03       0
0.10E-03  -  0.10E-01       0
      >  0.10E-01       0
  BH_8
      <  0.10E-08     489
0.10E-08  -  0.10E-06       0
0.10E-06  -  0.10E-03       0
0.10E-03  -  0.10E-01       0
      >  0.10E-01       0
.
.     >  0.10E-01       0
  BH_10
      <  0.10E-08     104
0.10E-08  -  0.10E-06      18
0.10E-06  -  0.10E-03     100
0.10E-03  -  0.10E-01      32
      >  0.10E-01     235
  BH_11
      <  0.10E-08     489
0.10E-08  -  0.10E-06       0
0.10E-06  -  0.10E-03       0
0.10E-03  -  0.10E-01       0
      >  0.10E-01       0

  BH_14
      <  0.10E-08     489
0.10E-08  -  0.10E-06       0
0.10E-06  -  0.10E-03       0
0.10E-03  -  0.10E-01       0
      >  0.10E-01       0
```

```
  BH_15
      <  0.10E-08     489
0.10E-08  -  0.10E-06       0
0.10E-06  -  0.10E-03       0
0.10E-03  -  0.10E-01       0
      >  0.10E-01       0
  BH_16
      <  0.10E-08     489
0.10E-08  -  0.10E-06       0
0.10E-06  -  0.10E-03       0
0.10E-03  -  0.10E-01       0
      >  0.10E-01       0
.
.
  BH_18
      <  0.10E-08     489
0.10E-08  -  0.10E-06       0
0.10E-06  -  0.10E-03       0
0.10E-03  -  0.10E-01       0
      >  0.10E-01       0
  BH_19
      <  0.10E-08     489
0.10E-08  -  0.10E-06       0
0.10E-06  -  0.10E-03       0
0.10E-03  -  0.10E-01       0
      >  0.10E-01       0
  BH_20
      <  0.10E-08     489
0.10E-08  -  0.10E-06       0
0.10E-06  -  0.10E-03       0
0.10E-03  -  0.10E-01       0
      >  0.10E-01       0
```

Figure 3.11 Example of risk_outfile.dat file

3.7 Flow and Transport model Packages

The synthetic contaminant concentrations released into the environment at any active model cell are propagated through the subsurface using a multi-species transport model, commonly referred to as MT3DMS (Zheng and Wang, 1999). This transport model requires a calibrated flow model prior to its execution. In this work, MODFLOW-2000 (Harbaugh *et al.* 2000) is used to develop the calibrated flow model.

3.7.1 Description of the selected groundwater flow model

The numerical code adopted for this work is the version of MODFLOW 2000 (version 1.18.01), downloaded from USGS Ground-Water Software (2004). This software is distributed as a compressed archive file, containing the source code and the relevant documentation. The program was activated in a typical serial processing mode.

MODFLOW-2000 is a blocked-centred finite-difference FORTRAN based code, which has the capability of representing a complex three-dimensional groundwater flow system. Unlike the earlier versions of MODFLOW, it directly incorporates the capability for sensitivity analysis. It provides options for using either inverse modelling approach for calibration or the conventional trial-and-error method. MODFLOW-2000 can simulate a wide range of geo-hydrological conditions under both steady and transient flow conditions, including interactions with the surface water regime.

MODFLOW-2000 consists of modular-structured algorithms, written in FORTRAN 90, and incorporates the capabilities for solving multiple simultaneous equations. The largest subdivision of the design concept of MODFLOW-2000 is called a Process. A Process solves a fundamental governing equation using a specified numerical method. The six Processes that are presently incorporated into MODFLOW-2000 are Groundwater Flow, Groundwater Transport, Observation, Sensitivity, Parameter Estimation and Global Processes. However, the Global Process does not solve any equation but merely controls the overall operation of the model. The Groundwater Flow Process is further subdivided into smaller units called packages. Each package solves a specific hydrologic process, while the solver packages solve the linear simultaneous equations that are generated by the application of the governing equation. The Groundwater Transport Process solves the solute transport equation (Konikow *et al.* 1996), while the Observation Process calculates

the simulated values that are used for comparison with the field measurements. The Sensitivity Process solves the sensitivity equation with respect to the hydraulic heads throughout the grid, while the Parameter Estimation Process minimizes the objective function by solving the modified Gauss-Newton equation in order to compute the optimal aquifer parameter values.

The modular structure of MODFLOW enhances its flexibility to be able to combine packages to simulate site specific geo-hydrological scenarios. The MODFLOW packages as well as the primary input files that were used in the demonstration of the field application of RAM are presented in Table 5.9. The model setup is then controlled by a *named file* in the MODFLOW algorithm. The software has a comprehensive freely available documented literature. The detailed description of these input files are contained in McDonald and Harbaugh (1988), Harbaugh and McDonald (1996), and Harbaugh *et al.* (2000). The model is widely acceptable among regulatory bodies and is intended for use on any computer operating system.

3.7.2 Description of the selected groundwater transport model

The transport model utilised in the setting up and simulation of the contaminant through the subsurface environment is the modular three-dimensional transport model for multi-species. The model is authored by Zheng and Wang (1999), and has a similar modular structure to that implemented in the U.S. Geological Survey modular three-dimensional finite-difference groundwater flow model, MODFLOW (McDonald and Harbaugh 1988; Harbaugh and McDonald 1996). The modular structure of MT3DMS enhances its capabilities for simulating advection, dispersion/diffusion and chemical reactions within groundwater under varied hydrological conditions. In addition, the modular structure provides capability to accommodate add-on reaction packages for modelling general biological and geochemical reactions. The chemical reactions included in the model are equilibrium-controlled or rate-limited linear or nonlinear sorption and first-order irreversible or reversible kinetic reactions.

MT3DMS includes three major classes of transport solution techniques namely finite-difference method, the particle-tracking-based Eulerian-Lagrangian methods, and the higher-order finite-volume Total Variation Diminishing (TVD) method. The iterative solver is based on the Generalized Conjugate Gradient (GCG) methods. The combination

of these solution techniques provides best approach for solving the most wide-ranging transport problems with efficiency and accuracy. MT3DMS is implemented with an optional, dual-domain formulation for modelling mass transport. This allows porous medium to be regarded as consisting of two distinct domains, a mobile domain where transport is predominately by advection and an immobile domain where transport is predominately by molecular diffusion. Two porosity values are used for each model cell to characterise the porous medium. One for the mobile domain and the other for the immobile domain, and the exchange between the mobile and immobile domains is specified by a mass transfer coefficient.

MT3DMS is developed for use with any block-centred finite-difference flow model and assumes that flow field is not significantly affected by changes in the concentration of the contaminant. Both flow and transport models are independently developed and linked by a file, where required data for flow model simulation are saved for the execution of the transport model. The MT3DMS model has enjoyed wide applications in areas of contaminant transport modelling and remediation assessment studies.

3.8 Implementation structure of the risk assessment method

The risk model is implemented by the directory structure presented in Figure 3.12. It consists of one directory (**bolded**) and 75 files, all of which occupied approximately 12 GB. The directory folder contains the generated spatial 2-D source terms for each stress period. The RAM is run within the Microsoft DOS environment, and the generated outputs can be viewed and evaluated within Windows based software packages. It is assumed that all the files and folder are installed in the same directory and the execution of RAM assumes a reasonable level of competence in MODFLOW, MT3DMS, WordPad, Microsoft Excel and MS DOS operating system.

[acute_indepe]

advance_flag.dat	bham._b	bham._nm
bham._os	bham._r	bham._w
bham._ws	bham._ww	bromsgrovebase.dat
driftbase.dat	filename.dat	fram.nam
fram.obs	ibound_1.dat	ibound_2.dat
ibound_3.dat	impact_assessment.bat	initial_conc_1.dat
initial_conc_2.dat	initial_conc_3.dat	initial_wl_1.dat
initial_wl_2.dat	initial_wl_3.dat	kidderminsterbase.dat
mf2k.exe	mf2kerr.p00	modbatch.rpt
modflow.bf	mt3dms5b.exe	ram.adv
ram.ba6	ram.btn	ram.cnf
ram.dis	ram.dsp	ram.ftl
ram.gcg	ram.glo	ram.hfb
ram.hob	ram.lmt	ram.lpf
ram.lst	ram.m3d	ram.mas
ram.mult	ram.nam	ram.obs
ram.oc	ram.pcg	ram.rch
ram.riv	ram.ssm	ram.ucn
ram.wel	ram_cell_by_cell.dat	ram_distribution.dat
ram_drawdown.dat	ram_files.dat	ram_head.dat
ram_input_file.dat	ram_output_file.dat	ram_recharge.dat
ram_river.dat	ram_well.dat	rech_mult.dat
risk_assessment.EXE	risk_assessment.f95	risk_model.EXE
risk_model.f95	risk_outfile.dat	source_term.dat
ssm_outfile.dat	topography.dat	wildmoorbase.dat

```
              75 File(s) 12,452,981,716 bytes
              1 Dir(s)  203,332,333,568 bytes free
```

Figure 3.12: Overview of the directory structure of the risk assessment method

3.9 Comparison of the RAM and other risk assessment methods

The contemporary techniques have been broadly discussed under three categories, namely: ranking index methods, process-based computer simulation, and post-pollution assessment methods. The first group are essentially qualitative and subjective in approach. Furthermore, the index methods serve primarily to provide a decision making tool in the management of groundwater resources, though water resources managers tend to take advantage of this, especially because of the low cost implications. However, these approaches generally lack good scientific judgement, because many important factors such as sorption capacity, contaminant travel times, dilution etc, are not accounted for. This is in addition to the following:

i. The choice of indices and the associated weights is largely subjective and requires considerable skill and experience of the user in assigning them. It is unlikely that any two users will obtain the same results.
ii. The ranking index methods tend to over-estimate vulnerability of porous media compared to fractured aquifers, perhaps because of its conservative approach.
iii. There is a tendency for the less important parameters to subdue the major determining factors, unless proper weighting values are assigned.
iv. There are varying degree of discrepancies between the vulnerability indexes estimated using a traditional approach such as DRASTIC, and the actual spatial field distributions (Barbash and Resek, 1996).
v. The complexity of the groundwater flow conditions and the transport properties of the subsurface limit the ability of the traditional assessment methods to effectively define the processes.

Hence, a more robust, scientifically based approach is required by water resources managers, in situations where there is a desire to eliminate or reduce the associated uncertainties in the predictions of risk to groundwater features, as well as where transport processes are required to be accounted for, without unnecessary complexities.

The second group are based on the physics of solute transport and are mostly analytical in approach. In addition, the parameters considered in the assessment are geo-hydrologic dependent and no consideration is given to the first dimensional component of the risk definition. Also, both the second and the third groups are post pollution incident

assessment method, largely for management of water resources and tend to evaluate the impacts of post pollution events on human health and the environment. The source-pathway-reception model also proffers a management tool for assessing the potential threat of a post pollution event to a receptor, rather than a more preferred preventive tool with anticipatory capability that incorporates the two-dimensional risk concept, for effective and quantitative prediction of pollution occurrence, which can provide a robust sustainability for water resources.

The risk assessment approach proposed in this work is generic and therefore can be applied to any geographical location where geological and hydrogeological concepts can be mathematically defined. Greater Birmingham is chosen as a case study (see Chapter 5) for the purpose of demonstrating the applicability of the method. Birmingham is chosen because of its proximity to the research base and the availability of the required data.

In a practical sense, all groundwaters are vulnerable because of their linkage with the ground surface, as replenishment of groundwater originates from recharge processes. Therefore, a more accurate approach for the measurement of the effective risk thereby becomes more dependent on environmental factors, including the occurrence and distribution of potential pollutant sources at the ground surface. This also includes the travel time of the contaminants to reach the water resources regime.

Hence, arising from the above, the approach developed in this work will constitute another dimension of the risk assessment approach, where the assessment of the risk to groundwater features will incorporate quantification of the probability of pollution occurrence. This will be based on the distribution of the potential pollution sources and the historical frequency of pollution incidents, in addition to the intrinsic geological properties. This anticipatory, preventive and management approach will predict risk to groundwater resources as a function of the probability distribution of historical pollution events, and therefore makes it possible to focus on prevention of the aquifer, rather than its management, in accordance with the principle of sustainable development.

Despite the specific advantages of this proposed fourth dimension of risk assessment approach (as highlighted above), this work also recognises the fact that the existing contemporary assessment methods possess their unique advantages in their own rights.

Therefore the proposed method in this work is not considered as an absolute alternative or rather 'either/or' solution, but 'both/and' philosophy, in order to provide a more encompassing complimentary approach in the assessment of risk to groundwater resources.

3.10 Summary of the Chapter

The conceptual and methodological approach of the risk assessment method is presented in this Chapter. The concept considers risk to groundwater features using synthetically generated source terms based on the knowledge of the frequency of the historical occurrence of the pollution incidents. The methodological approach involves algorithm development to carry out the scoping of the sources of potential pollutant, generation of synthetic pollution incidents and consideration of the resulting distribution of risks to the groundwater features. The risk posed to water features is quantified by computing the number of times at which concentration magnitude is exceeded at monitoring points during a given period of time. The more the exceedance value, the higher the risk posed to that water feature. The application of this method, where source terms are generated based on historical frequency of pollution incidents provides capability for anticipatory and predictive risk assessment for effective management of groundwater features. This approach has not been demonstrated in the current risk assessment methods.

Chapter 4: Application of risk assessment method using hypothetical data

4.1 Background

The Risk Assessment Method (RAM) developed in this work requires integrated flow and transport models for the simulation of the spatial and temporal representation of the effects of synthetic source terms generated by the risk model. The method is setup using MODFLOW-2000 (Harbaugh *et al.* 2000) and MT3DMS (Zheng and Wang, 1999), for flow and transport modelling, respectively. The detailed description of MODFLOW-2000 and MT3DMS are already presented in Section 3.7. The linkage between the flow and transport models is activated by a flow model interface called Link-MT3D package (Zheng and Wang, 1999), generated during the flow model simulation. The sensitivity of the method to sizes of the model cell grid and time steps, contaminant loading rates and probability of pollution occurrence were demonstrated using hypothetical models and scenario runs.

4.2 Choice of the model grid cell and time step sizes

The effects of the sizes of the model grid cells and time steps are more pronounced in the contaminant transport problems compared to flow related problems. This is partly because the mathematical properties of the transport governing equation are dependent on the dominant transport mechanism. This is further complicated by the heterogeneity of the subsurface environment. Where field transport problems are dominated by dispersion process, standard finite difference and finite element methods can provide accurate and efficient solution. However, many field-scale transport problems are dominated by advection process where relatively steep concentration gradient is moving through the subsurface system. In such cases, it is difficult to numerically preserve the sharp front of the contaminant transport, and therefore standard numerical methods often produce numerical errors which include numerical dispersion (smearing of the concentration front) and artificial oscillation (overshoot or undershoot of contaminant concentration).

One of the ways to mitigate these numerical errors is to make the model grid to be sufficiently refined. However, the refinement of the model has to be balanced against the available time and computational resources. For transport problems, the cell size that minimises the effects of the numerical dispersion is estimated using the Peclet number. The Peclet number is defined as the ratio of the advective to the dispersive terms. That is:

$$Peclet\ number = \frac{v_x d_x}{D_x}$$

where:

v_x : particle velocity in the x direction [L/T]

d_x : cell size in the x direction [L]

D_x : dispersion coefficient [L^2/T]

However,

$$D_x = v_x \alpha_x$$

where α_x is the dispersivity along the x direction [L]

Then

$$Peclet\ number = \frac{d_x}{\alpha_x}$$

The Peclet number is dimensionless, and needs to be less than 2 in order to ensure numerical stability and minimises numerical dispersion (Pinder and Gray, 1977).

The time interval during which model calculations are made is called the time step. In general, the smaller the time step the more accurate the predicted results. However, extreme cases can result into either excessive computational time or excessive number of iteration and possibly numerical dispersion. Therefore, the time steps that minimises numerical errors can be estimated using cell Courant number as shown below:

$$Courant\ number = v\frac{d_t}{d_x}$$

The cell Courant number needs to be less than unity in order to minimise numerical errors and ensure stability.

The three hypothetical scenarios (1 – 3) presented under this section were setup in order to be able to obtain sizes of the model grid cells that will provide acceptable trade off between the model accuracy and efficient implementation of the model. In order to satisfy the Courant number, the number of the time steps used per each stress period was kept constant as nine (9) in all the three scenarios.

4.2.1 Descriptions of the initial conditions

The initial conditions for scenario 1are summarised in Table 4.1. These consist of the flow and transport model input data as well as the initial groundwater levels. The locations of the 20 observation boreholes (H1 – H20) and the five abstraction boreholes (A1 – A5) are presented in Table 4.2.

Although this is a hypothetical model, it must be related to the size and configuration of a real groundwater resource. Chapter 5 considers the Birmingham aquifer in detail and this overall size and shape is representative of many aquifers. A very simple rectangular aquifer has therefore been constructed following the size of the Birmingham aquifer. The grid reference system given in Table 4.1 approximated to the British National Grid for the aquifer. Arbitrary boundary conditions of constant heads along each edge of the aquifer were constructed, falling from -5m in the north west corner to -23 in the south east. The initial head distribution was found by interpolating likely values across the aquifer then running the simulation model for 30 years with no abstraction. These heads are shown in Figure 4.1a as a profile and in Figure 4.1b as a spatial distribution, and this was used as the initial groundwater levels in all the subsequent scenarios.

Table 4.1: Model input data for the hypothetical scenario 1

Parameter	Scenario 1 (Baseline)
Dimension (m)	Length (West – East) = 15000; Width (South – North) = 18000
Grid reference	Bottom left hand corner : 400000: 279000 Top right hand corner: 415000:297000
Surface and base elevations (m OD)	Surface elevation = 0.0 ; Base elevation = -50
Grid size	Δx = 25 m; Δy = 25 m
Flow model discretization	No of layer(s) = 1; No of rows = 720; No of cols = 600 No of model cell = 432,000
No of observation BHs	20
MODFLOW & MT3DMS Packages	Discretisation (DIS), Basic (BA6), Layer Property Flow (LPF), Linked Mass Transport (LMT6), Preconditioned Conjugate Gradient (PCG), Well (WEL), Output Control (OC), Recharge (RCH), Basic Transport (BTN), Advection (ADV), Dispersion (DSP), Sink & Source Mixing (SSM), Generalised Conjugate Gradient Solver (GCG)
Boundary conditions for flow model	Constant head at all the four side boundaries, and no flow at the bottom; Specified flux from recharge at water table; No mass flux at all the boundaries as well as the bottom
Initial water head (m OD)	Distributed (see Figure 4.2)
S_y & S_s	0.12 & 1 x 10^{-4}
K_h (m/s)	1.84 x 10^{-3}
K_h/K_z	10.0
No of stress period	120
Length of stress period	90 - 91
Time step/stress period	9
Recharge (m/s)	2.900 x 10^{-9} (≈ 91.45 mm/yr)
Groundwater abstraction (m^3/sec)	Number of boreholes = 5 Rates per abstraction borehole: 9.744 x 10^{-2} (≈ 8418.82 m^3/d)
Porosity	30 %
Background concentration	0.0 mg/l
Initial contaminant mass	5500 kg
α_L α_T	20 m ; 0.1 m
Ratio of the vertical transverse dispersivity, to the longitudinal dispersivity	0.01
Effective molecular diffusion coefficient	0.0 m^2/s

Table 4.2: Observation (H1 – H20) and abstraction boreholes (A1 – A5)

BH Id	Easting	Northing	Scenario 1 (25m x 25m)		Scenario 2 (10m x 10m)		Scenario 3 (50m x 50m)	
			Row	Col	Row	Col	Row	Col
H1	403000	282000	549	167	1370	417	274	82
H2	406000	282000	549	267	1370	665	274	133
H3	409000	282000	549	366	1370	920	274	183
H4	412000	282000	549	466	1374	1168	274	232
H5	403000	285000	445	167	1115	417	223	83
H6	406000	285000	445	267	1115	665	223	133
H7	409000	285000	445	366	1119	916	223	183
H8	412000	285000	445	466	1115	1164	223	232
H9	403000	288000	342	167	856	417	171	83
H10	406000	288000	342	267	856	665	172	133
H11	409000	288000	342	366	860	913	171	183
H12	412000	288000	342	466	856	1168	171	232
H13	403000	291000	239	167	601	417	119	83
H14	406000	291000	239	267	598	665	119	133
H15	409000	291000	239	366	598	916	119	183
H16	412000	291000	236	466	598	1164	119	232
H17	403000	294000	137	166	346	417	68	83
H18	406000	294000	137	266	346	665	68	133
H19	409000	294000	137	366	343	916	68	183
H20	412000	294000	137	466	343	1164	68	232
A1	405362	284631	497	215	1243	541	248	108
A2	410327	284631	497	415	1243	1040	248	208
A3	410327	287213	395	415	988	1044	196	208
A4	410327	289745	292	415	729	1040	145	208
A5	410327	292277	189	415	470	1040	94	208

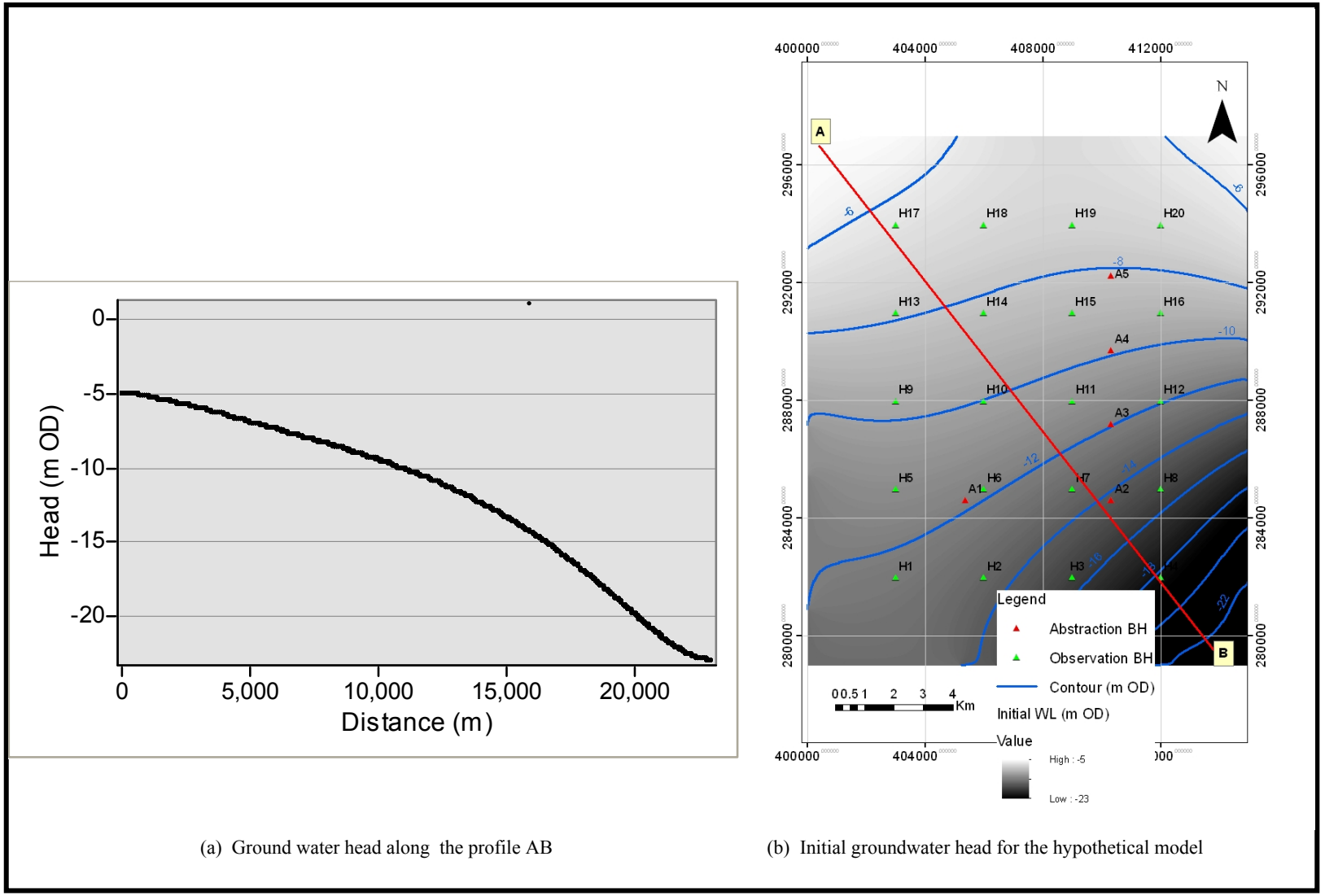

(a) Ground water head along the profile AB

(b) Initial groundwater head for the hypothetical model

Figure 4.1: Initial groundwater head for the hypothetical model

4.2.2 Setting up of the hypothetical scenarios for grid size assessment

Three hypothetical scenarios were setup in order to evaluate the required grid sizes needed for solute transport calculations. This requires introduction of a contaminant source and determination of the rate at which the contaminant travels within the model domain.

The initial conditions for the three hypothetical scenarios are based on those presented in Section 4.2.1. Scenario 1 (see Table 4.1) consists of a single layer model and represents the baseline conditions. Scenario 2 is similar to scenario 1, except that the model grid sizes are refined to $\Delta x = 10$ m, and $\Delta y = 10$ m. This makes the number of rows and columns to be 1800 and 1500, respectively. The total number of model cells then becomes 2,700,000. Also, scenario 3 is similar to scenario 1, with the exception that the model grid sizes are adjusted to $\Delta x = 50$ m, and $\Delta y = 50$ m. This makes the total number of rows and columns for the model to be 360 and 300, respectively. The total number of model cells then becomes 108,000. In addition, the longitudinal dispersivity is increase from 20 m (in scenarios 1 and 2) to 25 m (in scenario 3). An initial contaminant mass of 5500 kg was used in each of the three scenarios, and its location is shown in Figure 4.3a.

A constant lumped recharge value of 91.45 mm/yr was used for all the hypothetical runs. Therefore, the delay caused by the unsaturated zone was only implicitly represented because of the constant recharge values used in all the stress periods.

The integrated flow and transport model was run over a period of 30 years and the effects of variation of model grid size were assessed by observing the travel time of the contaminant, as well as the spatial and temporal concentrations at the 20 pre-defined monitoring points. In order to prevent the background contaminant concentration from masking the effects of the contaminant, the initial background concentration was set to be zero. Chloride was used as the contaminant in this study because of its conservative and non reactive nature within the natural subsurface environment.

4.2.3 Results of the hypothetical model run for grid assessment

In each of the scenarios 1- 3, the difference between the total inflow and outflow for each stress period is internally calculated by the model, using Equation 4.1 (McDonald and Harbaugh, 1988). The volumetric balance error obtained for scenarios 1 – 3 are presented in Figure 4.2a. The summary of the volumetric budget for scenarios 1 - 3 model runs for the simulation period of 30 years are presented in Figure 4.2 (b-d). Also, for each of these scenarios, the groundwater head and drawdown distributions are obtained directly as model outputs, and the values within the layer at the end of the simulation (30 years) are presented in Figures 4.3 to 4.5, for scenarios 1, 2 and 3, respectively.

$$PercentError = \frac{(IN - OUT)\,100}{(IN + OUT)/2} \qquad 4.1$$

The ranges of values of contaminant concentrations simulated at the 20 observation boreholes under scenarios 1 – 3 are presented in Figure 4.6, while the transient mass balance for each scenario are shown in Figure 4.7.

Chloride is not considered to be of health concern at the levels found in the drinking water and may only affect acceptability of the drinking water (WHO, 2011). Therefore chloride concentrations observed at the monitoring boreholes are considered to be insignificant if the value is less than 1×10^{-10} mg/l, though values that are lower than 1×10^{-5} mg/l are not plotted because of the masking effects of the higher concentrations. The breakthrough curves of the contaminant concentrations at the observation boreholes under scenarios 1 and 2 are lower than 1×10^{-5} mg/l, and therefore not plotted. Only those for scenario 3 are presented in Figure 4.8.

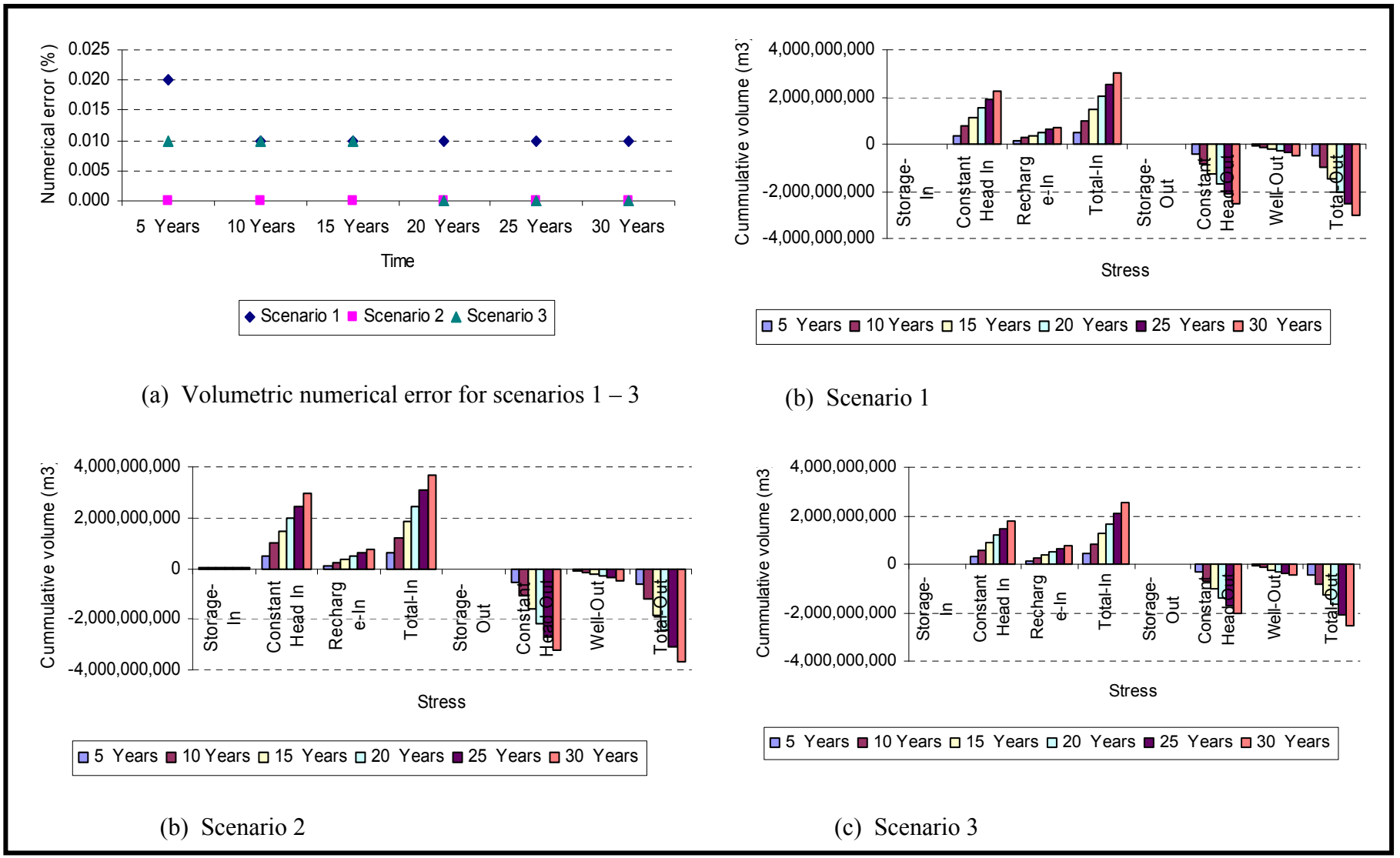

Figure 4.2: Numerical error and volumetric budget for scenarios 1 – 3

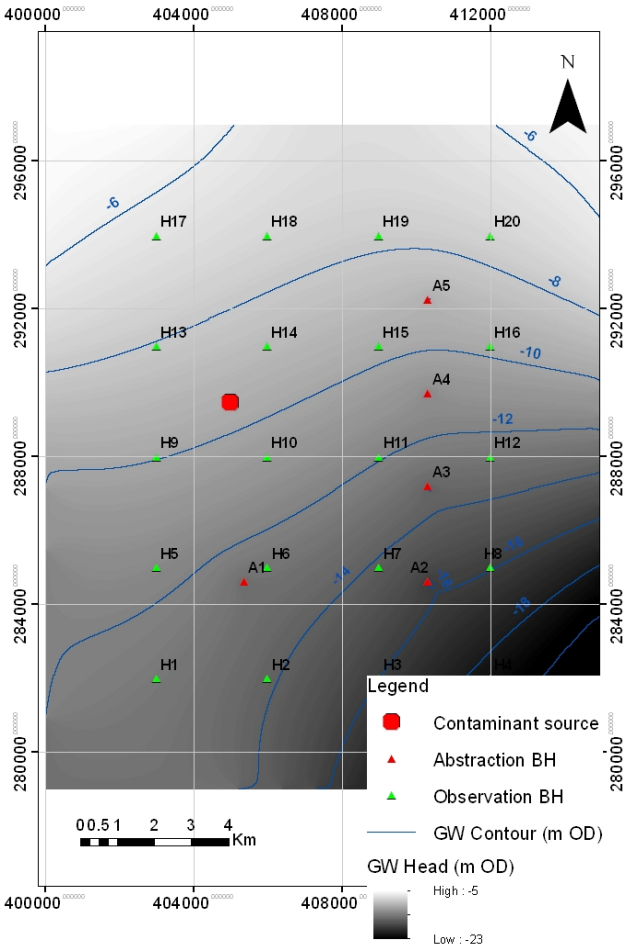

(a) Groundwater head after 30 years of simulation under scenario 1

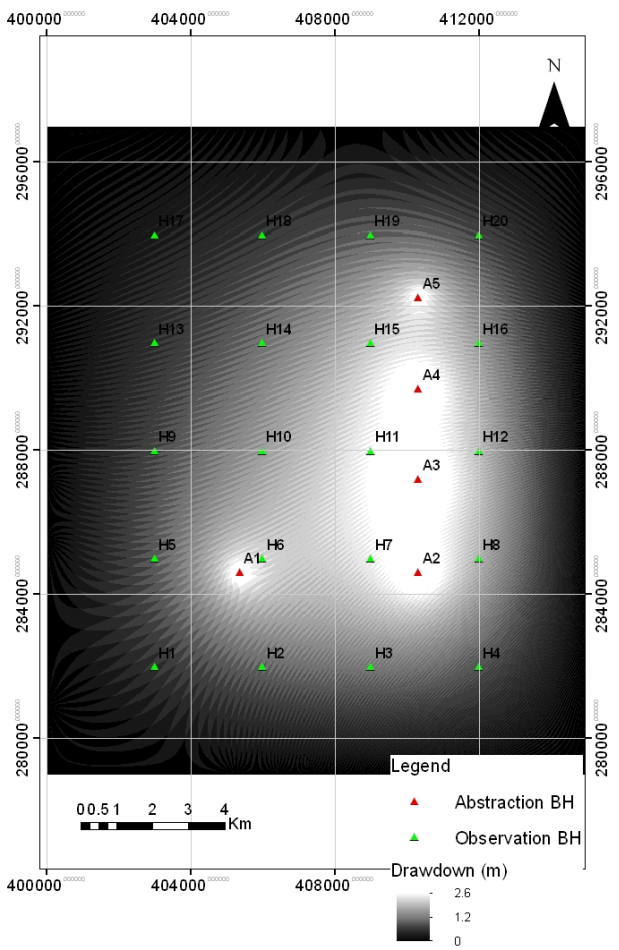

(b) Drawdown values after 30 years of simulation under scenario 1

Figure 4.3: Final groundwater head and drawdown under scenario 1

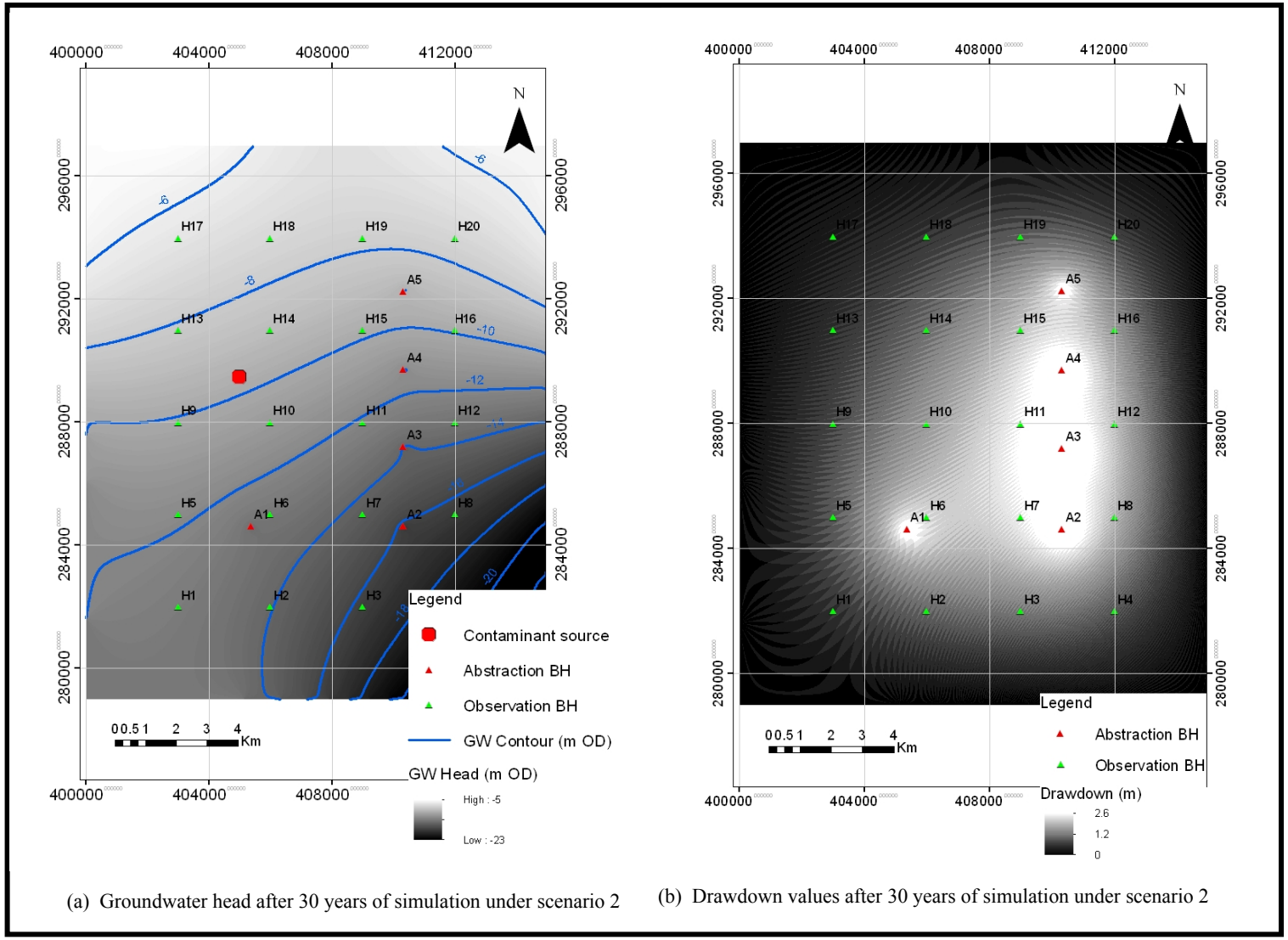

(a) Groundwater head after 30 years of simulation under scenario 2

(b) Drawdown values after 30 years of simulation under scenario 2

Figure 4.4: Final groundwater head and drawdown under scenario 2

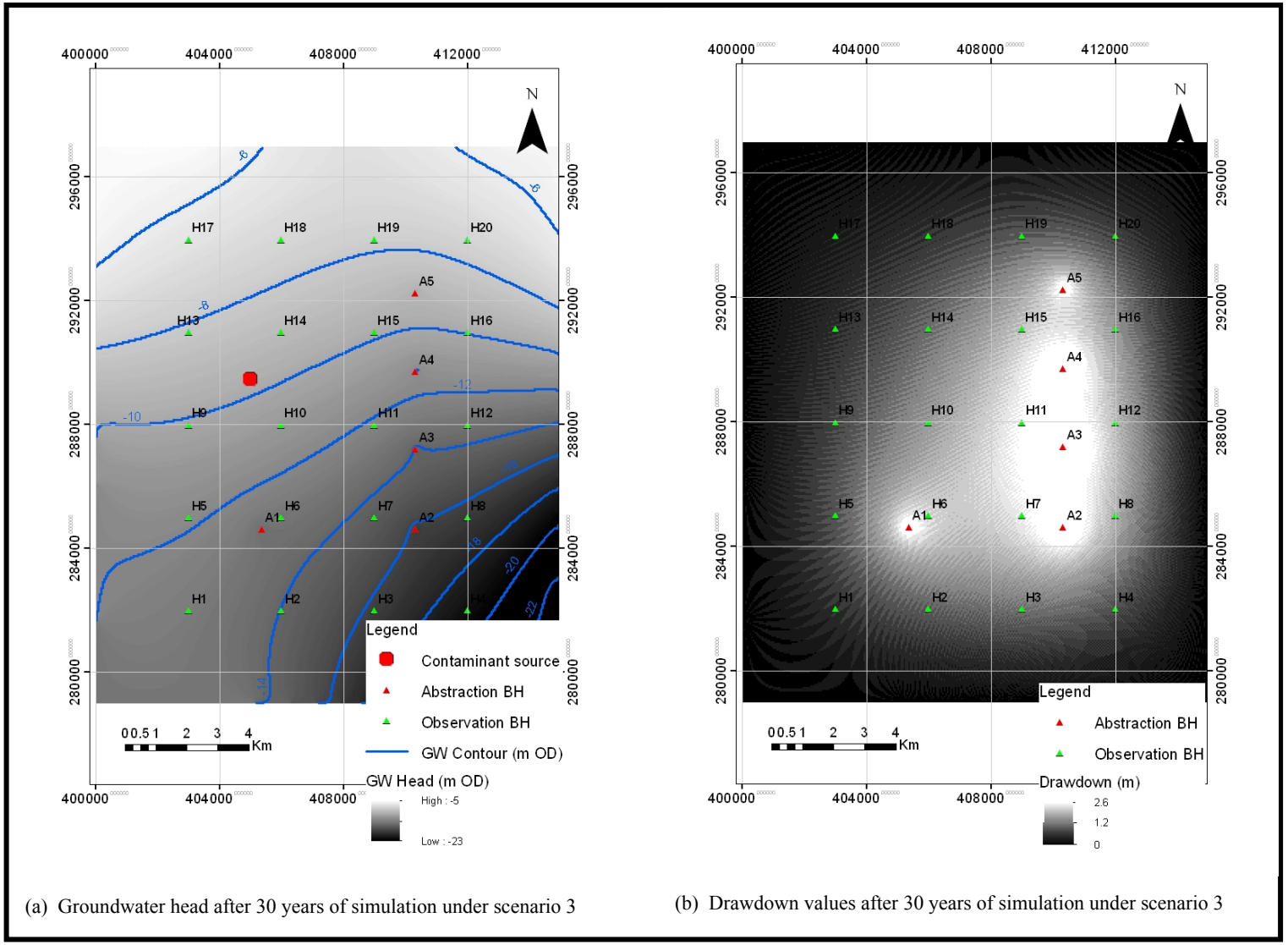

(a) Groundwater head after 30 years of simulation under scenario 3

(b) Drawdown values after 30 years of simulation under scenario 3

Figure 4.5: Final groundwater head and drawdown under scenario 3

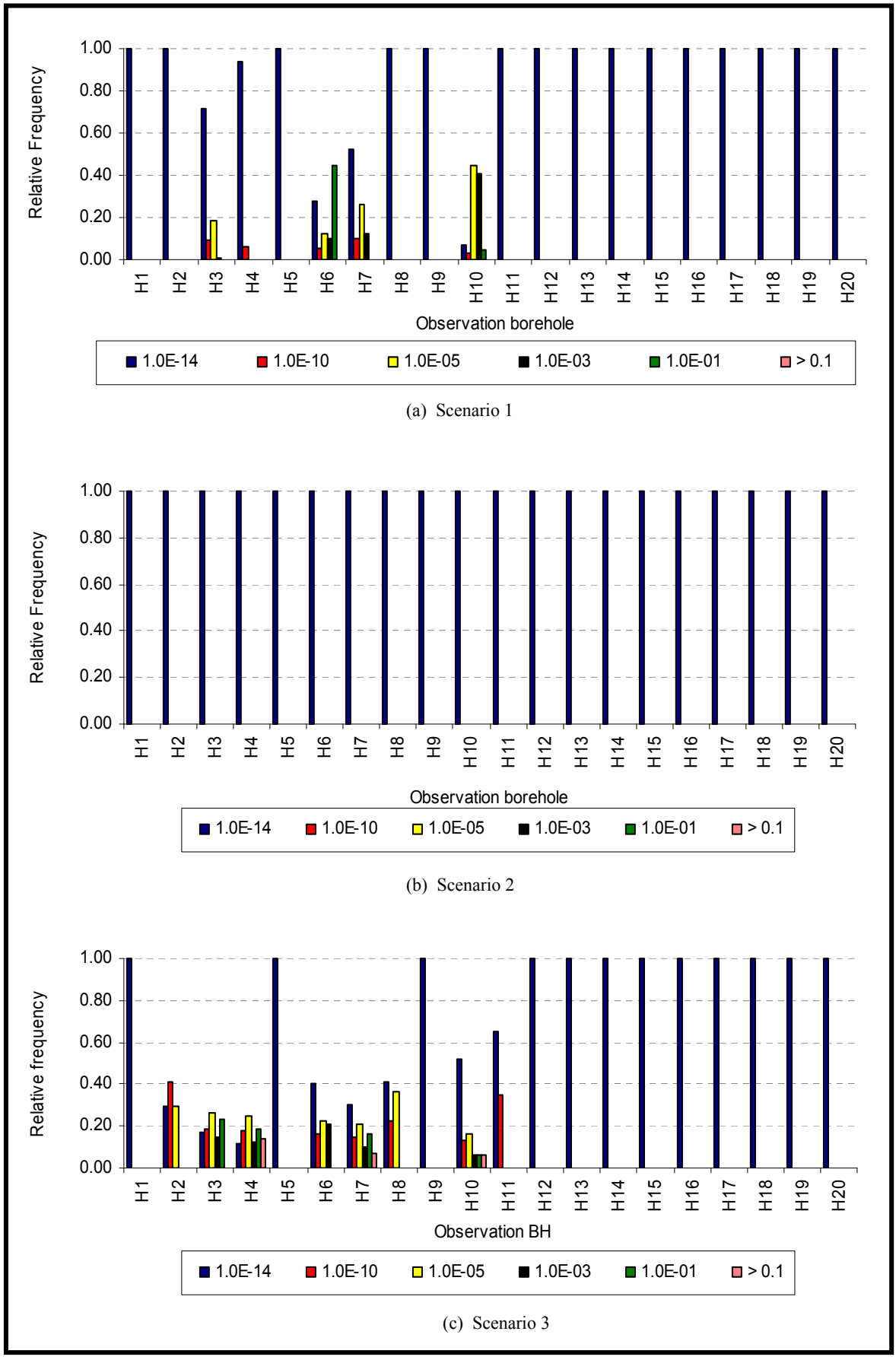

Figure 4.6: Contaminant concentrations (in mg/l) for scenarios 1 - 3

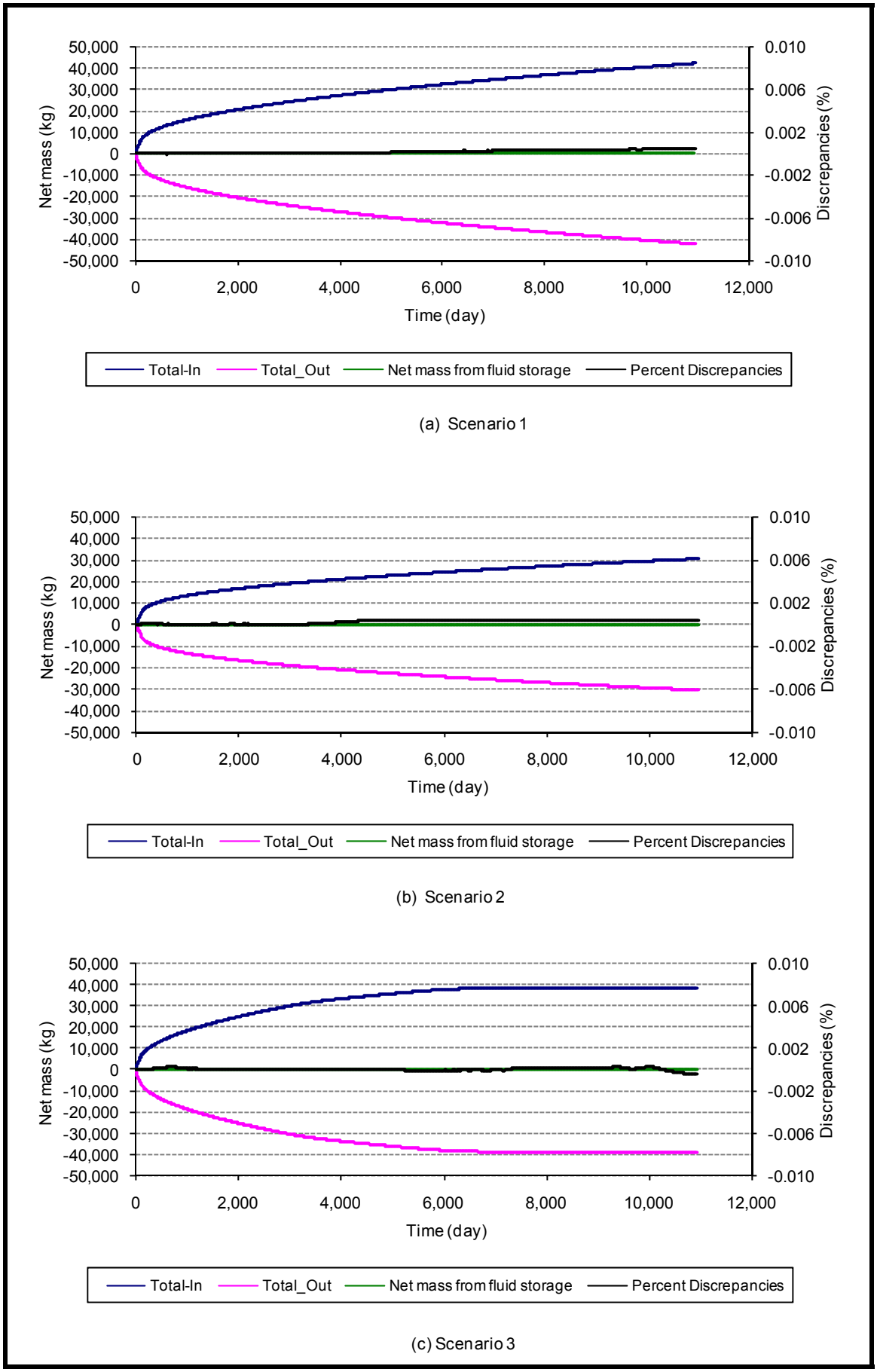

Figure 4.7: Contaminant mass balance for scenarios 1 – 3

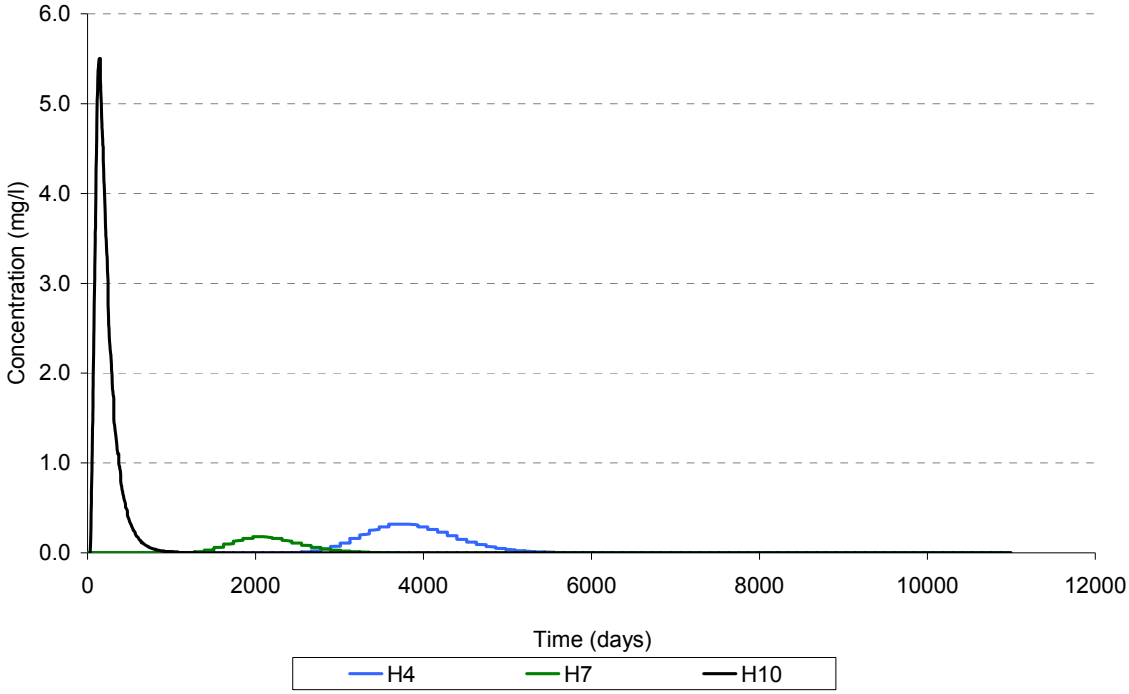

Figure 4.8: Contaminant breakthrough curves under scenario 3

4.3 Assessment of effects of stress periods and loading rates

This section utilizes the use of two hypothetical scenarios (4 and 5) to assess the effects of different mass loading rates of a contaminant on the risk assessment method developed in this work. The MT3DMS transport model represents the contaminant as point sources by specifying the cell indices (i.e. layer, row, and column) of the point source for which a mass or concentration needs to be applied for each stress period and each species. This capability is implemented by the sink and source mixing package of the software. In this work, the sink and source package is generated by the risk model and example of this input package has been presented Figure 3.10. The contaminant source terms are applied only to the first layer because the synthetic contaminant sources are assumed to have been generated at the ground surface.

4.3.1 Hypothetical scenarios for stress periods and loading rates assessment

The stress period is the time interval during which the boundary conditions for external stresses are constant. It simplifies the data entry by only entering values when the boundary conditions change and not for every time step of the model simulation. For

example a recharge rate may be held constant for the complete winter season rather than entered for every day. This implies that at any model cell where pollution source terms are generated by the risk model, the rates at which the contaminant mass are released into the sub-surface environment is defined by the length of the stress period. It is assumed that the pollutant is released uniformly over any given stress period. The two possible approaches that may be incorporated in the implementation the risk assessment method described in this work are presented below.

Approach 1

In the first approach, it is assumed that there are no existing flow and transport models and the risk model is the first to be setup. Therefore, the stress period design for the risk model will be adopted by both the flow and transport models. In which case, the stress periods for the simulation can be setup such that the length of the time spans are each defined to have exact overlap with the periods during which the contaminant discharge occurred, and larger or smaller stress periods are used when no discharges occurred during the simulation. For example, assuming historical records show 3 discrete discharges of contaminant mass of 450 kg each on 1st March, 13th June and 17th September of a particular year. For a simulation period of 365 days, and 10 stress periods, then under this approach, the model could be designed with 10 stress periods as shown in Table 4.3. In this case, the stress periods are designed such that a day is used to represent periods when there are pollution incidents and longer time periods (in days) are used to represent time span during which no discharge occurred. This causes the whole contaminant mass of 450 kg to be released into the subsurface on each day of the pollution. An example of risk model input file that uses this approach is presented in Figure 3.4a.

Approach 2

In the second approach, it is assumed that there are existing flow and transport models to which a new risk model is designed to be integrated into. Under this approach, the number and length of stress period for the risk model will be adopted from the existing flow and transport models. Assuming the same scenario for pollution incident presented for Approach 1, an example of the second approach is also presented in Table 4.3, where the rate of loading of contaminant mass is distributed across the entire length of the corresponding stress period. An example of risk model input file that uses this approach is presented in Figure 3.4b.

The first approach presents a scenario where a large mass of contaminant is loaded into the aquifer within a short period of time, while the second approach presents another scenario where the same mass of contaminant is loaded into the same aquifer over a longer period of approximately 36 days. The effects of the mass loading rate on the concentrations and travel time of contaminant observed at monitoring points are further considered in the following sections.

Table 4.3: Example of varying loading rate of contaminant mass

No of stress period	Stress Period start data	Stress Period end data	Length of stress period (days)	Mass loading rate (kg/day)	Comment
Approach 1					
1	01-Jan	28-Feb	59		
2	01-Mar	01-Mar	1	450	Pollution event on this day
3	02-Mar	30-Apr	60		
4	01-May	12-Jun	43		
5	13-Jun	13-Jun	1	450	Pollution event on this day
6	14-Jun	31-Jul	48		
7	01-Aug	16-Sep	47		
8	17-Sep	17-Sep	1	450	Pollution event on this day
9	18-Sep	31-Oct	44		
10	01-Nov	31-Dec	61		
Approach 2					
1	01-Jan	14-Feb	45		
2	14-Feb	22-Mar	36	12.50	Pollution event within this period
3	22-Mar	27-Apr	36		
4	27-Apr	02-Jun	36		
5	02-Jun	08-Jul	36	12.50	Pollution event within this period
6	08-Jul	13-Aug	36		
7	13-Aug	18-Sep	36	12.50	Pollution event within this period
8	18-Sep	24-Oct	36		
9	24-Oct	29-Nov	36		
10	29-Nov	31-Dec	32		

4.3.2 Setting up of the hypothetical scenarios for loading rate assessment

This section assesses the effects of the choice of stress periods and loading rates on the travel time and contaminant concentrations at monitoring points within the aquifer. Two hypothetical models (respectively referred to as scenario 4 and scenario 5) were setup based on the initial conditions presented in Table 4.1. The purpose is to demonstrate the effects of the two approaches described in Section 4.3.1 on the risk assessment method.

The differences between scenario 4 and scenario 5 are the length and number of stress periods i.e. *tspnumber,* and consequently different loading rates, as well as the number of time steps per stress period used to represent the same length of simulation of 30 years. In addition, the integrated flow and transport models (see Table 4.1) also incorporates risk model to generate initial contaminant source mass based on the algorithm presented in appendices A1.2 and A1.3.

4.3.3 Description of risk model runs for the loading rate hypothetical scenarios

The risk model in each scenario (4 and 5) is setup to generate temporal contaminant source terms over the same period of 30 years as the flow model, and then the generated sources are transported within subsurface groundwater environment using transport model over the same period of 30 years. The flow model input files for the scenarios are presented in appendices A4.1 – A4.16. The number of times at which threshold contaminant concentration magnitudes is exceeded, as well as the spatial and temporal distributions of the contaminant concentrations observed at pre-defined monitoring boreholes are assessed.

The execution of the risk model requires three input files namely ***ram1_input_file.dat***, ***advance_flag.dat***, and ***ram1_files.dat***. These files have already been described in Section 3.4. The local model grid (see Section 3.3.3) is set to equal to 74 rows and 130 columns. The maximum number of sources where pollution can potentially occur in any of the stress periods is 10, and they are represented as S1 – S10 in Figure 4.16. The row and column numbers for the local grid for the 10 potential sources under scenarios 4 – 5 are presented in Table 4.4. The global grid numbers that correspond to row 1 and column 1 of the local grid numbers under the scenarios are also included in Table 4.4, and these values were used by the risk model to convert the local grid references into global references for

transport simulations. The risk model input data for scenarios 4 and 5 are presented in appendices A2.1 – A2.3, and summarised in Table 4.5. The table shows that scenarios 4 and 5 consist of 929 and 120 stress periods, respectively (Figure 4.9). The previous number (or historical frequency) of pollution occurrence varies with the stress periods (see appendix A2.1).

The outputs of the risk model are presented in appendices A3.1 – A3.3, and these include the model output file (***ram1_output_file.dat***), frequency of the generated daily source terms (***ram1_distribution.dat***), and the synthetic source terms for transport model ***(ram1.ssm***). The detailed descriptions of these files are already presented in Section 3.5.2. The ***ram1.ssm*** contains generated source terms in a format that feeds directly into the transport model (see appendix A3.3).

Table 4.4: Location of potential pollution sources

Location ID	Local source grid system				Global source grid system	
					[Global row 1 / column 1 equivalent:301/201]	
	Easting	Northing	Row	Col	Row	Col
S1	405006	289481	17	30	317	230
S2	405193	289481	17	40	317	240
S3	405343	289481	17	50	317	250
S4	405568	289481	17	60	317	260
S5	405868	289481	17	70	317	270
S6	406093	289481	17	80	317	280
S7	406318	289481	17	90	317	290
S8	406506	289481	17	100	317	300
S9	406731	289481	17	110	317	310
S10	406956	289481	17	120	317	320

Table 4.5: Summary of risk model input data for scenarios 4 and 5

Record Number	Record	Record Value
File Name: *ram_input_file.dat*		
A1	*title_1*	HYPOTHETICAL SIMULATIONS
A2	*title _2*	SCENARIOS 4 AND 5
A3	*Layer, nrow, ncol*	1 74 130
A4	*tspnumber, itype, previousmult, min_mult, max_mult*	929 15 1 1.0 1.0 (Note: Sc 5 has 120 stress periods and not 929)
A5	*fwel, fdrain, frch, fevt, friv, fghb*	F F T F F F
A6	*Incrch, rarray1, buffer*	1 0 0.0
A7	*global_row, global_col*	See Table 4.5
A8	*spnumber, splength*	Stress period number and varied length are assigned to each stress period (see appendix A2.1)
A9	*npsource, nprevious*	10 number of potential sources per stress period. Varied frequency of pollution occurrence assigned to each stress period (see appendix A2.1)
A10	*sorrow, sorcol*	Row and column for each of the potential source in each stress period (see appendix A2.1)
A11	*min_mass, max_mass*	Minimum and maximum values of contaminant mass loading rate assigned to each potential source in each stress period (see appendix A2.1)
B1	***File Name: advance_flag.dat***	2D array with integer values between 0 and 5 (see appendix A2.2)
C1	***File Name: ram_files.dat***	funit, fname, fstatu (see appendix A2.3)

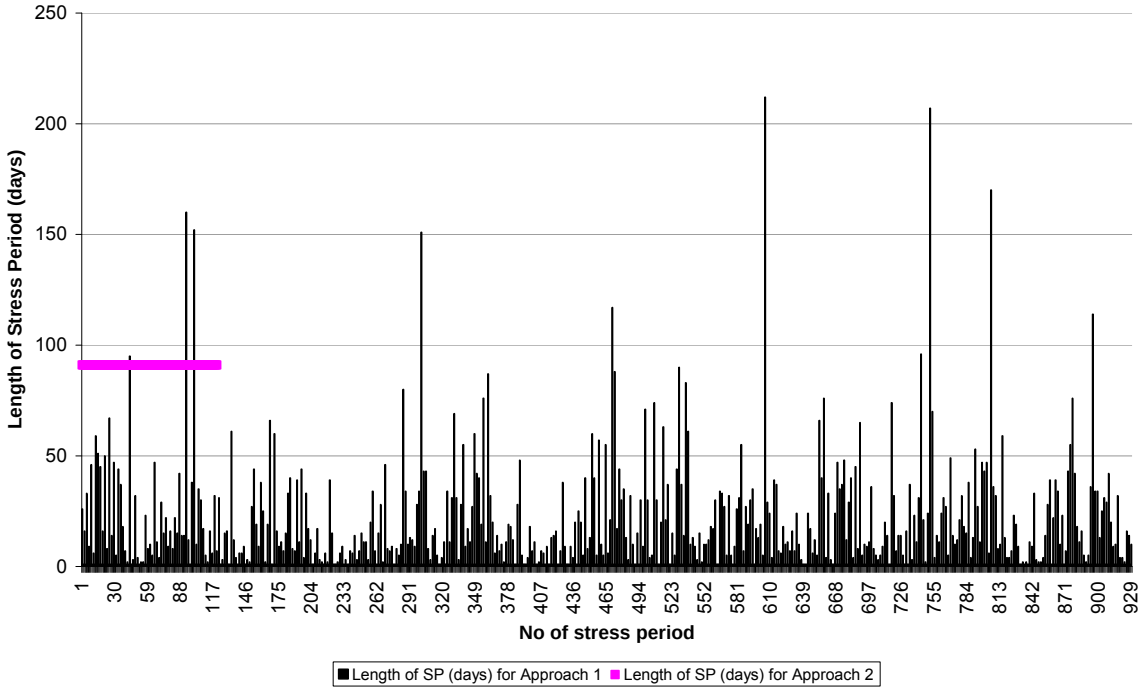

Figure 4.9: Stress periods for Approach 1 and Approach 2

4.3.4 Results of the hypothetical model run for loading rate assessment

The outputs of the flow, risk and transport models are presented as follow:

4.3.4.1 Results of the flow model run for scenarios 4 and 5

The volumetric balance error obtained for scenarios 4 – 5 are presented in Figure 4.10 (a,b). The summary of the volumetric budget for the model setup for the simulation period of 30 years is presented in Figure 4.10 (c and d). The groundwater head and drawdown distributions are obtained directly as model outputs, and the values within the layer at the end of the simulation (30 years) are presented in Figures 4.11 and 4.12, respectively for scenarios 4 and 5.

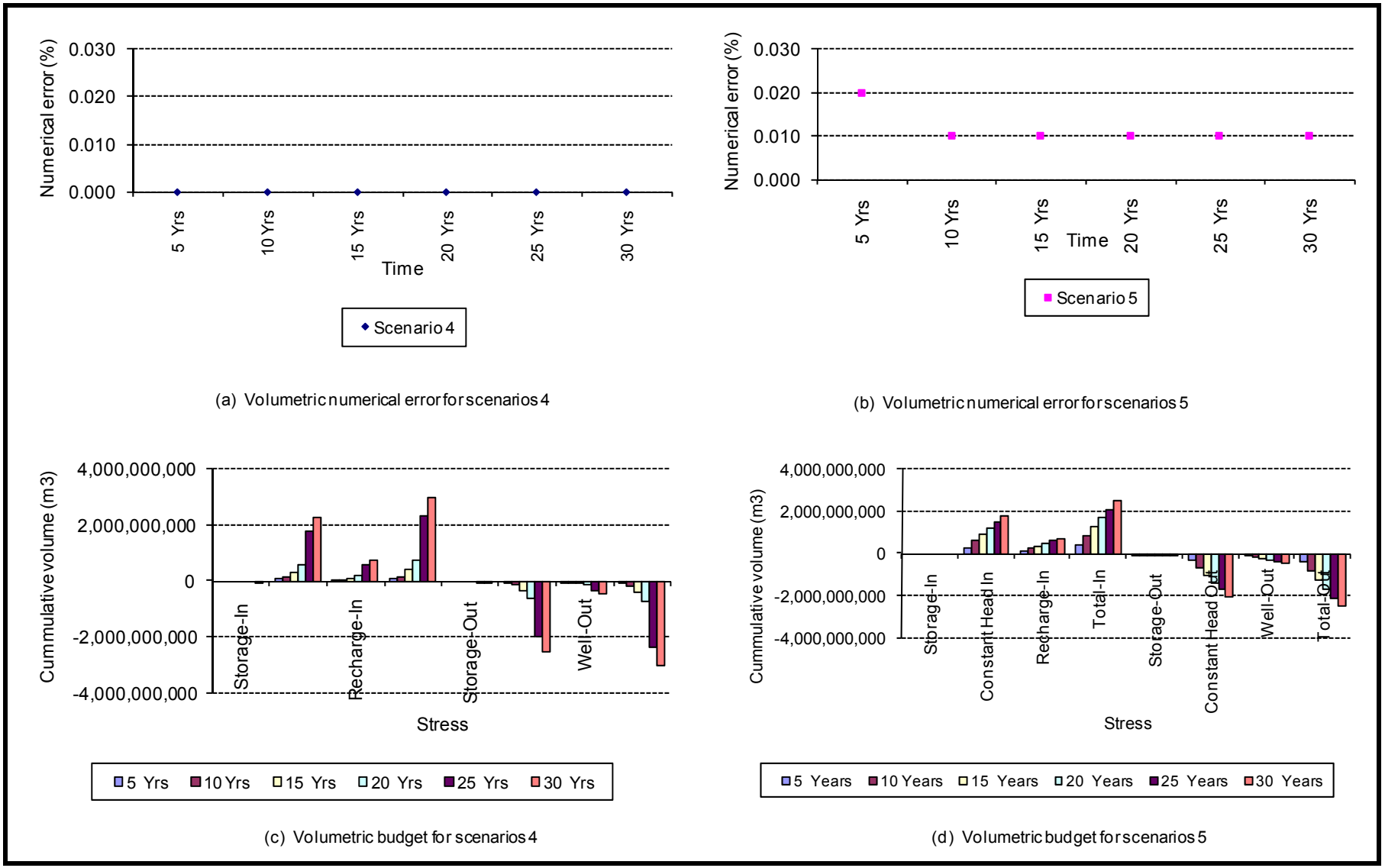

Figure 4.10: Numerical error and volumetric budget for scenarios 4 and 5

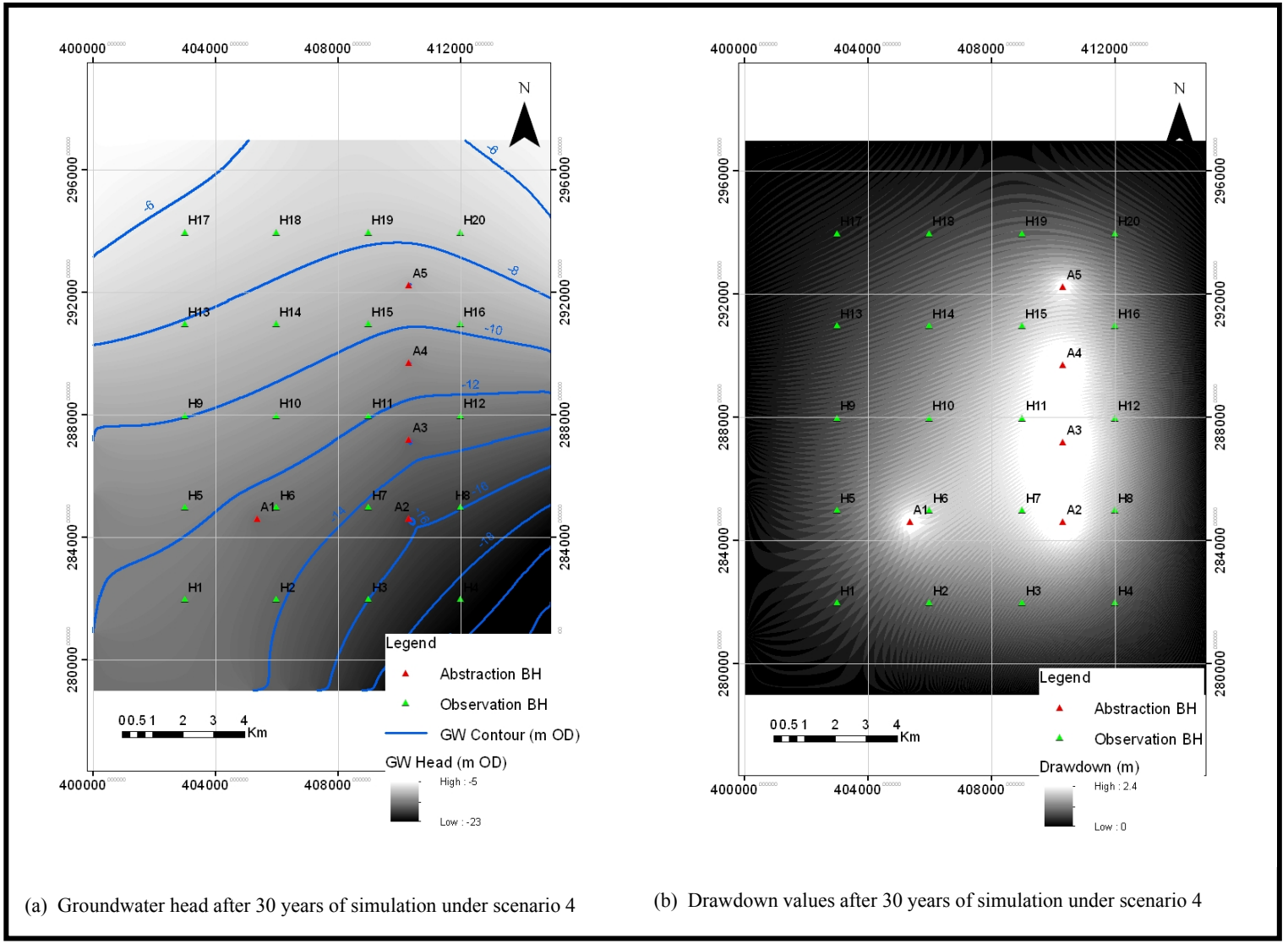

(a) Groundwater head after 30 years of simulation under scenario 4

(b) Drawdown values after 30 years of simulation under scenario 4

Figure 4.11: Final groundwater head and drawdown under scenario 4

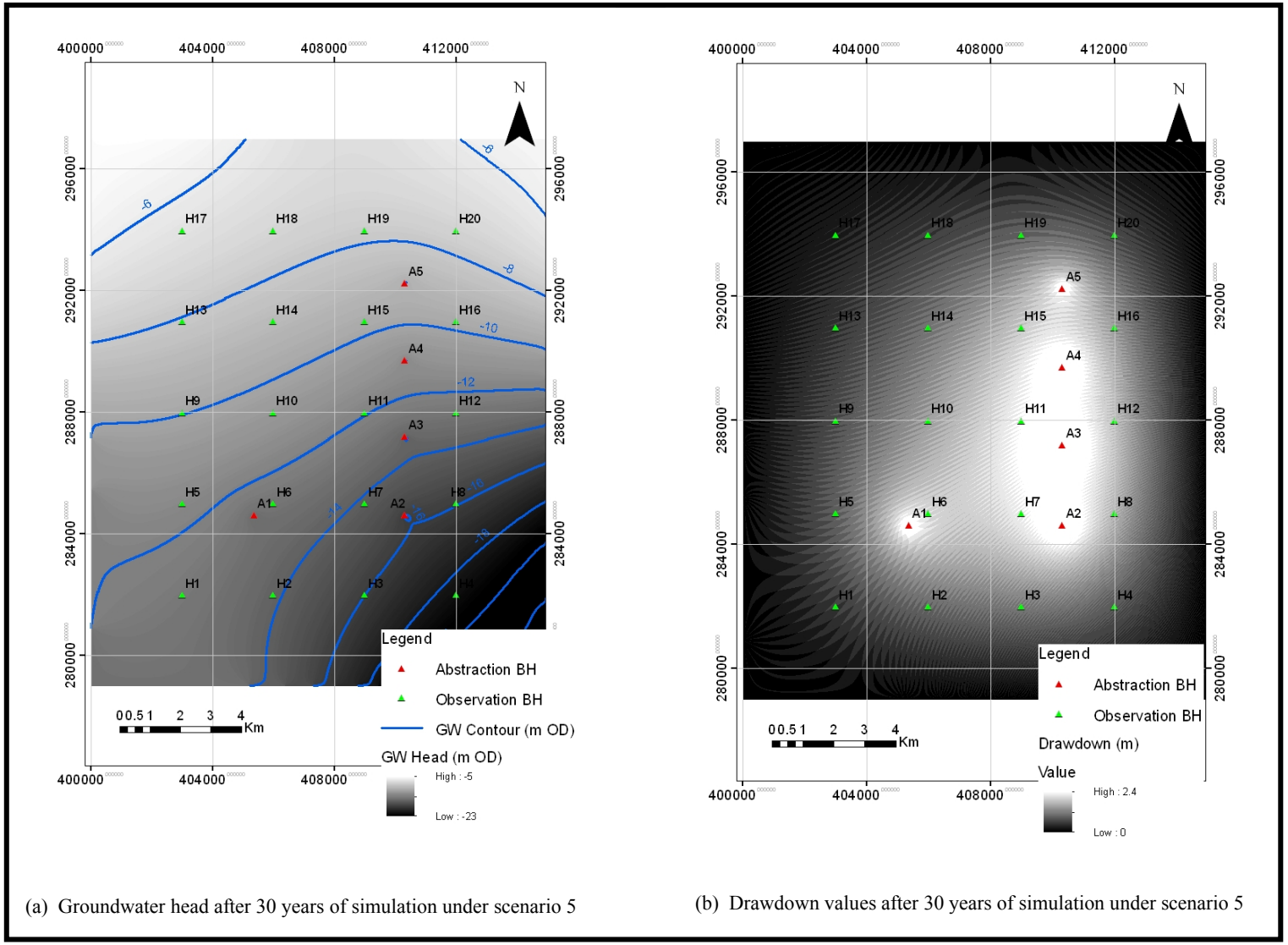

(a) Groundwater head after 30 years of simulation under scenario 5

(b) Drawdown values after 30 years of simulation under scenario 5

Figure 4.12: Final groundwater head and drawdown under scenario 5

4.3.4.2 Results of the risk and transport model run for scenarios 4 and 5

The frequency distribution of the occurrence of pollution events for the hypothetical scenarios 4 – 8 are presented in Figure 4.13. The ranges of values of contaminant concentrations simulated at the 20 observation boreholes under scenarios 4 and 5 are presented in Figure 4.14 while the mass balance are presented in Figure 4.15. The spatial distributions of the contaminant after 30 years of simulation are presented in Figure 4.16. Also, the breakthrough curves of the contaminant concentrations at the observation boreholes are presented in Figure 4.17.

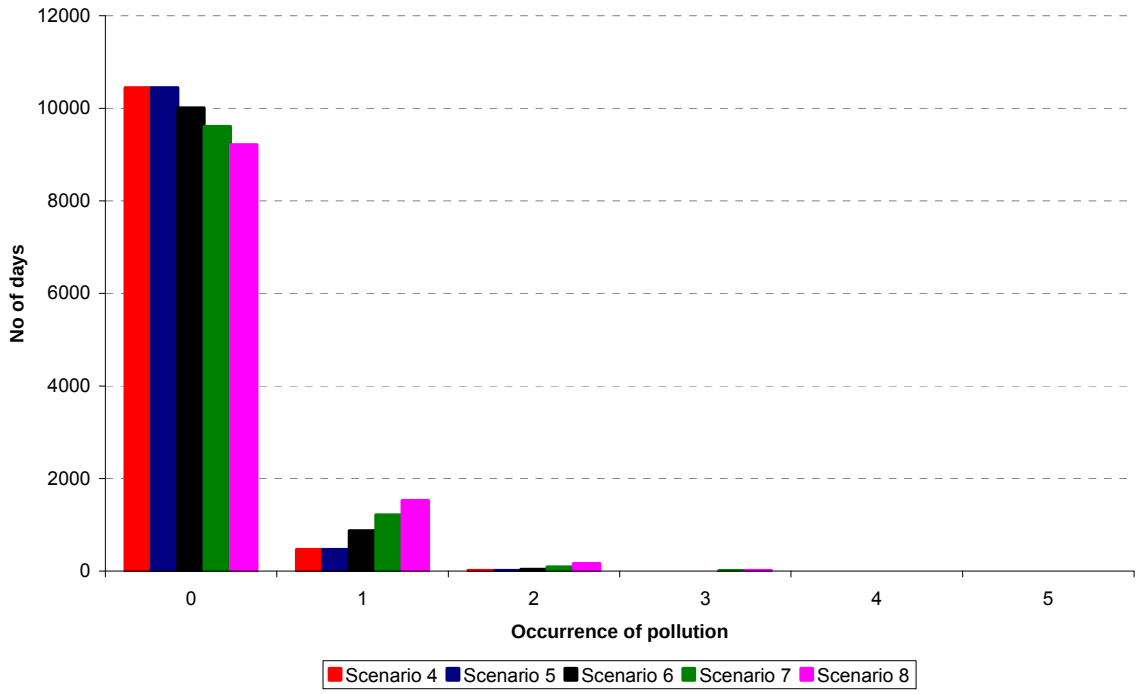

Figure 4.13: Source terms generated during the hypothetical scenarios

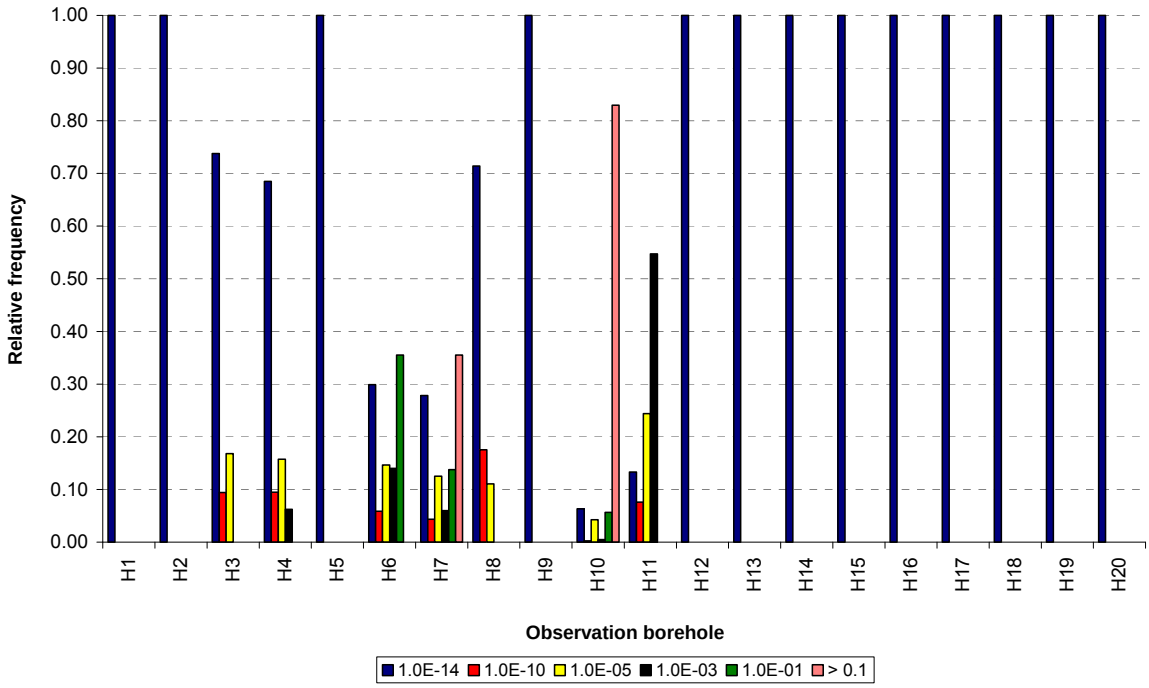

(a) Scenario 4

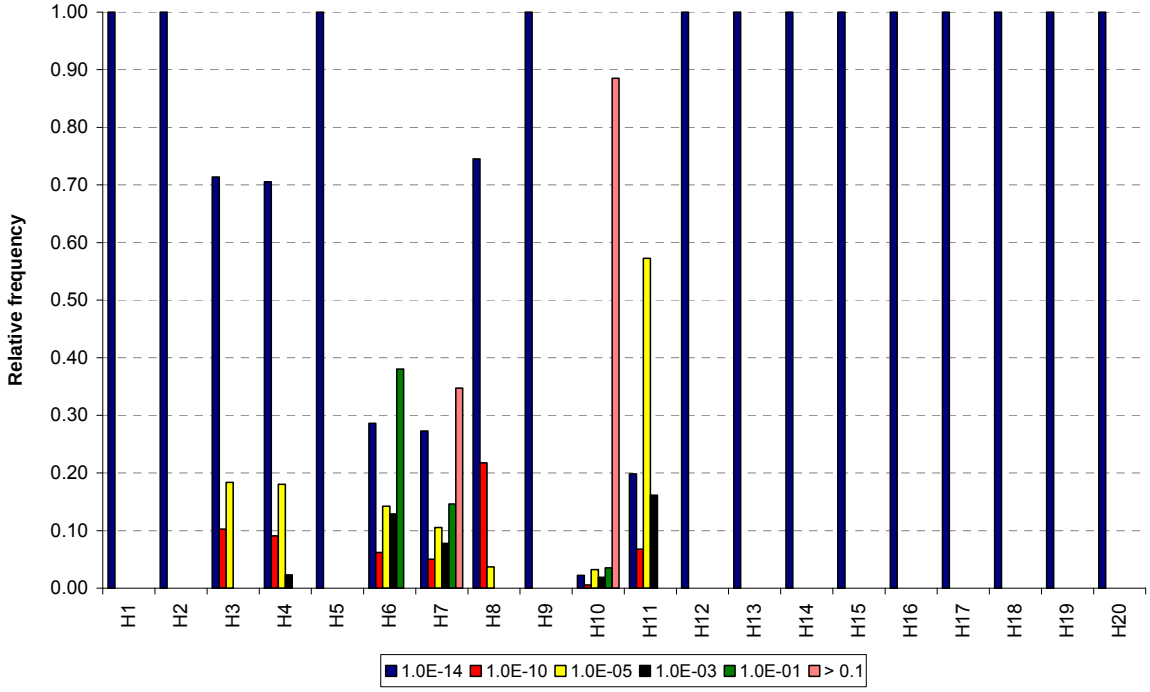

(b) Scenario 5

Figure 4.14: Contaminant concentrations (in mg/l) for scenarios 4 and 5

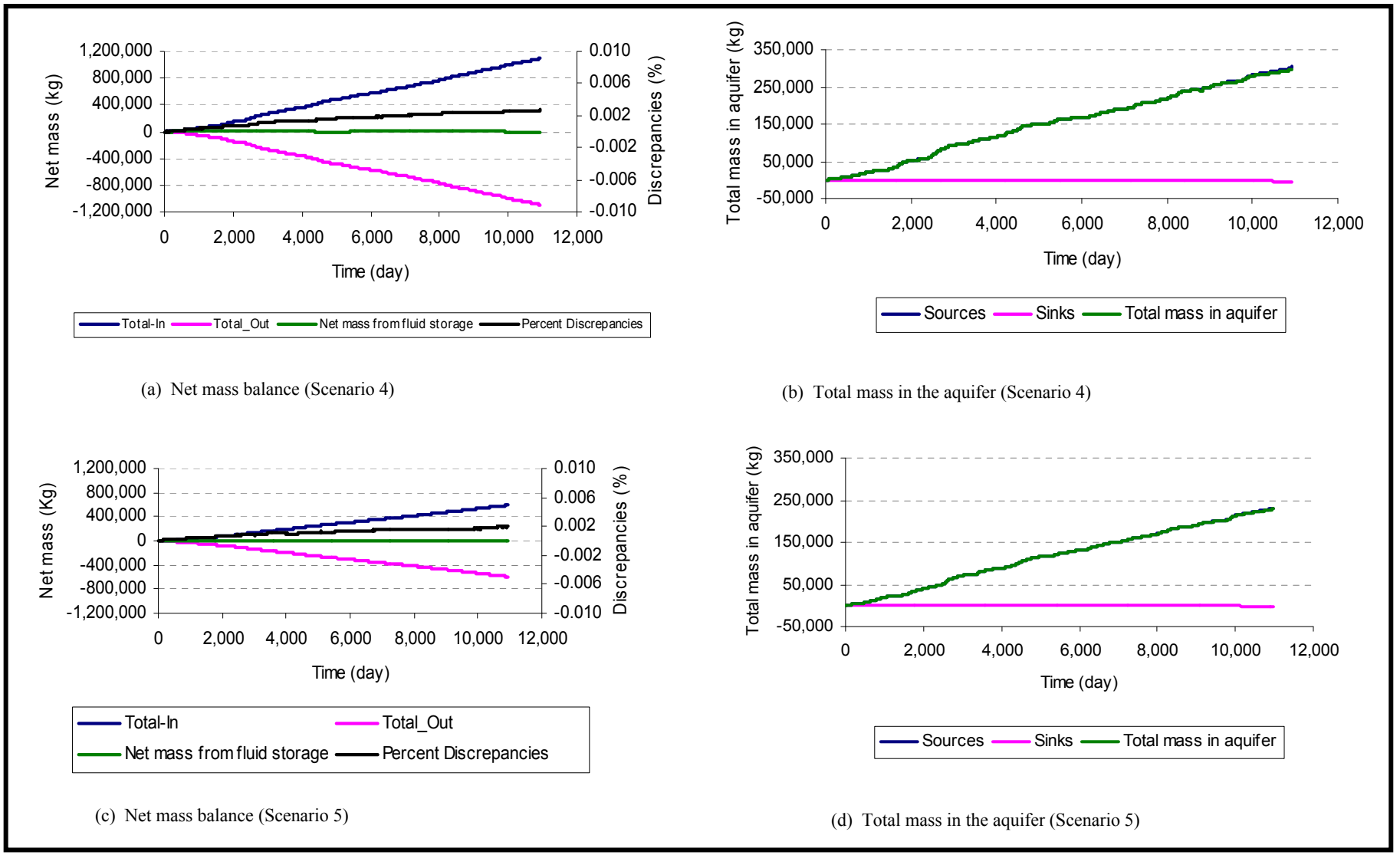

Figure 4.15: Contaminant mass balance for scenarios 4 - 5

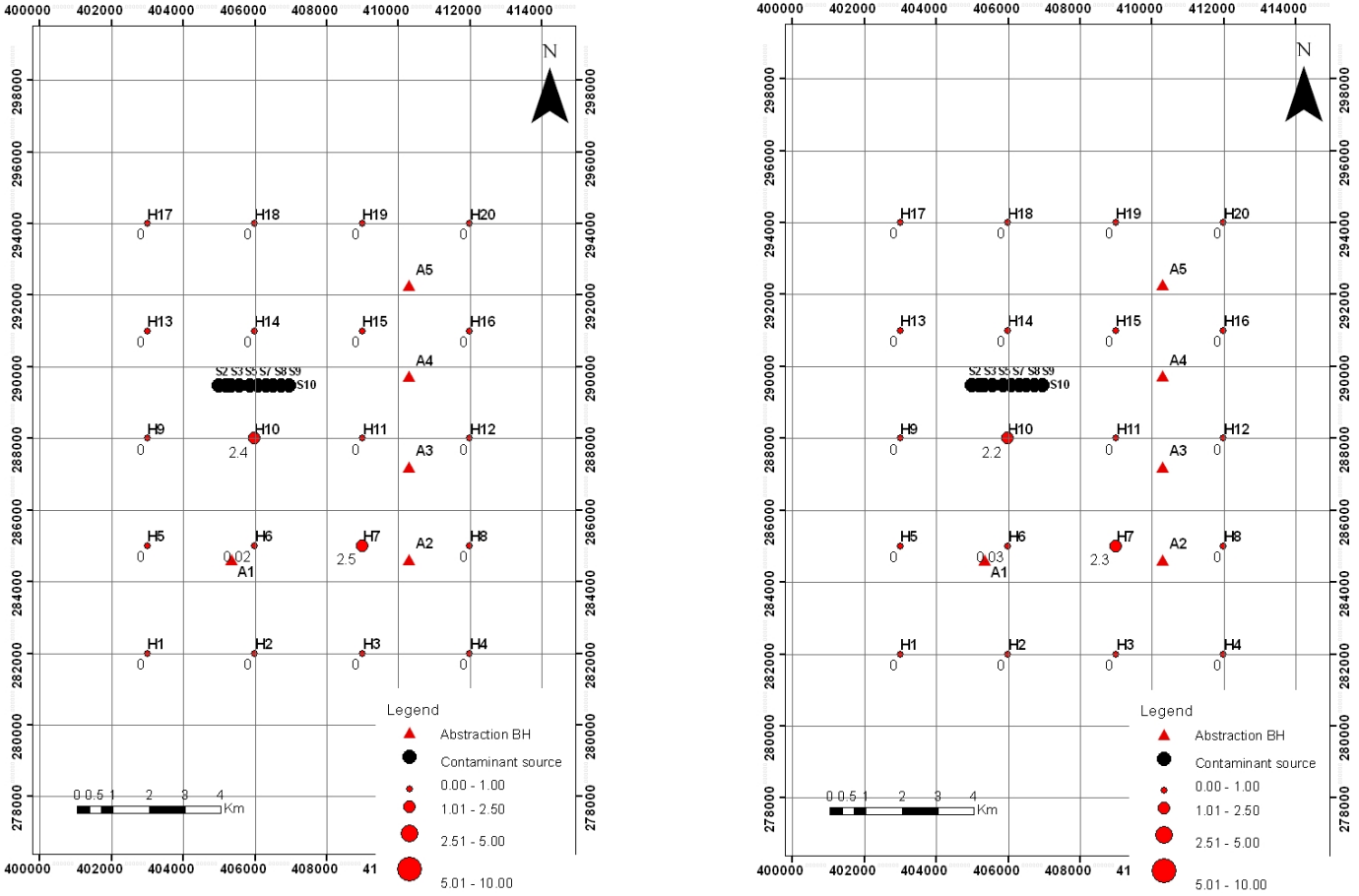

(a) Scenario 4

(b) Scenario 5

Figure 4.16: Contaminant distribution at the end of the simulation for scenarios 4 and 5.

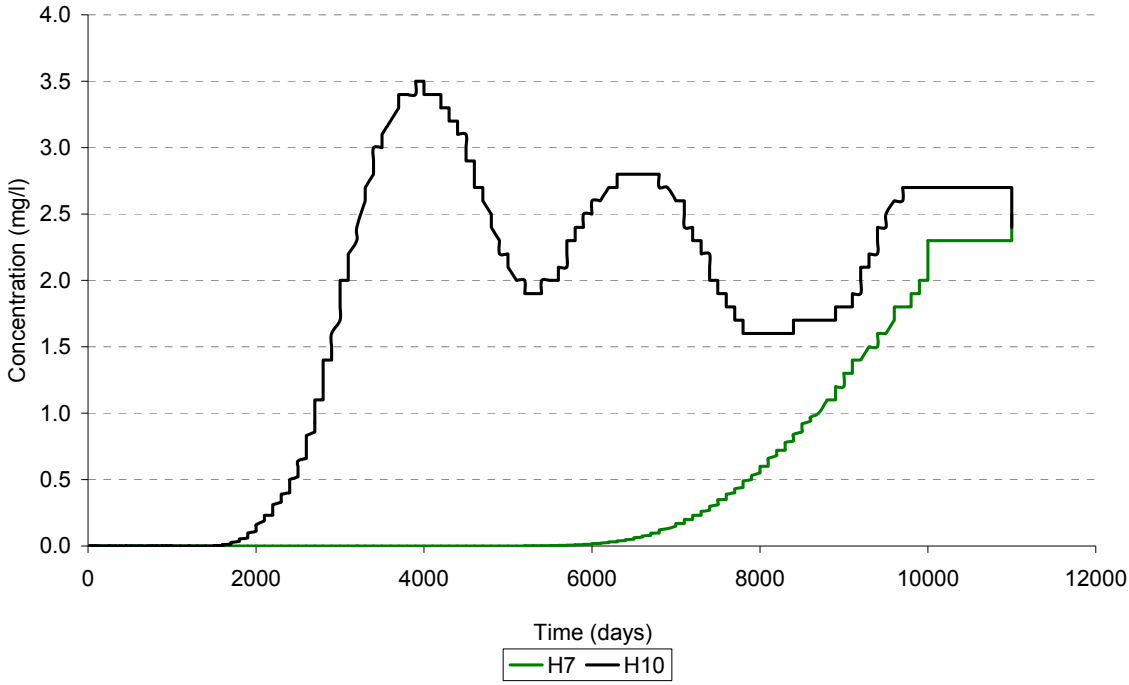

(a) Scenario 4

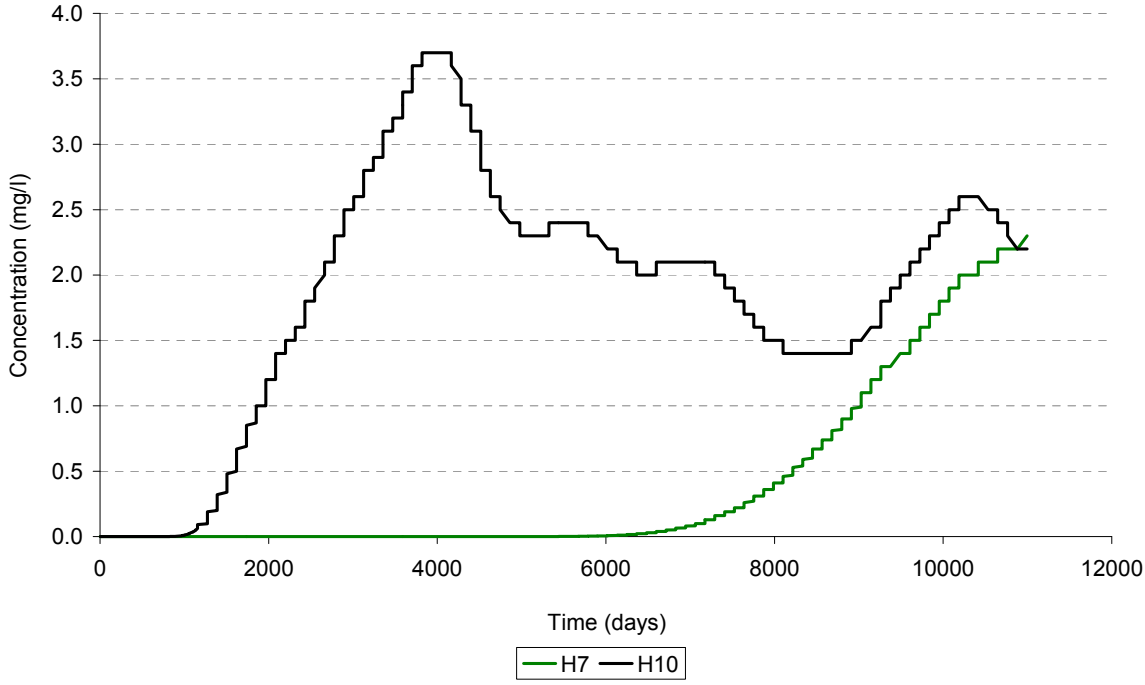

(b) Scenario 5

Figure 4.17: Contaminant breakthrough curves under scenarios 4 and 5

4.4 Evaluation of the probability of occurrence of pollution

The effect of the influence of the probability of occurrence of pollution incidents on the risk assessment method is assessed using three additional scenarios (6 – 8) where the number of previous occurrences (or historical frequency) of pollution incidents is progressively increased. The hypothetical model used in scenario 5 forms the baseline scenario and the number of historical occurrences of pollution incidents is progressively increased by multiplying the values for scenario 5 by two, three and four, to obtain corresponding values for scenarios 6, 7 and 8 respectively. The risk model output files for scenarios 6 – 8 are presented in appendices A5 – A7, respectively.

The flow model setup for scenario 5 was used for these scenarios (6 – 8). With the exception of the number of previous occurrence of pollution incidents, the input data for the risk model is the same as that presented in Table 4.5. The flow and transport models are setup based on the input data presented in Table 4.1. The daily source term frequency outputs of the risk model for scenarios 6 – 8 are already presented in Figure 4.13. The ranges of the values of contaminant concentrations simulated at the 20 observation boreholes under scenarios 6, 7 and 8 are presented in Figure 4.18, while the mass balance for the scenarios are also presented in Figure 4.19. The spatial distribution of the contaminant after 30 years of simulation under scenarios 6 – 8 are presented in Figure 4.20. The breakthrough curves of the contaminant concentrations at the 20 observation boreholes are presented in Figure 4.21.

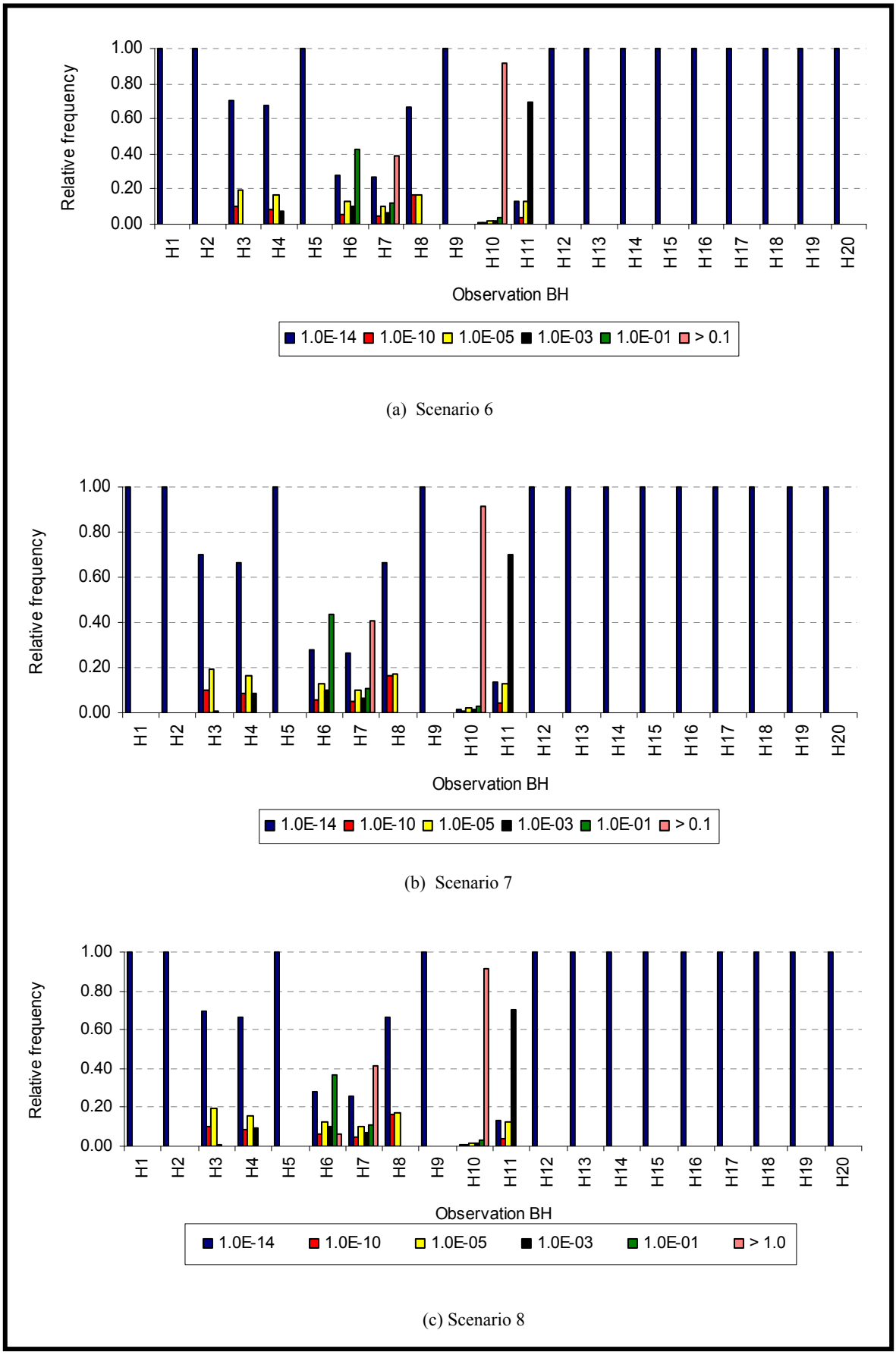

Figure 4.18: Contaminant concentrations (in mg/l) for scenarios 6 - 8

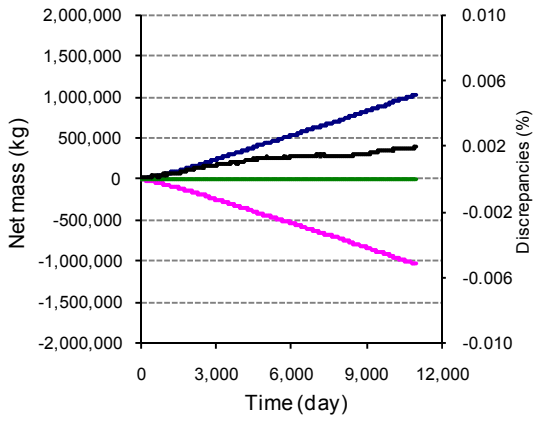

(a) Net mass balance for scenario 6

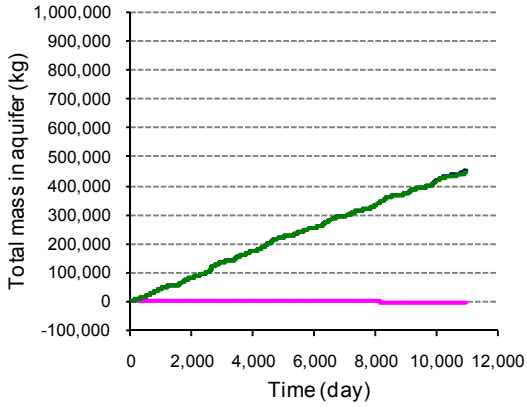

(b) Total mass in the aquifer for scenario 6

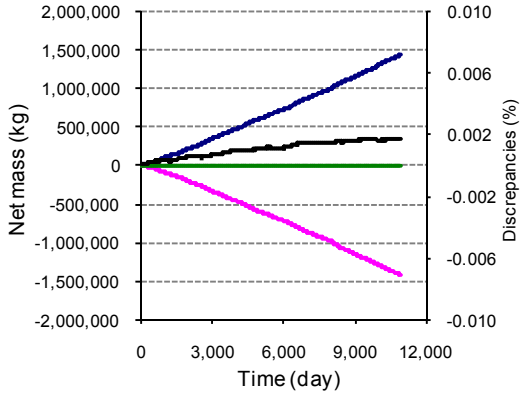

(c) Net mass balance for scenario 7

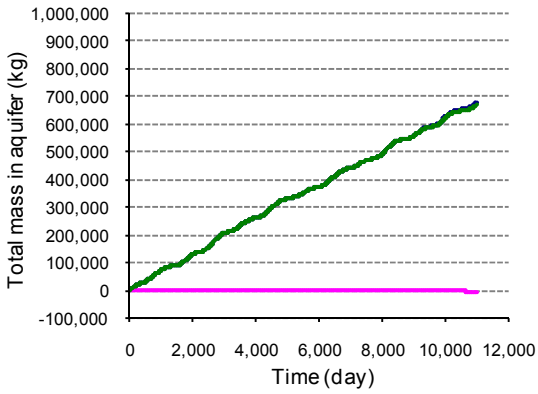

(d) Total mass in the aquifer for scenario 7

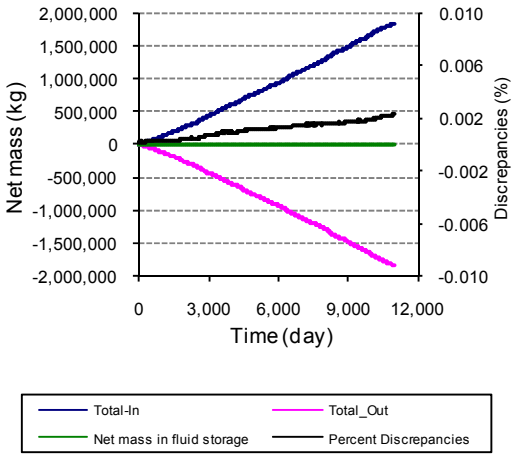

(e) Net mass balance for scenario 8

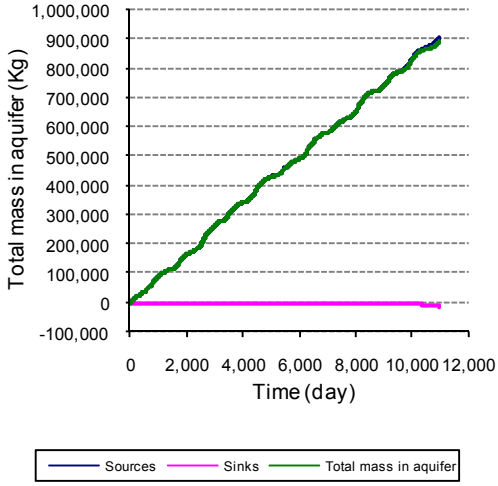

(f) Total mass in the aquifer for scenario 8

Figure 4.19: Mass balance for scenarios 6 - 8

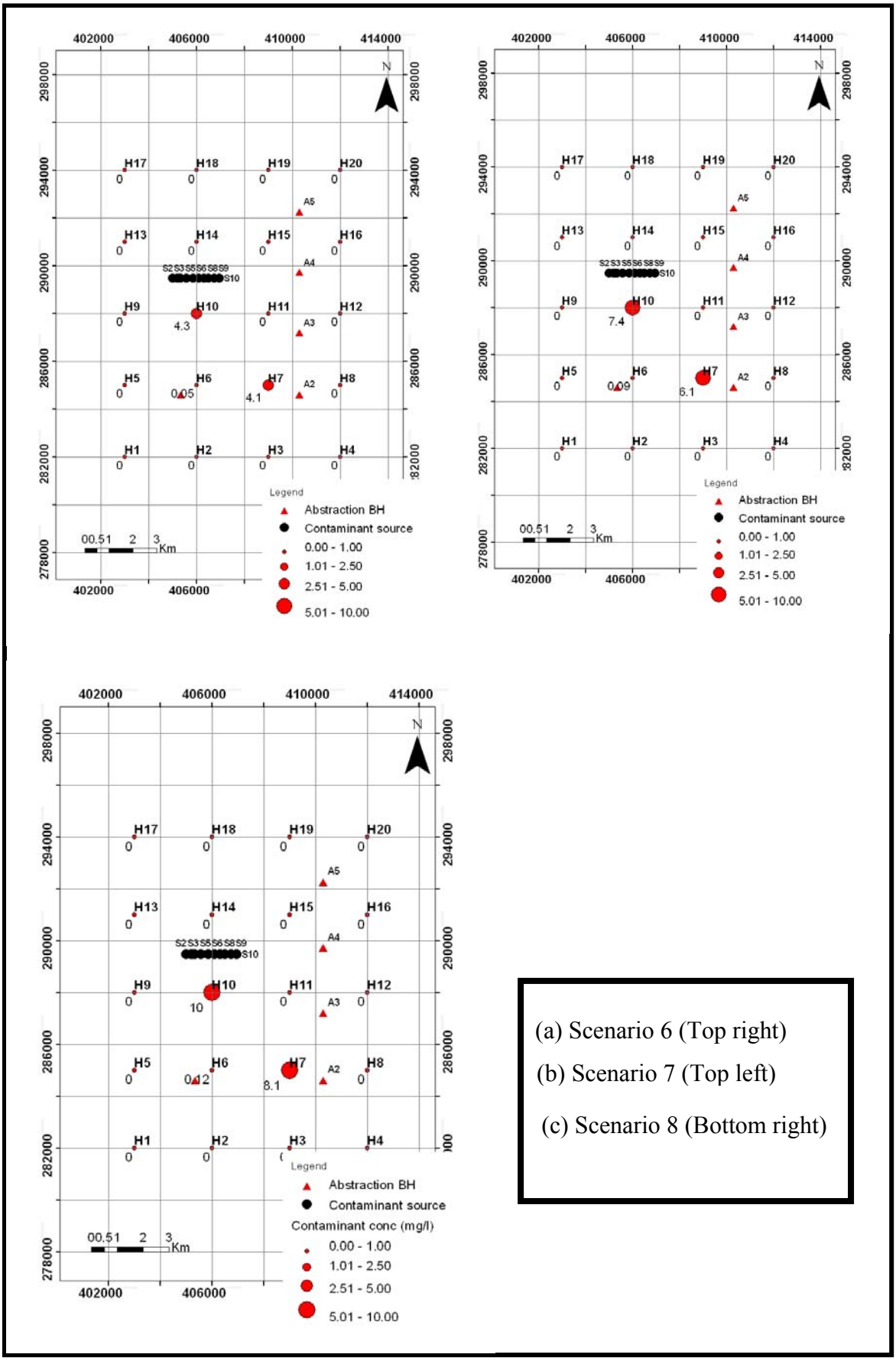

(a) Scenario 6 (Top right)

(b) Scenario 7 (Top left)

(c) Scenario 8 (Bottom right)

Figure 4.20: Contaminant distribution at the end of the simulation for scenarios 6 - 8

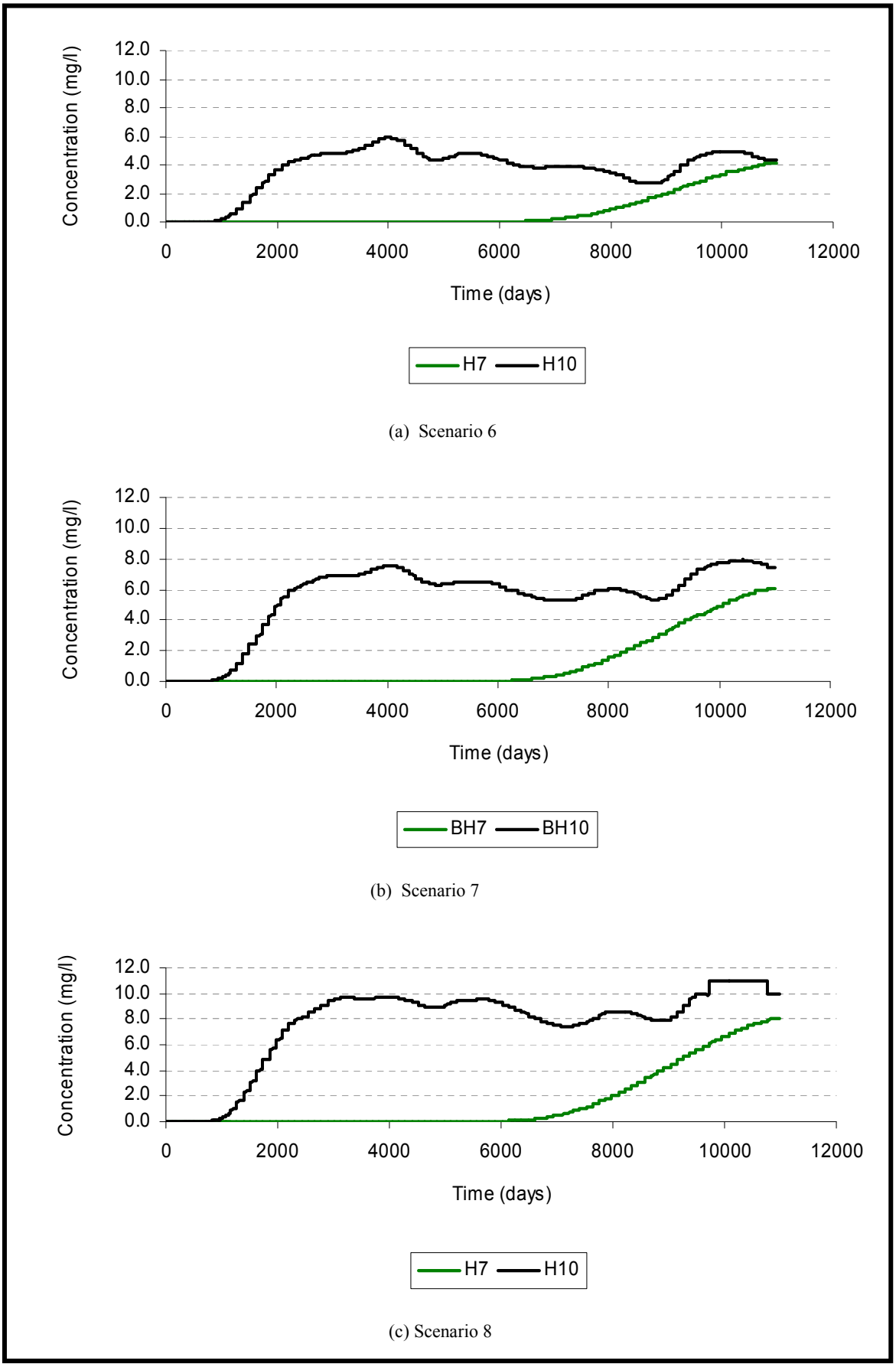

Figure 4.21: Contaminant breakthrough curves under scenarios 6 – 8

4.5 Assessment of impact of source terms on groundwater resource

The assessment of risk to groundwater resource is demonstrated using scenario 5 by repeating the simulation for 100 times, and then observing the distribution of contaminant concentrations at the observation boreholes. The sensitivity of the results to the number of iterations was accessed by carrying out sensitivity analysis of the number of iteration on the variability of the simulation output. The number of iteration was increased gradually from 1 to 200, and the exceedance values were assessed for 50, 100, 150, and 200 iterations. The time taken to complete a single iteration was approximately 2.5 hours.

Generally, the outputs of a Monte Carlo simulation are complex because they do not take the form of a single number. Rather, the results are expressed as a spectrum of possible outcomes, and the frequency with which each of these outcomes is expected is a distribution of values. However, it is normally convenient to summarize the results using a single representative value called a point estimate. In this work, the point estimate is calculated using Microsoft Excel spreadsheet as the mean of the number of exceedances for each of the user defined range of contaminant magnitude. The sensitivity of the number of iterations is assessed on the simulation output by considering the variability in this point estimate of the number of exceedances for each of the user defined range of contaminant magnitude, as the number of iteration increases.

The detailed results of the sensitivity analysis are presented in appendix A8.2. The monitoring boreholes that show variability in the contaminant concentration are presented in Figure 4.22, while in all other boreholes the contaminant concentration is less than 1 x 10^{-5} mg/l. Figure 4.22 shows that the variability in the point estimate appears to be largely the same across all the user defined ranges of contaminant concentration as the number of iteration increases from 50 to 200. Therefore, it is thought that 100 iterations is efficient in the use of the time and the computer memory, and could be employed in the Monte Carlo simulation for the implementation of this risk assessment method without losing significant details of the distribution of the input parameters. In this assessment, the repetition of the simulation is automated using the batch file presented in appendix A1.2. The graphs showing the probability of obtaining a particular concentration at a single point within the aquifer is presented in Figure 4.23, while Figure 4.24 presents risk maps which show the spatial distribution of the probability of exceeding a particular value of the user defined concentration magnitudes.

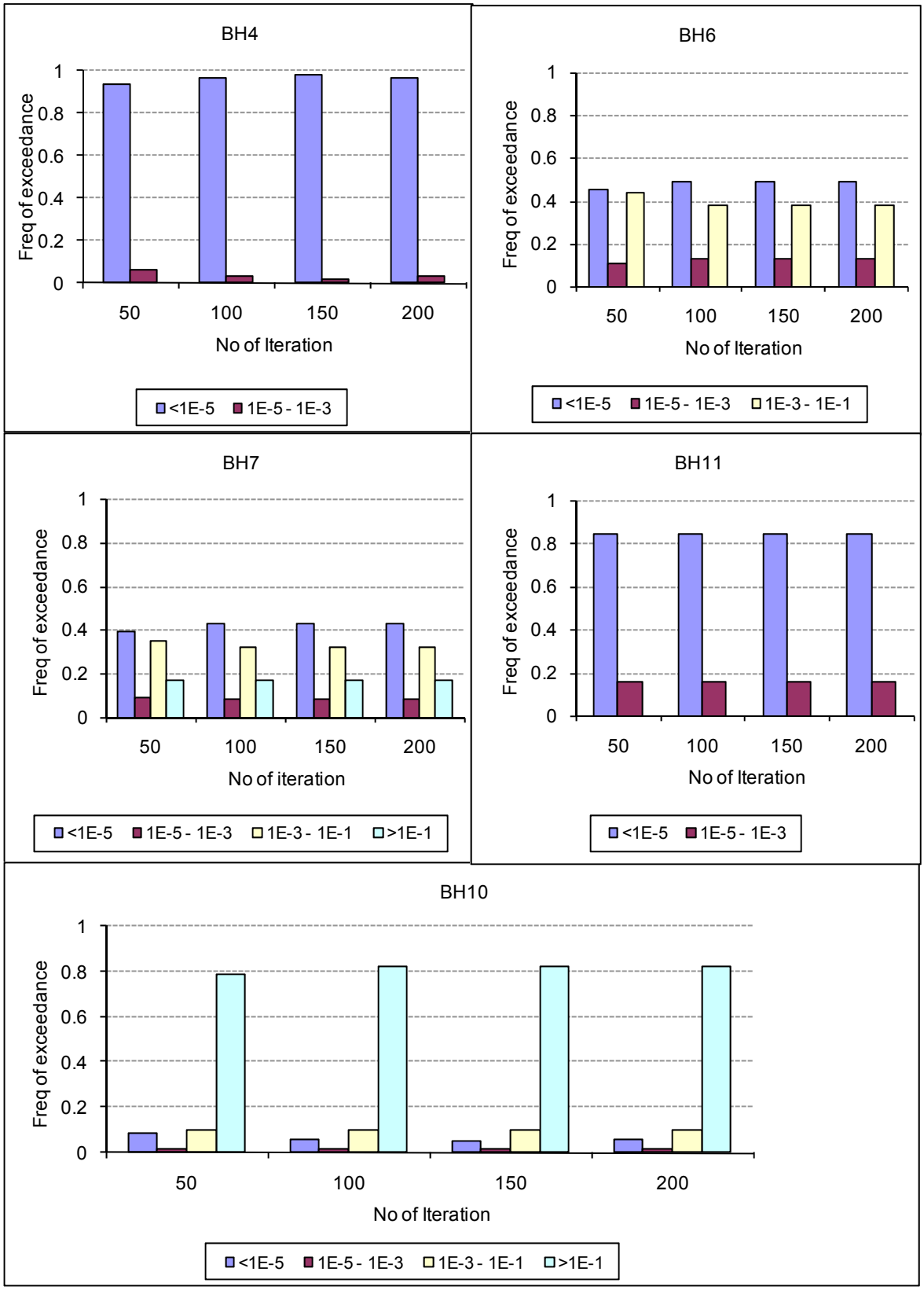

Figure 4.22: Sensitivity analysis for number of Monte Carlo iteration

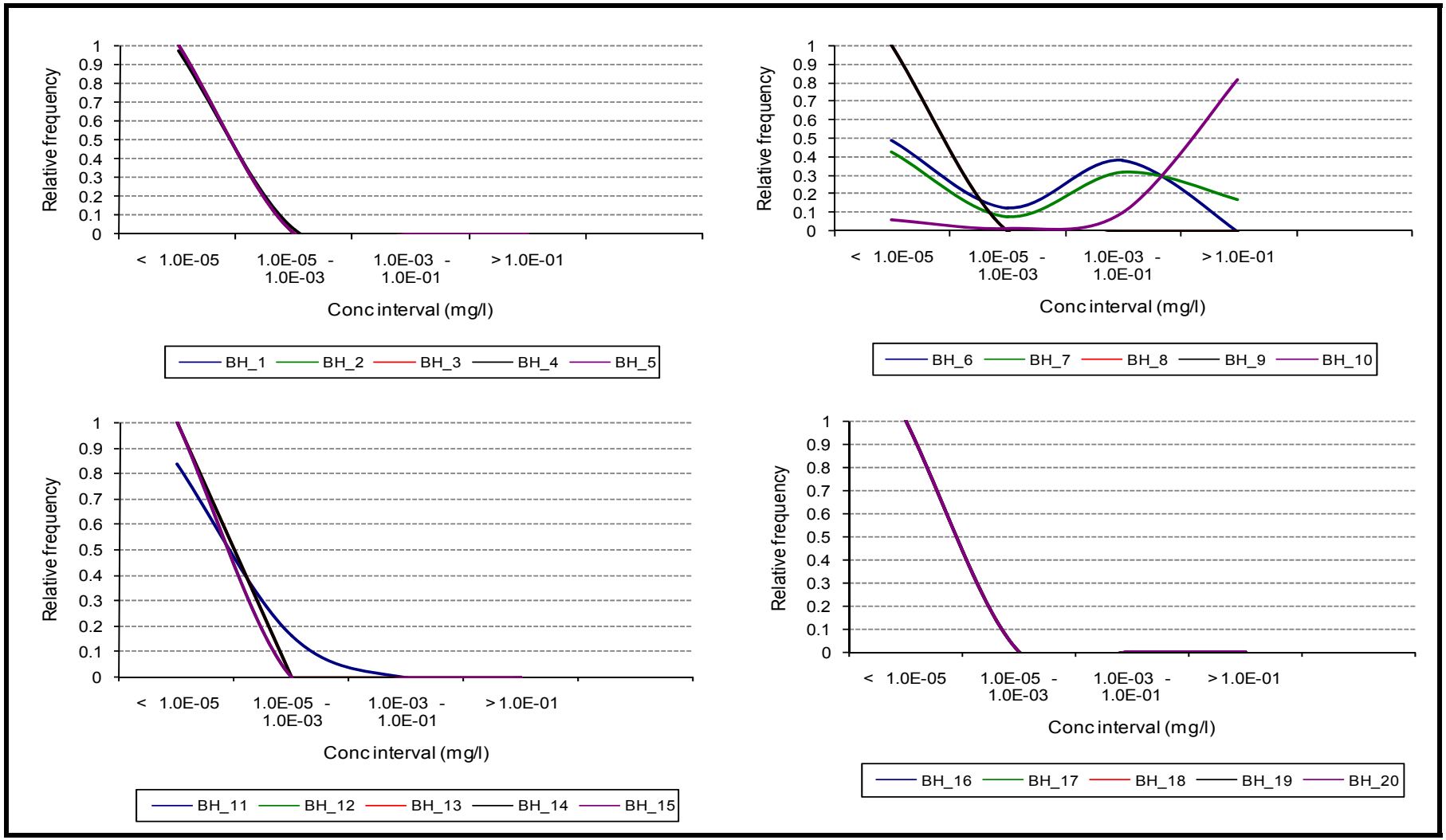

Figure 4.23: Probability of obtaining specific concentration at monitoring borehole

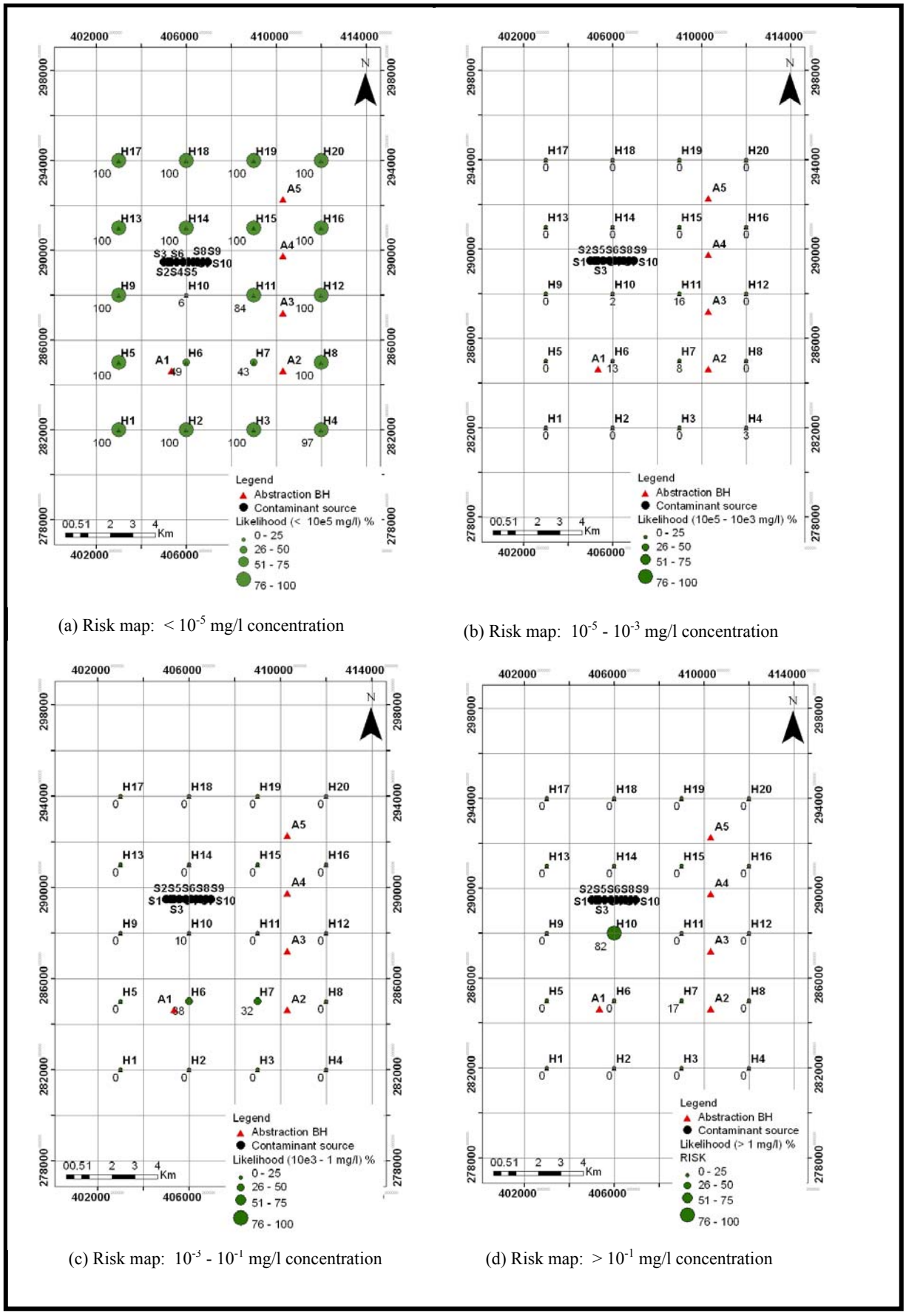

(a) Risk map: $< 10^{-5}$ mg/l concentration

(b) Risk map: 10^{-5} - 10^{-3} mg/l concentration

(c) Risk map: 10^{-3} - 10^{-1} mg/l concentration

(d) Risk map: $> 10^{-1}$ mg/l concentration

Figure 4.24: Risk maps for contaminant concentration

4.6 Deductions from the hypothetical scenarios

The risk assessment method was demonstrated using 8 scenarios to assess the effects of variations in the sizes of the model grid cells, stress period and the loading rate, as well as the historic frequency of pollution incident occurrence, on the method. The detailed discussions of the observations are presented in Chapter six.

The three scenarios (1, 2 and 3) with grid sizes 25 x 25 m, 10 x 10 m and 50 x 50 m, were used to assess the most efficient grid scales required for the solute transport calculations at the spatial and temporal scales required for decision making. The purpose of the assessment is to be able to balance the accuracy of the model outputs against the time resources. The numerical errors calculated by the model were used to indicate the accuracy of the scenarios. The volumetric balance errors for the flow models under the three scenarios are presented in Figure 4.2a. The maximum value obtained in the three scenarios was 0.02 %, and this indicates that the flow model scenarios were converging with insignificant numerical errors. The least percentage error value of 0.0 was obtained under the scenario 2 with the smallest grid sizes of 10 x 10 m. The percentage numerical error values of the transport model for all the three scenarios have similar values which are all much less than 0.001 %. The time taken for the simulations is presented in Table 4.6, and it shows that though the output of the scenario 2 appears to be more accurate compared to scenarios 1 and 3, however the time taken to complete the simulation under scenario 2 is more than five times greater than that of scenario 1, and ten times for scenario 3. Considering the fact that the implementation of the risk assessment methodology presented in this work requires multiple iterations, it is therefore considered not efficient to incorporate model grid size that is smaller than that used in scenario 1 (i.e. 25 x 25 m), and this is the grid size used in the field application of this risk assessment method presented in Chapter 5.

Table 4.6: Time taken for model runs (Scenario 1 – 3)

Scenario	Flow model (minutes)	Transport model (minutes)	Total time (minutes)
Scenario 1 (25 x 25 m)	11	108	119
Scenario 2 (10 x 10 m)	115	529	644
Scenario 3 (50 x 50 m)	8	52	60

The effect of the loading rates on this risk assessment method was demonstrated using scenarios 4 and 5. The comparison of the distribution of the stress periods used in scenario 4 (Approach 1) with those used in scenario 5 (Approach 2) is presented in Figure 4.9. The ranges of values of contaminant concentrations simulated at the same 20 observation boreholes are presented in Figure 4.14. The detailed input data (*ram_input_file.dat*) for risk model used in the assessment of Approach 2 is presented in appendix A2.1b, as compared to those used in Approach 1 (appendix A2.1a). The generated source terms (*ram.ssm*) by the risk model as input into transport model are respectively presented in appendix A3.3a and appendix A3.3b, for the Approach 1 and Approach 2. Finally, Figure 4.15 present the mass balance for both the Approaches 1 and 2, while the breakthrough curves of the contaminant concentrations obtained during Approaches 1 and 2 at the same observation boreholes are presented in Figure 4.17. The comparison of the values of relative frequency of exceedance for Approaches 1 and 2 at the monitoring points are presented in Figure 4.25.

The breakthrough curves (Figure 4.17) show that the contaminant appears in the downstream observation borehole (BH10) faster under Approach 2 (scenario 5) compared to Approach 1 (scenario 4). Though the breakthrough curves are interesting the true output of this risk assessment methodology is the frequency of exceedance at the points of interest within the aquifer. These are shown in Figure 4.25, and it can be seen that these values are almost identical under Approach 1 and Approach 2 with no detectable pattern in the discrepancies. Indeed due to the stochastic nature of the generating mechanisms these may represent the natural variations within the methodology. The combination of similar frequency distributions of pollutant levels within the aquifer and the pattern of the breakthrough curves indicates that no benefit is gained in adopting Approach 1 over the computationally more efficient Approach 2. Therefore, the Approach 2 (scenario 5) where loading rate is distributed over the stress period is considered to have greater flexibility and ease of integration into existing flow and transport models. It uses fewer number of stress periods which enhances its efficiency in terms of the required simulation time and memory, without posing unacceptable compromise for accuracy, and therefore it is the approach adopted in the subsequent implementation of the method in Chapter 5.

Finally, scenarios 6 – 9 assess the effects of variation of frequency of pollution occurrence on the risk assessment method. The historic frequency of pollution incidents were

respectively doubled, tripled and quadrupled compared to the values used in scenario 5. All other input data were kept constant. Source terms were subsequently generated using the new variations, and the effects of the variation on the groundwater heads as well as contaminant concentrations at the 20 observation boreholes were assessed. The results show that the number of source terms generated increases with increasing historic frequency of pollution incidents. Consequently, the mass of contaminant in the aquifer during simulation appears to be directly proportional to the historic frequency of pollution incidents and the number of source terms generated. Also, the simulated concentrations at the monitoring boreholes appear to increase in a non linear pattern, as the historic frequency of incidents increases. That is, tripling the numbers of historic frequency of pollution occurrence in scenario 8 (compared to the baseline conditions in scenario 5) do not have corresponding increase in the amount of contaminant concentrations observed in the monitoring boreholes (see Figure 4.21).

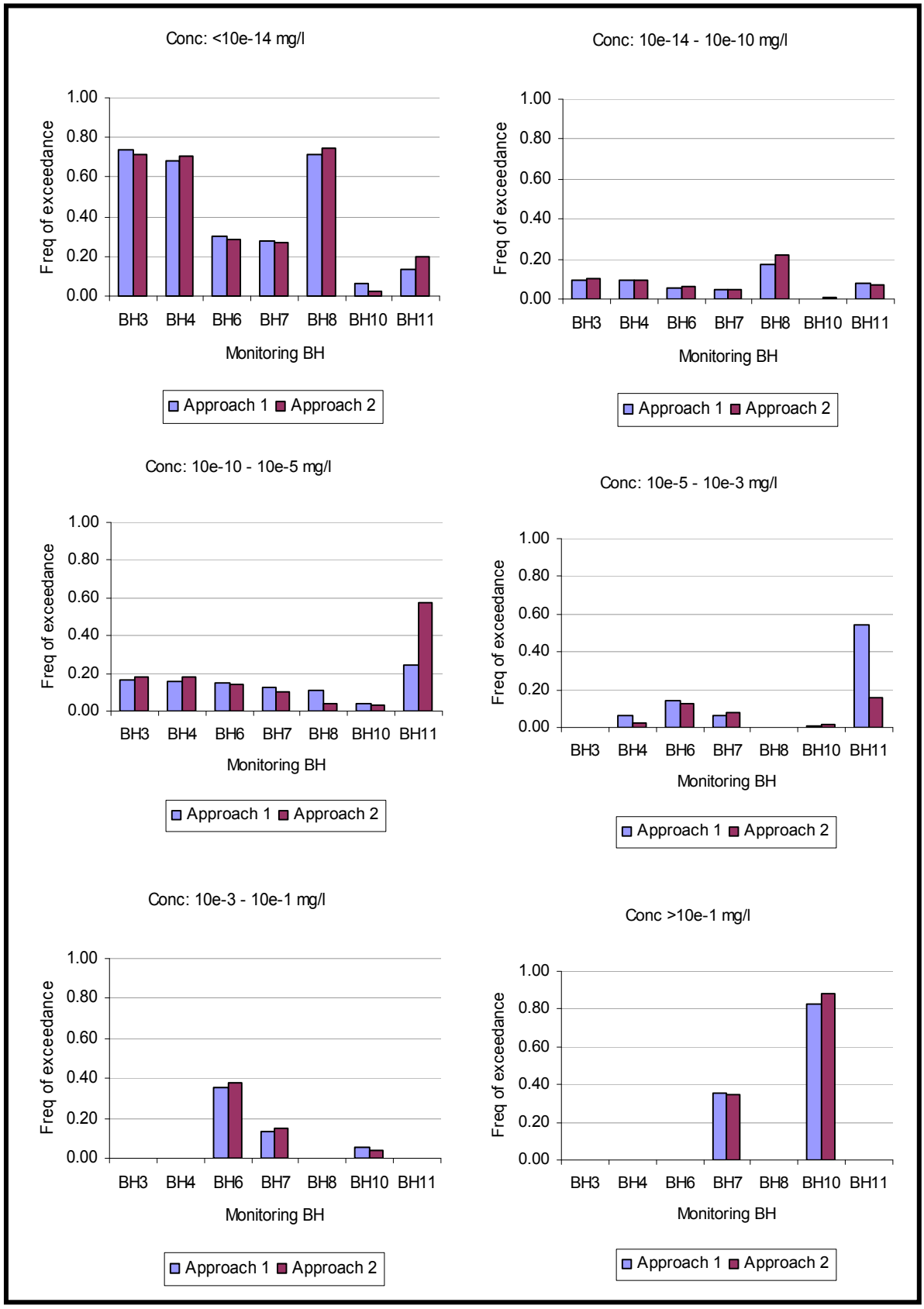

Figure 4.25: Exceedance of contaminant concentration under Approaches 1 and 2

4.7 Summary of the Chapter

The functionalities of the risk assessment method developed in this work is demonstrated by using 8 hypothetical scenarios to evaluate the dependency of the methodology on variations in model grid sizes, contaminant loading rates and the historic frequency of pollution events. Under scenarios 1 to 3, the grid sizes were 25x25, 10x10, and 50x50 m, respectively. The effect of the loading rates on this risk assessment method was demonstrated using scenarios 4 and 5, while that of the probability of occurrence of pollution incidents was also assessed under scenarios 6 to 8, by multiplying the baseline values (scenario 5) by a factor of 2, 3 and 4, respectively.

Each scenario integrates flow, risk and transport models in the assessment of risk to groundwater features. The models under each scenario were setup over a 30-year period. The results of the hypothetical application of the methods are presented in form of tables, graphs and spatial maps. This also includes the calculated risk at each of the observation boreholes based on the user defined contaminant magnitudes. The sensitivity analysis of the grid sizes using the hypothetical scenarios provided the basis for the choice of grid size of 25x25 m used in the subsequent field applications. Also, the Approach 2 (scenario 5) where loading rate is distributed over the stress period is considered to have greater flexibility and ease of integration into existing flow and transport models. It uses fewer number of stress periods which enhances its efficiency in terms of the required simulation time and memory, without posing unacceptable compromise for accuracy, and therefore it is the approach adopted in the subsequent implementations of the method. Finally, varying the historic frequency of occurrence shows that the number of source terms generated increases with increasing number of historic frequency of pollution incidents, and consequently the mass of contaminant generated within the aquifer during simulation. However, the simulated contaminant concentrations within the observation boreholes appear to increase in a non linear pattern as the historic frequency of incidents increases.

The assessment of risk to groundwater resource is demonstrated by repeating the simulation for 100 times, and then observing the number of times at which the user defined contaminant concentration intervals was exceeded. The risk of pollution from a number of sources all occurring by chance together was evaluated, and the results presented as graphs and risk maps.

Chapter 5: Application of risk assessment method using field data

This Chapter presents the development of a three-dimensional calibrated flow model of Birmingham area, hereafter referred to as the study area. The model is in turn integrated with a transport model, and is used as a framework for the application of the risk assessment method (RAM) developed in this work.

5.1 Description of the study area

This section presents a detailed description of the study area. This involves the climatic conditions, geology, groundwater abstractions, hydrological systems and conceptual understanding of the area.

5.1.1 Location and demography

The location of the study area is presented in Figure 5.1. The area is bounded by the 279000N : 296000N and 400000E : 413000E of the British National Grid. It extends 17 km from south to north, and 13 km from west to east, covering approximately 221 km^2. This area encompasses Birmingham city with a population of 977,087 (UK National statistics, 2006), and also forms part of the larger West Midlands conurbation. Birmingham has been a major manufacturing centre for over a century, and contains many industrial processes that may constitute risk to groundwater.

5.1.2 Topography

The surface topography of the study area is presented in Figure 5.2a. The landscape is dominated by higher elevation on the western part, as compared to relatively low elevation towards the eastern part. The highest point is approximately 170 m OD, located in the western part of the area, while the lowest point is approximately 92 m OD, located in the central part. According to Powell *et al.* (2000), the surface elevation is greatly influenced by the underlying geology.

5.1.3 Solid geology

The generalised solid geology of the study area is presented in Figure 5.3a. The descriptions of the geology are deduced from a number of sources including the acquired borehole lithologic logs, geological cross sections constructed from the lithologic logs and

the literature. The vertical geological cross sections are prepared using WinLog (Version 4) and WinFence (Version 2) software. The lines along which the geologic cross sections are drawn are shown in Figure 5.2b, while the corresponding geologic cross sections are presented in Figure 5.4. The depth of the lithologic logs defined the basal part of the geologic cross-sections and the model area. The information yielded by the borehole logs includes the stratigraphy, aquifer geometry in terms of the elevations of the constituent strata, thicknesses and lateral extents. Additional information obtained from the borehole logs is presented in appendix A8.1.

The borehole logs (appendix A8.1) including the associated elevation records, as well as the account of the generalized geology of Birmingham on a scale 1:50000 (Powell *et al.* 2000) indicate the presence of Triassic sandstone, overlying the Westphalian Formations. The Triassic sandstone consists of fluvioglacial thick successions of the sandstone deposit, commonly referred to as the Sherwood sandstone Group. These are mostly fluviatile in origin, well sorted conglomerates and cross-bedded sandstones, with abundant fining upward sequences. The constituent geological strata of the Triassic sandstone are the Kidderminster, Wildmoor, and Bromsgrove sandstone Formations.

5.1.3.1 Westphalian Formations

Underlying the Triassic sandstone are members of the older geologic formation ranging from Cambrian to Permian, which are largely impermeable. For the purpose of this research work, these formations constitute the basal rocks of the study area. The top elevation of the Westphalian Formations corresponds to the base elevation of the overlying Triassic sandstone, represented by the Kidderminster Formation, and presented in Figure 5.5.

5.1.3.2 Kidderminster Formation

The Kidderminster Formation which is formerly known as the Bunter Pebble Beds or the Cannock Chase Formation constitutes the basal part of the Triassic sandstone. The formation is often covered by thin layer of drift, or sometimes man-made ground, and its base elevation as well as its thickness are presented in Figure 5.5. Maximum thickness of

approximately 160 m occurs at the south central part of the study area, and consequently pinches out towards the north east and the southern areas.

Generally, the formation consists essentially of pebbles, conglomerates, and coarse-grained sandstones, with intercalations of thin mudstone beds. A gradational boundary exists between the Kidderminster Formation and the overlying Wildmoor sandstone Formation. The basal part of Kidderminster Formation consists of well-rounded conglomerates, and medium-grained micaceous sandstones. The formation is generally friable and weakly cemented, with local occurrence of calcite-cemented beds. Petrological and mineralogical studies of the formation show that quartzite of various shades of colours constitutes over 80 per cent, while the remaining constituents are aggregates of mineral assemblages from igneous, metamorphic and sedimentary rocks. Exposures of Kidderminster Formation within the study area occur around Sutton Coldfield (BNG: 410750: 296630), as well as quarries along the Barr Beacon escarpment (BNG: 405920: 296720), and Perry Barr (BNG: 406300: 294400), among other locations.

5.1.3.3 Wildmoor Formation

The Wildmoor sandstone Formation is formerly known as the Upper Mottled sandstone. It is sandwiched between the underlying Kidderminster Formation and the overlying Bromsgrove sandstone Formation. The base elevation and its thickness are presented in Figure 5.6.

The Wildmoor Formation consists of reddish fine-grained micaceous sandstones, with occasional occurrences of thin beds of marl. The grains of the sandstones are often poorly cemented, which promotes its use for foundry purposes. The Wildmoor Formation is generally fine grained, red coloured and of mottled appearance and these characteristics distinguishes it from the underlying Kidderminster Formation. The upper part of Wildmoor Formation consists of red to brown quartzite- and calcite-rich pebbly sandstone, with ferruginous cementation. Mineralogical analyses show silica as the major constituent, as much as 85 %, while alumina, iron oxide, and potassium carbonates form the remaining constituents. Less than 2 % of the grain sizes are coarse, while medium- and fine-grained sizes range from 40 - 67 % and 28 – 46 %, respectively. Exposures of the Wildmoor Formation within the case study area have been reduced due to urbanisation and drift

deposits. Outcrops of the formation occur around central Birmingham (BNG: 405980: 288150 to 406000: 288060), as well as along the Midland railway line located at BNG: 405210: 288490.

5.1.3.4 Bromsgrove Formation

The Bromsgrove sandstone Formation is formerly known as Lower Keuper sandstone. It caps the Triassic Sherwood sandstone Group. The base elevation and its thickness are presented in Figure 5.7. The formation consists of red to brown, medium- to coarse-grained sandstones. The grains are sub-angular with a matrix of occasional occurrences of the pebbles of conglomerates and thin beds of mudstone and siltstone. Dominant constituents at the base of the formation are rounded granules and pebbles of quartz, quartzite and feldspar. Old *et al.* (1991) sub-divided the formation into three upward sequence members, namely: Burcot, Finstall and Sugarbrook. The Bromsgrove sandstone Formation rests unconformably on the underlying Wildmoor Formation or Kidderminster Formation in the absence of the former. Also, factors such as urbanisation and drift deposits have reduced the outcroppings of the Bromsgrove Formation. The formation outcrops at the following localities, namely railway cuttings in central Birmingham (BNG: 406920: 286740, 407400: 286800), and in the Calthorpe fields (BNG: 405270: 285190 to 405380: 285240).

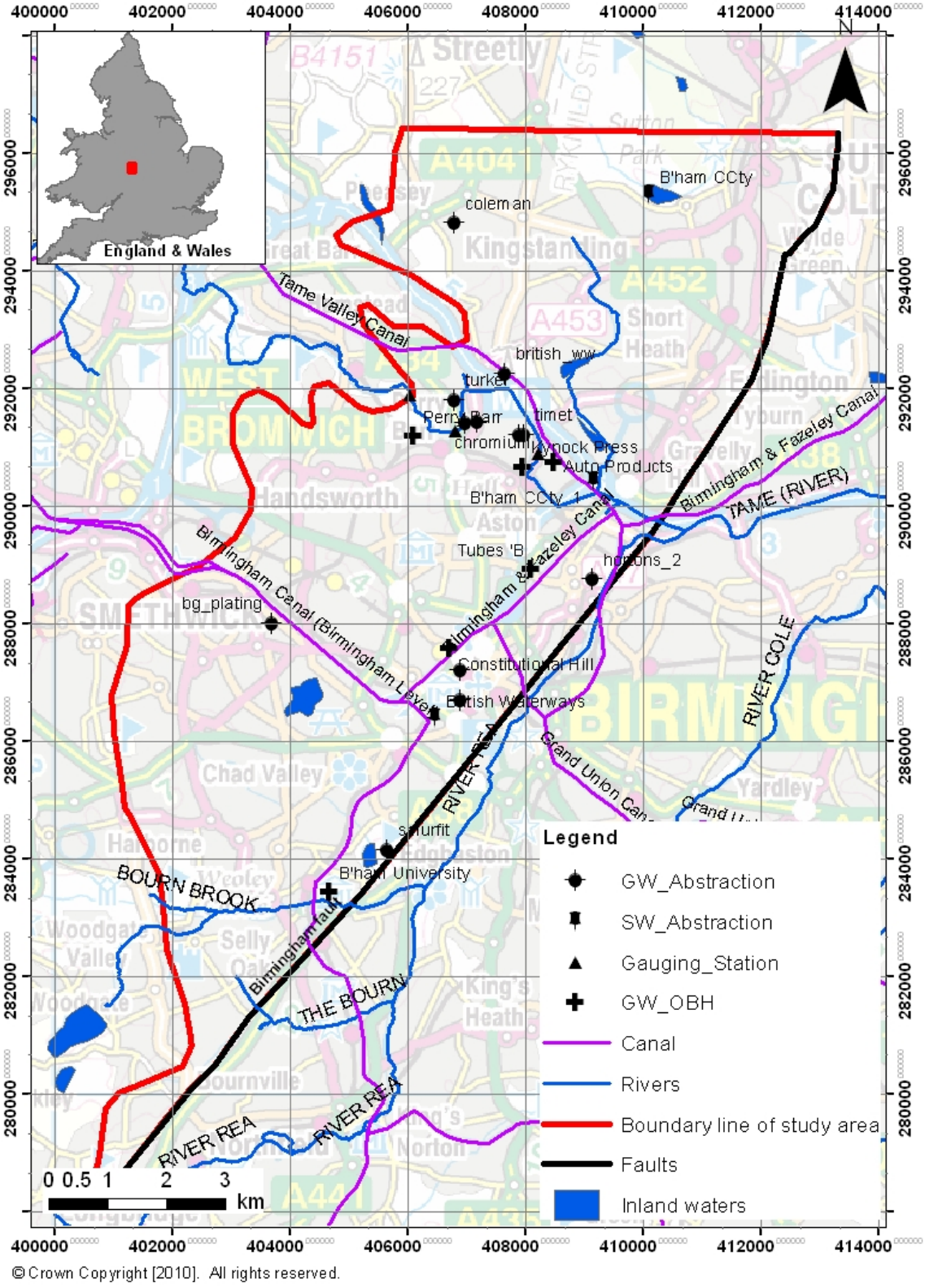

Figure 5.1: Location of the study area

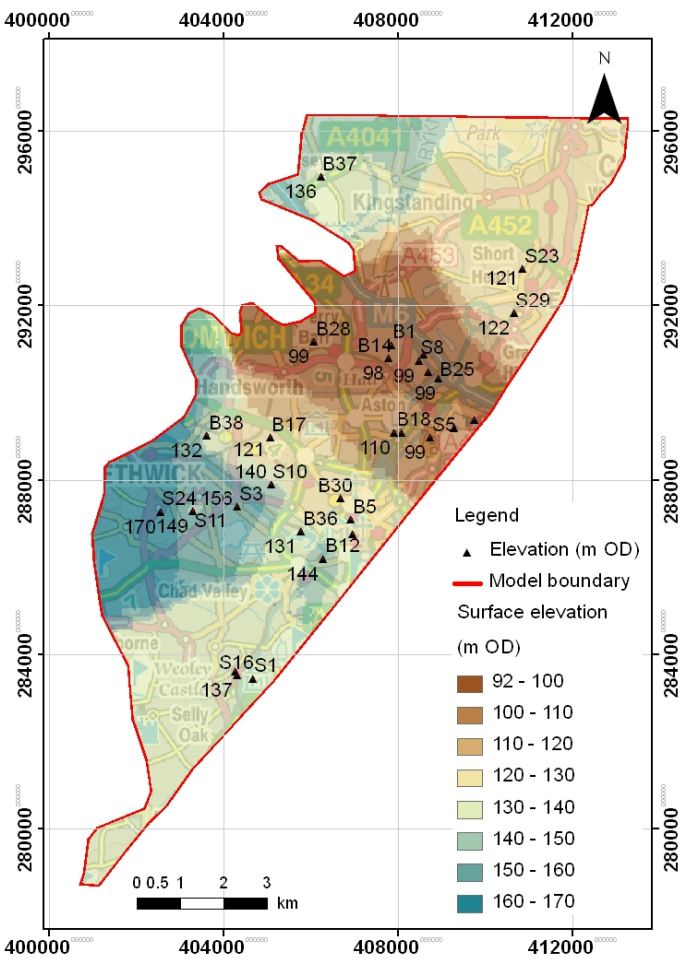

(a) Topography of the study area

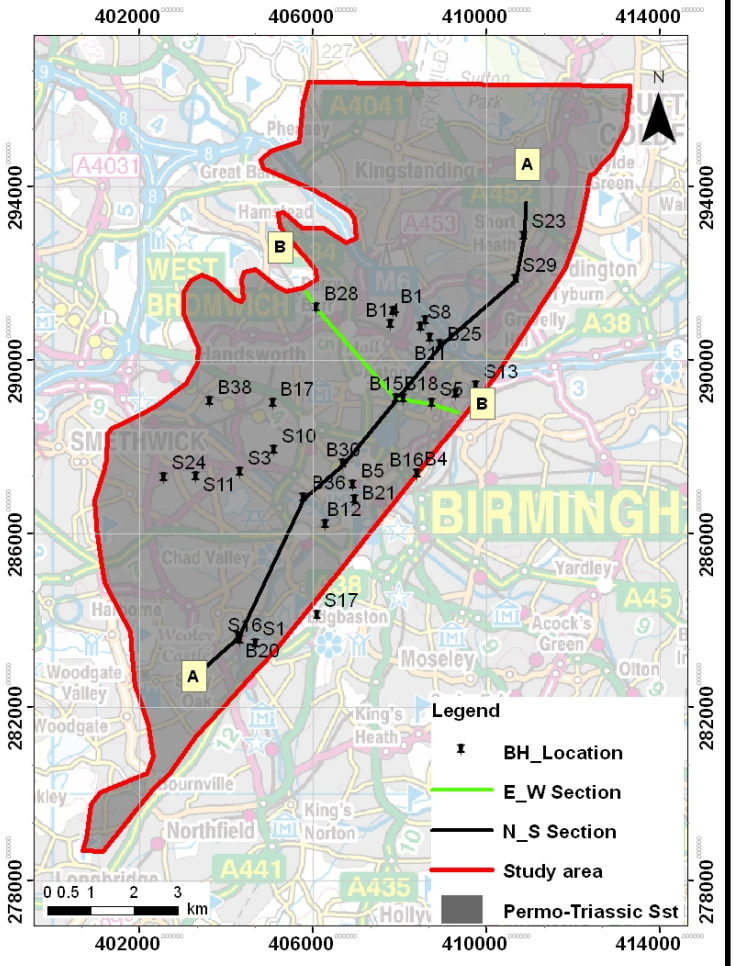

(b) Borehole logs and cross section lines

Figure 5.2: Surface elevation and borehole log locations

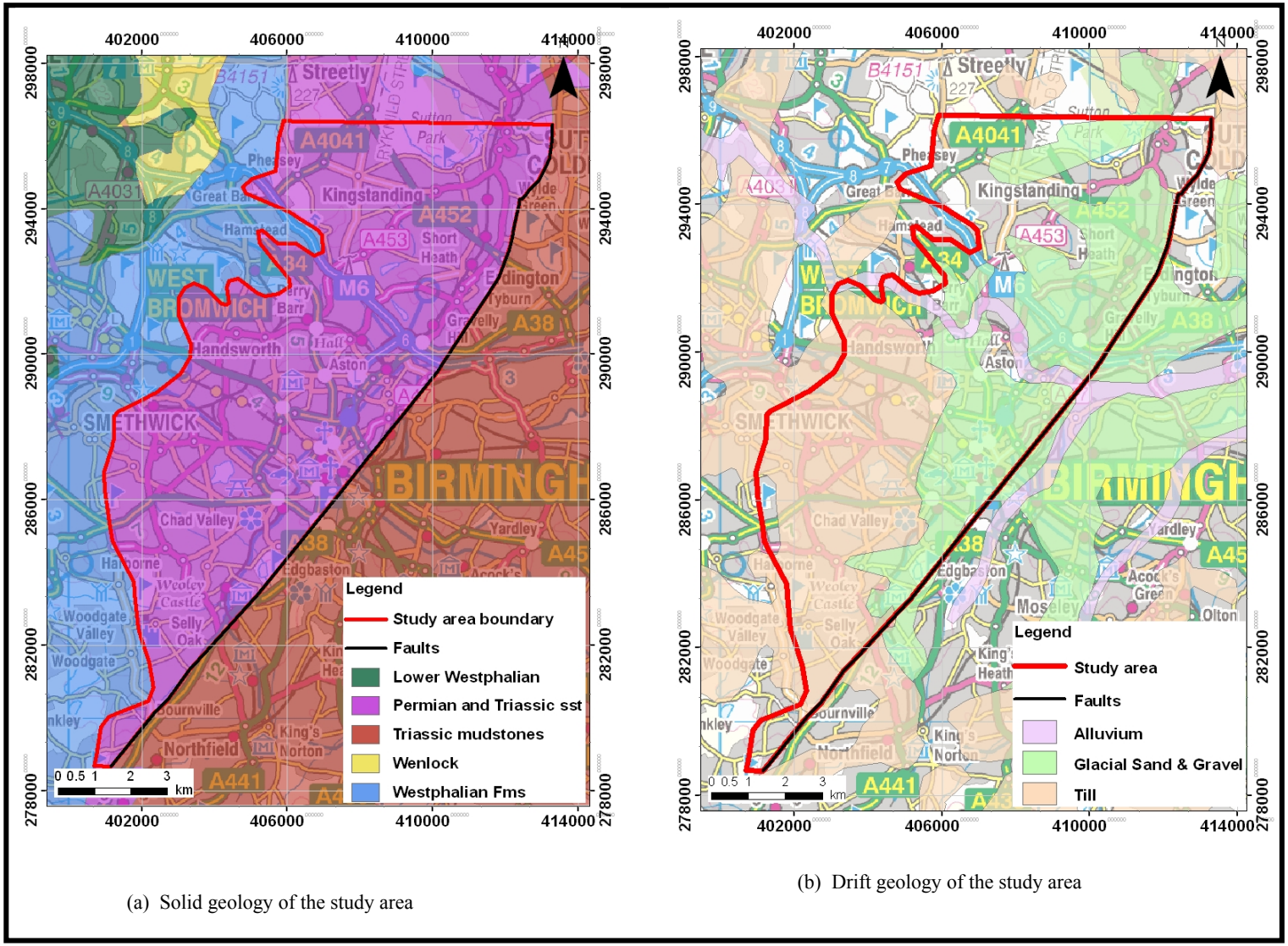

(a) Solid geology of the study area

(b) Drift geology of the study area

Figure 5.3: Geology of the study area

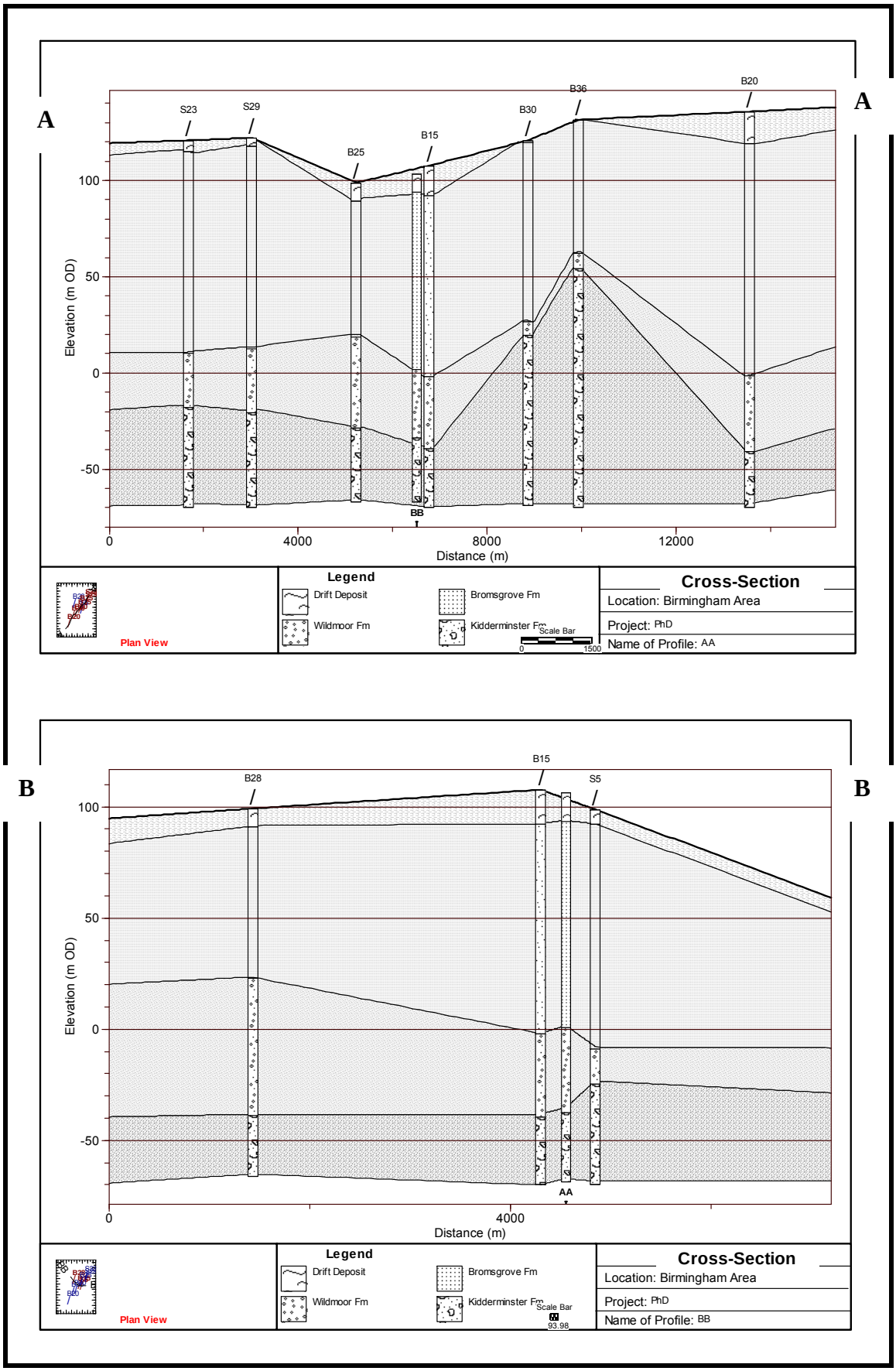

Figure 5.4: Geological cross sections

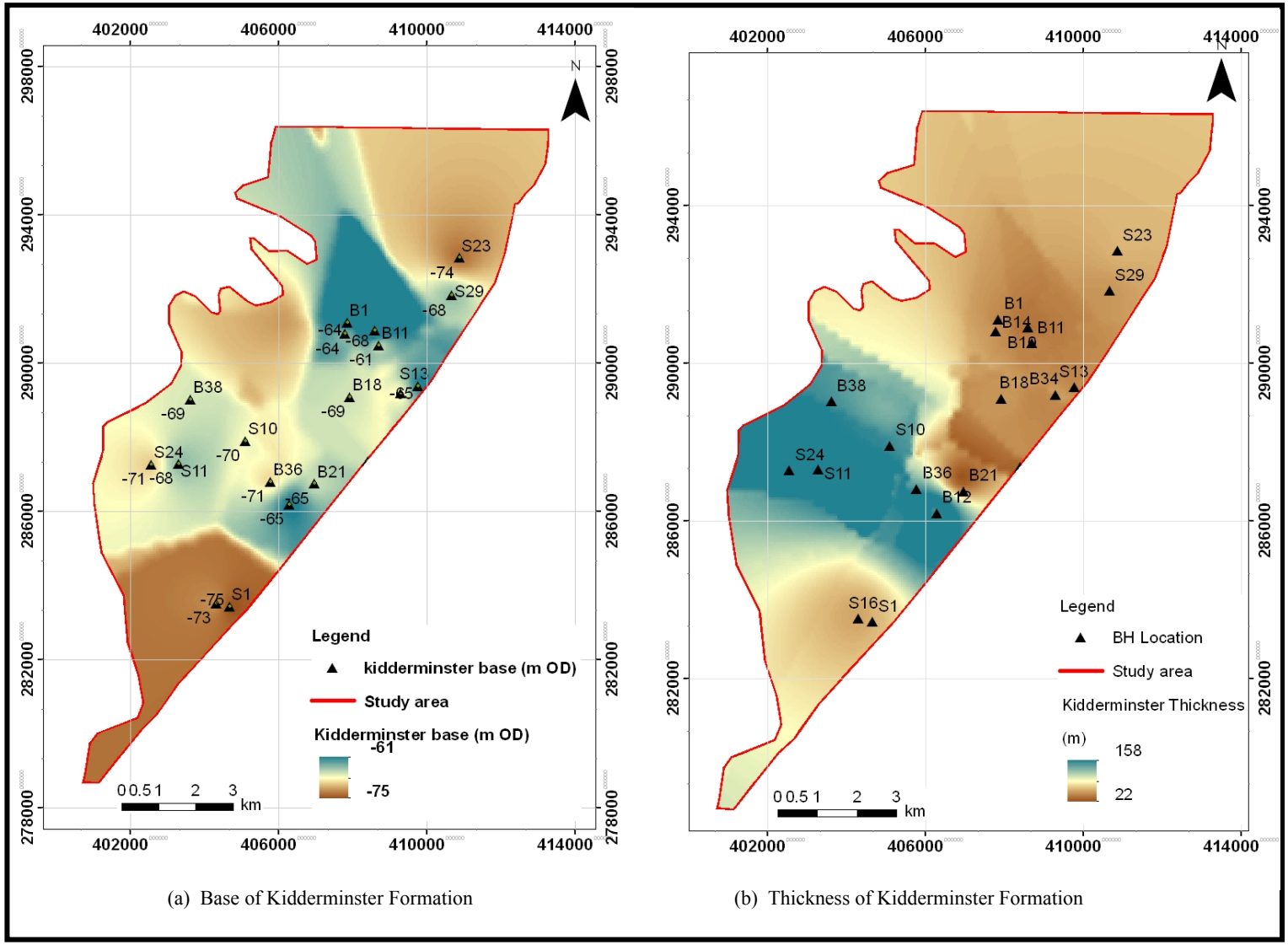

(a) Base of Kidderminster Formation

(b) Thickness of Kidderminster Formation

Figure 5.5: Base and thickness of the Kidderminster Formation

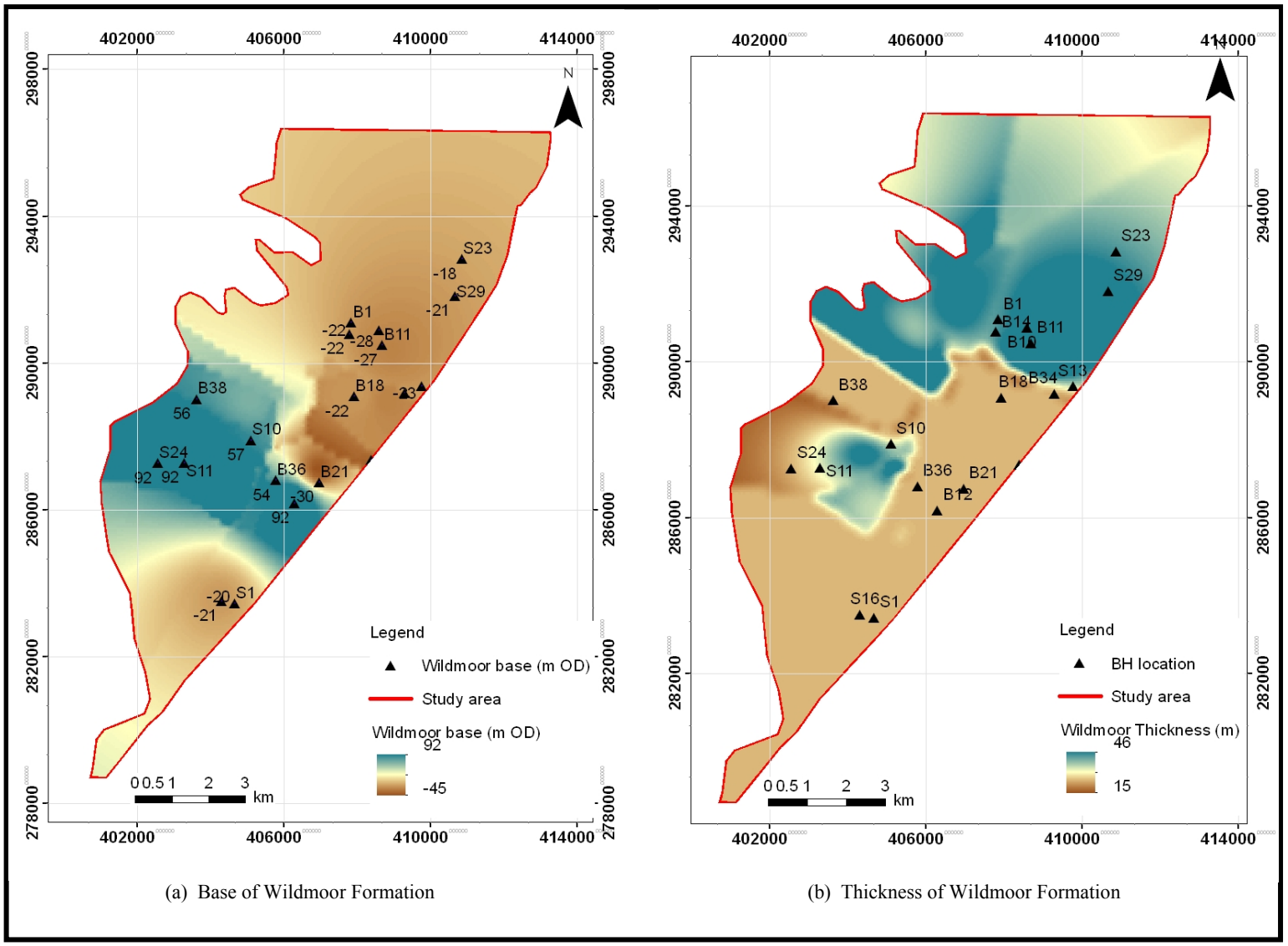

Figure 5.6: Base and thickness of Wildmoor Formation

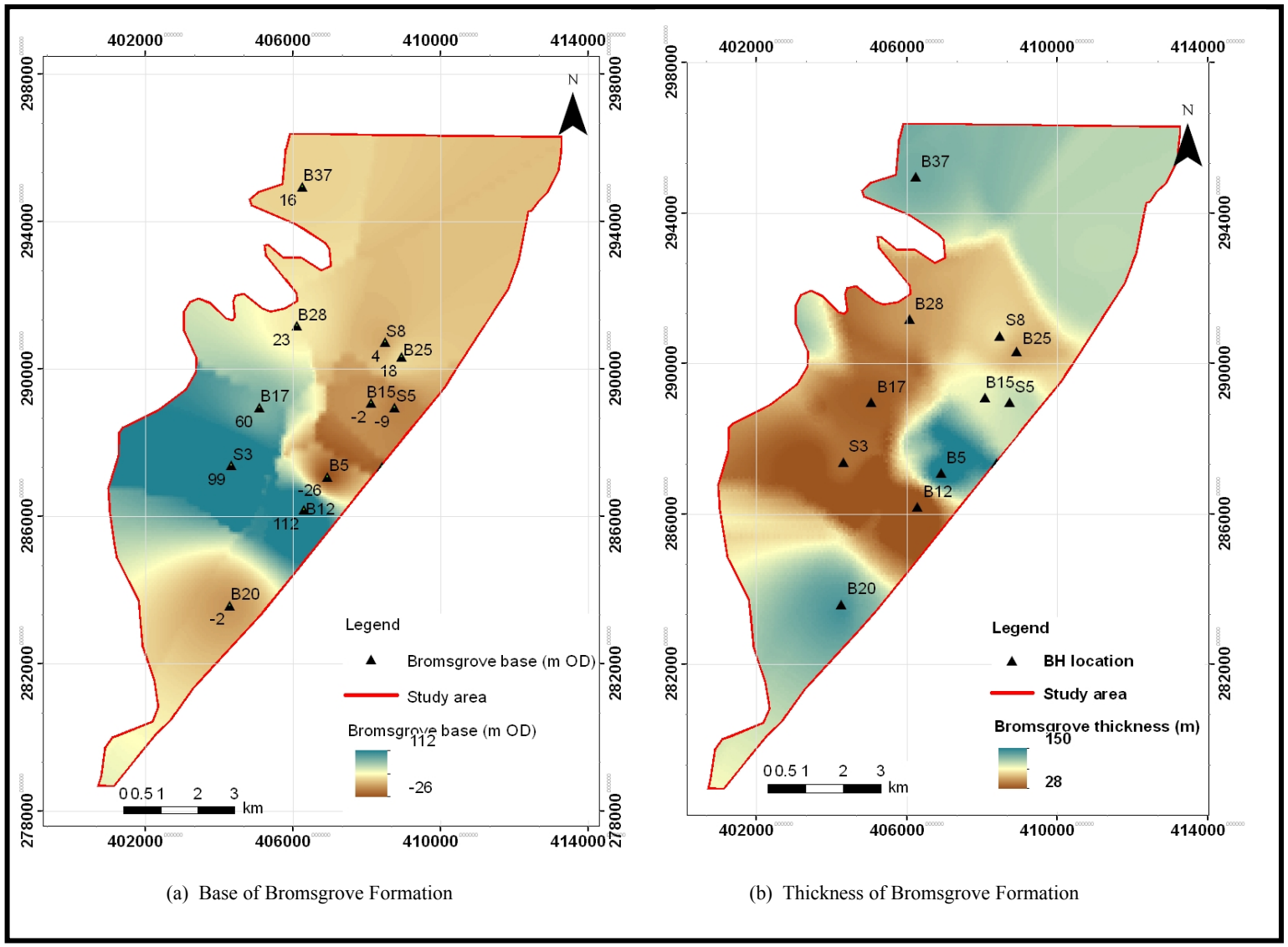

(a) Base of Bromsgrove Formation

(b) Thickness of Bromsgrove Formation

Figure 5.7: Base and thickness of Bromsgrove Formation

5.1.4 Superficial geology

The superficial geology is presented in Figure 5.3b. It consists of clayey, sand, gravel and alluvium, which are products of glaciation and of the Quaternary Period. It overlies the Triassic geological successions and underlies the surface waters. The clayey materials as well as the sand and gravel largely dominate the south western and north eastern parts of the study area. The base elevation as well as the thickness of the superficial deposits obtained from the borehole records are shown in Figure 5.8. The deposits show maximum thickness of 24 – 35 m in the west, as compared to the central and the north east, where the thickness vary between 0 – 4 m.

5.1.5 Soils

The distribution of predominant soil types across the study area is shown in Figure 5.9a while their descriptions are presented in Table 5.1. According to Powell *et al.* (2000), factors such as climate, geology, geomorphology and hydrology greatly influenced the distribution and composition of the highly varied and complex soils within the case study area.

The Hydrology of Soil Types (HOST) is a hydrologically-based classification of the soil types of the United Kingdom. A detailed description is presented by Boorman *et al.,* (1995). The classification is based on the conceptual model of the processes occurring within the soil and the substrate. The modelled concept consists of three major scenarios described as follow:

1. A soil on a permeable substrate in which there is a deep aquifer or groundwater (i.e. at > 2 m depth).
2. A soil on a permeable substrate in which there is normally a shallow water table (i.e. at ≤ 2 m depth).
3. A soil (or soil and substrate) which contains an impermeable or semi-permeable layer within 1 m of the surface.

The concept further consists additional scenarios for assessing variability of different soil properties such as peaty top layer, wetness regime etc. The resulting scheme has 29

classes based on 11 modelled scenarios. Soils are assigned to classes on the basis of their physical properties, and with reference to the hydrogeology of the substrate. The final product of the HOST Project is a computer data set based on a 1 km grid that covers the entire UK.

The distributions of the natural vegetation are largely man-made, and greatly influenced by water availability and soil types.

5.1.6 Land use

The study area is urban, covering the Birmingham conurbation and includes Selly Oak, Weoley Castle, Harbourne, and Chad Valley in the south; Sutton Coldfield, Kingstanding and Short Heath in the north; while Smethwick, Handsworth, Perry Barr and Aston covers the central part. The landuse pattern (EA, 2008b) within the study area is presented in Figure 5.9b.

5.1.7 Rivers

The major rivers and inland waters present within the study area are presented in Figure 5.1. The River Tame flows from the Black Country, through the north-eastern part of the case study area into the River Trent near Alrewas. The River Cole is a tributary of the River Tame, and feeds into the River Blythe. The River Cole is a relatively short river, about 44 km long. It rises at Wythall, south of Birmingham and passes through Coleshill, joining the River Blythe at Ladywalk.

The inland waters are mostly artificially created either as canal feeders or for drinking purposes, but currently been maintained for leisure purposes and nature conservation.

There are three locations within the study area where continuous stream level data are available, and one location for continuous flow data (Table 5.2). All these gauging stations are shown in Figure 5.1. The level data as well as the flow data are presented in Figure 5.10.

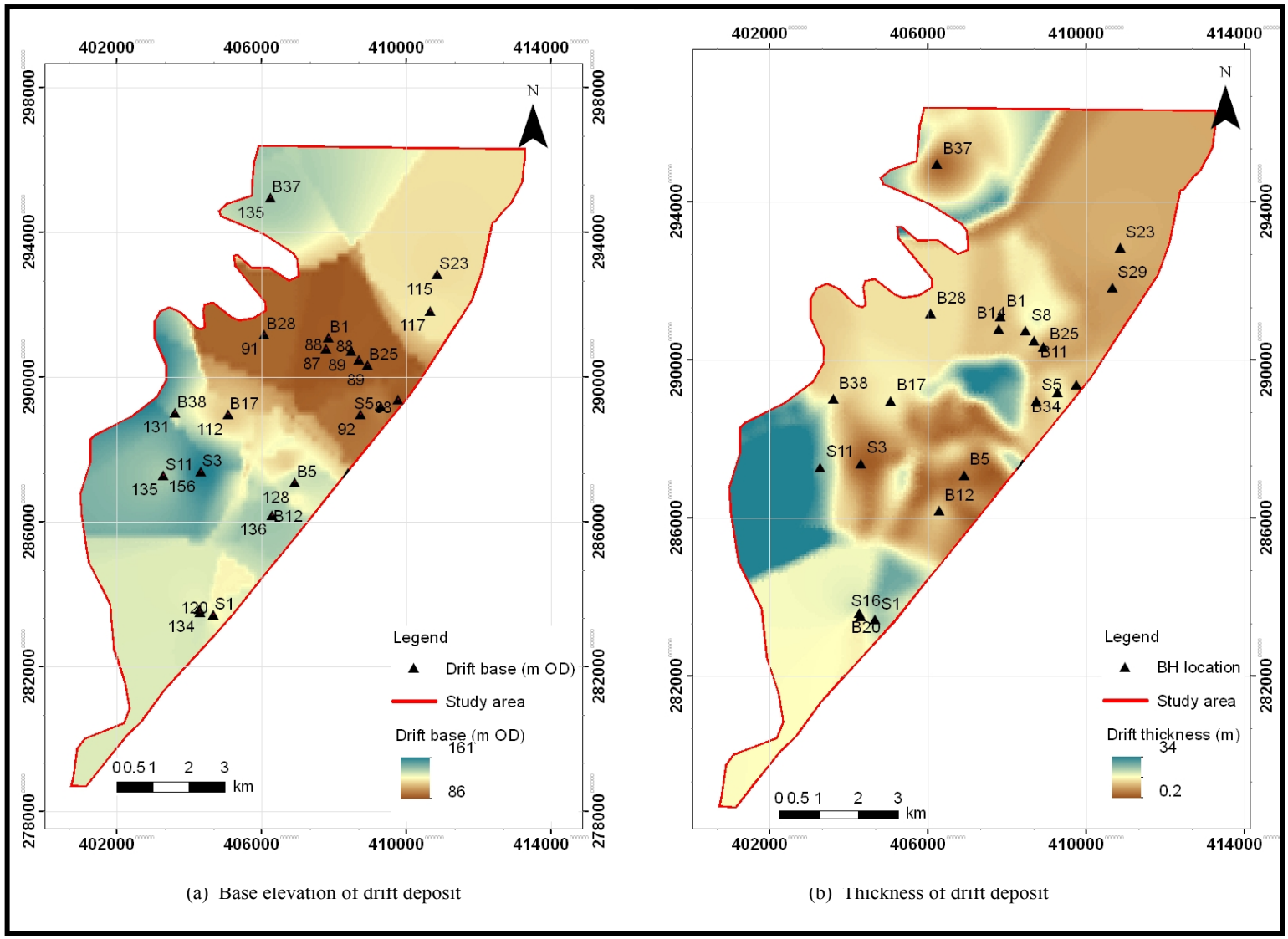

Figure 5.8: Base and thickness elevation of drift deposit

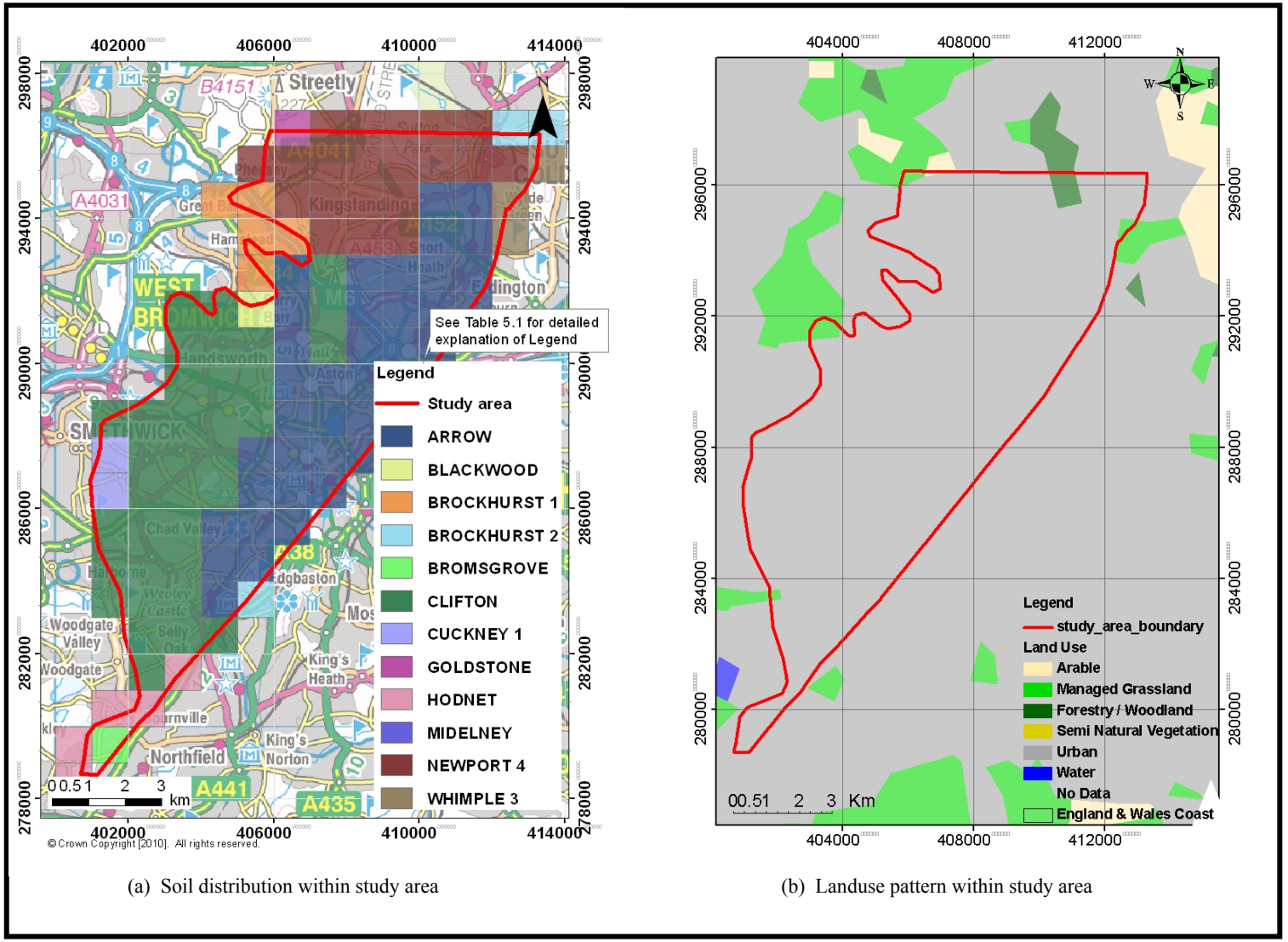

(a) Soil distribution within study area

(b) Landuse pattern within study area

Figure 5.9: Soil distribution and landuse pattern

Table 5.1: Description of the soil types[#]

Soil Name	Description	Soil cover	[*]Host Class	Model recharge Zone	Approximate drift thickness (m)	Landuse (as % of soil type)
Arrow	Deep permeable coarse loamy soils affected by groundwater	38 km^2 / 33.04 %	7	12	2.68 – 19.62	Continuous urban: 100
Blackwood	Seasonally wet, deep permeable sandy and coarse loamy soil	1 km^2 / 0.87 %	10	11	8.23	
Brockhurst 1	Seasonally wet loam to clayey over red shale. Slowly permeable seasonally water logged, reddish fine loamy over clay soils.	5 km^2 / 4.35 %	24	10	7.13 – 23.37	
Brockhurst 2	Seasonally wet loam to clayey over red shale. Slowly permeable seasonally water logged, reddish fine loamy over clayey and clayey soils.	3 km^2 / 2.61 %	24	9	5.29 11.89	
Bromsgrove	Deep loam, well drain reddish coarse loamy soils mainly over soft sandstone but deep in places.	1 km^2 / 0.87 %	3	8	9.83 – 9.85	
Clifton	Seasonally wet deep loam. Slowly permeable seasonally waterlogged, reddish fine and coarse loamy soils	35 km^2 / 30.43 %	24	7	6.43 – 29.39	

Soil Name	Description	Soil cover	*Host Class	Model recharge Zone	Approximate drift thickness (m)	Landuse (as % of soil type)
Cuckney 1	Sandy over sandstone. Well drained sandy and coarse loamy soils	2 km^2 / 1.74 %	3	6	17.72 – 27.65	Continuous urban: 100
Goldstone	Stony, sandy over sand stone. Well drained, very acidic, very stony sandy soils with a bleached subsurface horizon over conglomerate	1 km^2 / 0.87 %	3	5	6.96 – 8.78	
Hodnet	Silty over red shale. Reddish fine and coarse loamy soils with slowly permeable subsoils and slightly seasonal waterlogging	5 km^2 / 4.35 %	18	4	9.31 – 9.87	
Midelney	Seasonal wet deep clay over peat. Stoneless clayey soils mostly overlying peat	1 km^2 / 0.87 %	9	3	6.29 – 9.08	
Newport 4	Deep sandy, well darin sandy soil	20 km^2 /17.39 %	5	2	3.77 – 14.03	
Wimple 3	Deep red loam to clay. Reddish fine loamy or fine silty over clayey soils with slowly permeable subsoils and slightly seasonal waterlogging	3 km^2 / 2.61 %	21	1	5.30 – 5.43	

[#] Source: National Soil Resources Institute (NSRI) GIS Data

[*]Hydrology of soil type. See Section 5.1.5.

Table 5.2: Description of the gauging station within the study area

Site Name	Brookvale Road	Walsall Road	Perry Park
Grid Reference	408220E: 290900N	406820E: 291291N	406042E: 291887N
River Gauged	Tame	Tame	Tame
Data type	Level	Level	Flow & Level
Record frequency & length	Daily/ 01/06/2000 - 25/11/2009	Daily/ 06/03/2000 - 26/01/2009	Daily/ 01/04/1984 - 25/11/2009

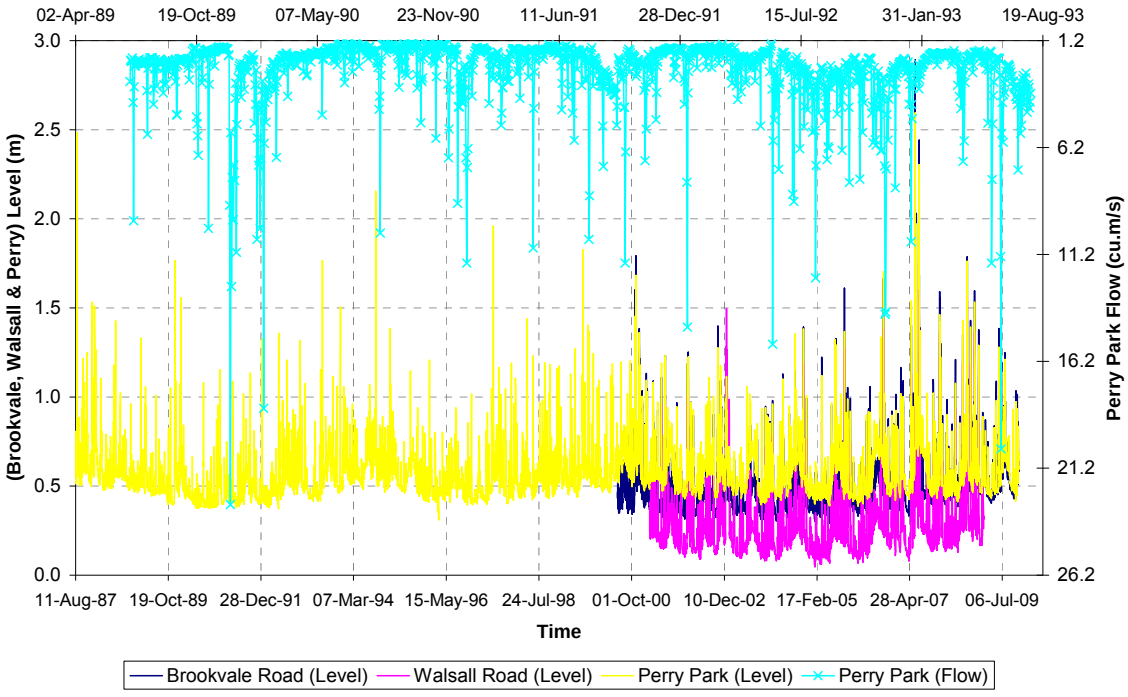

Figure 5.10: Gauged level and flow data within the study area

5.1.8 Geological structures

A major geological structure within the study area is the Birmingham Fault. This is shown in Figure 5.1. The fault juxtaposes the Triassic mudstone to the east against the Triassic sandstone to the west.

Generally, faults have implications for the regional hydrogeology of an area. Dilation and the fault plane irregularities of active faults can enhance the associated hydraulic conductivity of an aquifer, while vertical displacement and the associated grain size reduction can lead to substantial reduction in the hydraulic conductivity. According to Allen *et. al.,* (1997), transmissivity is generally reduced across the Birmingham Fault. Also, Knipe *et. al.,* (1993) modelled the zone across the fault as a reduced aquifer thickness in order to represent the reduced transmissivity across the fault.

Boak (1992b) reported a year long pumping test at the Wheatmoor Wood (BNG: 413680E: 298040N) and St George's Barracks (BNG: 413700E: 296600N) abstraction boreholes for public water supply (PWS). The two PWS boreholes are completed within Bromsgrove sandstone Formation beneath the Triassic Mercia Mudstone Group, on the east of the Birmingham Fault. In addition, 10 of the 11 observation boreholes located on the west of the fault were monitored during the test. A drawdown of 4 m was observed at the Good Hope Hospital monitoring borehole (BNG: 412800E : 296680N) over the test period, though South Staffs Water (2000) attributed the groundwater head decline to natural recession caused by reduced recharge.

Additional work carried out by Buss *et al.* (2008) indicates that in the southern part of their investigation area, the Birmingham Fault has a displacement of approximately 80 m. The authors concluded that a substantial part of the Sherwood sandstone is likely to be in contact with the less permeable fault phase. The faulting in the Permo-Triassic sandstones is older than the sandstone formations; therefore faults are likely to exhibit reduced conductivity. Also, Buss *et al.* (2008) reported evidence that faults inhibit flow from the Severn Trent Water's groundwater scheme pumped well on Adelaide Street, Highgate (BNG: 407630E: 285790N). This deduction appears to be reinforced by Jackson and Lloyd (1983) who, based on the interpretation of groundwater chemistry, concluded that lateral flow is restricted across the Birmingham fault.

5.1.9 Hydraulic properties of aquifers

The constituent formations of the Triassic sandstone Group form the major aquifers in the study area. The descriptions of the properties of the aquifers are based on the borehole logs and associated records, as well as the literature (Jones *et al.,* 2000; Allen *et al,* 1997; and Buss *et al.,* 2008). The distribution and values of hydraulic conductivity, transmissivity and porosity for the undivided Triassic sandstone aquifer obtained from British Geological Survey (BGS) for sites located within the study area are presented in Table 5.3.

According to Allen *et al.*, (1997), the hydrogeological characteristics of Triassic sandstones are dominantly controlled by lithological variations, vertical heterogeneity, anisotropy, fractures, scale of measurement, as well as uneven variations in the aquifer thickness. The authors viewed the aquifer properties of the Triassic sandstone at three levels of scale measurement namely; the core sample, the field (regional) test and the use of models. The summary of the Allen *et al.* (1997) results is presented in Table 5.4. Also, the one-layer numerical flow model developed by Knipe *et al.* (1993) used hydraulic conductivity value of 1.0 – 1.5 m/day in the model run. Theoretically, the storage coefficient of an unconfined aquifer is expressed as presented in Equation 5.1.

$$S_C = S_S h + S_Y \qquad 5.1$$

where S_S : specific storage; h : saturated thickness; S_Y : specific yield.

In any simulation, the two storage terms (i.e. specific storage and specific yield) are required as input into the flow package of the MODFLOW 2000. The respective values used by Knipe *et al.* (1993) for the specific storage and specific yield were 5 x 10^{-4} and 0.15, respectively. Buss *et al.,* (2008) developed a three-layered numerical flow model for the Birmingham-Lichfield area, and defined the aquifer properties of the Sherwood sandstones Group, using values presented in Table 5.5.

5.1.10 Groundwater levels

There are six groundwater level monitoring boreholes within the study area, with data available for the time period over which the model was calibrated, and their locations are presented in Figure 5.1. The depths of the boreholes are completed within different geologic layers as shown in Table 5.6. Long term groundwater hydrographs for each of the monitoring borehole are presented in Figure 5.11.

Table 5.3: Aquifer properties for Triassic sandstones (Source: British Geological Survey)

Note: No further classifications of the geological layers are provided in the source.

Table 5.4: Hydrogeological properties of Permo-Triassic sandstone aquifer (Source: Allen *et al.* 1997)

Table 5.5: Hydrogeological properties of Permo-Triassic sandstone aquifer (Source: Buss *et al.* 2008)

Table 5.6: Descriptions of the groundwater level monitoring boreholes

Site Name	Birmingham University	Kynock Press	Auto Products	Constitutional Hill	Tubes 'B'	Perry Barr
Grid Reference	SP04688345	SP07959068	SP08499075	SP06708759	SP08108893	SP06099119
BH Id	S1	S7	S8	B30	S6	B28
BH depth (m bgl)	60.0	90.0	91.0	86.0	Unknown	76.2
Geologic layer	Bromsgrove	Kidderminster	Bromsgrove	Bromsgrove	Bromsgrove	Bromsgrove
Rest water level (m OD)	127.12	91.42	87.72	97.23	95.78	94.12
Date RWL measured	07-Jun-94	18-Mar-86	03-Dec-85	29-May-74	03-Dec-85	20-Dec-72
Length of available records	June 1994 – Feb 2008	March 1986 – Feb 2008	Dec 1985 – June 2003	May 1974 – Feb 2008	Dec 1985 – Feb 2008	Dec 1972 – Sept 2001

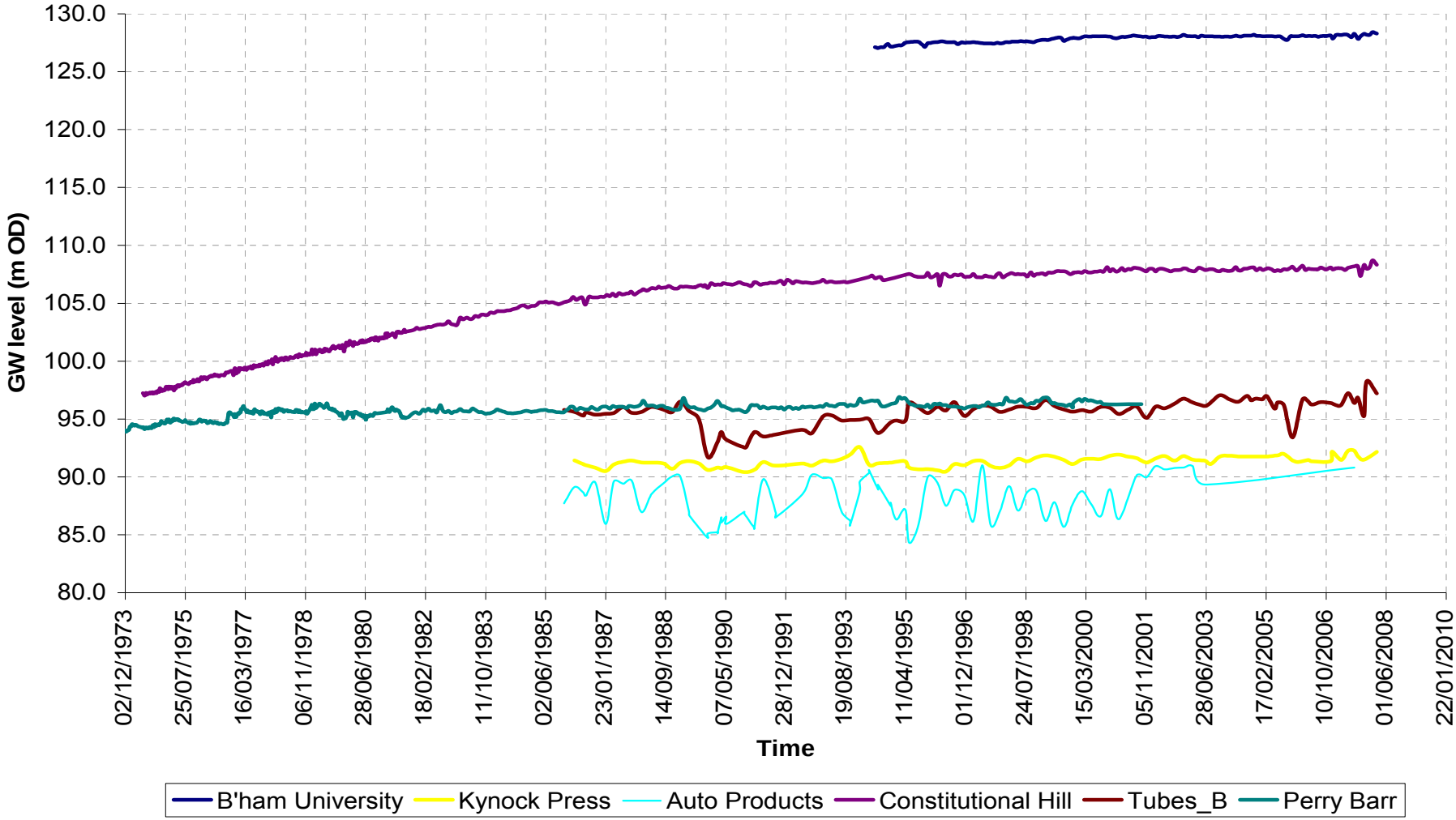

Figure 5.11: Groundwater hydrographs for the monitoring boreholes

5.1.11 Hydrogeochemistry

The inorganic, organic contamination and the pollution related acidification within the urban aquifer of Birmingham area have been respectively presented by Ford and Tellam, (1994), Rivett *et al.* (1990), and Ford *et al.* (1992). The authors describe the groundwater contained within the aquifers of the Permo-Triassic sandstones of the Birmingham urban area as not containing excessive contamination despite the fact that the city has a long established history of industrial activities. The chemistry of the waters within the Permo-Triassic aquifers has been influenced by a substantial number of potential sources of major and minor ions. Some of the sources include rainfall recharge, chemical composition of the aquifer materials, anthropogenic sources and land use patterns.

The analyses of groundwater samples obtained from the Permo-Triassic sandstone aquifers through pumped boreholes represent a mixture of the water samples drawn from the composite geological formations. Therefore, most of the results of the chemical analyses of groundwater within the sandstone formations represent the chemistry of the water of the composite formations.

Ford and Tellam (1994) shows that most groundwater samples obtained from the western part of the Birmingham fault contain Ca^{2+} and HCO_3^- as their dominant ions. Further to this, the groundwater within the Wildmoor sandstone Formation on the western part of Birmingham fault has relatively low pH and alkalinity, with SO_4^{2-} and Cl^- as the dominant anions, which are perhaps of anthropogenic origin. The waters underlying the Mercia mudstone group (adjacent to the study area) on the eastern part of Birmingham Fault contain Ca^{2+} and SO_4^{2-} as the dominant ions. Generally, based on the samples obtained from the pumped boreholes, only NO^{3-} and Ba^{2+} consistently show relatively high concentration values, and sometimes exceed the European Community Maximum Admissible Concentrations Standards for drinking water. The authors also observed a high correlation between the various localized anomalous ionic occurrences and the land use pattern. No regional pattern in the groundwater chemistry was concluded.

According to Rivett *et al.* (1990), chlorinated solvents are widespread within the groundwater of the Birmingham Triassic sandstone aquifers. Particularly, trichloroethylene concentrations of 30 – 5500 μg/l occur in 40 % of the sampled boreholes.

Also, the effect of the hydrogeological control on the distribution of the organic contaminants is apparent. Generally, a severe contamination occurrence is associated with the portions of the aquifer with relatively thin layers of superficial deposits and clayey content materials.

Ford *et al.* (1992) observed increasing pollution related to acidification of the groundwater within the Permo-Triassic sandstones. Shepherd *et al.* (2005) show that the groundwater obtained from abstracted wells within the Birmingham Triassic sandstone aquifer are of the Ca-HCO_3-SO_4 type, and with average pH value of 6.9. These findings agree with Ford and Tellam (1994) which attributed the dominant ionic concentrations to anthropogenic inputs.

5.1.12 Groundwater and surface water abstraction

The extensive Permo-Triassic sandstone that underlies the study area had previously served as a major source of water supply, especially in the wake of the British industrial revolution (Knipe *et al.* 1993). This has caused declination in the groundwater level within the sandstone aquifer. The estimated historical total groundwater abstraction rates for the Birmingham aquifer are presented in Figure 5.12. The peak of the abstraction rate was 78 Ml/day in 1940, and the subsequent periods experienced significant reduction in the abstraction rate. At the end of 1989, the peak abstraction rate has reached 11.7 Ml/day, and it appears (based on recent data) that only slight decrease has been recorded thereafter. This is partly caused by the decline in the manufacturing industries within the area. Currently, the aquifer is being exploited to support public water supply.

The available groundwater abstraction data for the boreholes within this study area starts in 1987, though it is probable that abstraction at these boreholes predates 1987. This dearth of data of the abstraction rates restricts the use of the actual historical abstraction rates in the model calibration. The pressure posed to the groundwater resources by the impacts of the climate change and the need to reduce global carbon and water footprints suggests that the downward trend in the abstraction rates is not likely to be reversed soon. Since the purpose of this modelling work is to assess future risk to groundwater resources, then it thought that the 1990 abstraction rates will be more representative of the future permitted demands. The available groundwater abstraction data were averaged for each of the borehole in order to obtain a constant daily rate and this value was used for both the

historical runs as well as the future predictions. The calculated average abstraction rates for each stress period are presented in Figure 5.13.

Also, there are 3 locations where surface water abstraction is being abstracted within the study area (Figure 5.1). The British Waterway and Birmingham City Council_1 (B'ham CCty_1) are from the Birmingham Canal and therefore no interaction with the underlying aquifer is assumed. The third location B'ham CCty is from a lined inland waters and also not represented in the model.

Figure 5.12 Historical abstraction rates for Birmingham area (Source: Knipe *et. al.*, 1993)

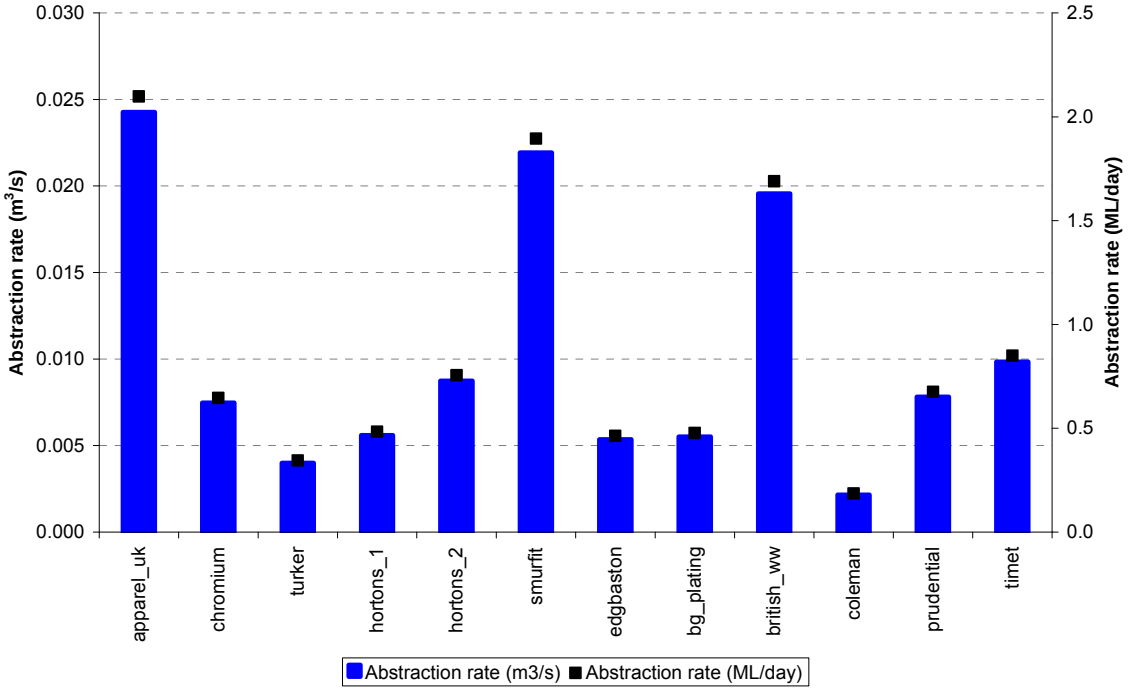

Figure 5.13: Abstraction rate for each stress period in the flow model

5.2 Recharge estimations

Daily recharge values were calculated for the study area using the Environment Agency Water Framework Directive recharge calculator spreadsheet (Environment Agency, 2007). The recharge calculator was developed through collaboration between the Environment Agency and the Scotland and Northern Ireland Forum for Environmental Research (SNIFFER). The flow chart for the recharge toolbox is presented in Figure 5.14. This is based on series of spreadsheet calculations using Food and Agricultural Organisation (FAO) methodology. The recharge toolbox provides the capability to quantitatively explore the influence of various catchment parameters on recharge estimations. However, the toolbox did not directly incorporate the capability to consider the effect of a possible delay factor that can potentially be caused by the thickness of the overlying superficial deposits.

The study area is divided into 12 recharge zones (Figure 5.17a) based on the distribution of the different soil types present. Each recharge zone is represented in the flow model using the zoning and multiplier capability of the MODFLOW 2000. These packages allow each model cell to be categorised into a zone, with associated multiplier factor which is used to scale the value of the recharge flux assigned to the model cell.

Figure 5.14: EA WFD recharge calculator (Environment Agency, 2007)

The multiplier factor is set to between 1.0 – 1.1 and 0.9 -1.0, for soil types with HOST value equal or less than 12, and for those greater than 12, respectively. The cell value for the multiplier factor was arrived at during the trial and error approach adopted for the model calibration. Furthermore, in order to represent the processes occurring within the unsaturated zone, a delay factor was applied to the recharge flux time series generated by the recharge toolbox to be infiltrated into the aquifer. The delay was implemented in the model by dividing the study area into two regions, based on the thickness of the unsaturated zone (Figure 5.18). The first region represents those areas where the thickness of the unsaturated zone is less than 15 m, while the second region represents those areas where the thickness of the unsaturated zone is greater than 15 m. The choice of two parts is to reduce complexity of the model. The length of delay applied is based on evidence

from examination of groundwater hydrographs and rainfall events. Buss *et al*., (2008) reviewed the groundwater hydrographs within the Birmingham and Lichfield groundwater bodies. The analysis shows that there is a lag time between the recharge events and the response in the observation boreholes. There appears to be a weak correlation between the thickness of the unsaturated zone and the time lag, but it is thought that given the high vertical heterogeneity of the sandstone formations, the lag may be controlled more strongly by the presence of low permeability horizons within the sandstone sequence. The analysis of the hydrographs shows that there is a lag time of 4 - 6 and 1 - 3 months, between the recharge events and the response in observation boreholes at patches where the unsaturated zone is greater than 15 m, and those where the unsaturated thickness is less than 15 m, respectively. Following the analysis of the lag times, the periods of time over which the recharge is estimated for the patches where the unsaturated zone is greater than, and less than 15 m are July 1969 – December 1989 and November 1969 – December 1989. The recharge time series outputs of the recharge toolbox over these periods are applied to the flow model calibrated over the period of January 1970 – December 1989. The shift in the time period is to account for the estimated delays caused by the unsaturated zone.

The detailed descriptions of the input data into the recharge calculator are presented in Table 5.7. A continuous daily rainfall data set spanning January 1961 – August 2005 is obtained for the Frankley Waterworks site (BNG: 400720E: 280150N) and presented in Figure 5.15. This time series data shows that the long-term average (LTA) annual rainfall for the study area is approximately 715 mm/yr. The study area is within the MORECS square 125 (Hough and Jones, 1997), and the daily PE data for the most recent forty-year period (1969 – 2009) is presented in Figure 5.16. The distribution of household numbers per recharge zone is presented in Figure 5.17b. The calculated daily time series recharge values for the two regions of the unsaturated zone thickness are presented in Figure 5.19 (a,b). No observable difference is indicated in the two outputs possibly because the lag times are not significantly different. The annual average recharge values for the two regions are 111.21 and 112.60 mm/yr, respectively. This time series gives average annual recharge value for the study area as 112 mm/yr or 67.8 ML/day, and represents the final recharge value distributed across each stress period in the flow model (Figure 5.19c). The recharge value of 112 mm/yr obtained in this work is comparable to 132 mm/yr (or 40 ML/day) obtained by Knipe *et al.*, (1993). Buss *et al*., (2008) obtained similar value of 121 mm/yr for year 1996 and relatively higher value of 431 mm/yr for year 2000.

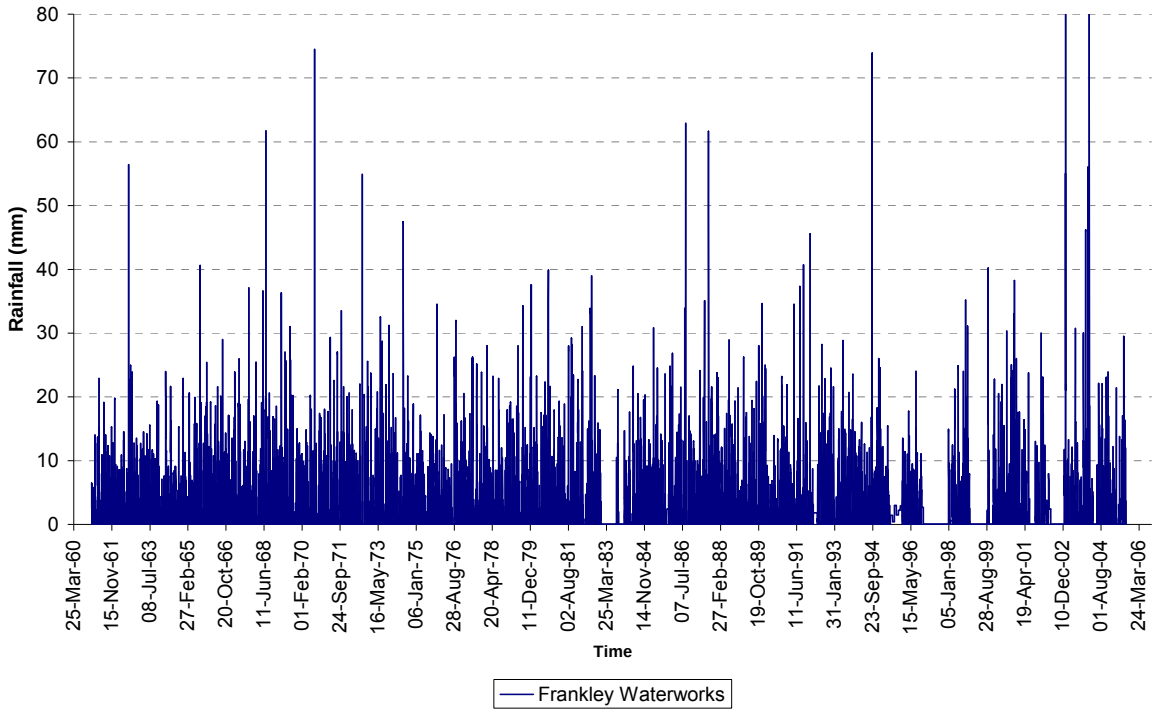

Figure 5.15: Daily rainfall data at Frankley Waterworks rainfall station

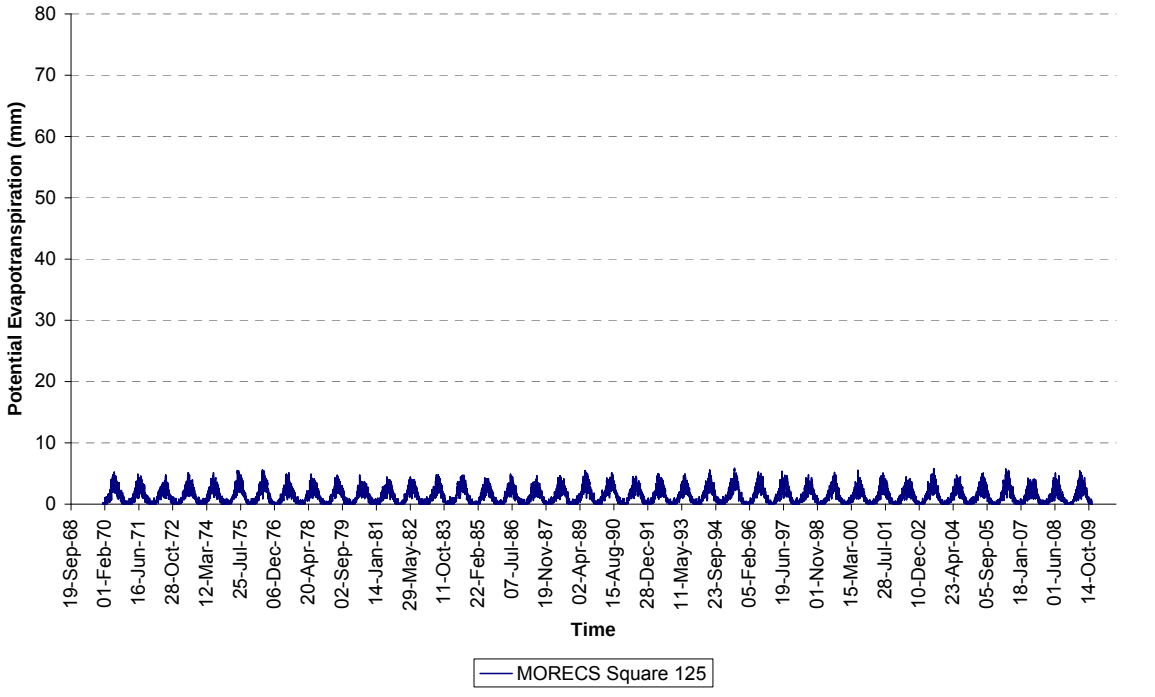

Figure 5.16: Daily potential evapotranspiration data for MOREC square 125

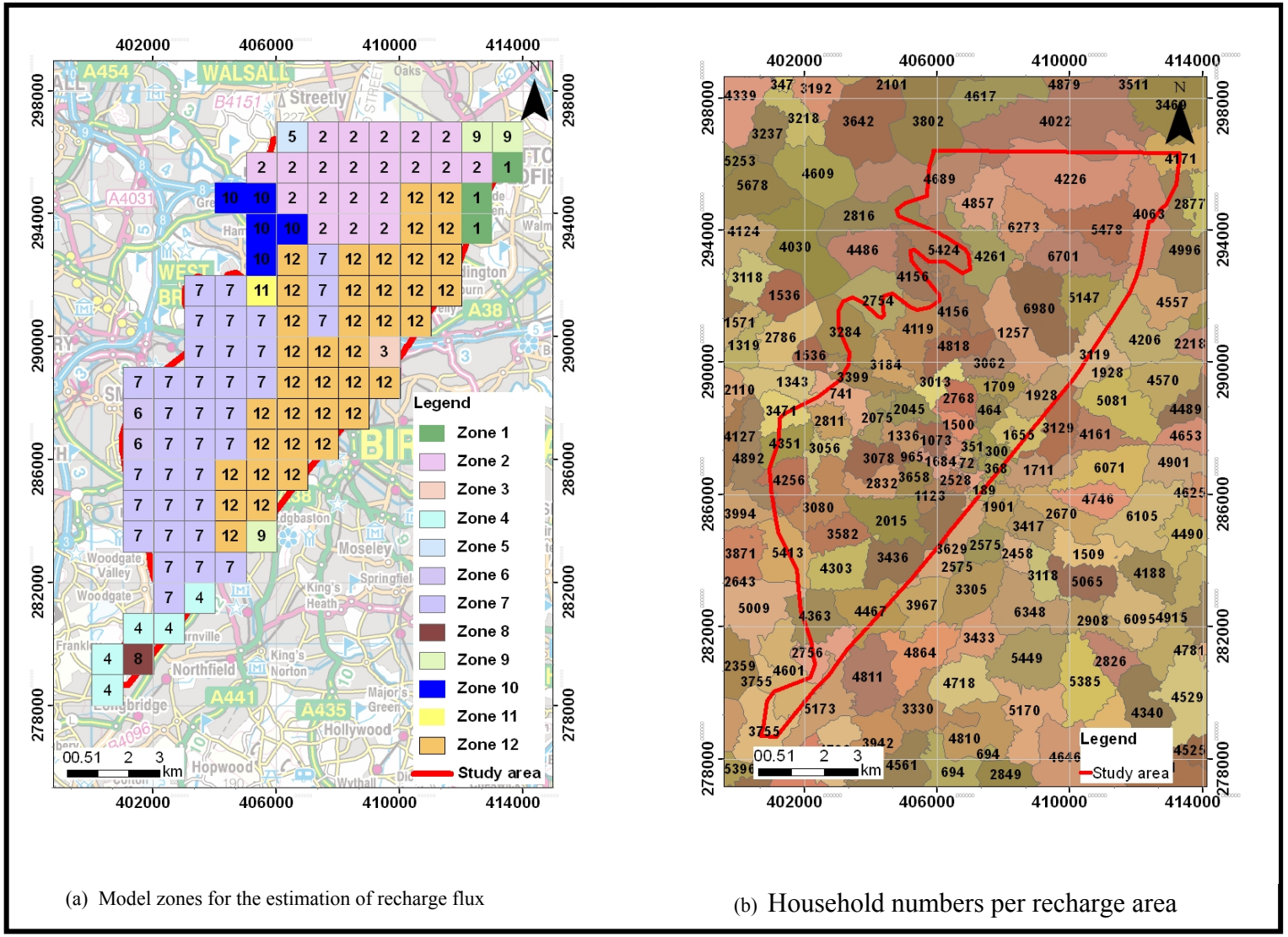

(a) Model zones for the estimation of recharge flux

(b) Household numbers per recharge area

Figure 5.17: Model zones and the associated number of the households

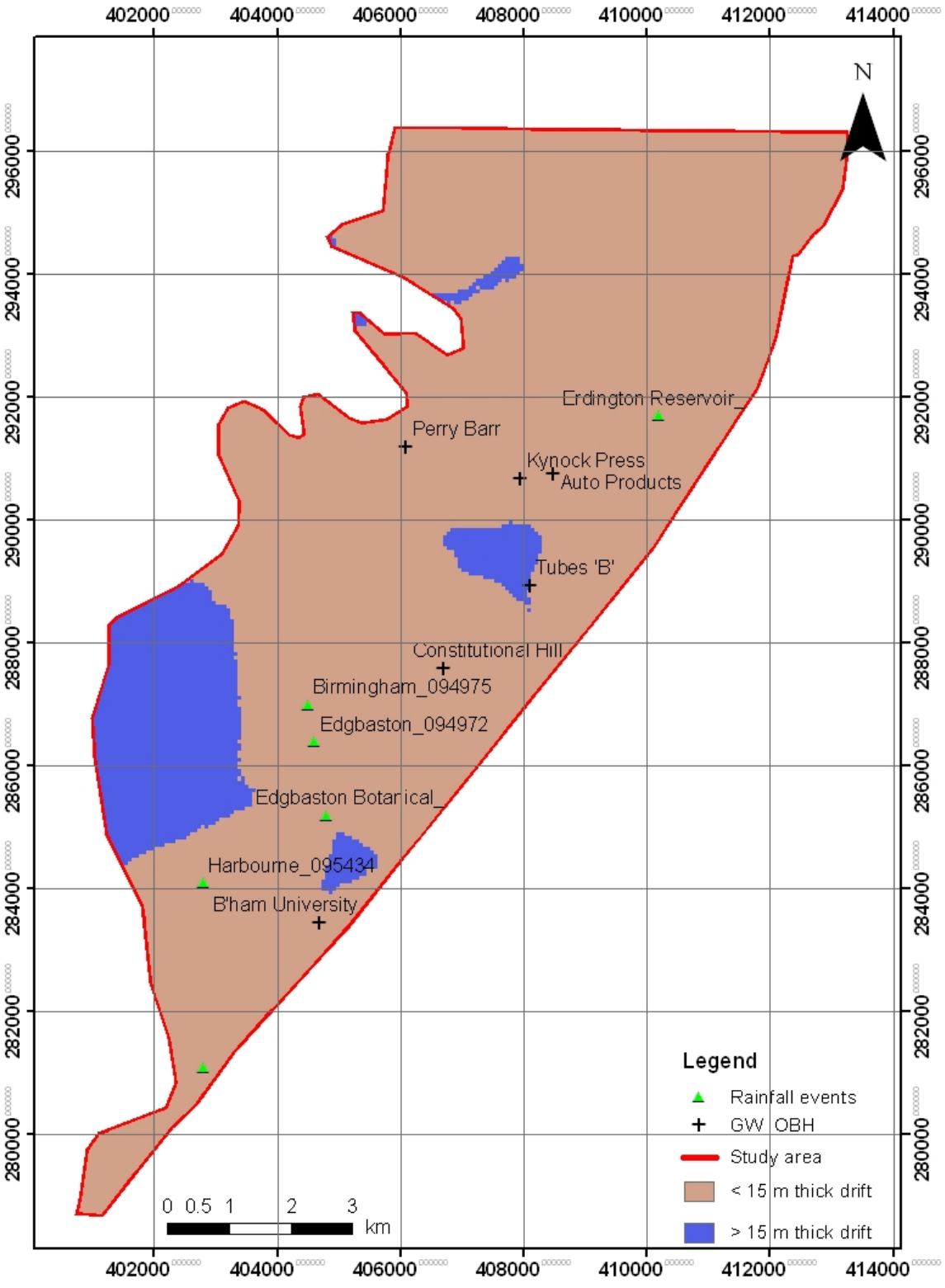

Figure 5.18: Classification of the thickness of the unsaturated zone

Table 5.7: Recharge calculator input data

No	Input Parameter	Value	Remarks
1	Groundwater Body	Study area (model domain)	This is used only for reporting purpose
2	Rainfall data	Frankley Waterworks Rainfall Station	See Figure 5.15. The period July 1969 – December 1999 was used for the estimation of the recharge flux for the model area.
3	Potential Evaporation data	Daily potential evapo-transpiration (PE) MOSES data for MORECS square 125	Potential Evaporation data was used for the estimation of recharge flux.
4	Total Zone Recharge Area (km^2)	221	This is the entire model area.
5	Soil Type	Silt clay loam	The dominant soil type for the model area is represented as Silt-clay-loam. See Table 5.1 for details. The recharge calculator toolbox links the soil type to the required soil properties in the estimation of the recharge flux
6	Land Use/Crop	Urban	The land use for the model area is urban. See Figure 5.9b. The recharge calculator toolbox links land use to corresponding properties in the estimation of the recharge flux. No crop type is used in this estimation.
7	Host Class	7	The partitioning of the processes between surface and ground-water is calculated using the host class of the soil. The assigned host class were obtained from the GIS based Environment Agency's version of the National Soil Resources

No	Input Parameter	Value	Remarks
			Institute. See Table 5.1 and Section 5.1.5 for details.
8	Name of SW Catchment	Plant Brooks_Borne Brooks_River Tame	This is the name of the WFD surface water body. It is used only for reporting purpose.
9	SW Catchment Area	3 % (0.51km^2)	This is estimated as percentage of model area.
10	Bypass Flows	0	This is the water that does not interact with the soil zone, and it is calculated as the percentage of rainfall. Sensitivity analysis (Buss *et al.*, 2008) shows that this has a large effect on the calculated recharge. Bypass flows of 20% increase the recharge by 13%. There are no field data to constrain the size of this parameter. Also, the HOST value indicates that the soil types have relatively high permeability therefore flow bypass is less likely to occur. Hence the value is set to zero.
11	Interflow (slow runoff)	70	This represents the portion of water that moves to surface water through the soil zone. A value of 30% was used in this work based on the superficial drift coverage (Figure 5.3b).
12	Urban area	95	This is the percentage of the recharge zone that is urban (see Figure 5.9b).
13	Area of paved cover	55	The percentage of urban area that is covered by impermeable layer. This is estimated as percentage of urban area
14	Snow cover	5	This is the percentage of zone area covered by snow during the winter months. It is estimated as percentage of total area.
15	Mains Leakage - Total no of Properties	310882	Estimated from Figure 5.17b
16	Mains Leakage-Leakage (m^3/property/day)	0.02573	This represents additional recharge flux from mains leakages. The parameter is

No	Input Parameter	Value	Remarks
			calculated from two variables namely the total number of households per recharge zone, and the leakage per household. Knipe *et al.* (1993) suggested a value of 8.5 Ml/d for 1989 recharge to the aquifer from service leakages. The leakage per household value is obtained as follows: Estimated total number of properties: 310882; Estimated daily leakages from mains services (*Knipe et al*. 1993): 8000 m^3/day; Estimated leakage per property: 8000 / 310882 = **0.02573** m^3/day/property
17	Surface Water Leakage – Area (km^2)	0.51	This is the estimated recharge zone area covered by surface water.
18	Surface Water Leakage -- Bed Coefficient (m/day)	1	Bed Coefficient is the amount of daily leakage of surface water into groundwater. A default value of 1 m/day is used.
19	Crop type and parameters	Crop type: The study area is classified as continuous urban (see Figure 5.9b & Table 5.1), and therefore crop type was not used in the estimation of the recharge flux. Kc Coefficient: This is the combined soil and crop coefficient. Zr Coefficient: This is rooting depth. Depletion factor, cropping dates & percent cover: These values are not used in the estimation of the recharge flux because of the urban landuse classification.	

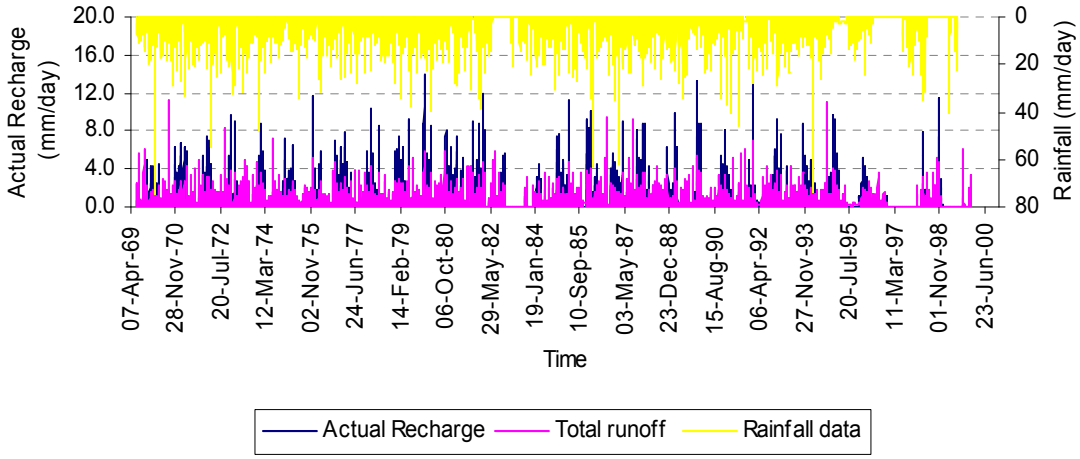

(a) Unsaturated zone greater than 15 m

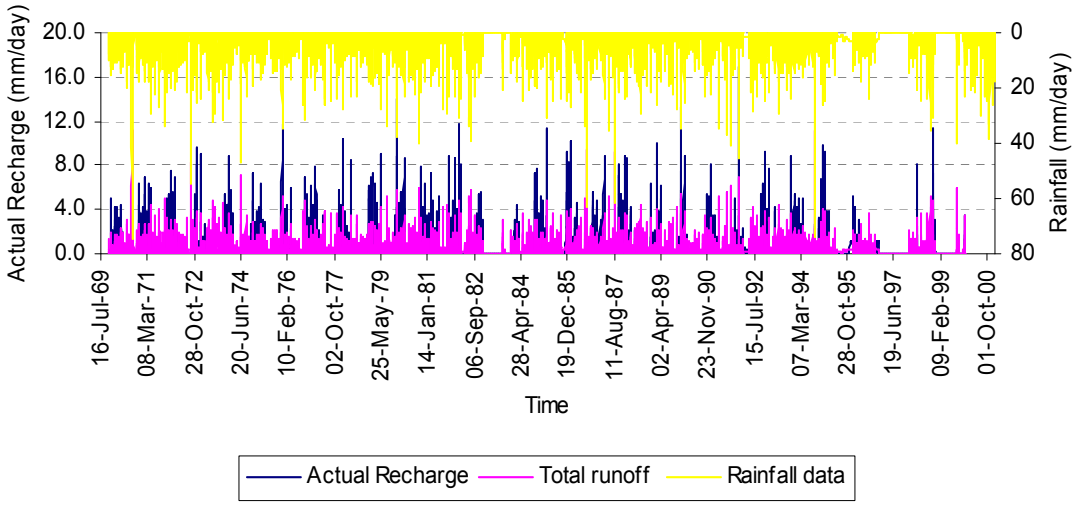

(b) Unsaturated zone lower than 15 m

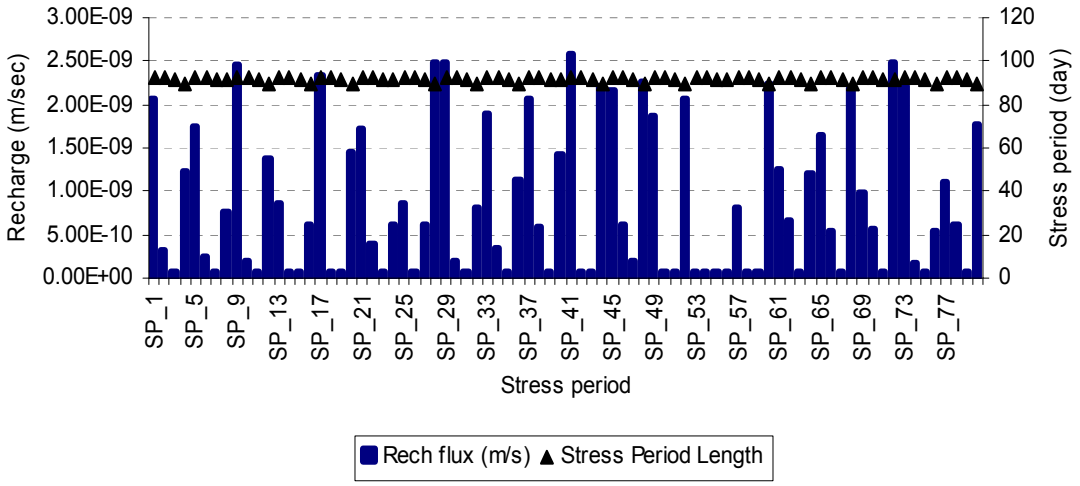

(c) Final recharge values for each stress period

Figure 5.19: Model recharge values

5.3 Conceptual understanding of the study area

This section presents the conceptual framework of the study area through the synthesis of the lithological, hydrological and geological data. It presents the understanding and interpretations derived from the acquired geological and hydrological information, as well as the literature.

The borehole lithological data indicates that three major sandstone aquifer horizons underlie the study area. The basal aquifer unit is the Kidderminster sandstone Formation, overlain by the Wildmoor and Bromsgrove sandstone Formations. The acquired data as well as the literature suggest that the three sandstone aquifer horizons have distinct hydrogeological properties, and therefore are represented as distinct layers in the model development. The drift geology, which is widely varied both in composition and thickness, overlays the Bromsgrove Formation. The drift deposit consists of clayey, sand, gravel and alluvium material. The drift is not considered as a separate model layer in this work, but as part of the thickness of the first model layer (Bromsgrove sandstone Formation), and acts much as an extension to the unsaturated zone. Although, considering the drift deposit as a separate layer could improve the proper representation of the layer, however it thought that this would involve a significant amount of additional work that is beyond the scope of this work.

The lithology of the aquifer materials suggests the existence of hydraulic connectivity between the groundwater and the surface water. Hence, head-dependent flow between the sandstone aquifer and the surface waters is incorporated into the model development. The presence of the Birmingham fault demarcates the eastern and southern boundaries of the aquifer geometry. The fault acts as a low permeability barrier and therefore restricts the easterly component of the groundwater flow across the study area. The western boundary is defined by the presence of Westphalian Formations, which are essentially crystallised rocks and coal measures. These geologic materials are considered to inhibit flow across them. The northern boundary of the model is also defined as no flow boundary. According to Knipe *et al.* (1993), this boundary corresponds to a surface water divide along a ridge of higher ground and a groundwater divide along an anticlinal axis on the base of Triassic sandstones. Land (1966) described this boundary as the line that separates the Lichfield groundwater unit to the north and the Birmingham groundwater unit to the

south. The river depths are relatively shallow and therefore are considered to be contained within the first layer.

Based on the LTA (1961 – 2005) annual rainfall data for the Frankley waterwork station, the average annual rainfall for the study area is 715 mm/yr. The EA WFD recharge calculator predicts the average annual actual recharge and evapotranspiration over the study area to be 112 mm/yr (or 67.8 ML/day) and 376 mm/yr, respectively. Generally, the data available for the site conceptualisation is considered to be sufficient for this work. However, the depth elevation of the individual aquifer horizon of the Sherwood sandstone represents areas where a dearth of field data poses degree of uncertainty.

5.4 Description of the numerical groundwater flow model

This section presents a description of the setting up and calibration of the flow model. The U.S. Geological Survey numerical finite-difference groundwater flow model MODFLOW 2000 forms the basis for the model development and the subsequent calibration process. Detailed description of MODFLOW-2000 has earlier been presented in Section 3.7.1. This section describes how each of the hydrologic condition is represented in the model.

5.4.1 Pre- and post-processing utilities

The preparation of the input data and the presentation of the modelling output are largely based on manipulation within both the ArcGIS 9.1 and GRASS GIS 5.7 software. This is also largely complimented by customised FORTRAN utility programs, Microsoft Excel and MS WordPad. Table 5.8 lists the specific applications of each utility.

The detailed description of GRASS GIS is documented at the official GRASS site (GRASS site, 2004). The package was originally developed by the US Army Construction Engineering Research Laboratory (CERL) in 1985 – 1995, in Champaign, Illinois to support land management at military installations (Neteler and Mitasova, 2004). Baylor University continued the development of GRASS after CERL stopped its development in 1995, and released version 4.2 in 1997. At the moment however, the development of GRASS has become a collaborated Open Source project. GRASS currently possesses the capability to provide tools for raster, vector and point analyses as well as surface visualization and image processing. The open source nature of GRASS has provided the capability for users to customize the package according to specific needs. On the other

hand, ArcGIS 9.1 is a proprietary, industry standard, Microsoft Windows environment based, GIS package. The detailed description of the capabilities of ArcGIS is presented by Ormsby *et al.,* (2001).

5.4.2 Setting up of the flow model

The selected MODFLOW 2000 packages that are combined together in this model development are listed in Table 5.9. The detailed descriptions of the packages are contained in McDonald and Harbaugh (1988) and Harbaugh *et.al.* (2000).

Table 5.8: Utility roles in the preparation of input and output model data

Name of utility	Pre/post data functionality
MS Excel	1. Prepare database to create shapefile within GIS 2. Prepare data to be saved in another format readable by the model. 3. Post processing of model output
ArcGIS 9.1	1. Prepare geo-referenced data for presentation 2. Prepare geo-referenced data for export into GRASS GIS
GRASS GIS 5.7	1. Interpolation of discrete data into raster format 2. Export of spatial discrete data as MODFLOW compatible cell values. 3. Setting up of the regions in order to obtain the required number of row and columns
MS WordPad	Preparation of model input data
Fortran utilities	Sorting, filtering, formatting, generation of model input data in the required syntax, etc

Table 5.9: List of MODFLOW packages used in the flow model

MODFLOW Package	MODFLOW file type	Description
Named file	NAM	It activates all the capabilities of the model setup
Global output file	GLO	It contains information that applies to model run as a whole
List output file	LIST	It contains information from the Groundwater Flow Process that appears within the Parameter Estimation Loop
Basic	BA6	Provides overall program control
Layer Property flow package	LPF	It is an internal flow package that computes the conductance coefficients and storage. It calculates terms of finite difference equations which represent flow in a porous medium, specifically flow from cell-to-cell and into storage.
Discretization	DIS	It enables capability for spatial and temporal model framework
Horizontal Flow Barrier	HFB6	It provides the capability to simulate thin, vertical, and low-permeability geologic features within the model domain
Zone	ZON	It allows only some of the model cells of a layer to be associated with a layer parameter value.
Well	WEL	It adds terms representing flows to wells in the finite difference equations, thereby enables hydrological capability for abstraction from and recharging into boreholes/wells.
River	RIV	Enables hydrological capability for interactions between surface water and groundwater
Recharge	RCH	It adds terms representing spatially distributed recharge to the finite difference equations, thereby enables hydrological capability for the recharge process
Preconditioned Conjugate Gradient	PCG2	It iteratively solves the system of finite difference equations using the Pre-Conditioned Gradient solver.
Output Control	OC	It controls the details and frequency of model output in a flexible way using words rather than code.
DATA	DATA	To save formatted data onto files

5.4.3 Stress periods and time steps of the flow model

The two time intervals used in modelling are the stress periods and the time steps. The stress period is the time interval during which the boundary conditions for external stresses are constant, while the time steps are intervals during which model calculations are made. In MODFLOW-2000, the user specifies the number and length of the stress period(s) as well as the corresponding number of time step(s) for each of the stress period. The length of the first time step is computed by the model. Where the user intends to use the same length of time step in any given stress period, the model divides the length of the stress period (*PERLEN*) by the number of time step (*NSTP*). However, where subsequent time steps are intended to be calculated as multiples of initial time step within any given stress period (i.e. *TSMULT* > 1.0) then the model uses Equation 5.2 to calculate the length of the first time step.

$$\Delta t = PERLEN\left(\frac{TSMULT - 1}{TSMULT^{NSTP} - 1}\right) \qquad 5.2$$

where

Δt : length of the first time step [t]

PERLEN: length of the stress period [t]

TSMULT: user defined time step multiplier.

NSTP: number of time step

The model developed in this Chapter has been set up to run under transient conditions covering 20 years from January 1970 to December 1989, for the purpose of model calibration. The average length of the stress period is 90 days, making a total number of 80 stress periods. Each stress period is in turn divided into nine time steps, corresponding to approximately 10-day time step. The total number of time step is 720.

5.4.4 Spatial grid and vertical layering of the model

In MODFLOW-2000, the spatial grid dictates the model cell sizes, which in turn determines the overall model resolution. The spatial grid and vertical layering provide the required mathematical framework for the development and execution of a numerical model. The spatial grid of the model has been setup using 760 rows and 600 columns, with cell dimensions (Δy and Δx) of 25 x 25 m, making a total of 456,000 cells and

covering 221 km^2. The origin of the grid is the upper left hand corner, which corresponds to 400000E and 296000N of the British National Grid.

The model is set up as three layers representing the constituent aquifer horizons namely, Bromsgrove, Wildmoor and Kidderminster Formations. These layers represent model layer 1, 2 and 3, respectively. The three layers are defined in the groundwater model as varying saturated thickness. The ground surface and the base elevations of the Kidderminster, Wildmoor and Bromsgrove have already been presented in Figures 5.2a, 5.5a, 5.6a and 5.7a respectively.

5.4.5 Boundary conditions of the flow model area

The interface between the model domain where hydraulic heads are computed and the surrounding environment is referred to as the model boundary. The mathematical expressions of the boundary conditions are required for a well-posed modelling problem. The specification of the condition of each cell within the model area is permitted in MODFLOW through the *ibound* array, where a cell can be designated as variable, constant head, or no-flow/inactive.

The aquifer geometry within the model area is defined using variable active cells while other areas of the model domain that are outside the aquifer geometry are defined using no-flow boundary cells. The selection of the model active cells is based on the consideration of the complexities of the aquifer geometry, distribution of the available data, as well as the desire to optimize the model domain by taking advantage of the natural boundaries and constraining computation efforts. Although, the entire model boundary is defined by both the variable and no-flow model cells, the finite difference equations are solved only for the variable (active) cells.

The model boundary cells are defined as no flow boundaries. The boundary conditions are necessary to isolate the aquifer geometry which is the actual area of interest. The flows across the eastern and the southern boundaries of the aquifer geometry are restricted by imposing low hydraulic conductivity values along the fault paths, using the Horizontal Flow Barrier Package. The imposed restriction is due to the presence of Birmingham Fault, which is assumed to inhibit flow across it (Section 5.1.8). The presence of the Westphalian Formations (Figure 5.3a) along the western parts of the site supports the

choice of the defined no-flow cells along the western boundary of the model. The northern boundary of the model is also defined as no flow boundary because of the presence of surface water divide along a ridge of higher ground and a groundwater divide along an anticlinal axis on the base of Triassic sandstones (Knipe *et al.*, 1993).

5.4.6 Initial conditions of groundwater elevations

The initial groundwater heads within the aquifer horizons are interpolated from the rest water levels already presented in Table 5.6, and the interpolated heads across the study area are presented in Figure 5.20. The interpolation technique used is presented in Section 3.3.2. Where the river path exists, the initial groundwater head is set to equal to the river stage.

5.4.7 Initial estimate for aquifer hydraulic properties

The hydraulic properties that were assigned initial values prior to the model refinement procedures are the hydraulic conductivities (both horizontal and vertical), as well as the specific yield and specific storage. The initial values used are obtained from Buss *et al*. (2008) as presented in Table 5.5. These initial values are subsequently optimised during calibration process in order to obtain a good match between the field and calculated groundwater heads.

5.4.8 Zone Package

The model setup utilizes the zoning capability of MODFLOW-2000. One zone file, rchzones, was created (see Figure 5.17a), and it allows recharge values to be distributed across the 12 recharge zones.

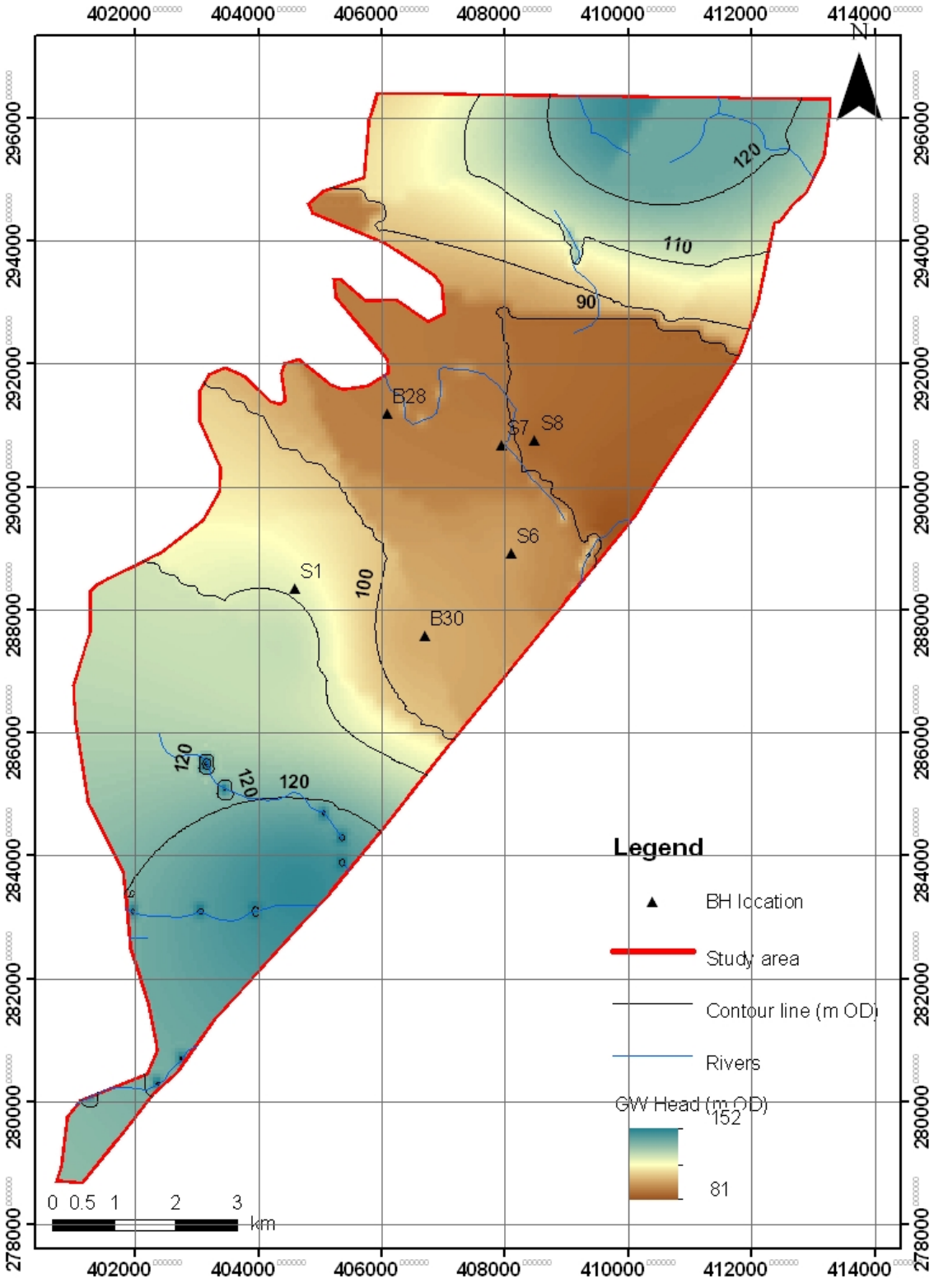

Figure 5.20: Initial groundwater head within the aquifer horizons

5.4.9 Model representation of the rivers

The rivers present within the model domain are contained within the first layer. The MODFLOW-2000 head dependent river package allows the model to calculate the amount of streambed percolation and groundwater inflow to each river reach, using river bed conductance and the difference between the calculated model cell hydraulic head and the stage of the river.

The river paths contained within the model boundary (see Figure 5.1) were divided into reaches. The interaction with the underlying aquifer is simulated between each reach and the model cell that contains that reach. The basic input data include the conductance of the river bed, river stage, and the river bottom elevation. The river bed conductance interfaces the surface and groundwater system. According to Allen *et. al.,* (1997), the rivers within the model domain are underlain by the river terrace materials.

The MODFLOW river bed conductance controls the rate of flow to or from the river according to the difference between the river stage and the modelled groundwater head in the uppermost active cell. River bed conductance also defines the maximum leakage rate to the aquifer when heads fall below the bed of the river, and it can be estimated using Equation 5.3.

$$Riverbedconductance = \frac{K}{b} A \qquad 5.3$$

where:
K is the hydraulic conductivity of the river bed material
b is the thickness of the river bed
A is the cross sectional area of the river bed

Very little information is available regarding the conductance of the river bed. Entec (2001) carried out water resources investigations for the parts (Worfe, Stour and the Penk catchments) of the West Midlands Permo-Triassic sandstone. The purpose of the investigation was to develop understanding of the water resources systems of the area and help the Environment Agency to manage the systems effectively and sustainably. As part of this study, the field river conductance values were estimated to vary from 70 m^3/d per metre head difference per cell (200 x 200 m cells) for most of the smaller brooks, to 350

m^3/d/m/cell for the Penk, 500 m^3/d/m/cell for the Stour, Smestow Brook and Worfe, and 1000 m^3/d/m/cell for the Severn. All the rivers within the current study area are assumed to be small rivers, and therefore, an initial value of 70 m^3/d per metre head difference per cell (25 x 25 m) or $1.296x10^{-5}$ m/s was used and progressively adjusted during the refinement of the model.

Also, no river bed survey data were available. Therefore the river bed elevations of the MODFLOW river cells were estimated from the digital elevation map (DEM), and assumed to be 1.0 m below the ground surface. The rivers within the study area are represented in the model by using the river package of the MODFLOW 2000. This package specifies the river stage at the beginning of the simulation and held constant throughout the simulation. The river stage was assumed to be 0.5 m above the estimated river bed. It is thought that the use of stream flow package will provide a more flexibility in the representation of the rivers because the river stages could be allowed to be calculated based on the flow rates during the simulation. Also, there may be some uncertainties associated with the values used for river bed conductance in the model.

5.4.10 Well Package

Groundwater abstraction constitutes a key element in this model because it represents a major component of groundwater outflow from the model domain. The MODFLOW-2000 well package is a constant flux boundary condition that allows a user-defined quantity of water to be added or removed from any active model cell. This package was used to simulate pumping from the 12 abstraction boreholes located within the model domain (Figure 5.1).

Historical data (see Figure 5.12) shows that the peak abstraction rate was 78 Ml/day in 1940, and subsequent periods experienced significant reduction in the abstraction rate. At the end of the 1989, the peak abstraction rate has reached 11.7 Ml/day. The Environment Agency records show that the available groundwater abstraction data for the abstraction boreholes within the study area starts in 1987, though it is probable that groundwater abstraction at these boreholes predates 1987. However, this dearth of data of the abstraction rates restricts the use of the actual historical abstraction rates in the model calibration. The available groundwater abstraction data were averaged for each of the borehole in order to obtain a constant daily rate and this value was used for both the

historical runs as well as the future predictions. The calculated average abstraction rates for each stress period are presented in Figure 5.13.

5.4.11 Recharge

The recharge to the groundwater system occurs both as infiltration from precipitation and as leakages from the mains services. The EA Water Framework Directive Recharge Calculator (Environment Agency, 2007) was used to estimate the daily recharge into the aquifer. The recharge package of the MODFLOW then applies the recharge flux calculated for each stress period from the daily recharge values onto the model. The recharge flux used in the flow model for each stress period is presented in Figure 5.19c.

5.4.12 Solver package and model acceptance criteria

The MODFLOW-2000 solver Package adopted for this work is the Preconditioned Conjugate Gradient 2 (PCG2). A detailed documentation of PCG2 is presented by Hill (1990). The PCG type solution method is more robust when compared to other solver packages (Hill *et al.* 2000). The maximum number of outer and inner iterations was set to 100 and 50 respectively. The convergence criterion for the hydraulic head observations was set to 0.01 m. The PCG2 MODFLOW-2000 package iteratively refines the initial estimates of the solution until either an acceptable measure of residual is achieved or the difference between the results of successive iterations is less than a user specified convergence criteria. The model is said to converge when the maximum absolute change in groundwater head in all the cells is less than the convergence criteria.

Five of the groundwater level monitoring data presented in Section 5.1.10 as well as Table 5.6 and Figure 5.11, were used as targets for assessing the effectiveness of the calibration process. The observed and simulated data were compared, and the criteria considered for model acceptance are the residual between the simulated and the observed values, the user defined convergence criteria, and the matching trend between the observed and simulated data, based on the simulated equivalent produced by the Observation Process of the MODFLOW-2000 Package.

5.4.13 Calibration of the numerical flow model

The initial values for the hydraulic properties of the flow model are based on the final calibrated model of Buss *et al.* (2008) because of the overlap that exists between the

northern part of the case study area used in this work and the southern part of the Buss *et al.* (2008) model.

The conceptual model was setup based on the understanding of the geology, hydrology and hydrogeology of the study area, and forms the numerical framework of the model. The model was calibrated by minimizing the residuals between the observed and the simulated groundwater head data using trial and error approach. This is coupled with the graphical analysis of the model fit and constrained by the conceptual understanding of the study area. This process was aided by the Observation Process of the MODFLOW 2000 which calculates the simulated equivalents of the observations and compares the observed values with the simulated equivalent values. The plot of the observations and the corresponding residual is presented in Figure 5.21c.

The river package requires data for the river boundary gain or loss along the length of a river, defined by the river reaches. This requires a minimum of two points of measurement on the river stretch in order to calculate the observed river boundary gain/loss. In this work, the available data for river levels at Brookvale Road and Walsall Road covers March 2000 – January 2009 (see Table 5.2). These ranges of data are outside the time period used for the model calibration. The flow and level data at Perry Park are therefore not sufficient to allow for flow observation to be incorporated in the calibration process of the flow model. The hydraulic heads are the only field observation data used to compare the simulated values. These include groundwater head observations obtained from five monitoring points (see Figure 5.11). The Birmingham University borehole has water level data that covers June 1994 – February 2008, and therefore are not used for model calibration. The model is refined with data spanning over 20-year period, from January 1970 and December 1989. Subsequently, the Observation Process of MODFLOW 2000 was used to calculate simulated equivalents of the observation and compares the measured field data with the simulated equivalents. Table 5.10 summarises the model data for both the pre and post calibration processes, and detailed input files are contained in appendices A11.1 – A11.20.

A detailed description of the solid geology of the study area has been presented in Section 5.1.3. The borehole logs, geological cross sections as well as reviewed literature (Powell *et al.*, 2000; Allen *et. al.,* 1997) suggest that the principal lithostratigraphic formations

have distinct hydrogeological characters. Therefore each of this formation is represented as a distinct layer within the model framework. The Bromsgrove, Wildmoor and Kidderminster Formations consist largely of sequences of sandstone layers, interbeded with argillaceous sediments, which limit vertical hydraulic conductivity and retard the vertical movement of groundwater within these formations. Refinement of both the horizontal and vertical hydraulic conductivities of the constituent formations of the Permo-Triassic sandstone were carried out on a regional based scale, and the groundwater model is considered to accurately simulate the observed groundwater levels within the study area (see Figures 5.21c and 5.25). Hydraulic layering within the Permo-Triassic sandstone aquifer is thought to account for the large vertical anisotropy in the final calibrated hydraulic conductivity values. Comparative values for the vertical hydraulic conductivities are also reported around the West Midlands-Worfe area (Entec, 2001).

The percentage numerical error values for the flow model are presented in Figure 5.21a, while the volumetric budget is presented in Figure 5.21b. The simulated groundwater heads and associated drawdown distributions for the study area at the end of the 20-year simulation are presented in Figures 5.22 – 5.24, for layers 1 – 3, respectively. The plot of field observation data against the corresponding simulated data for the 5 observation boreholes are presented in Figure 5.25.

Table 5.10: Summary of initial and final flow model data

S/n	Input parameter	Initial Value	Source of data	Final Value
1	Elevations (m OD)	Distributed values	Borehole records from British Geological Survey (Figures 5.2a, 5.5 – 5.7)	Same as initial value
2	Boundary Conditions	No flow conditions for the west, east, north and south boundaries.	Dictated by site geology and extent of the area of interest.	
3	Geometry	3 Layer model; 1: Bromsgrove sst Formation; 2: Wildmoor sst Formation 3: Kidderminster Formation	Model conceptualisation	
4	Spatial discretization (m)	No of rows: 760; No of columns: 600; $\Delta x=25$; $\Delta y=25$	Model conceptualisation	
5	No of abstraction boreholes	12	Model conceptualisation	
6	Abstraction rates (m^3/day)	Varied, (see Figure 5.13)	Environment Agency	
7	Observation boreholes and levels	5 boreholes, see Figure 5.11 for groundwater levels time series	Environment Agency	
8	No of river reaches	3051	Model conceptualisation	
9	River bed conductance (m/s)	1.296×10^{-5} m/s	Entec, 2001	9.2593×10^{-6} m/s
10	River stage (m OD)	Varied	Calculated from surface elevation data to be 0.5 m above the estimated river bed	

11	River Bottom (m OD)	Varied	Calculated from DEM and topographic contours to be 0.5 – 1.0 m below the surface elevation	Same as initial value
12	Recharge rate (m/s)	Recharge rates for stress periods are presented in Figure 5.19c.	Calculated, using the Environment Agency WFD Recharge Calculator	
13	Horizontal hydraulic conductivity (m/s)	Bromsgrove Fm =5.787×10^{-6} Wildmoor sst Fm =2.315×10^{-5} Kidderminster Fm =3.472×10^{-5}	Initial values taken as the final calibrated value for the Lichfield sandstone Model (Buss *et al.* 2008)	
14	Vertical hydraulic conductivity (m/s)	Bromsgrove Fm =5.787×10^{-8} Wildmoor sst Fm =1.157×10^{-7} Kidderminster Fm =5.787×10^{-8}	Initial values taken as the final calibrated value for the Lichfield sandstone Model (Buss *et al.* 2008)	
15	Groundwater abstraction rates	Values for stress period presented in Figure 5.13 for individual borehole	Return data obtained from the Environment Agency	
16	Specific yield	Bromsgrove Fm = 0.12 Wildmoor sst Fm = 0.10 Kidderminster Fm = 0.12	Initial values taken as the final calibrated value for the Lichfield sandstone Model (Buss *et al.* 2008)	
17	Specific storage	Bromsgrove Fm =1×10^{-4} Wildmoor sst Fm =5×10^{-4} Kidderminster Fm = 1×10^{-4}	Buss *et al.* 2008	
18	Hydraulic conductivity across the vertical barriers (m/s)	1.0×10^{-12}	Model refinement	1.0×10^{-9}

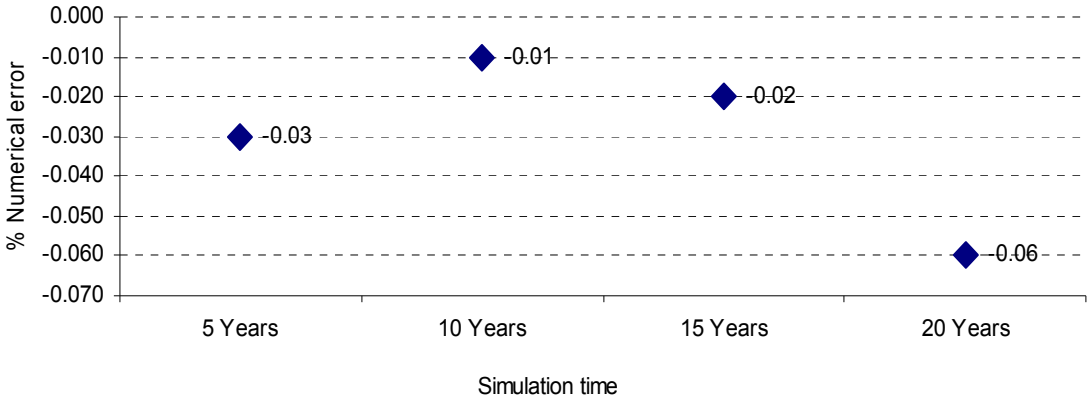

(a) Volumetric numerical error for calibrated flow model

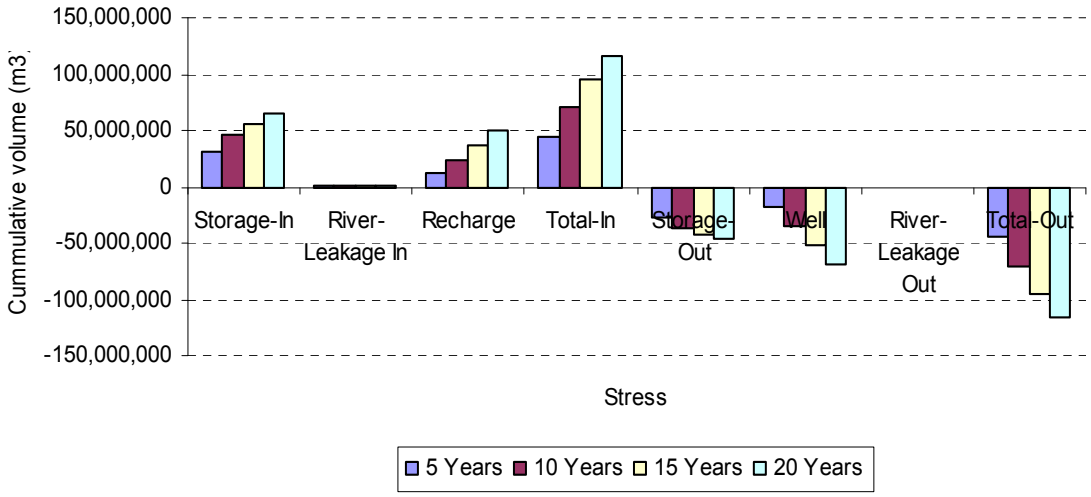

(b) Volumetric budget for calibrated flow model

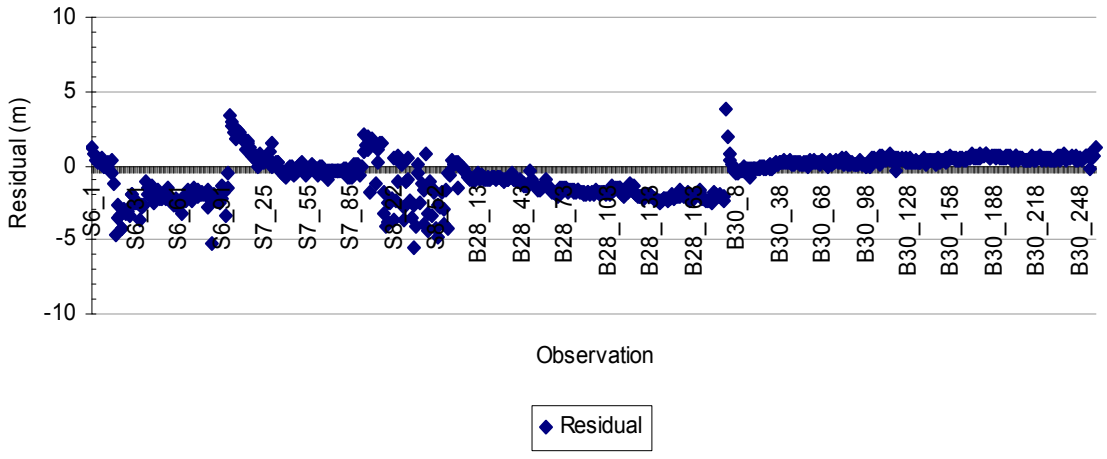

(c) GW head against the residual after the model calibration

Figure 5.21: Graphical analysis of the model fit

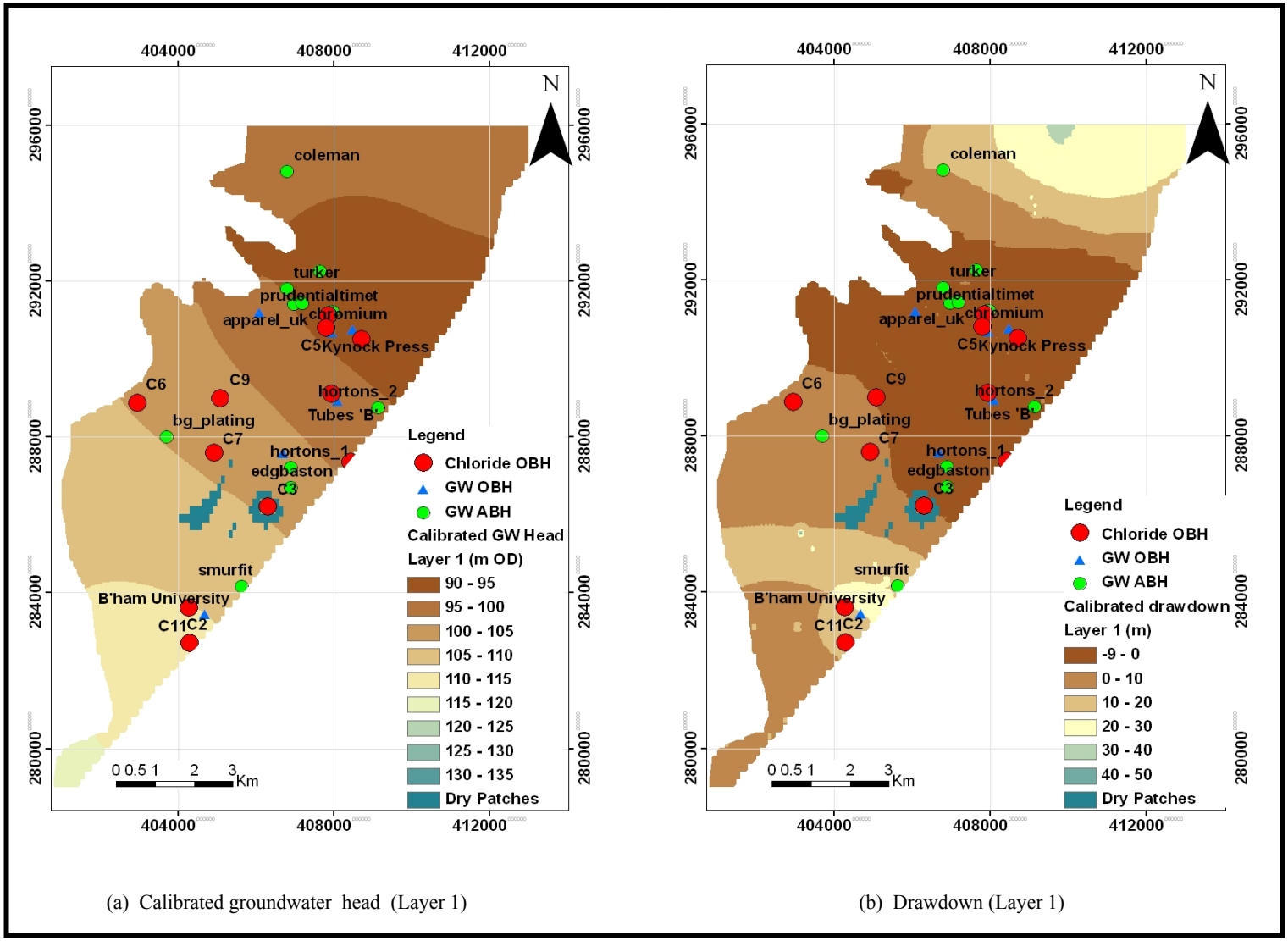

(a) Calibrated groundwater head (Layer 1)

(b) Drawdown (Layer 1)

Figure 5.22: Calibrated head and drawdown in layer 1 after 20 years

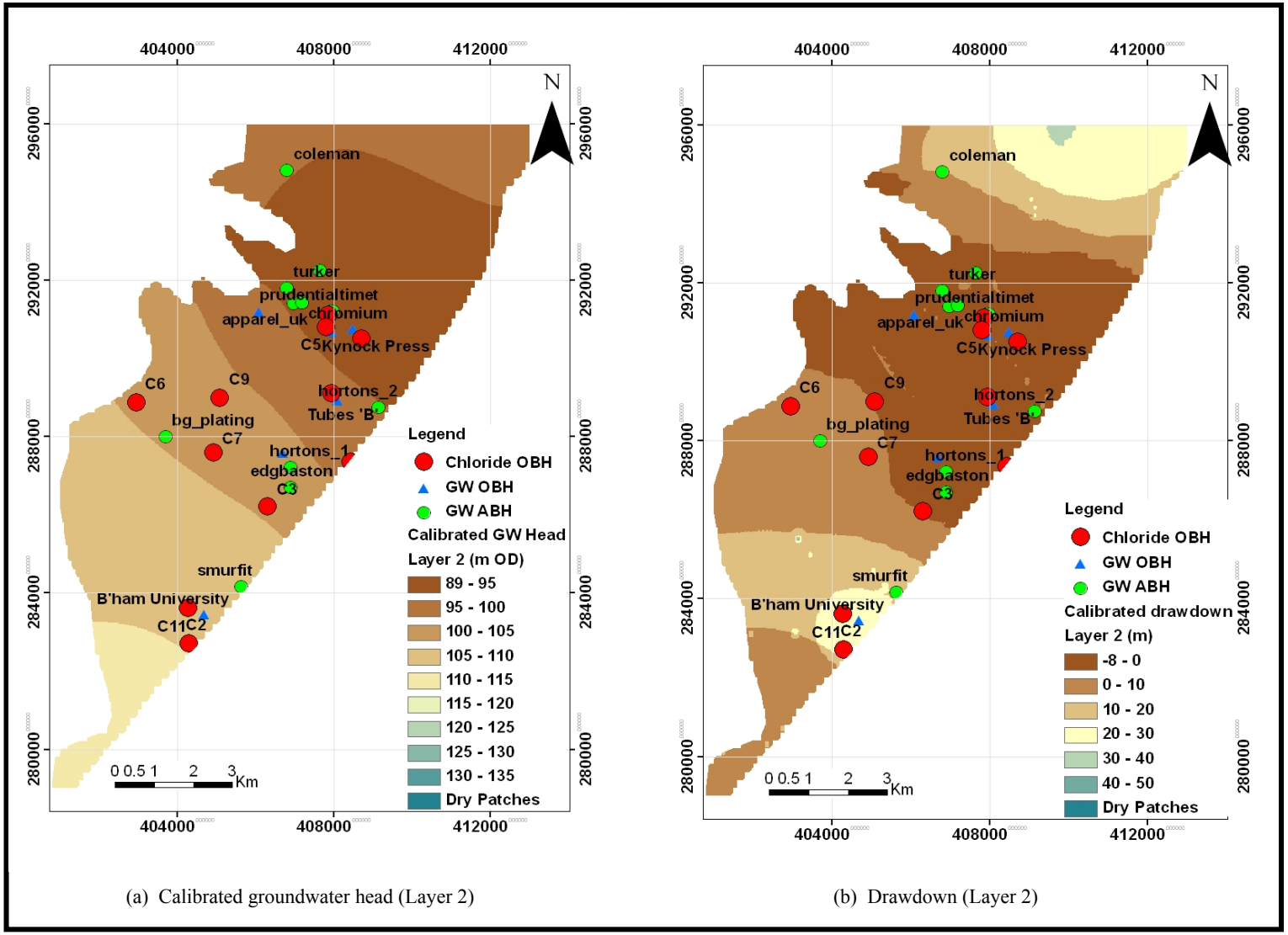

(a) Calibrated groundwater head (Layer 2)

(b) Drawdown (Layer 2)

Figure 5.23: Calibrated head and drawdown in layer 2 after 20 years

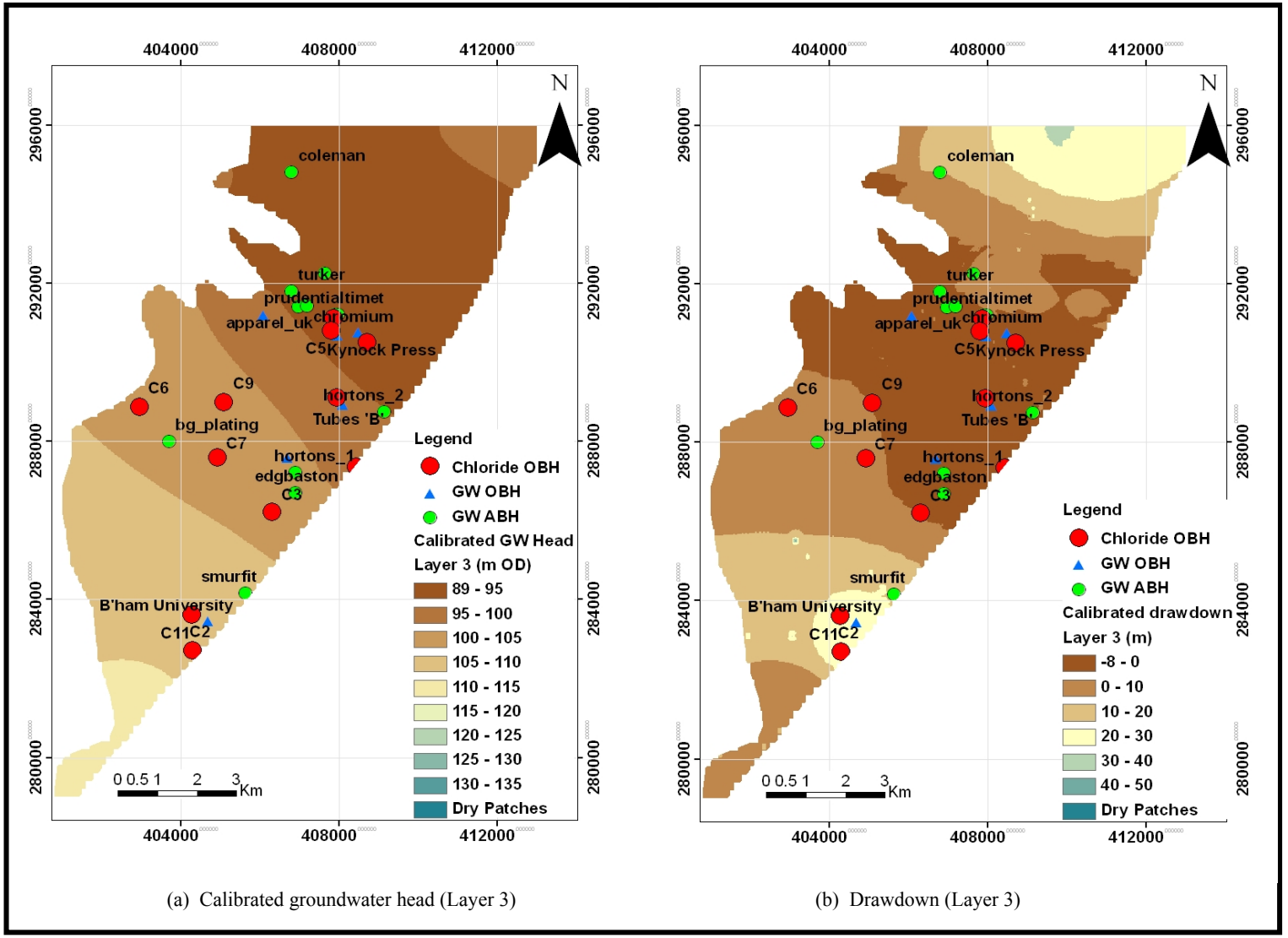

(a) Calibrated groundwater head (Layer 3)

(b) Drawdown (Layer 3)

Figure 5.24: Calibrated head and drawdown in layer 3 after 20 years

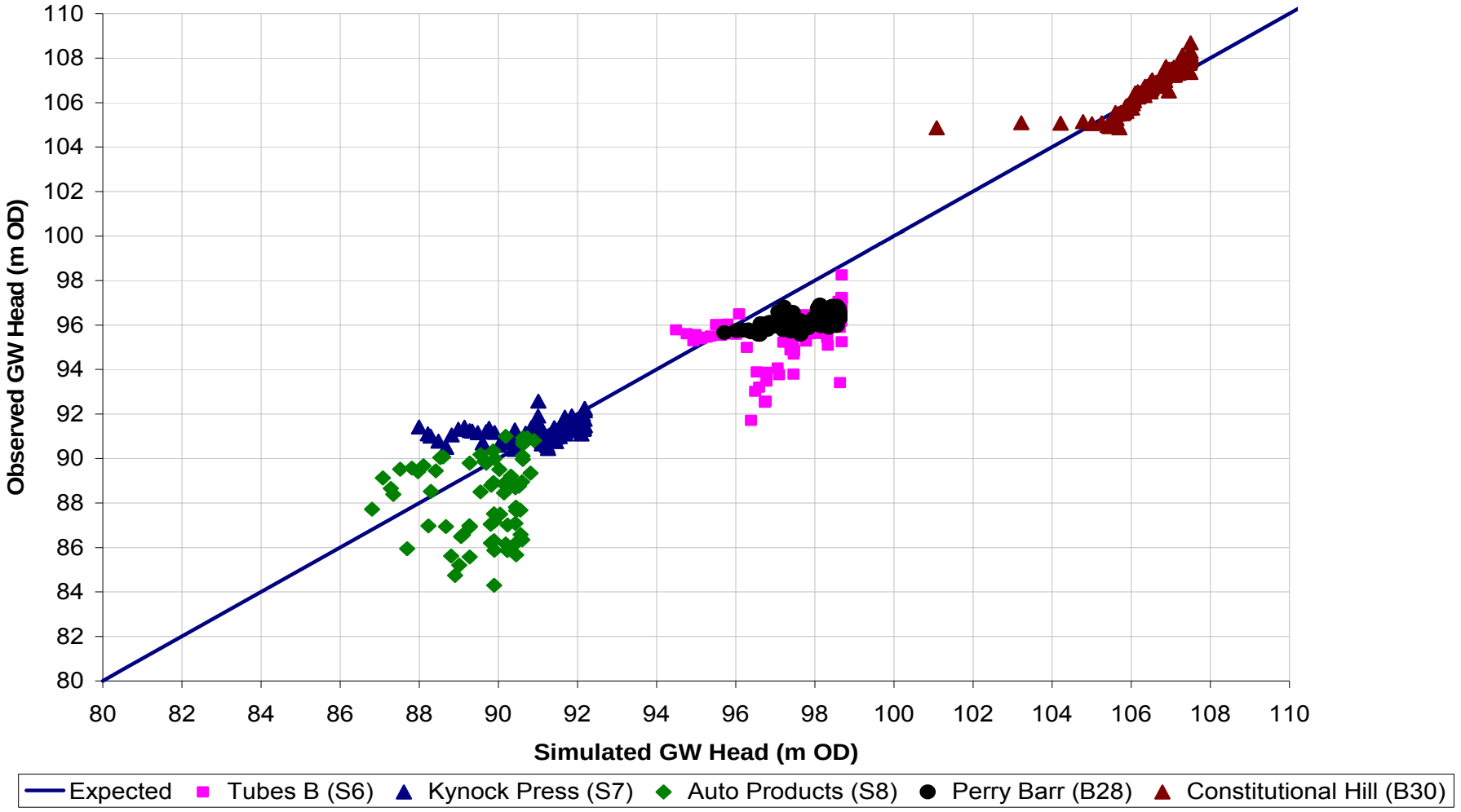

Figure 5.25: Observed and simulated groundwater heads

5.5 Risk Assessment Method

The risk assessment method integrates the flow model, risk model and the transport model.

5.5.1 Groundwater flow model in the risk assessment method

In order to determine the risk to the groundwater resource, the flow model was setup to run under transient conditions covering 30 years from March 1985 to February 2015. The simulation length consists of 120 stress periods, with the length of each stress period varying between 90 – 91 days. Each stress period is in turn divided into nine time steps, corresponding to approximately 10 days time step length. The total number of time steps is 1080. In order to obtain the initial conditions for this predictive simulation, the head distribution obtained from the calibration runs was used. The corresponding groundwater head computed at the beginning of March 1985 (stress period number 60) of the calibrated transient flow model is presented in Figure 5.26, and were set to be the initial groundwater heads for model layers 1 - 3 under predictive transient simulation. The required additional model input files for the predictive simulation are presented in appendices A12.1 – A12.10. The groundwater heads and drawdown distributions after 30 years (March 1985 – February 2015) of the simulation are presented in Figures 5.27 – 5.29.

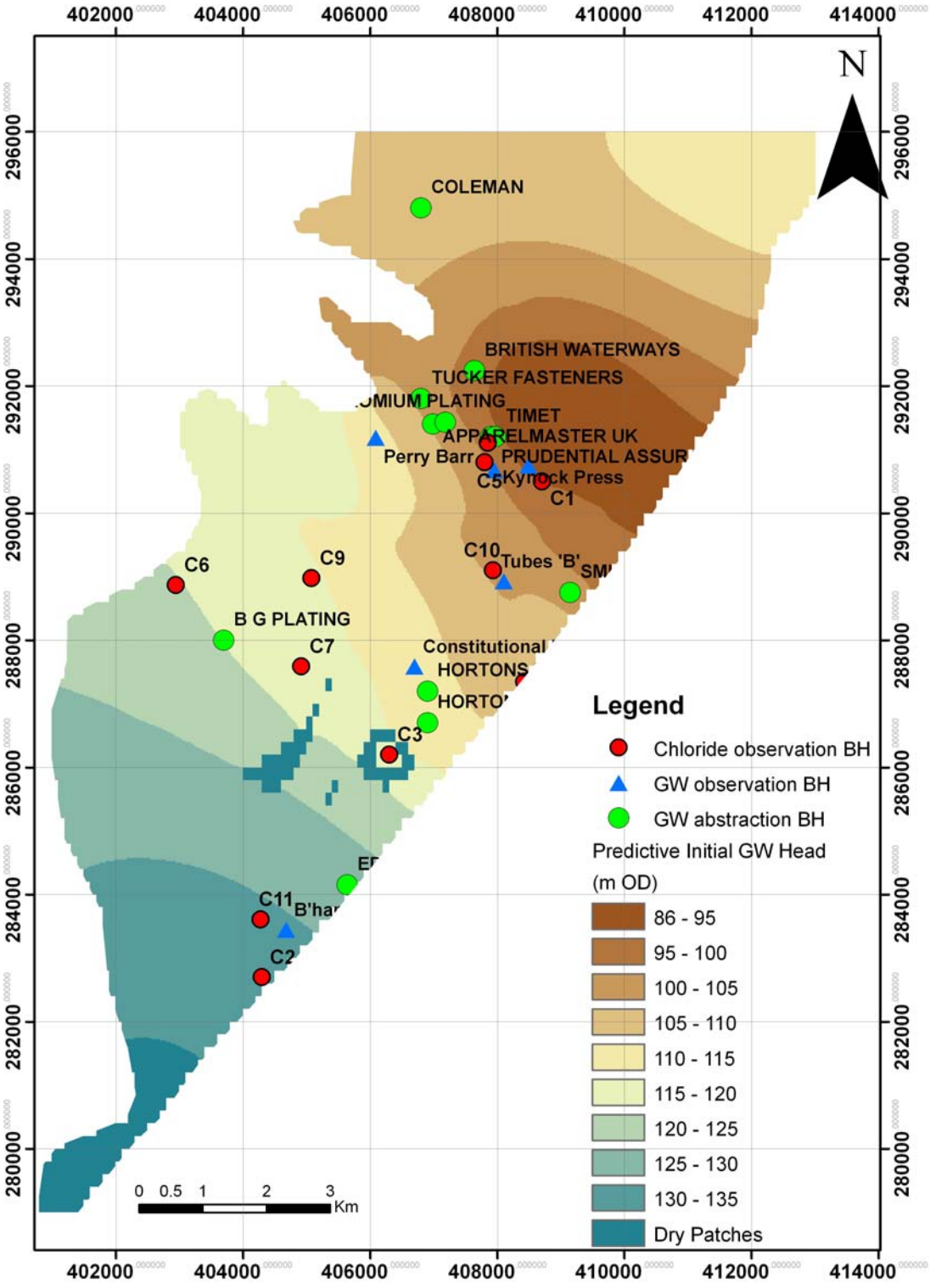

Figure 5.26: Initial (March 1985) groundwater head for predictive model

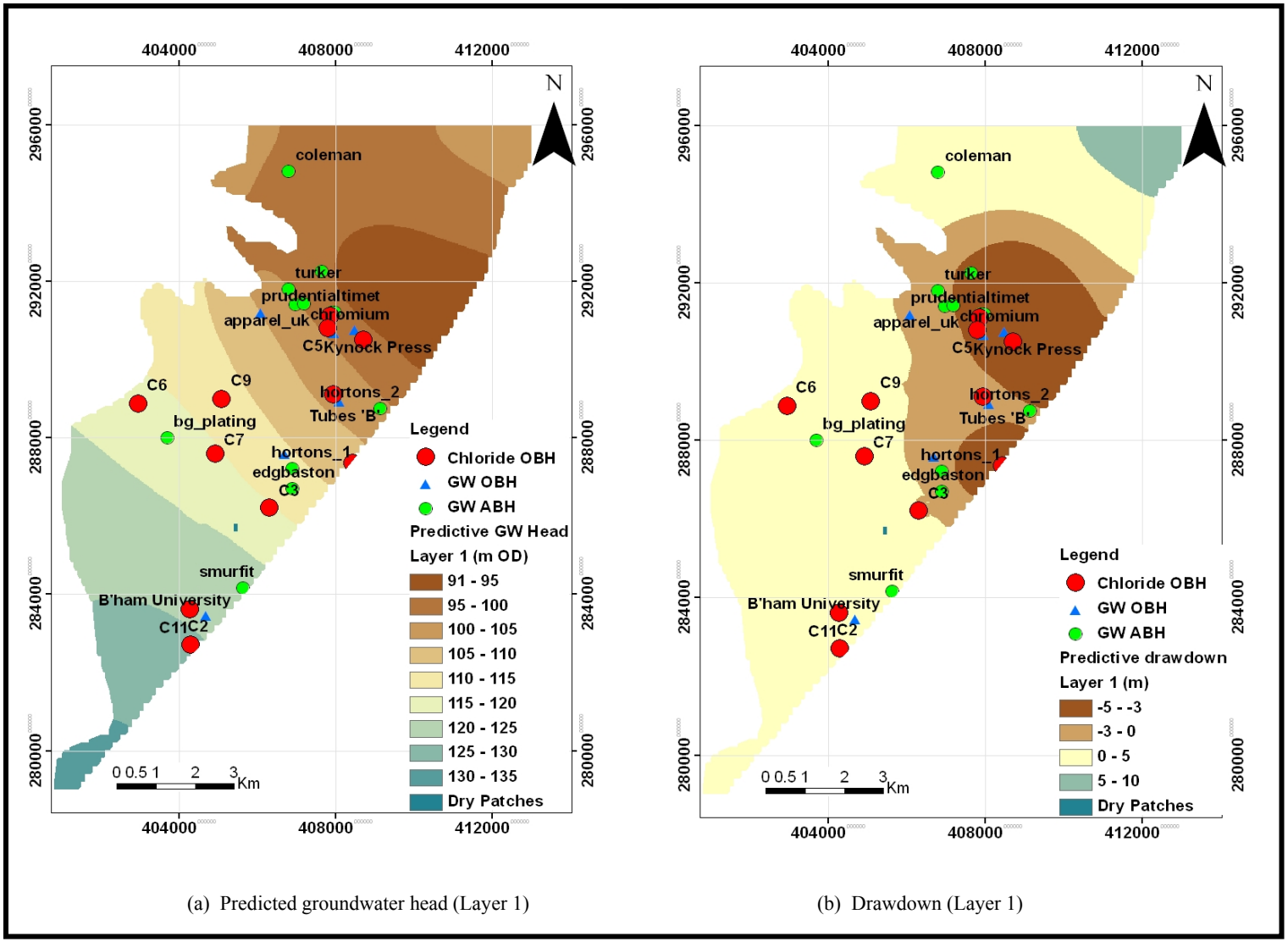

(a) Predicted groundwater head (Layer 1)

(b) Drawdown (Layer 1)

Figure 5.27: Predicted head and drawdown in layer 1 after 30 years

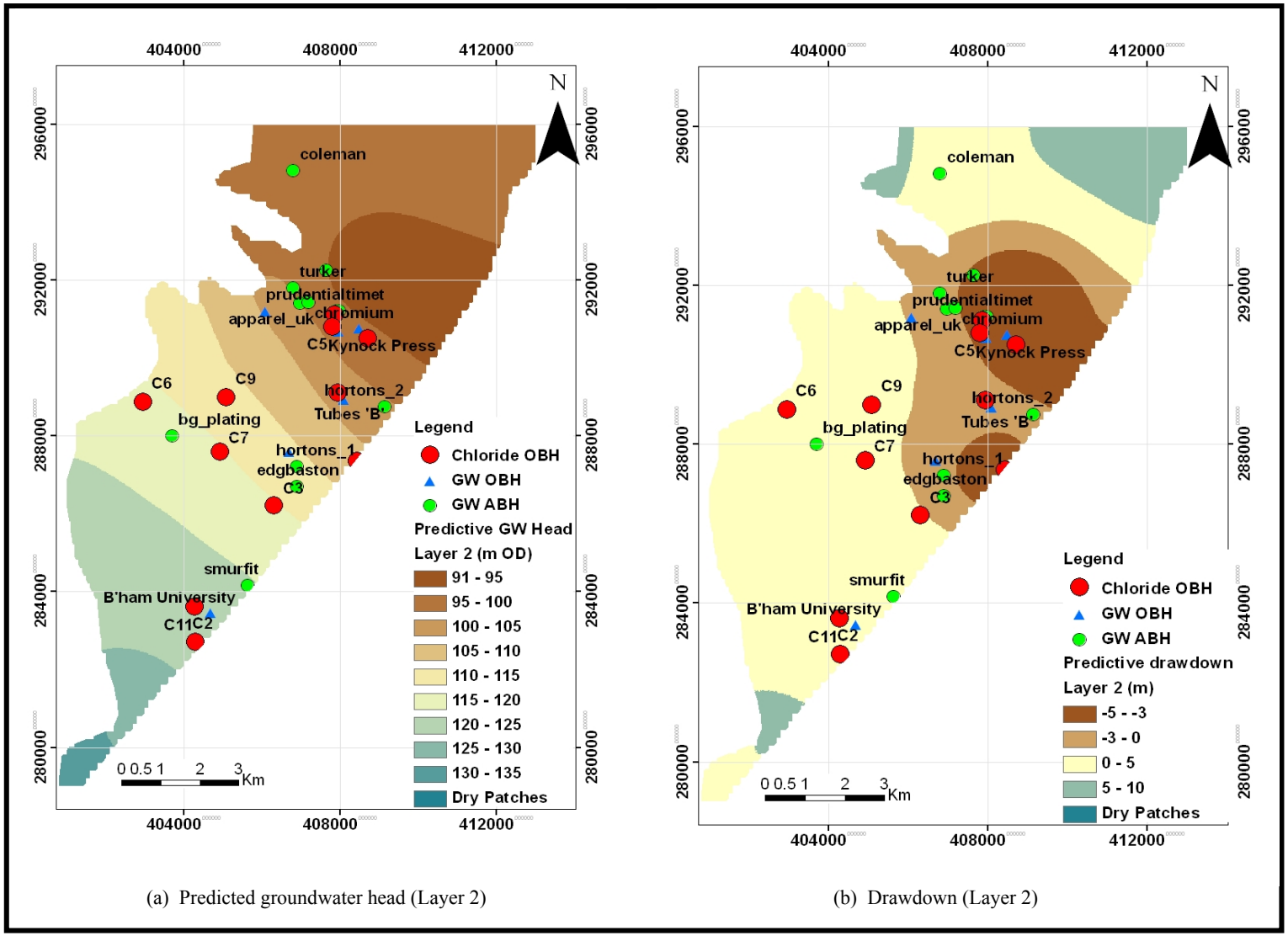

(a) Predicted groundwater head (Layer 2)

(b) Drawdown (Layer 2)

Figure 5.28: Predicted head and drawdown in layer 2 after 30 years

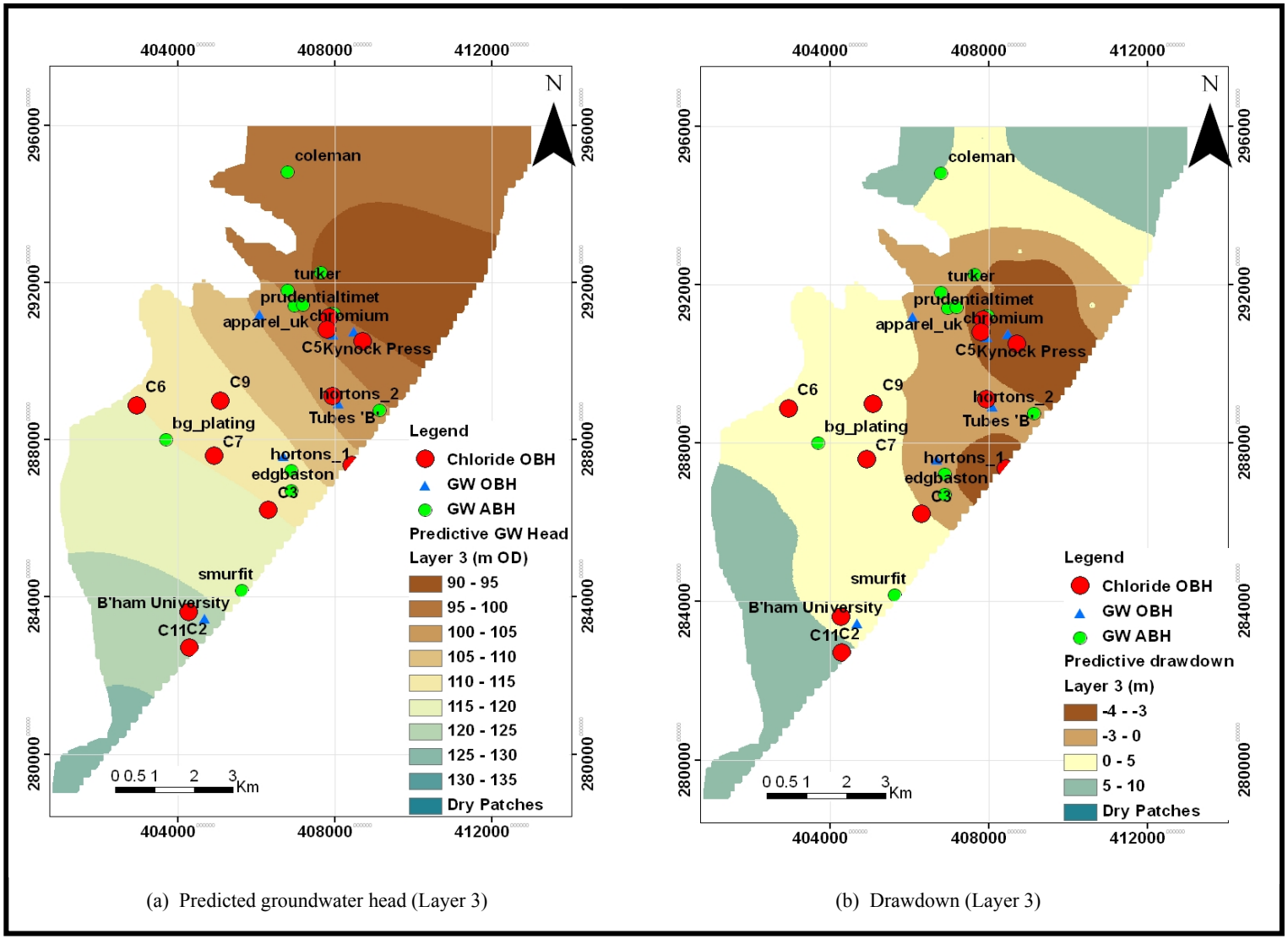

(a) Predicted groundwater head (Layer 3)

(b) Drawdown (Layer 3)

Figure 5.29: Predicted head and drawdown in layer 3 after 30 years

5.5.2 Risk model

This section demonstrates the application of the risk model, using the field data. The risk model was set up in a format presented in Chapter 3. The synthetic source terms were generated for the same period of time (March 1985 to February 2015) as the flow model. The field applications involve the scoping, reviewing and compilation of all the possible sources of chloride related pollutant within the study area. This required applying numerical values to the qualitative descriptions. For example, Table 3.1 shows that 250 – 5000 kg of chloride pollution is qualitatively described as Minor pollution.

The National Incident Recording System (NIRS) of the Environment Agency (EACD, 2006), is a data capture tool that supports pollution incident management across the England and Wales. This tool is underpinned by a Microsoft Access database and it contains records of occurrence of pollution incidents, and how they were managed. The Environment Agency is a statutory Agency for ensuring regulatory compliance of the Government environmental policies. Most of the records of previous occurrence of pollution incidents since the organization's establishment are therefore expected to be captured by this database. As part of this work, all the available records (i.e. 2002 – 2009) within the NIRS database were searched for the occurrence of chloride related pollution incidents in Birmingham area. The results are presented in appendix A9.4, and summarised in Table 5.11 and Figure 5.30a. The length of the available records of pollution incidents is considered to be sufficient in the demonstration of the applicability of the risk assessment method presented in this work. However, it is thought that longer record length will be more representative of the historical occurrence of pollution incidents within the study area.

The NIRS presents the records of the historical pollution incidents using qualitative descriptive terms. Therefore, it was necessary to estimate the quantitative loading rate of mass of the chloride contaminant that is capable of causing the corresponding effects described by the NIRS database and Table 3.1 was used for this purpose. The search of the NIRS database was complimented by further search of the internet for the locations of the industries that could possibly act as potential sources of chloride pollution within the study area. The websites searched include the UK Birmingham Business Directory as well as the People, Businesses and places (192.com). In order to keep the model simple, this work

considered pollution sources from only five commonly available industries within the Birmingham area, and these include food, chemical, garages, mining and mineral industries. The British National Grid references of the scoped potential sources of pollution were imported into the basemap within the GIS environment, in order to determine their locations in terms of the row and column numbers. This was required to allow their representations into the risk model.

The results presented in Table 5.11 were used to compute the Probability of Pollution Occurrence (PPO) for the study area, and these show that the average number of chloride related pollution incidences from the selected industries for the study area is 35 events per stress period of 91 days. The total number of pollution sources (both potential and actual) is 281. Using Equation 3.3, the probability of pollution occurring at any of the sources over a given stress period of 91 days is computed as:

$$PPO = \frac{35/281}{91} = 0.0014$$

This calculated PPO was applied to each of the active nodes for each stress period. The risk model input files are presented in appendices A9.1 – A9.3 and summarised in Table 5.12. The distribution of the generated synthetic contaminant sources and the number of the generated sources per stress period are presented in Figure 5.31. The effects of the generated source terms are observed over a period of 30 years at the observation boreholes shown in Figure 5.30a. Although, the method as demonstrated in this work assumed that all the industry types have the same probability of pollution occurrence across all of the stress periods. However, this method can be setup to assess the risk from the individual type of industry with varying probability of pollution occurrences per stress period for each of the industry.

Table 5.11: Scoping analysis of pollution incidence

Parameters	Value	Comments
List of industries considered in the study	Garages, Food, Mining & Quarries, Mineral, Chemical	
Average number of events occurring every 91 days	35	Detail presented in appendix A9.4
No of potential pollution sources where incident has not previously occurred but has the same likelihood of occurrence	246	Location presented in Figure 5.30a
Description of historical pollution events	Minor	Description based on Table 3.1
Total number of sources in any stress period	281	This include both actual and potential sources

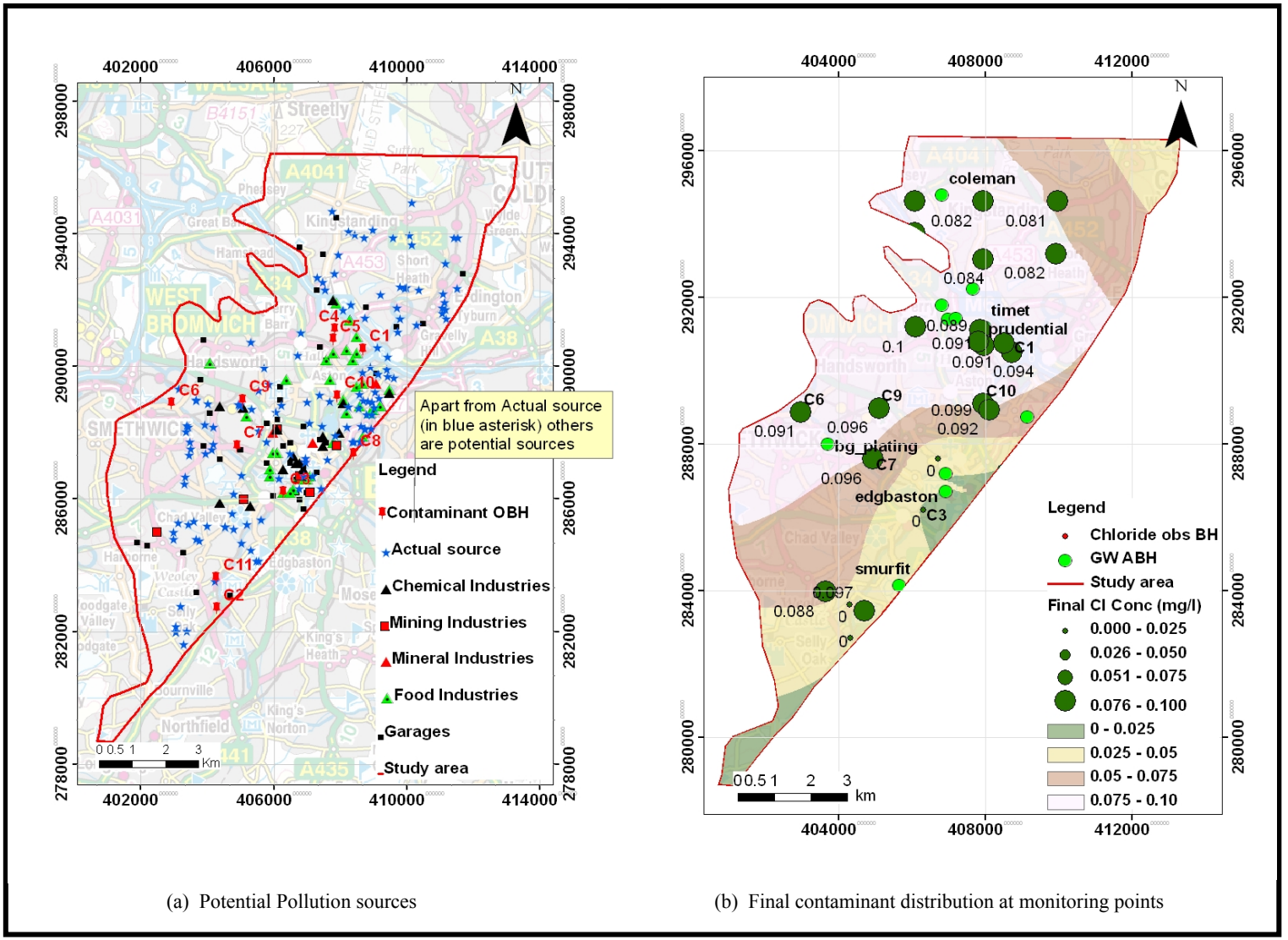

(a) Potential Pollution sources

(b) Final contaminant distribution at monitoring points

Figure 5.30: Pollution sources and modelled contaminant distribution

Table 5.12: Summary of risk model input data

Record Number	Record	
File Name: *ram_input_file.dat*		
A1	*title_1*	RISK ASSESSMENT METHOD
A2	*title _2*	USING FIELD DATA
A3	*lnlay, lnrow, lncol*	1 550 500
A4	*tspnumber, itype, previousmult, min_mult, max_mult*	120 15 1 1.0 1.0
A5	*fwel, fdrain, frch, fevt, friv, fghb*	F F T F F F
A6	*Incrch, rarray1, buffer*	1 0 0.0
A7	*global_row, global_col*	46 87
A8	*spnumber, splength*	Spnumber, 91
A9	*npsource, nprevious*	281 35
A10	*sorrow, sorcol,*	Location of potential source in each stress period (see appendix A9.1)
A11	*Min_mass, max_mass*	Minimum and maximum values of comtaminant mass assigned to each potential source in each stress period (see appendix A9.1)
File Name: *advance_flag.dat*		
B1	2D array with integer values between 0 and 5	Data read from advance_flag.dat (See appendix A9.2)
File Name: *ram_files.dat*		
C1	*funit, fname, fstatu*	Data read from ram_files.dat (See appendix A9.3)

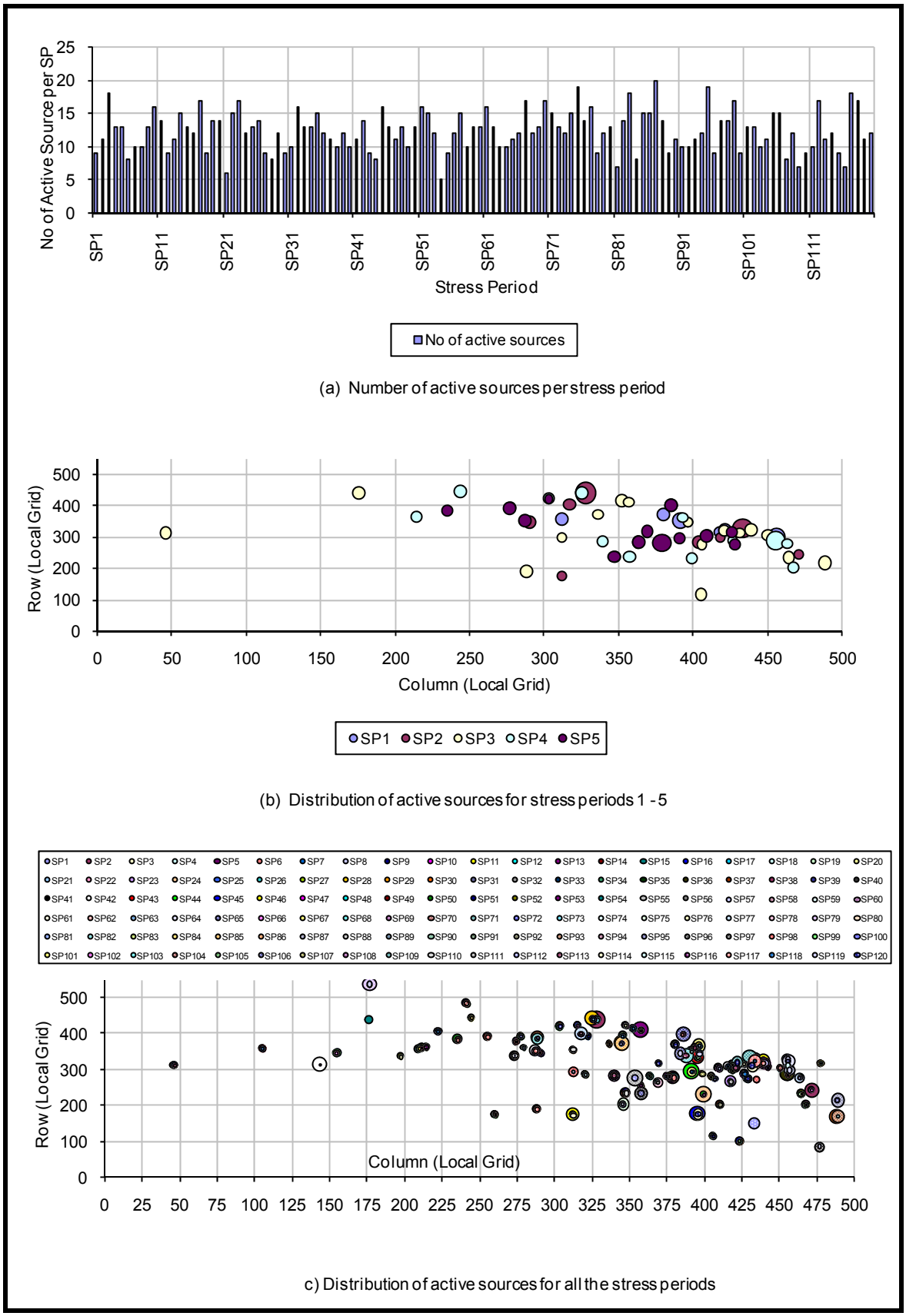

Figure 5.31: Distribution of active sources per stress period

5.5.3 Application of Transport model in risk assessment method

The transport model used in this work is the modular three-dimensional transport model commonly referred to as MT3DMS (Zheng and Wang, 1999). The detailed description of MT3DMS has already been presented in Section 3.7.2, and the model setup is presented in this section. The selected MT3DMS packages and standard output files that were combined together in this model development are listed in Table 5.13. The descriptions of the packages are contained in Zheng and Wang, (1999).

The predictive transport model is set up to run under transient conditions covering 30 years from March 1985 to February 2015. The length of each stress is the same as the flow model. However, the transport model has an internal capability to adjust the length of the time step in order to ensure numerical stability and therefore, limiting the control of the user.

Chloride was used in this case study because of its non reactive nature, and only indicates a conservative extent to which a typical contaminant could potentially migrate under the prevailing field conditions. The background chloride concentration was set to be zero in order to prevent the background concentration from masking possible effects of the synthetically generated source terms. The transport model input files are presented in appendices A12.1 – A12.10, and summarised in Table 5.14.

Table 5.13: List of MT3DMS packages used in the transport model

MT3DMS Package	MT3DMS file type	Description
Named file	-	It contains the names of input and output files used in a model simulation and controls the parts of the model program that are active.
List output file	LIST	This is the standard MT3DMS output file, and must always be specified in the Named File for MT3DMS as the first non-comment record.
Basic Transport	BTN	It handles basic tasks such as problem definition, boundary specification, initial conditions, determination of the step size, preparation of mass balance information and printout of the simulation results
Flow Model Interface	FMI	It interfaces with a flow model, and contains hydraulic heads and flow terms in the form required by the transport model.
Advection	ADV	It solves the concentration change due to advection process with an explicit scheme or formulates the coefficient matrix of the advection term for the matrix solver.
Dispersion	DSP	It solves the concentration change due to dispersion explicitly or formulates the coefficient matrix of the dispersion term for the matrix solver.
Sink & Source Mixing	SSM	It solves the concentration change due to sink/source mixing explicitly or formulates the coefficient matrix of all sink/source terms for the matrix solver.
Generalized Conjugate Gradient Solver	GCG	It solves the matrix equations resulting from the implicit solution of the transport equation.
MT3Dnnn.UCN	UCN	Default unformatted output file for dissolved-phase concentration
MT3DnnnS.UCN	UCN	Default unformatted output file for sorbed-phase concentration
MT3Dnnn.OBS	OBS	Default formatted observation concentration files
MT3Dnnn.MAS	MAS	Default formatted mass budget summary files
MT3D.CNF	CNF	It stores spatial discretization information needed by post-processing programs.

Table 5.14: Transport model input data

Record Number	Variable Name	Description	Value	Remarks
Basic Transport Package				
A1	HEADNG(1)	Heading for simulation run	Transport model using field data	
A2	HEADNG(2)			
A3	NLAY	Number of layers	3	Based on flow model setup
	NROW	Number of rows	760	
	NCOL	Number of columns	600	
	NPER	Number of stress periods	120	
	NCOMP	Number of chemical species included in the current simulation	1	The only contaminant being considered by the risk model is Chloride
	MCOMP	Number of mobile species	1	
A4	TUNIT	Unit of time	Second	Based on flow model setup
	LUNIT	Unit of length	Metres	
	MUNIT	Unit of mass	Kilograms	
A5	TRNOP	Logical flags for major transport and solution options	ADV = T	Activated transport options are advection, dispersion, sink & source and generalized conjugate gradient solver
			DSP = T	
			SSM = T	
			RCT = F	
			GCG = T	
A6	LAYCON (NLAY)	1-D integer array indicating the type of model layer	1 for the three layers	Model layer is convertible between confined and unconfined
A7	DELR (NCOL)	Cell width along rows	25 metres	Based on flow model setup
A8	DELC (NROW)	Cell width along columns		
A9	HTOP (NCOL, NROW)	2-D array defining the surface elevation	Interpolated two dimension surface elevation (see Section 5.1.2, & Figure 5.2a)	
A10	DZ(NCOL, NROW)	Thickness of cells in each model layer	Interpolated two dimension layer thickness (see Section 5.1.3, & Figure 5.5 - 5.7)	
A11	PRSITY (NCOL, NROW)	Effective porosity of the porous medium	Bromsgrove (Layer 1) = 26.8 %	Obtained from Allen *et al.* (1997),
			Wildmoor (Layer 2) = 23.8 %	
			Kidderminster (Layer 3) = 26.4 %	

Record Number	Variable Name	Description	Value	Remarks
A12	ICBUND (NCOL, NROW)	Integer array specifying the boundary condition type	Based on flow model damain	
A13	SCONC (NCOL, NROW)	Set to be zero	To prevent background concentration from masking the effects of the synthetic source term	
A14	CINACT	Value for indicating an inactive concentration cell	-777	Arbitrary distinct number
	THKMIN	Minimum saturated thickness in a cell below which cell becomes inactive	0.01	Suggested default value Zheng and Wang, (1999)
A15	IFMTCN	Flag indicating whether the calculated concentration should be printed	1	Concentration is printed in the wrap form
	IFMTNP	Flag indicating whether the number of particles in each cell should be printed	0	Number of particles in each cell is not printed
	IFMTRF	flag indicating whether the model-calculated retardation factor should be printed	0	Model-calculated retardation factor is not printed
	IFMTDP	flag indicating whether the model-calculated, distance-weighted dispersion coefficient should be printed	0	Model-calculated, distance-weighted dispersion coefficient is not printed
	SAVUCN	Logical flag indicating whether the concentration solution should be saved in a default unformatted format	T	Concentration of each species will be saved in the default file
A16	NPRS	Flag indicating the frequency of the output and also indicating whether the output frequency is specified in terms of total elapsed simulation time or	10	Suggested default value Zheng and Wang, (1999)

Record Number	Variable Name	Description	Value	Remarks
		the transport step number.		
A17	TIMPRS (NPRS)	Total elapsed time at which the simulation results are printed to the standard output	Varied	
A18	NOBS	Number of observation points at which the concentration of each species will be saved	11	Suggested default value Zheng and Wang, (1999)
	NPROBS	Integer indicating how frequently the concentration at the specified observation points should be saved	3	
A19	KOBS, IOBS, JOBS	Cell indices in which the observation point is located	Varied	Model discretization
A20	CHKMAS	Logical flag indicating whether a one-line summary of mass balance information should be printed	T	The mass balance information for each transport step will be saved in file MT3Dnnn.MAS
	NPRMAS	Integer indicating how frequently the mass budget information should be saved in the mass balance summary file	6	Suggested default value Zheng and Wang, (1999)
A21	PERLEN	Length of the current stress period	90 days	Model discretization
	NSTP	Number of time-steps in the current stress period	9	
	TSMULT	Time steps multiplier	1	
A23	DT0	DT0 is the user-specified transport step size within each time-step of the flow solution	0	Model-calculated transport step size to be used in the simulation

Record Number	Variable Name	Description	Value	Remarks
	MXSTRN	Maximum number of transport steps allowed within one time step of the flow solution	10000	Maximum number of transport steps allowed within one time step of the flow solution
	TTSMULT	Multiplier for successive transport steps within a flow time-step if the GCG solver is used and the solution option for the advection term is the standard finite-difference method	1.1	Suggested default value Zheng and Wang, (1999)
	TTSMAX	Maximum transport step size allowed when transport step size multiplier TTSMULT > 1.0.	0	No limit is imposed. Suggested default value Zheng and Wang, (1999)
Advection Transport Package				
B1	MIXELM	Integer flag for the advection solution option	0	Standard finite-difference method with upstream weighting. Suggested value Zheng and Wang, (1999)
	PERCEL	Courant number. That is, the number of cells, or a fraction of a cell	1	Suggested default value Zheng and Wang, (1999)
	MXPART	Maximum total number of moving particles allowed	50,000	Suggested default value Zheng and Wang, (1999)
	NADVFD	Integer flag indicating which weighting scheme should be used	1	Upstream weighting. Suggested default value Zheng and Wang, (1999)
Dispersion Transport Package				
C1	AL (NCOL, NROW)	Longitudinal dispersivity for every cell of the model grid (unit, L).	20.0 m	Model refinement
C2	TRPT (NLAY)	1D real array defining the ratio of the horizontal transverse dispersivity to the longitudinal dispersivity,	0.1	

Record Number	Variable Name	Description	Value	Remarks
C3	TRPV (NLAY)	Ratio of the vertical transverse dispersivity to the longitudinal dispersivity,	0.01	
C4	DMCOEF (NLAY)	Effective molecular diffusion coefficient (unit, L^2T^{-1}).	0.0	Suggested default value when molecular diffusion is inactive Zheng and Wang, (1999)
Sink & Source Mixing Package				
D	See appendix A10.3			
Generalized Conjugate Gradient Solver Package				
F1	MXITER, ITER1, ISOLVE, NCRS	MXITER: maximum number of outer iterations; ITER1: maximum number of inner iterations; ISOLVE: Precondi-tioner parameters; NCRS: Integer flag for treatment of dispersion tensor cross terms	100, 200 3, 0	Suggested default value Zheng and Wang, (1999)
F2	ACCL, CCLOSE, IPRGCG	ACCL: Relaxation factor CCLOSE: Convergen-ce criterion IPRGCG: Printing interval	1.000 0.001 0	Suggested default value Zheng and Wang, (1999)

5.5.4 Results of the risk assessment method

The ***ram_output_file.dat, ram_distribution.dat,*** and ***ram.ssm*** files are generated as output from the execution of the risk model and are respectively presented in appendices A10.1, A10.2 and A10.3. The simulation was run for a single realisation as a control to check the accuracy of the risk assessment method. For the single iteration, the relative frequency distribution of the occurrence of the pollution events is presented in Figure 5.32. The ranges of values of contaminant concentrations simulated at the observation boreholes are presented in Figure 5.33, while the mass balance for the transport simulation is presented in Figure 5.34. The spatial distribution of the contaminant after 30 years of simulation is presented in Figure 5.30b, while the breakthrough curves of the contaminant concentrations at the observation boreholes are presented in Figure 5.35.

The assessment of risk to groundwater resource is demonstrated by repeating the simulation for 100 times, and then observing the number of times at which the user defined contaminant concentration intervals was exceeded. The sensitivity analysis of the variability of the contaminant concentrations to the number of Monte Carlo iterations was presented in Section 4.5, and the results indicate that 100 iterations are efficient in the use of the time and the computer memory, and could be employed in the Monte Carlo simulation for the implementation of this risk assessment method without losing significant details of the distribution of the input parameters. The graphs showing the probability of obtaining a particular concentration at a single point within the aquifer is presented in Figure 5.36, while Figures 5.37 – 5.38 present risk maps showing the spatial distribution of the probability of exceeding a particular value of the user defined concentration magnitudes.

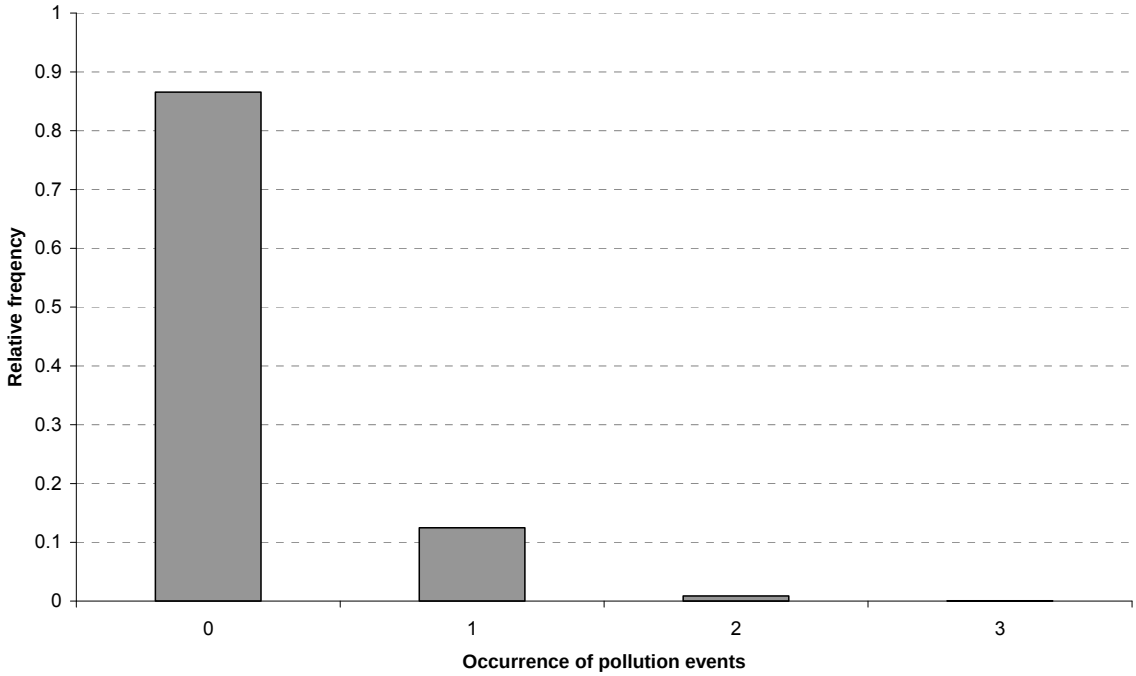

Figure 5.32: Source terms generated during the 30-year simulation period

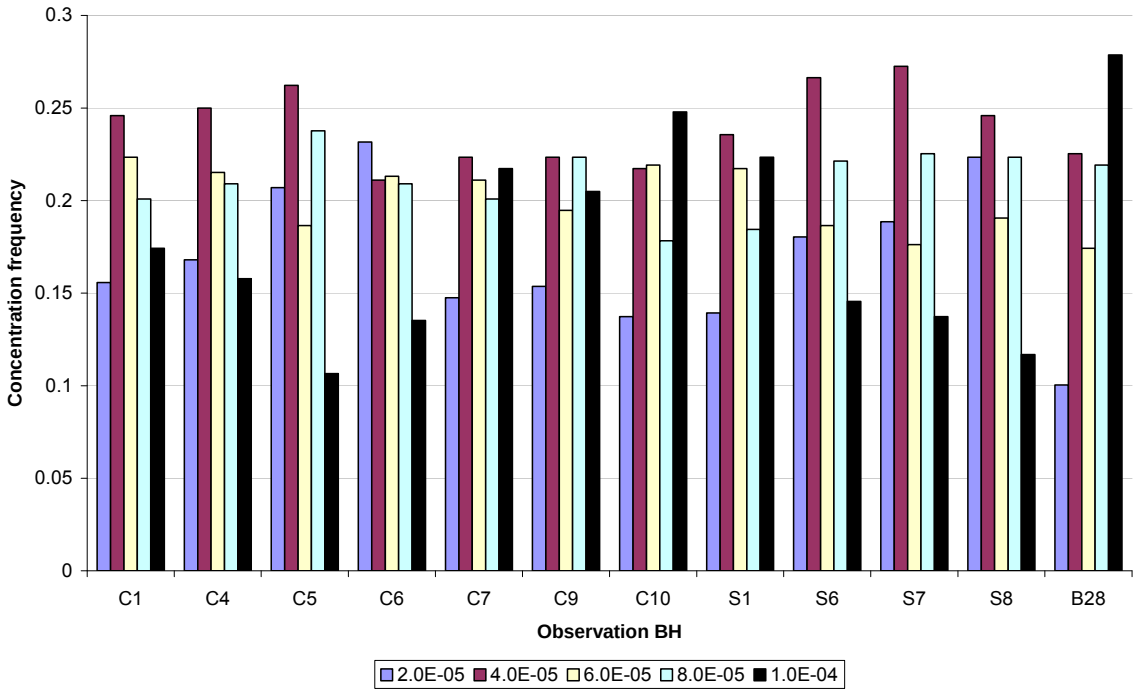

Figure 5.33: Relative frequency of contaminant concentrations (in mg/l)

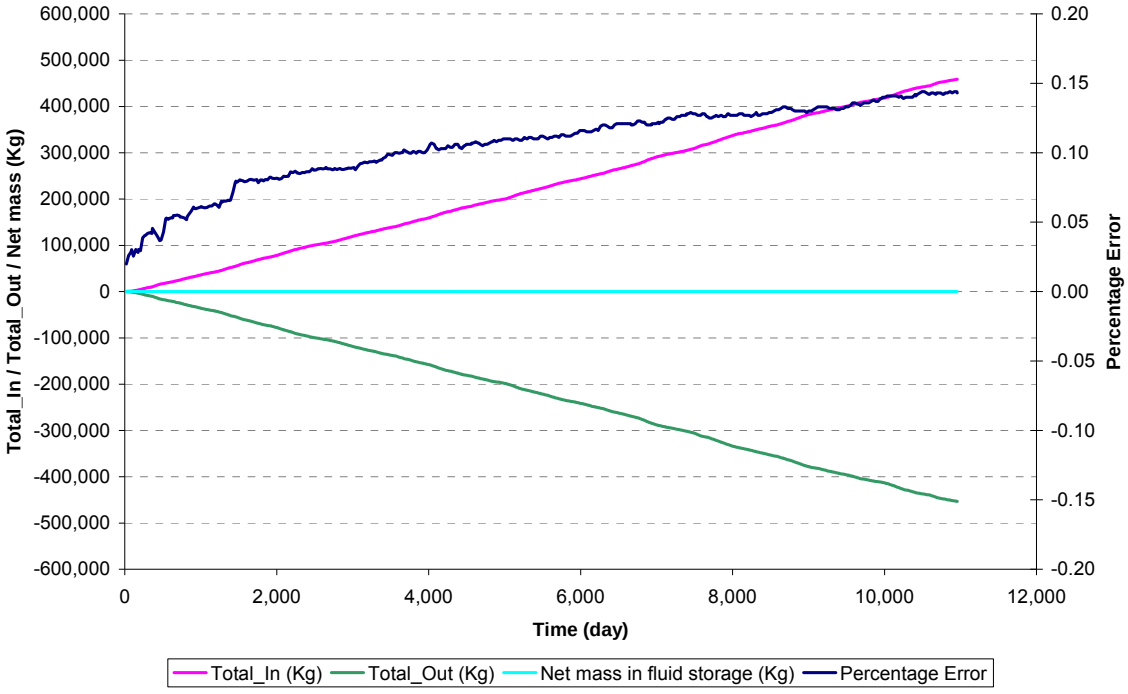

(a) Net mass balance from fluid storage

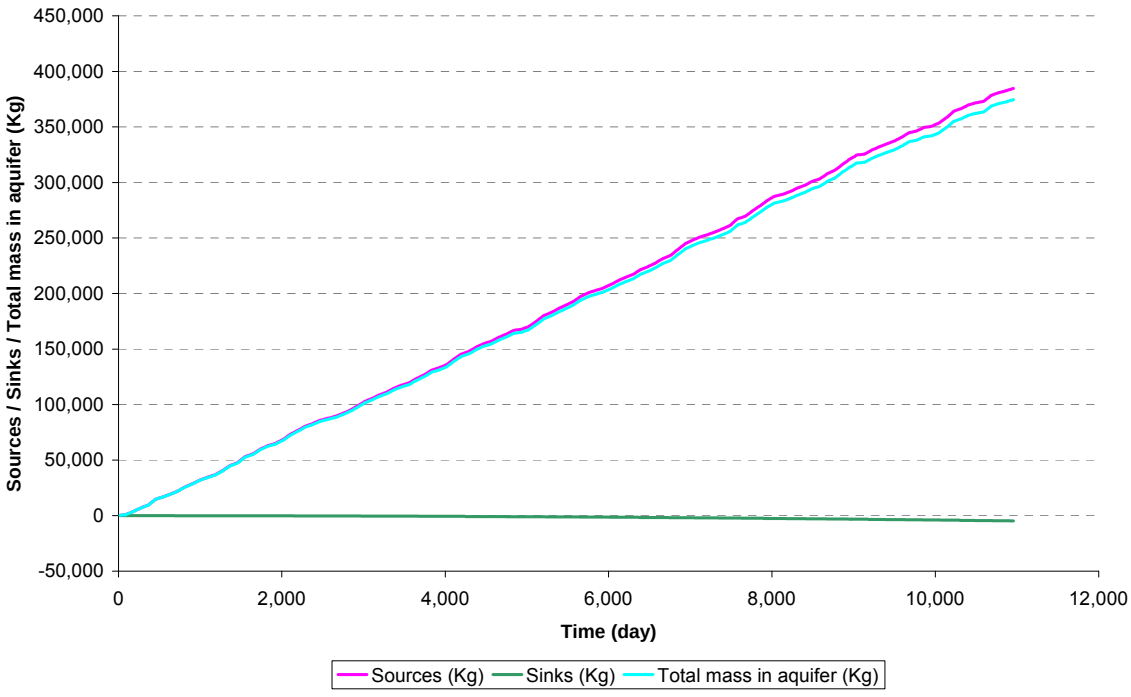

(b) Total mass in the aquifer

Figure 5.34: Mass balance over the 30 years of simulation

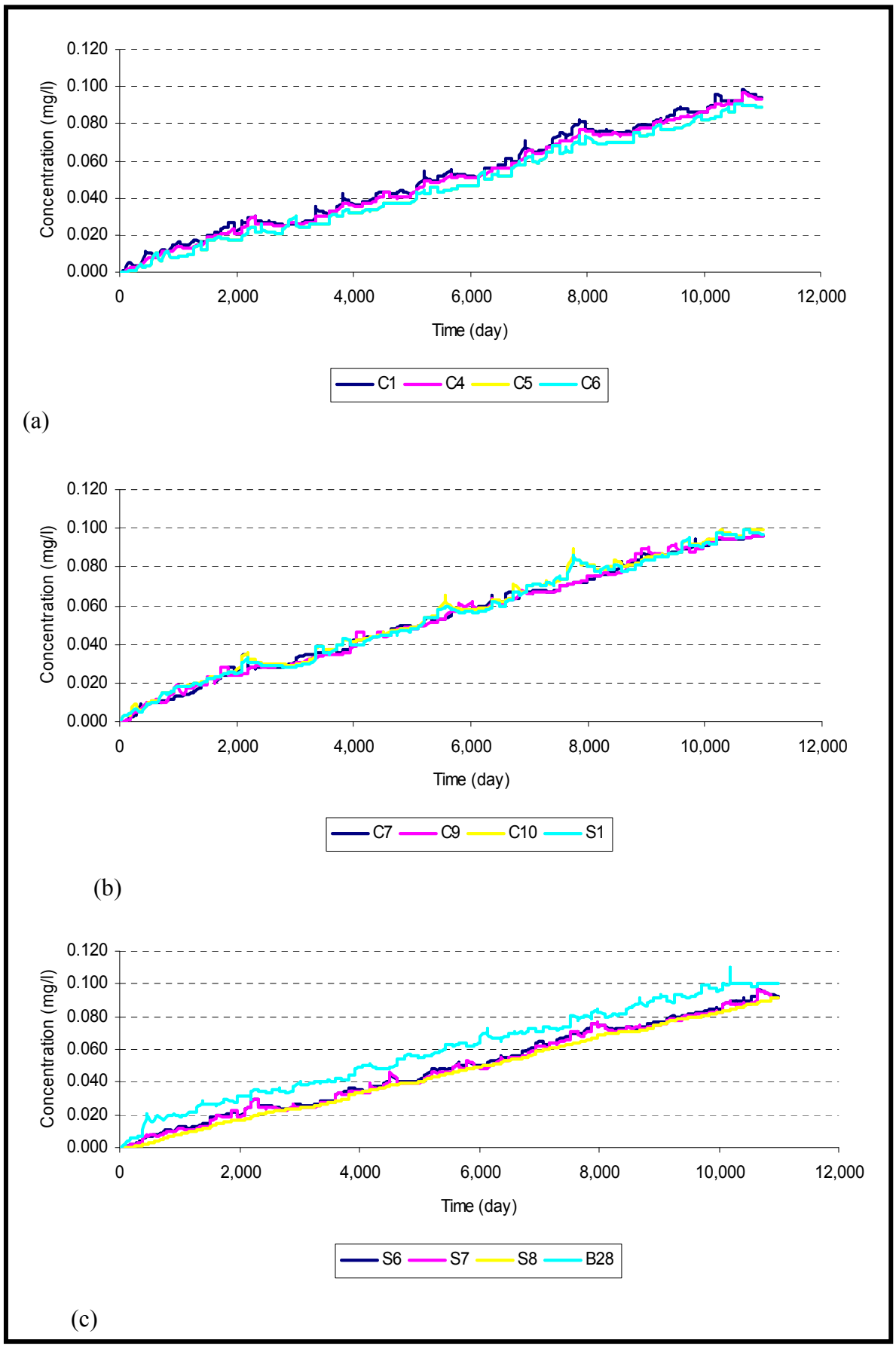

Figure 5.35: Contaminant breakthrough curves at the observation boreholes

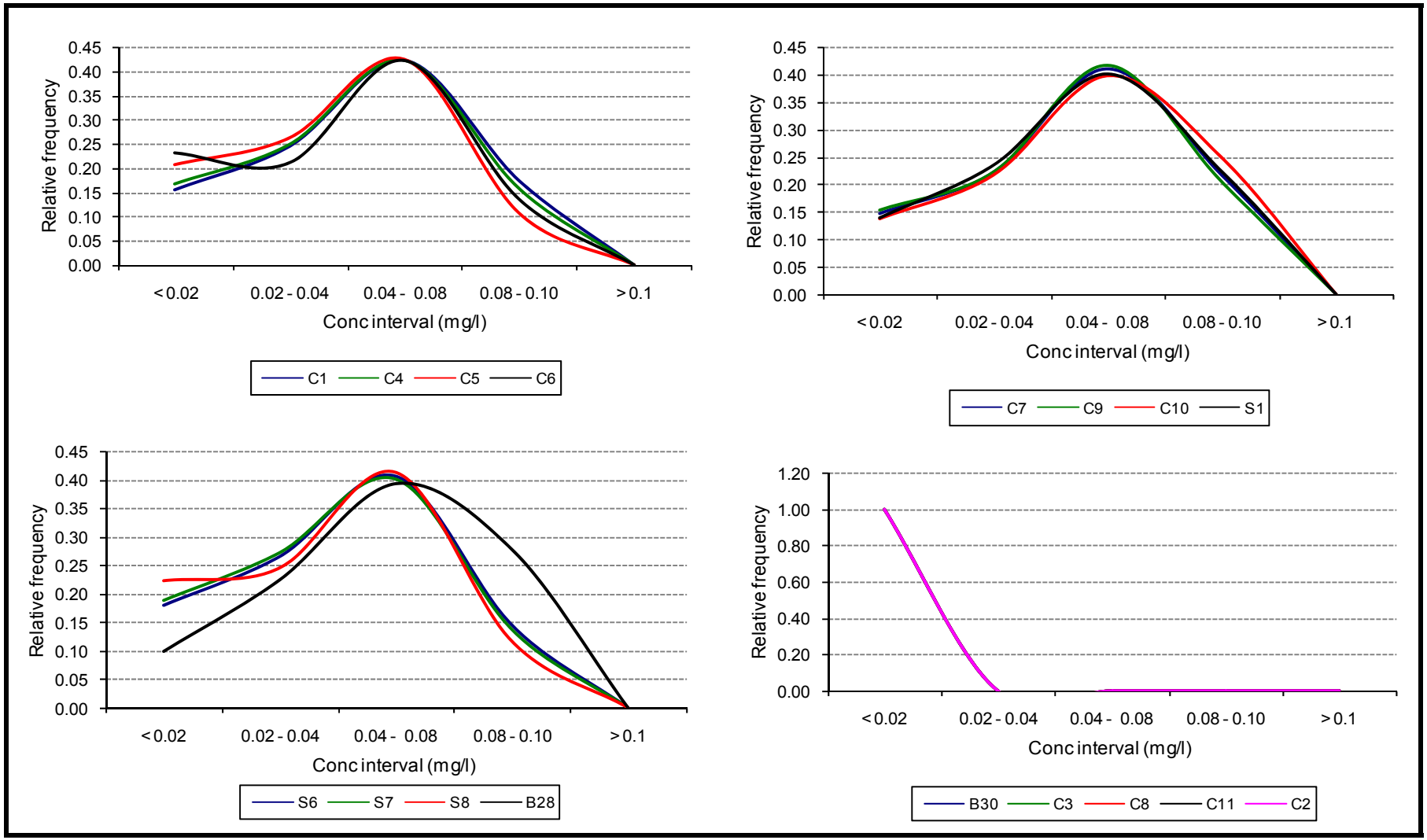

Figure 5.36: Probability of obtaining specific concentration at monitoring borehole

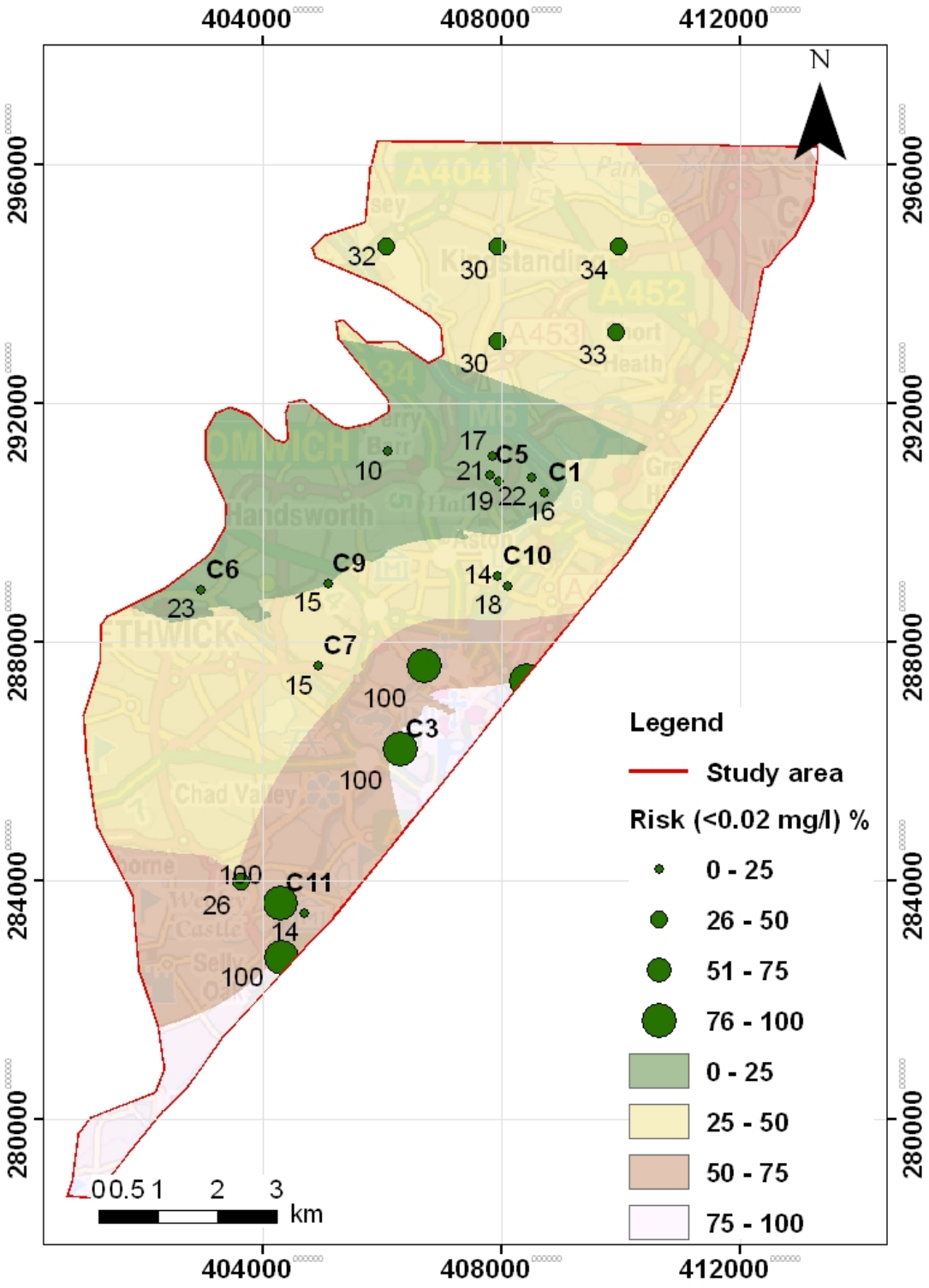

Figure 5.37: Risk maps for concentration less than 0.02 mg/l

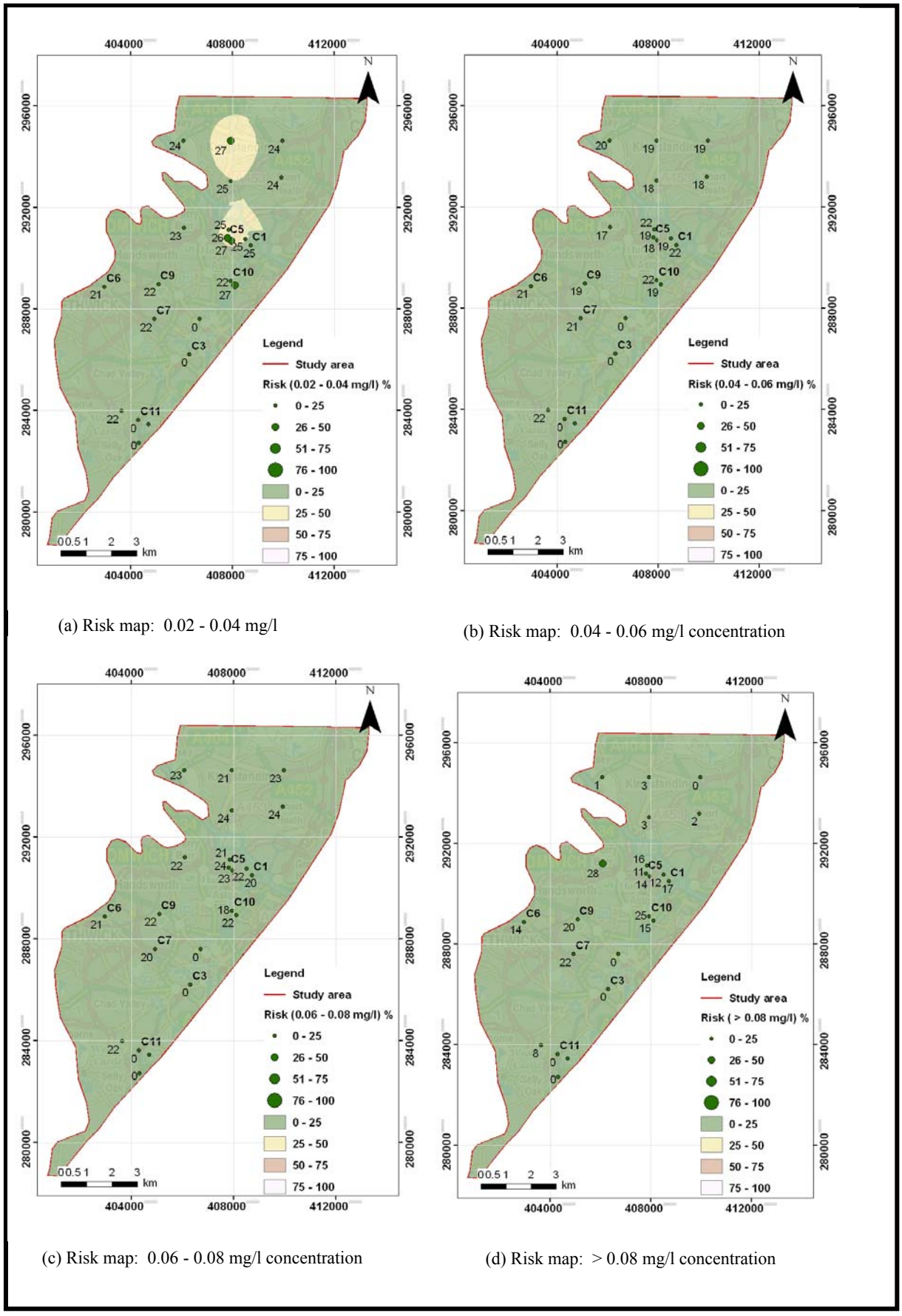

(a) Risk map: 0.02 - 0.04 mg/l

(b) Risk map: 0.04 - 0.06 mg/l concentration

(c) Risk map: 0.06 - 0.08 mg/l concentration

(d) Risk map: > 0.08 mg/l concentration

Figure 5.38: Risk maps for contaminant concentration (0.02 – 0.08 mg/l)

5.6 Summary of the Chapter

The demonstration of the risk assessment method using field data is presented in this Chapter. The conceptual framework of the case study area was developed through synthesis of the lithological, hydrological and geological features. The area covers approximately 221 km^2, and is underlain geologically, by a multi-layer setup with varied hydraulic properties. Based on the borehole lithologic data, geological cross sections, distinctive hydraulic properties and literature, three major sandstone aquifer horizons are identified to underlie the study area. The basal aquifer unit is the Kidderminster sandstone Formation, overlain by the Wildmoor and Bromsgrove sandstone Formations. The drift geology which overlays the Bromsgrove Formation has varied composition and thickness. The drift deposit is not considered as additional layer in this work, but as part of the Bromsgrove Formation and acts much as an extension to the unsaturated zone. Although, considering the drift deposit as a separate layer could improve the representation of the layer, however it thought that this would involve a significant amount of additional work that is beyond the scope of this work.

The presence of the Birmingham fault demarcates the eastern and southern boundaries of the model domain. The fault acts as low permeability barrier and therefore restricts the easterly component of the groundwater flow within the study area. The western boundary is defined by the presence of Westphalian Formations, which are essentially crystallised rocks and coal measures. These geologic materials are considered to inhibit flow across them. The northern boundary is defined by a groundwater divide, and therefore is represented as a no flow boundary. The river depths are relatively shallow and are considered to be contained within the first layer. The EA WFD recharge calculator was used to estimate average actual recharge to be 112 mm/yr.

The framework for the risk application was built on the calibrated flow and transport model that were developed using MODFLOW and MT3DMS software. The flow model was calibrated over a 20-year (January 1970 – December 1989) transient condition, and subsequently setup as predictive model to run over 30 years from March 1985 – Feb 2015. The flow model was calibrated using observed transient groundwater head data obtained from five observation boreholes. The ranges of values obtained for horizontal and vertical hydraulic conductivities are 5.787×10^{-6} - 2.315×10^{-5} m/s and 5.787×10^{-8} - 1.157×10^{-7} m/s, respectively. The ranges of values obtained for the specific yield and specific storage are

0.10 - 0.12, and $1x10^{-4}$ - $5x10^{-4}$, respectively. The calculated model error is generally much less than 0.1 %. Hydraulic layering within the Permo-Triassic sandstone aquifer is thought to account for the large vertical anisotropy in the final calibrated hydraulic conductivity values.

The risk and transport models were set up to run over the same period of 30 years, from March 1985 to February 2015 for which the flow model was setup and run. The results of the field application of the methods are presented in the form of tables, graphs and spatial maps. The estimated historical frequency of pollution occurrence per stress period is 35, while the probability of pollution occurring at any of the sources over a period of stress period of 91 days is calculated as 0.0014. The risk model was run to generate synthetic source terms that were subsequently transported. The initial background chloride data for the transport model was set to be zero in order to prevent masking of the effects of the generated source terms by the background concentration levels. Time variant chloride concentrations were observed at the 12 observation boreholes and the values vary between 0.0 – 0.10 mg/l.

The assessment of risk to groundwater resource is demonstrated by repeating the simulation for 100 times, and then observing the number of times at which the user defined contaminant concentration intervals was exceeded. The results of the sensitivity analysis of the variability of the contaminant concentrations to the number of Monte Carlo iterations indicate that 100 iterations are efficient in the use of the time and the computer memory, and could be employed in the Monte Carlo simulation for the implementation of this risk assessment method without losing significant details of the distribution of the input parameters. The risk of pollution from a number of sources all occurring by chance together was evaluated, and the results presented as graphs and risk maps.

Chapter 6: Discussions of results

The results of the simulations of the hypothetical (Chapter 4) and field (Chapter 5) applications are discussed in this Chapter.

6.1 RAM applications using hypothetical data

The risk assessment method was demonstrated using 8 scenarios to assess the effects of variations in the sizes of the model grid cells, the contaminant loading rates, as well as the historic frequency of the pollution incident occurrences, on the method. In all the 8 scenarios, the effects of the contaminant on the groundwater resources were observed at 20 monitoring boreholes, and the results are presented for each scenario in terms of the water balance error, volumetric budget, as well as the groundwater head and drawdown in the model layers. Other considerations include the frequency of pollution incident occurrences, mass balance for the transport model, and the time variant contaminant concentrations at the 20 observation boreholes.

6.1.1 Variation of the dimensions of model grid cell

The dimensions of the model grid cells were varied through 25x25 m, 10x10 m, and 50x50 m under scenarios 1 to 3, respectively. A contaminant mass of 5500 kg was introduced at a single source (see Figure 4.3a) and the effects of the transport of the source terms were assessed at the monitoring points under the varying grid cells. Apart from the grid sizes, all other input data were kept constant (Table 4.1) for the three scenarios.

Volumetric numerical error

The time variant volumetric numerical errors for scenarios 1 - 3 are presented in Figure 4.2a. With the exception of scenario 2 (10x10 m) where the numerical error was zero throughout the simulation, the trends of the volumetric numerical errors for scenarios 1 and 3 are similar, with values generally ≤ 0.020 % during the 30 years of simulation. The volumetric numerical errors indicate that scenario 2 (10 x 10 m) has relatively greater accuracy compared to scenarios 1 and 3, where the grid sizes were 25 x 25 m and 50 x 50 m, respectively. This is probably because scenario 2 has a lower Peclet number of 0.5 compared to scenarios 1 and 3, with Peclet values of 1.25 and 2.0, respectively. The truncation error which is the difference in hydraulic head between two successive iterations generally tend to become greater as the mesh spacing and time step length are increased

(McDonald and Harbaugh, 1988), and this consequently reduces the accuracy of the model. However, Table 4.6 shows that the time taken for the completion of the simulation was five times higher under scenario 2 compared to scenario 1, and ten times higher when compared to scenario 3. The simulation time for scenario 2 is considered inefficient for the required number of iteration in the implementation of the risk assessment method.

Volumetric Budget

The volumetric budgets for scenarios 1 – 3 are presented in Figure 4.2 (b-d). The external stress components are the constant head boundary conditions, recharge and groundwater abstraction from the five boreholes. The cumulative volumetric water budget increases with the decreasing grid sizes and with the increasing total number of the model cells. The change in storage was very low in all the scenarios, with the highest value obtained in scenario 2.

The transformation of the groundwater flow equation into the finite difference form is underpinned by continuity equation. That is, the difference between total inflow and total outflow should be equal to the total change in storage. In MODFLOW 2000, the water budget is calculated independently of the equation solution process, and therefore provides an independent check for the validity of the solution. The flow component package of the model calculates the rate of flow into and out of the system due to the processes simulated by the package for every time step. The flow per unit cross sectional area is calculated using Darcy's Law, as the product of the hydraulic conductivity and the hydraulic gradient. It is therefore thought that the refinement of the model grid sizes will affect how the variability of the hydraulic gradient is characterized. That is, the gradient will be averaged over a larger distance for a coarse meshed model compared to the fine meshed model. A larger gradient will result in larger flow rate and consequently larger volumetric budget. However, it is expected that the difference between inflow and outflow of the scenarios should be the same, and this is confirmed by the similar values obtained for the numerical errors for the scenarios 1 – 3.

Groundwater levels

The initial groundwater levels for the model layer are presented in Figure 4.1b, while the levels after 30 years of simulations under scenarios 1 – 3, and associated drawdown are respectively presented in Figures 4.3, 4.4, and 4.5. The maximum drawdown values under scenarios 1 – 3 were 2.4, 2.6 and 2.3 m, respectively. The measured drawdown values

appear to decrease slightly with increasing grid sizes and this is thought to be due to the coarse representation of the domain with the scenarios 1 and 3, as compared to a more refined model grid in scenario 2. No other changes were observed in the groundwater heads and drawdown as the dimensions of the grid sizes are being varied.

Frequency of occurrence of pollution incidents

No source terms were generated for scenarios 1 – 3. A single contaminant source was applied in order to facilitate comparison between the three scenarios.

Mass balance and associated numerical error values

The transient mass balance plots for transport models under scenarios 1 – 3 are presented in Figure 4.7. The components of the mass balance plots include the total contaminant mass in and out of the model, masses accumulated through sources and sinks, as well as total mass of contaminant in the aquifer. The calculated smallest contaminant mass of 30,000 kg within the aquifer was obtained after 30 years of simulation under scenario 2, while approximately 40,000 kg was obtained in scenarios 1 and 3. The values of the mass balance error under the three scenarios were generally less than 0.002 %. These results show that variations in the dimensions of the model cells affect the mass balance, with the total mass accumulated within the aquifer appears to be higher in the coarse grid size scenarios. However, similar to the volumetric budget, it is expected that the difference between the total contaminant mass in and out of the model for the three scenarios should be the same, and this is confirmed by the similar values obtained for the scenarios 1 – 3 where the errors associated with the differential contaminant mass were less than 0.002 %.

Time variant and spatial contaminant concentration

The time variant chloride concentrations were observed as breakthrough curves in the 20 observation boreholes under scenarios 1 – 3. The initial background concentration was zero for all the scenarios. Chloride is not considered to be of health concern at the levels found in the drinking water and may only affect acceptability of the drinking water (WHO, 2011). Therefore chloride concentrations observed at the monitoring boreholes are considered to be insignificant if the value is less than 1×10^{-10} mg/l, though values that are lower than 1×10^{-5} mg/l were not plotted because of the masking effects of the higher concentrations. The breakthrough curves for observation boreholes where the presence of contaminant is indicated under scenario 3 are presented in Figure 4.8. Lower contaminant

concentration values were obtained at the corresponding observation boreholes under scenarios 1 and 2, and therefore not plotted. The summary of the distribution of the contaminant concentration at the monitoring boreholes for scenarios 1 - 3 are presented in Figure 4.6.

In scenario 3, three observation boreholes namely BHs 4, 7, and 10 indicate significant presence of the contaminant (see Figure 4.8). The BH10 is on the downstream point to the contaminant source, and contained highest peak concentration of approximately 5.5 mg/l, with values less that 1.0 mg/l at BHs 4 and 7. Also, in scenario 3, the contaminant appears in BH10 immediately the contaminant mass was introduced, and then peaked in BH7 and BH4 after 2000 and 4000 days of the simulation.

The variation of model grid cells as demonstrated in scenarios 1 – 3 has shown great implications for the simulated concentrations at the observation boreholes. The rate of advancement of the contaminant plume along the groundwater flow path appears to increase as the model grid sizes increase. The smallest model grid size evaluated is the 10x10 m (scenario 2), and the contaminant has the longest transport time. Under this scenario, no indication of the contaminant occurs at BH10 which is the closest downstream monitoring point, before the completion of the simulation. The MT3DMS defines the extent to which advection of contaminant will be allowed in any direction in one transport step in terms of the number of model cells or a fraction of a cell. This implies that the larger the model cell sizes, then the larger the distance over which advection advances the contaminant in each time step. That is, the extent of advection of the contaminant will be smaller for fine grid sizes compared to a coarse model mesh. This condition is apparent in this work as no indication of the contaminant was observed in all the monitoring boreholes under scenario 2 with model grid cells of 10x10 m. The degree at which the contaminant appears in the monitoring boreholes increases with the increasing mesh sizes in scenarios 1 and 3.

The contaminant concentration peaked at 0.0011 and 0.02 mg/l in BH10 and BH6, respectively, after 4000 and 8000 days of simulation for model grid of 25x25 m (scenario 1). Also, the time taken for the completion of the simulation is more than five times higher under scenario 2 as compared to scenario 1, and ten times higher compared to scenario 3. Therefore scenario 1 is considered to be more time efficient because of the relatively shorter time taken for the completion of the simulation as well as the low numerical error

of 0.01 %, and it is the grid size (25 x 25 m) that was used in the subsequent field application of the method.

6.1.2 Assessment of the effects of stress periods and loading rates

The effects of the stress periods and loading rates were assessed using scenarios 4 and 5. The details of the model setup are presented in Table 4.1. Scenarios 4 and 5 represent the Approach 1 and Approach 2 (see Section 4.3.1), with the number of the stress periods being 929 and 120, respectively.

Volumetric numerical error

The time variant volumetric errors for scenarios 4 and 5 are presented Figure 4.10 (a,b). The numerical errors were 0.00 and 0.01 % under scenarios 4 and 5, respectively. These values appear to be constant during the simulations, and it show that scenario 4 with 929 stress periods appears to be more relatively numerically accurate compared to scenario 5 with 120 stress periods.

Volumetric Budget

The volumetric budgets for scenarios 4 and 5 are presented in Figure 4.10 (c,d). The external stress components were the same for both scenarios and include constant head boundary condition, recharge and groundwater abstraction from the five boreholes. The volumetric budgets were the same for the two scenarios and no significant effect appears to have been indicated in the flow budget.

Groundwater levels

The groundwater heads and drawdown distributions after 30 years of simulations under scenarios 4 and 5 are respectively presented in Figures 4.11 and 4.12.

Generally, the distributions of the groundwater heads under scenarios 4 and 5 were the same. The maximum drawdown value obtained under the two scenarios was 2.4 m. Therefore, no significant effect appears to have been indicated in the groundwater levels by varying the stress periods.

Frequency of occurrence of pollution incidents

The frequency of daily occurrence of pollution incidents for the two scenarios is presented in Figure 4.13. The numbers of days when 0, 1, and 2 incidents occurred were the same under the two scenarios. Therefore the frequency of pollution occurrence appears to be independent of the length of the stress period, as well as the pattern of the loading rates.

Mass balance and associated numerical error values

The mass balance plots for transport models under scenarios 4 - 5 are presented in Figure 4.15. The calculated total mass in the aquifer under scenario 4 after 30 years of simulation was approximately 300,000 kg, as compared to 250,000 kg obtained under scenario 5. It appears that the total accumulated mass in the aquifer over the period of simulation is been influenced by the pattern of the mass loading rates as well as the number of stress period. In this work, this results show that more contaminant was generated within the aquifer under Approach 1 compared to Approach 2.

Time variant chloride concentration

The breakthrough curves for scenarios 4 and 5 are presented in Figure 4.17. The figure indicates the presence of significant level of contaminant concentration in BHs 7 and 10. In both scenarios, the peak contaminant concentration of approximately 3.5 mg/l occurred in BH10 after 4000 days of simulation. The concentration also peaked in BH 7 at 2.2 mg/l at the end of the simulation. The spatial variation of the contaminant concentrations at the end of the simulations under scenarios 4 and 5 are presented in Figure 4.16. Generally, the concentration at the observation boreholes appears to reflect no effect of the variation in the loading rates and the number of stress periods. The length of the time step of 1 day used in scenario 4 is less than those used in scenario 5 (9 days). The calculated Courant number for scenarios 4 and 5 were 0.1 and 0.36, respectively. In general, the smaller the time step, the more accurate the predicted results become. That is, as the time-step size increases, the accuracy of the transport solution usually deteriorates. This situation is reflected in scenarios 4 and 5. The numerical error for scenario 4 is zero throughout the simulation while scenario 5 shows a maximum value to 0.02 %.

6.1.3 Variation of the historic frequency of pollution occurrence

The historic frequency of pollution incidents were respectively doubled, tripled and quadrupled compared to the values used in scenario 5. All other input data were kept

constant (Tables 4.1) for the three scenarios (6 – 8). Source terms were subsequently generated using the new values, and the effects of the variation on the groundwater heads as well as contaminant concentrations at the 20 observation boreholes were assessed.

Volumetric numerical error, Volumetric Budget and Groundwater levels

No flow model simulation was run. The results obtained for scenario 5 were used.

Frequency of incident occurrence

The frequency of daily incident occurrence under scenarios 6 – 8 is presented in Figure 4.13. The figure shows that the numbers of days of occurrence of 0, 1, and 2 pollution incidents increases with increasing number of historic frequency of pollution incidents. That is, the number of source terms generated increases with increasing historic frequency of pollution incidents.

Mass balance and associated numerical error values

The mass balance plots for transport models under scenarios 6 – 8 are presented in Figure 4.19. The components of the mass balance plots include the total mass in and out of the model, as well as the total mass of contaminant in the aquifer. The simulated time variant contaminant mass of approximately 500,000, 700,000 and 900,000 kg within the aquifer were obtained after 30 years of simulation under scenarios 6, 7, and 8, respectively. These values appear to be directly proportional to the numbers used in the scaling of the historic frequency for scenario 5. However, the trend of the mass balance error was the same under the three scenarios and values were generally less than 0.002 %. It therefore appears that the mass of contaminant in the aquifer during simulation is directly proportional to the historic frequency of occurrence of pollution incidents and consequently to the number of source terms generated.

Time variant chloride concentration

The time variant chloride concentrations were observed as breakthrough curves in the 20 observation boreholes under scenarios 6 – 8. The initial background concentration was zero for all the scenarios. The summaries of the distribution of the contaminant concentration for scenarios 6 - 8 are presented in Figure 4.18. The breakthrough curves at the observation boreholes where the presence of contaminant was indicated under scenarios 6, 7 and 8, are presented in Figure 4.21. Under the three scenarios, two

observation boreholes namely BHs 7 and 10 indicate significant presence of the contaminant. The BH10 is the closest downstream point to the potential sources, and contained the highest concentration of approximately 6.0, 8.0 and 10.0 mg/l in scenarios 6 – 8, respectively after 3000 days into the simulation. BH 7 is located further downstream and correspondingly contains approximately 4.0, 6.0, and 8.0 mg/l at the end of the simulations.

The variation of the historic frequency of pollution incidents as demonstrated in scenarios 6 – 8 has shown great implications for the simulated concentrations at the observation boreholes. The simulated concentrations appear to increase as the number of the historic frequency of occurrence of pollution incidents increase. The simulated concentrations appear to increase in a non linear pattern, as the historic frequency of incidents increase. That is, tripling the numbers of historic frequency of pollution occurrence in scenario 8 (compared to the baseline conditions in scenario 5) do not have corresponding increase in the amount of the contaminant concentrations observed in the monitoring boreholes. Also, the increased concentration caused by increased historical frequency appears to show no effect on the time delays before the contaminants appear in the observation boreholes. This is probably because the amount of recharge required to mobilise the transport of the contaminant was constant for the three scenarios (6 – 8). Therefore, the amount of contaminant that was transported at each transport time step apparently remains largely the same across the three scenarios, despite the increase in the amount of the synthetic source terms generated. It is thought that this is the reason why the contaminant concentrations observed at the monitoring boreholes show a non-linear proportionality to the rate of increase in the generation of the contaminant from scenario 6 through to scenario 8.

6.1.4 Assessment of risk to water resources

The risk to groundwater features was expressed as the number of times the user defined contaminant concentration intervals were exceeded. This capability was demonstrated using the scenario 5 hypothetical model setup. The simulations were repeated 100 times, where for each realisation a pattern of contaminant magnitudes and location was randomly generated as input into the transport model. Based on the ranges of observed concentration of contaminant, the user defined ranges of concentration intervals were set to include $<10^{-5}$, $10^{-5} – 10^{-3}$, $10^{-3} – 10^{-1}$ and $>10^{-1}$ mg/l.

The frequency plots for the number of incidents for each concentration interval in the 20 observation boreholes are presented in Figure 4.23. The graphs show the probability of obtaining a particular concentration at a single observation borehole. The frequency plots (Figures 4.23) show that BHs 6 and 7 have fair distribution of magnitudes of contaminant concentrations With the exception of BH10 that was skewed towards the high concentration of $>10^{-1}$ mg/l, all other observation boreholes have skewed distribution of contaminant concentrations largely restricted to $<10^{-5}$ mg/l. Risk maps showing the spatial distribution of the exceedance number for each of the user defined concentration interval are presented in Figure 4.24. The Figure 4.24a presents a risk map where concentration values are less than 10^{-5} mg/l, and 75% of the monitoring boreholes indicated high likelihood (100 %) of having concentration less than 10^{-5} mg/l throughout the entire simulation. Exception occurs at BHs 4, 6, 7, 10 and 11, where there is varying degree of likelihood that the contaminant concentration will exceed 10^{-5} mg/l during the simulation (Figure 4.24 b - d). This capability to quantify risk to groundwater features at a greater resolution is considered to be significant in the assessment of risk to groundwater resource, compared to the current blanket, conservative approach of assessing risk to groundwater resources.

6.1.5 Conclusions from the hypothetical scenarios

The following have been demonstrated by the simulations run under the 8 scenarios:

6.1.5.1 Variation of the dimension of the model grid cell

1. The volumetric numerical error increases as the model grid size increase. This indicates that finer grid sizes have relatively greater accuracy compared to larger grid sized model. However, the time taken for the completion of the simulation was five times under scenario 2 (10x10), and ten times under scenario 3 (50x50), compared to scenario 1 (25x25).

2. The cumulative volumetric water budget increases with decreasing grid sizes and increasing total number of the model cells.

3. The measured drawdown values appear to decrease with increasing grid sizes. No other changes are observed in the groundwater heads as the dimensions of the grid sizes are being varied.

4. The variations in the dimensions of the model cells affect the mass balance; with a higher value of accumulated contaminant mass within the aquifer under the fine grid (scenario 2) compared to the coarse grid scenarios.

5. The rate of advancement of the contaminant plume along the groundwater flow path appears to increase as the model grid sizes increase.

6.1.5.2 Assessment of the effects of the stress periods and the loading rates

1. The numerical error reduces with increased number of stress period and reduced time step length.

2. The volumetric budgets are the same for the two scenarios and no significant effect appears to have been indicated in the flow budget.

3. No effect appears to have been indicated in the groundwater levels by varying the stress periods.

4. The frequency of the pollution occurrence is independent of the length of the stress period as well as the pattern of the loading rates.

5. It appears that the total mass in the aquifer over the period of simulation is been influenced by the pattern of the mass loading rates as well as the number of stress period.

6. Generally, the concentration at the observation boreholes appears to reflect no effect of the variation in the loading rates and the number of stress periods.

6.1.5.3 Variation of the historic frequency of pollution occurrences

1. The number of source terms generated increases with increasing the historic frequency of the pollution incidents.
2. The mass of contaminant in the aquifer during simulation appears to be directly proportional to the number of the historic frequency of pollution incidents and consequently the number of synthetic source terms generated.

3. The simulated concentrations observed at the monitoring points appear to increase in a non linear pattern, as the historic frequency of occurrence of pollution incidents increases. That is, tripling the numbers of historic frequency of pollution occurrence in scenario 8 (compared to the baseline conditions in scenario 5) do not have corresponding amount of increase in the amount of contaminant concentrations observed in the monitoring boreholes. Also, increased concentration caused by increased historical frequency appears to show no effect on the time taken for the contaminants to appear at the observation boreholes.

6.2 RAM applications using field data

This section discusses the results of the application of the risk assessment method using field data. This includes the setting up of both the flow and transport models.

6.2.1 Flow model results

The flow model was setup and calibrated over a 20-year period spanning January 1970 – December 1989. The model setup and calibrated results are presented in Table 5.10. The model refinement was carried out using trial and error approach, and the Observation Package of MODFLOW-2000 was used to calculate the simulated equivalents of the field observations. The hydraulic heads from five observation boreholes were used as the observed data during the model calibration process. The objective of the calibration process was to reduce the residuals between the observed and simulated hydraulic heads. A convergence criterion of 0.01 m was set within the solver package, such that the solution is considered to converge either when the difference between two successive solutions for the calculated hydraulic heads is less than the convergence criteria, or when the difference between the simulated and observed values is less than the convergence criteria.

The model input data namely, horizontal and vertical hydraulic conductivities, as well as specific yield and specific storage, were assigned using the zonation capability of MODFLOW 2000. The initial values for the hydraulic properties were obtained from the final calibrated model of Buss *et al.* (2008). The model was setup as a three-layer model, which represents (from top) the Bromsgrove, Wildmoor and Kidderminster sandstone Formations. The respective final horizontal hydraulic conductivity values were 5.787×10^{-6}, 2.315×10^{-5}, and 3.472×10^{-5} m/s. The corresponding values for vertical hydraulic

conductivity were $5.787x10^{-8}$, $1.157x10^{-7}$, and $5.787x10^{-8}$ m/s, respectively. Hydraulic layering within the Permo-Triassic sandstone aquifer is thought to account for the large vertical anisotropy in the final calibrated hydraulic conductivity values. The final horizontal conductivity values are within the same ranges compared to the values obtained by Allen *et al.* (1997) and Jones *et al.* (2000) from field test data, for the respective aquifer horizons, as well as to those values obtained by Knipe *et al.* (1993) (see Table 5.4).

Furthermore, the final values for the specific yield were 0.12, 0.10 and 0.12, and for the specific storage were $1x10^{-4}$, $5x10^{-4}$, and $1x10^{-4}$, respectively for Bromsgrove, Wildmoor and Kiderminster Formations. The value reported by Allen *et al.* (1997) for the specific yield of the undivided Sherwood sandstone Group is 0.12. Knipe *et al.* (1993) and Rushton and Salmon (1993) respectively reported specific yield value of 0.15, and 0.10 for the Bromsgrove sandstone Formation. The values obtained in this work are similar to these referenced values.

The five observation boreholes (see Table 5.6) were used in the model calibration. Generally, a sufficient degree of match was obtained between the measured head observations and the simulated equivalents as presented in Figure 5.25. The simulated data are within ± 5 m of the observed data, though majority of the simulated data falls below this deviation (see Figure 5.25). The percentage numerical error associated with the volumetric balance is less than 0.01 % throughout the duration of the simulation (Figure 5.21a). The calibration target of ± 5 m and the obtained percentage error of below 0.01 % are similar to the results obtained by Buss *et al*., (2008). The groundwater heads and corresponding drawdown in layers 1 – 3 at the end of the 20 years of simulation are presented in Figures 5.22 - 5.24. Generally, the drawdown figures show patches of distributed increase of between 0.0 – 8.0 m in groundwater heads of the three layers within the central part of the model area and average decline of approximately 0.0 – 10.0 m at both the north and southern parts of the area. There are also dry patches at the south central portions of the first layer. The high drawdown values greater than 10 m were obtained in places where the initial water levels were defined using the depth of the surface rivers.

The flow model was subsequently setup as a predictive model for a 30-year period spanning March 1985 – February 2015. The March 1985 groundwater head output of the calibrated model (Figure 5.26) was used as the initial water levels for the predictive model.

The final groundwater heads as well as associated ranges of drawdown after 30 years of predictive model simulations are presented in Figures 5.27 – 5.29, for layers 1 – 3, respectively. The calculated drawdown values are generally lower than that obtained for the calibrated flow models (Figures 5.22b – 5.24b). This is probably because a more representative initial water level conditions (Figure 5.26) were used.

The final refined value for the hydraulic conductance along the Birmingham fault is 1.0 x 10^{-9} m/s. This value is less than the hydraulic conductivity values obtained for the sandstone layers ($5.787x10^{-6}$ - $3.472x10^{-5}$ m/s), and therefore confirms that the fault acts as a barrier to groundwater flow, and not conduits. This conclusion agrees with the earlier work of Knipe *et al.* (1993), who modelled the faults as reduced thickness to achieve the required lower transmissivity value along the fault path.

6.2.2 Risk model results

The risk assessment method (RAM) was set up in a format presented in Chapter 3, over the same period of 30 years, from March 1985 to February 2015 for which the flow and transport models were setup and run. The input data for the risk assessment method are presented in Table 5.12.

The global grid system for the risk model is the same as that of the flow and transport model. The number of potential sources of chloride pollution within the case study area was determined through identification, review and compilation of all the possible sources of chloride related pollutant within the case study area. The identification process was carried out using the Environment Agency NIRS database as well as the internet to exhaustively search all possible potential sources of chloride pollution within the study area. The sources of chloride pollutants considered are from the food processing, garages, quarries, mineral and chemical industries. The locations of the identified potential sources of pollution are presented in Figure 5.30a. The grid references are subsequently converted into row and column numbers using GIS utilities in order to allow their representations into the numerical models. Furthermore, using the NIRS database of the Environment Agency, the annual occurrence of chloride related pollution incidents from these industries within the study area over a period of 8 years (2002 – 2009) were obtained.

The summary of the records of previous incidents of chloride related pollution incidents over the period of 8 years is presented in Table 5.11. The average occurrence of chloride pollution incidents over the eight-year period was calculated as 35 events per 91 days, which is the length of a stress period. Based on the data available, these values were taken to be representative for the study area. NIRS described all the previous pollution incidents that occurred within the study area as Minor. According to the classification presented in Table 3.1, all the reported pollution incidents will have associated range of probable contaminant mass of 250 – 5000 kg per each incident. This represents the range of values within which the probable contaminant mass loading rate was sampled on each occasion a synthetic pollution incident occurred.

Also, Figure 5.30a presents the locations of the 281 (see Table 5.11) actual and potential sources of the pollutant. Where sources overlap, the effects of the corresponding number of sources were repeated at the respective grid cells. The probability of pollution occurrence was computed using Equation 3.3, which gives the probability of pollution occurring at any of the potential sources over a period of 91 days, as:

$$PPO = \frac{35/281}{91} = 0.0014$$

The risk model was run to generate source terms that were subsequently transported. The actual number of pollution occurrence per stress period and the distribution of the sources as generated by the risk model are presented in Figure 5.31. The frequency of pollution generated for each day is presented in Figure 5.32, and the figure shows that zero incident occurred in 9,453 days out of the total 10,920 days. Single daily events occurred in 1363 days, two daily events in 98 days, while three daily events occurred in only 6 days.

Given the generating mechanism used to create pollution events, the frequency of occurrence of 0, 1, 2… events per day should follow a Poisson distribution, and was verified by the Chi squared test presented in Table 6.1. The Chi squared test shows that the probability that these are by chance from different distributions is 1.02937×10^{-6}, very remote. This test confirms that the mechanism for generating random events is correct.

Table 6.1: Chi square test

p =	0.12
n =	10920

Number	Probability	Expected number	Actual number
0	0.88	9641.80	9453
1	0.11	1200.28	1363
2	0.01	74.71	98
3	0.00	3.10	6
4	0.00	0.10	0
5	0.00	0.00	0
Sum	**1**	**10919.99**	**10920**

where

P: The probability of the field data and, obtained by multiplying the calculated probability of pollution occurrence of 0.001368 by 91, which is the length (in days) of a stress period.

n: The number of elements is 10920, which is the length of simulation (in days).

6.2.3 Transport model results

The transport model was setup over a 30-year period (March 1985 to February 2015). The summary of the input data for transport model is presented in Table 5.14. The initial background contaminant concentration was set to zero in order to prevent the background concentration from masking the effects of the generated source terms. The ranges of contaminant concentrations within each of the observation boreholes are presented in Figure 5.33, and shows temporal variability in the contaminant concentrations over the simulation period. The mass balance plot for the transport models is presented in Figure 5.34. The components of the mass balance plots include the total mass in and out of the model, total mass of contaminant in the aquifer, as well as the transient masses from sources and sinks. The calculated total mass of contaminant in the aquifer after 30 years of simulation was approximately 375,000 kg. The mass balance error is generally less than 0.2 %.

The spatial distribution of the contaminant after 30 years of simulation is presented in Figure 5.30b, and shows that the contaminant concentration within the study area varies

between 0.0 – 0.1 mg/l. The highest concentration values occur at the central part of the study area, and decreases outwardly. The time variant chloride concentrations were observed as breakthrough curves in the 12 observation boreholes and presented in Figure 5.35. The range of concentration values is 0.0 – 0.1 mg/l. The trend of the breakthrough curves of the contaminant concentrations in all the 12 observation boreholes are similar, and reflect the continuous load rates of the synthetically generated source terms.

6.2.4 Risk assessment results

The risk to groundwater resources within the study area was determined as the number of times which chloride concentrations at the 12 observation boreholes exceed user defined concentration intervals during the 100 simulations. The five user defined concentration intervals used were < 0.02, 0.02 – 0.04, 0.04 – 0.06, 0.06 – 0.08, and > 0.08 mg/l. The number of times at which the concentration interval at each of the observation borehole is exceeded during the computed average of 100 simulations is presented in Figure 5.36. Risk maps showing the spatial distribution of the exceedance number for each of the user defined concentration interval are presented in Figures 5.37 – 5.38. The frequency plots (Figure 5.36) show that the graphs peaked at the concentration range of 0.04 – 0.08 mg/l, and this suggests that this concentration interval dominates the simulations at the observation boreholes, except BHs B30, C2, C3, C8 and C11, where the simulated contaminant concentrations is generally less than 0.02 mg/l. The risk maps for the user defined concentration intervals presented in Figures 5.37 – 5.38, show the likelihood of occurrence of specified contaminant concentration magnitudes relative to other concentration interval.

This approach of risk assessment presents a more resolved definition of risk distribution within the study area. The existing groundwater vulnerability maps classified the study area as high vulnerability area. However, considering the potential pollution sources present within the study area, this work has further delineated and temporally quantified regions within the area that are prone to risk from the contamination. This involves isolating the specific risk of exceedance to the individual source as well as the relative trend of the risk distribution within the study area. The roles played by the incorporation of the occurrence and distribution of potential pollution sources at ground surface are not accounted for in the contemporary vulnerability and risk maps. Also, Ford and Tellam (1994) concluded that few abstraction boreholes within the Birmingham area have highly

contaminated groundwaters and attributed this to localized high concentration recharge. What the authors referred to as 'localized concentrated recharge' appears to be localized potential pollution sources', as there are no geological evidence that support significant differential recharge at this location. In addition, existing risk assessment methods do not have the capability to isolate such localized events at the same resolution that could be possible with the method presented in this work.

Some setbacks of this method include considerable time investment, additional data requirement and expert knowledge. However the following capabilities make this RAM to be uniquely different from the existing methods.

1. Predictive anticipatory assessment of the risk to groundwater sources that is based on the prior knowledge of the historic frequency of pollution incidents.
2. The risk estimate is not only based on the static hydrogeologic aquifer properties, but also on additional parameters (as presented in Section 3.4) that enabled temporal assessment in the generation of synthetic pollution incidents.
3. The major additional input parameter of RAM is historically based and therefore objective in approach, rather than conceptual and hence, subjective.
4. Like the process-based computer simulation group of methods, RAM incorporates processes that govern contaminant transport within the subsurface and therefore it is considered to have more precision of forecast compared to the risk index based methods.
5. The capability to combine the risk to a groundwater feature from numerous potential sources of pollution is a great asset to the methodology. The risk of pollution from a number of sources all occurring by chance together can be evaluated. This is a large benefit over traditional risk and vulnerability methods.
6. The risk maps (see Figures 5.37 – 5.38) allow for either a fixed probability of an occurrence of pollution to be examined over the aquifer or for the frequency distribution (see Figures 5.36) of contaminant concentration to be examined at fixed locations. There is no other method of risk assessment to groundwater resources that gives such detailed information.

Although, it is generally difficult to make definitive statements about the predictive accuracy of one risk assessment method as compared to another, the proposed method does

offer a greater insight in the quantification of risks to a groundwater source. Therefore, the application of the RAM is preferred in circumstances where the anticipatory assessment of the risk to groundwater is required as a function of previous occurrence of pollution incidents, and where the occurrence and distribution of potential pollution sources are relevant in the risk estimation.

Generally, any vulnerability assessment approach requires continuous and dynamic reviewing and update. This process may span over several years. Also, it is generally difficult to test regional vulnerability assessment methods on a field scale in a similar way as site specific risk assessment methods such as concept of Source-Pathway-Receptor will be tested or validated. Alternative validation approach is to apply more than one method to the same site and compare the results.

6.3 Summary of the Chapter

This Chapter discusses the results of the application of the risk assessment method, using both hypothetical and field data. The results are presented in the form of tables, charts and maps. The risk to groundwater resources was evaluated based on the measurement of the frequency at which user defined concentration intervals were exceeded at the observation boreholes. The RAM assumes direct proportionality between the frequency of exceedance and the risk associated with groundwater source.

In this work, eight hypothetical scenarios and 20 observation boreholes were used to assess the effects of the variability of input data on the results. The volumetric numerical error slightly increases as the model grid size increase, and this indicates that the finer grid sizes have relatively greater accuracy compared to the larger grid sized model. However, the time taken for the completion of the simulation was ten times under scenario 2 compared to scenario 3. The cumulative volumetric water budget increases with decreasing grid sizes and increasing total number of the model cells. The measured drawdown values appear to decrease slightly with increasing grid sizes and no other changes were observed in the groundwater heads as the dimensions of the grid sizes are being varied. Also, the variations in the dimensions of the model cells affect the mass balance, with the total mass in the aquifer tends to increase with the increasing grid sizes. The rate of advancement of the contaminant plume along the groundwater flow path appears to increase as the model grid sizes increase.

The assessment of the stress period and the loading rates shows that the numerical error increases with reduced number of stress period. The volumetric budgets are the same for the two scenarios (4 and 5) and no significant effect appears to have been indicated in the flow budget. Also, no effect appears to have been indicated in the groundwater levels by varying the stress periods, and the frequency of pollution occurrence appears to be independent of the length of stress period as well as the pattern of the loading rates. Furthermore, it appears that the total mass in the aquifer over the period of simulation could slightly be influenced by the pattern of the mass loading rates as well as the number of stress period. Generally, the concentration at the observation boreholes appears to reflect no effect of the variation in the loading rates and the number of stress periods.

Also, the number of source terms generated increases with increasing historic frequency of pollution incidents. This suggests that the mass of contaminant in the aquifer during simulation is directly proportional to the historic frequency of occurrence of pollution incidents and consequently to the number of source terms generated. The simulated concentrations at the observation boreholes appear to increase in a non-linear pattern as the historic frequency of incidents increase. However, increased concentration caused by increased historical frequency appears to show no effect on the time delays before the contaminants appear in the observation boreholes.

The results of the field application of the methods are also presented in form of tables, graphs and spatial maps. Calibrated flow model was setup, integrated with risk and transport models and used as predictive tool to assess effects of the generated source terms at the observation boreholes. The risk of pollution from a number of sources all occurring by chance together was evaluated, and this capability to combine the risk to a groundwater feature from numerous potential sources of pollution proved to be a great asset to the method. The risk maps allow for either a fixed probability of an occurrence of pollution to be examined over the aquifer or for the frequency distribution of contaminant concentration to be examined at fixed locations. There is no other method of risk assessment to groundwater resources that gives such detailed information. This is a large benefit over the contemporary risk and vulnerability methods.

Chapter 7: Conclusions and Recommendations

7.1 Summary of the Thesis

This Chapter presents the summary and the conclusions of the development of a risk assessment method for groundwater features. The methodology is borne out of the need to be able to justify acceptable trade-offs between the utilization of groundwater resources and industrialization and to quantify the risk posed from potential pollution sources. The primary aim was to develop and demonstrate the applicability of a generic modelling approach that utilizes coupled groundwater models and GIS technologies for the purpose of assessing the risk to groundwater quality. The novelty of the work is based on the fact that the risk assessment assesses the effects of probabilistic source terms, based on the historic frequency or externally determined probability distributions of pollution incidents, on groundwater source. The review of literature presents the current methods of assessing risk to groundwater sources, which largely revolve around mapping vulnerable recharge areas using the intrinsic properties of the aquifer, as well as estimating the risk to the aquifer resulting from a single pollution incident.

The conceptual development of this risk assessment method (RAM) is based on a methodological tool to assess the risk to groundwater quality. The method incorporates a Monte Carlo mechanism for generating synthetic pollution events from a probability distribution. The risk is calculated in terms of the frequency at which user defined contaminant concentration magnitudes are exceeded at observation boreholes over a period of time. The RAM generally consists of three integrated main components which include a flow model, risk model and transport model. The flow and transport models provide the facilitating framework for the risk model. The risk model generates synthetic pollution events for a defined period of time, and the generated events are subsequently incorporated into a transport model in order to assess the event concentrations that appear at pre-defined observation boreholes. This work considered chloride as the contaminant because of the conservative and non reactive nature of chloride within the natural subsurface environment.

The utilities of the risk assessment method (RAM) were demonstrated using hypothetical models and scenario runs. The hypothetical models were run under 8 scenarios. Each of the hypothetical models consists of 20 observation boreholes. Parameters such as model

grid sizes, contaminant loading rates, and number of previous pollution events were varied under different scenarios in order to assess the influence that these parameters wield on the risk assessment method. The risk model in each scenario was setup to generate synthetic source terms over the same period of 30 years, and then the generated incidents were transported within the subsurface groundwater environment using the integrated flow and transport models. The simulation was repeated 100 times and the number of times at which user defined contaminant concentration magnitudes were exceeded, as well as the spatial and temporal distributions of contaminants observed at pre-defined monitoring boreholes were assessed. The groundwater flow model used is the MODFLOW-2000 (Harbaugh *et al.* 2000), while the transport model utilised in the setting up and simulation of the contaminant through the subsurface environment is the modular three-dimensional transport model for multi-species, commonly referred to as MT3DMS (Zheng and Wang, 1999).

The results of the hypothetical application of this method were presented in the form of tables, graphs and spatial maps. The empirical assessment carried out using hypothetical scenarios show that the volumetric numerical error increases with the model grid size, and this indicates that finer grid sizes have relatively greater accuracy compared to larger grid sized model. However, the time taken for the completion of the simulation was ten times under scenario 2 (10x10 m) compared to scenario 3 (50x50 m). The cumulative volumetric water budget increases with decreasing grid sizes and increasing total number of the model cells. The measured drawdown values appear to decrease with increasing dimensions of the model grid sizes and no additional changes were observed in the groundwater heads as the dimensions of the grid sizes were varied. Also, the variations in the dimensions of the model cells affect the mass balance, with the total mass in the aquifer tends to increase with increasing grid sizes. The rate of advancement of the contaminant plume along the groundwater flow path appears to increase as the model grid sizes increase. Considering the fact that the implementation of the risk assessment methodology presented in this work requires multiple iterations, it is therefore thought not efficient to incorporate model grid size that is smaller than that used in scenario 1 (i.e. 25 x 25 m), and this is the grid size used in the field application of this risk assessment method.

The assessment of the stress period and the loading rates shows that the numerical error increased with reduced number of stress period. The volumetric budgets were the same for

the two scenarios (4 and 5) and no significant effect appears to have been indicated in the flow budget. Also, no effect appears to have been indicated in the groundwater levels by varying the stress periods, and the frequency of pollution occurrence appears to be independent of the length of stress period as well as the pattern of the loading rates. Furthermore, it appears that the total mass in the aquifer over the period of simulation is dependent on the pattern of the mass loading rates as well as the number of stress periods. Generally, the concentration at the observation boreholes appears to reflect no effect of the variation in the loading rates and the number of stress periods. Also, the number of source terms generated increases with increasing the historic frequency of occurrence of pollution incidents. This suggests that the mass of contaminant in the aquifer during simulation is directly proportional to the historic frequency of occurrence of pollution incidents and consequently to the number of synthetic source terms generated. The simulated contaminant concentrations observed at the monitoring boreholes appear to increase as the historic frequency of occurrence of pollution incidents increase. However, increased concentration caused by the increased historical frequency appears to show no effect on the time delays before the contaminants appear in the observation boreholes. The assessment of risk to groundwater resource is performed by repeating the simulation for a number of realisations, and then observing the number of times at which the user defined contaminant concentration intervals was exceeded. The results of the sensitivity analysis of the variability of the contaminant concentrations to the number of Monte Carlo realisations indicate that 100 were efficient in the use of the time and the computer memory. Increasing the number of realisations did not markedly alter the frequency distribution of exceedance values. The risk to the groundwater resources was presented as graphs showing the probability of obtaining a particular concentration at a single point within the aquifer, as well as risk maps showing the spatial distribution of the probability of exceeding a particular value of the user defined concentration magnitudes.

The setting up and application of RAM based on field data as a case study involves flow model, setup as a three-layer model and calibrated over a 20-year period spanning January 1970 – December 1989. The model refinement was carried out using trial and error approach, with the incorporation of the Observation Package of MODFLOW 2000. Hydraulic heads from five observation boreholes were used as the observed data during the model calibration process. The final horizontal hydraulic conductivity values for the three model layers (from top) are 5.787×10^{-6}, 2.315×10^{-5}, 3.472×10^{-5} m/s. The corresponding

values for vertical hydraulic conductivity are $5.787x10^{-8}$, $1.157x10^{-7}$, and $5.787x10^{-8}$ m/s, respectively. Hydraulic layering within the Permo-Triassic sandstone aquifer is considered important and it is thought to account for the large vertical anisotropy in the final calibrated hydraulic conductivity values. The final horizontal conductivity values are within similar range of values obtained by Allen *et al.* (1997) and Jones *et al.* (2000) from field test data, for the respective aquifer horizons, as well as those obtained by Knipe *et al.* (1993). Also, the calibrated values for the specific yield are 0.12, 0.10 and 0.12, and for specific storage are $1x10^{-4}$, $5x10^{-4}$, and $1x10^{-4}$, respectively for Bromsgrove, Wildmoor and Kiderminster Formations. The value reported by Allen *et al.* (1997) for the specific yield of undivided Sherwood sandstone Group is 0.12. Knipe *et al.* (1993) as well as Rushton and Salmon (1993) reported specific yield value of 0.15, and 0.1 for the Bromsgrove sandstone Formation. The values obtained in this work are similar to these referenced values. Generally, a high degree of match is obtained between the measured head observations and the simulated equivalents. The calculated model error is generally much less than 0.1%.

The flow model was subsequently setup as a predictive model for a 30-year period spanning March 1985 – February 2015. The risk assessment method (RAM) was set up in a format presented in Chapter 3, over the same period of 30 years, from March 1985 to February 2015 for which the flow and transport models were setup and run. The historic frequency of occurrence of pollution incidents per stress period was 35, while the probability of pollution occurring at any of the sources over a period of stress period of 91 days was calculated as 0.0014. The risk model was run to generate source terms that were subsequently incorporated into the transport model.

The initial background chloride data for the transport model was set to be zero in order to isolate the effects of the surface generated contaminants. The time variant chloride concentrations were observed as breakthrough curves in the 12 observation boreholes with values varying between 0.0 – 0.10 mg/l. The risk to groundwater resources within the study area are presented as maps based on the exceedance of concentration levels. The number of times at which the concentration at each of the observation borehole was exceeded during the computed average of 100 simulations of 30 years is presented. The risk maps show the spatial distribution of the exceedance number for each user defined concentration interval. These maps allow for either a fixed probability of the occurrence of

pollution to be examined over the aquifer or for the frequency distribution of contaminant concentration to be examined at the fixed monitoring points. There is no other method of risk assessment to groundwater resources that provides this detailed approach of information. The risk maps have presented the quantitative likelihood of risk to the groundwater sources at a greater resolution for the study area compared to the conservative approach of the current risk assessment methods. The methodology presented the approach of assessing risk of the occurrence and distribution of ground surface potential pollution sources to groundwater features.

7.2 Limitations of the risk assessment method

1. Lack of sufficient understanding of the unsaturated zone could potentially introduce uncertainty in the computed travel times of the contaminants. The effect of the unsaturated zone was simulated by using a simplistic delay approach based on the observed lag times in the hydrographs. It may be that representing the unsaturated zone as a separate layer will improve the accuracy of the model. However, it is thought that this type of representation would involve a significant amount of additional work that is beyond the scope of the work.

2. It is not possible to calibrate and validate the probabilistic component of the risk model. Also, it is very difficult to determine the probability of occurrence of extreme events because of lack of historical records. Furthermore, high pollution incidents usually have higher correlation compared to low pollution events, and the capability for assessing this type of correlation is not incorporated in the current level of the development of this risk assessment method.

3. Although, the length of available records (8 years) for the previous occurrence of pollution incidents is sufficient for the demonstration of the risk assessment method presented in this work. However it is thought that longer record length will provide a more representation of the historical pollution occurrence and therefore improves the forecast capability of the method. Further work is required in determining the probability and magnitude of different potential polluters, for example petrol filling stations or chemical processes, to provide a generic database applicable to any location

4. The rivers within the study area were represented in the model by using the river package of the MODFLOW 2000. This package specifies the river stage at the beginning of the simulation and held constant throughout the simulation. It is thought that the use of stream flow package will provide more flexibility in the representation of the rivers because the stream stages could be allowed to be calculated based on the flow rates during the simulation.

5. Reliable historical abstraction data are only available for the time periods outside those used for the model calibration. There may be some uncertainties associated with the use of constant abstraction rates as well as the values used for river bed conductance in the model.

7.3 Conclusions of the Thesis

In conclusion, a risk assessment approach that utilizes Monte Carlo methods, GIS technology and coupled groundwater models has been developed and its applicability demonstrated. The developed approach uses enhanced input parameters, where the distribution of the potential sources of pollution at the ground surface played an important role in the estimation of risks posed to groundwater sources. The method considers the risk to groundwater features arising from any number of potential pollution sources, and treats risk, more as a function of the threats posed to the aquifer system, rather than mainly based on geo-hydrologic properties. The developed method is more of preventive, anticipatory measures and focuses on pollution prediction and prevention in accordance with the principle of sustainable development. The application of the method has been demonstrated and the utilities discussed. The capability to combine the risk to a groundwater feature from numerous potential sources of pollution proved to be a great asset to the method, and a large benefit over the contemporary risk and vulnerability methods. Although, considerable time investment, additional data and expert knowledge are required, however, the generated risk maps and frequency distributions provides a wider capability for risk quantification which has not been produced by any existing risk assessment methods.

7.4 Recommendations for further work

1. The programs and methodology presented in this thesis are in the form of research tools. A good user friendly interface will be required for a full implementation and commercialisation of the methods.

2. For the purpose of the validation of this work, its application to different geographical locations with distinctive socio-economical and technological developments and with extensive continuous groundwater quality monitoring over an extended period of time may be required.
3. The groundwater model has been refined over 20 years using hydraulic heads only. The model is considered as a valid tool for providing the required framework for the risk assessment method. However, in order to use the model for predicting the effects of changes in groundwater abstraction within the study area, further surface water flow data will be required to improve the current state of the model refinement.
4. Further investigation is required for application of this method in the implementation of chronic and spatially related pollution events.

References

Aiuppa, A., Bellomo, S., Brusca, L., D'Alessandro, W., and Federico, C. 2003. Natural and anthropogenic factors affecting groundwater quality of an active volcano (Mt. Etna, Italy). Applied Geochemistry; 15: 863 – 882.

Al-Adamat, R. A., Foster I. D., and Baban, S. M. 2003. Groundwater vulnerability and risk mapping for the Basaltic aquifer of the Azraq basin of Jordan using GIS, Remote sensing and DRASTIC. Applied Geography; 23 (4): 303-324.

Ali B. A., Christophe S. B., Gabriel B. C., and Jean L. M. 2006 (a). Heavy metal contamination from mining sites in South Morocco: 1. Use of a biotest to assess metal toxicity of tailings and soils. Chemosphere; 63: 802–810.

Ali B. A., Christophe S. B., Gabriel B. C., Wafae A. A., Ahmed O. D., and Jean L.M., 2006 (b). Heavy metal contamination from mining sites in South Morocco: 2. Assessment of metal accumulation and toxicity in plants. Chemosphere; 63: 811–817.

Allen, D.J., Brewerton, L.J., Coleby, L.M., Gibbs, B.R., Lewis, M.A., MacDonald, A.M., Wagstaff, S.J., and Williams, A.T. 1997. The physical properties of major aquifers in England and Wales. British Geological Survey Technical Report WD/97/34. 312pp.

Aller, L., Bennett, T., Lehr, J. H., Petty, R,J., Hackett, G. 1985. Drastic: a standardised system for evaluating groundwater pollution potential using hydrographic settings. US-EPA Report 600/287-035.

Aven, T., 2007. A unified framework for risk and vulnerability analysis and management covering both safety and security. Reliability Engineering and System Safety 92: 745–54.

Aven, T. and Renn, O., 2009. On risk defined as an event where the outcome is uncertain. Journal of Risk Research, 12: 1, 1 — 11.

Bachmat, Y., and Collin, M., 1987. Mapping to assess groundwater vulnerability to pollution. In: Vrba, J., and Zoporozec A., (eds.) 1994. Guidebook on mapping groundwater vulnerability. International Association of Hydrogeologists. International contributions to Hydrogeology Volume 16, Verlag Heinz Heise, Hannover, germany, 131p.

Barbash, J.E., and Resek, E.A. 1996. Pesticides in Groundwater – distribution, trends, and governing factors. Chelsea, Michigan, Ann Arbor Press, Inc. 588p.

Boak, R., 1992b. *Report on the Long Term Pumping Test, East Sutton Borehole Scheme*. Report by School of Civil Engineering, Birmingham University for South Staffs Water Company. In: Buss, S.R., Streetly, M.J., and Shepley, M.G., (Ed); 2008. Lichfield Permo-Triassic sandstone Aquifer Investigation (Final Report). Environment Agency (Midlands Region).

Boorman, D.B., Hollist, J.M. and Lilly, A. 1995. Hydrology of soil types: a hydrologically-based classification of the soils of the United Kingdom (Report No. 126); Institute of Hydrology 137 pp.

Brugnot, G. 1998. http://www.infotheque.info/fichiers/JSIR-AUF-Hanoi07/ presentations/AJSIR_ pwt_2-7_Amharref.pdf Accessed on 24/08/2010.

Buss, S.R., Streetly, M.J., and Shepley, M.G., (Ed); 2008. Lichfield Permo-Triassic sandstone Aquifer Investigation (Final Report). Environment Agency (Midlands Region).

Cabinet Office. 2002. Risk: Improving government's capability to handle risk and uncertainty. Strategy Unit report. London: Strategy Unit.

Clark, A., Turner, T., Dorathy, K.P., Goutham, J., Kalavati, C. and Rajanna, B. 2003. Health hazards due to pollution of waters along the coast of Visakhapatnam, east coast of India. Ecotoxicology and Environmental Safety; 56: 390-397

Connell, L.D., Daele Gerd van den, 2003. A quantitative approach to aquifer vulnerability mapping. Journal of Hydrology; 276: 71 – 88.

Delleur, J. D., 1999. The Handbook of Groundwater Engineering. CRC Press, USA; and Springer-Verlag GnbH & Co. Germany.

Dimitra R., and Carmela V., 2006. Geochemical evidences of landfill leachate in groundwater. Engineering Geology; 85: 111–121.

Egbu, A.U., 2004. Constraints to effective pollution control and management in Nigeria. The Environmentalist; 20 (1): 13 – 17.

Entec UK Limited, 2001.West Midlands Permo-Triassic sandstones Water Resources Study (Final Report). Prepared for Environment Agency, Olton Court, Solihull, B92 7HX

Environment Agency Controlled Document (EACD), printed 03/12/06. Explanatory notes to accompany Common Incident Classification Scheme (CICS) Methodology. Environment Agency Management System Document. 42p.

Environment Agency, 1997. Policy and practice for the protection of groundwater. Groundwater vulnerability of South Staffordshire and East Shropshire Sheet 22. Prepared by Cartographic Department, Soil Survey and Land Research Centre, Cranfield University, Silsoe, Bedford, MK45 4DT.

Environment Agency, 2007. Water Framework Directive (WFD) recharge calculator spreadsheet version 2.59 and manual (draft). Developed by the Environment Agency and the Scotland and Northern Ireland Forum for Environmental Research (SNIFFER).

Environment Agency, 2008a. http://www.environment-agency.gov.uk/maps/info/groundwater/?version=1&lang=_e; Accessed on 15/03/2008.

Environment Agency, 2008b. ArcGIS Shapefiles; Accessed on 04/03/2008.

Environmental Systems Research Institute (ESRI). 1995a. Understanding GIS – the ARC/INFO Method: Self study workbook, version 7 for UNIX and Open VMS. New York, John Wiley and Sons.

Evans, B. M. and Mayers, W. L., 1990. A GIS based approach to evaluating regional groundwater pollution potential with DRASTIC In: Al-Adamat, R. A., Foster I. D., and Baban, S. M. 2003. Groundwater vulnerability and risk mapping for the Basaltic aquifer of the Azraq basin of Jordan using GIS, Remote sensing and DRASTIC. Applied Geography; 23 (4): 303-324.

Ford, M. and Tellam, J.H., 1994. Source, type and extent of inorganic contamination within the Birmingham urban aquifer system, UK. Journal of Hydrology; 156: 101 – 135.

Ford, M., Tellam, J.H. and Hughes, M., 1992. Polluted – related acidification in the urban aquifer, Birmingham, UK. Journal of Hydrology; 140: 297 – 312.

Foster, S.S.D., 1987. Fundamental concepts in aquifer vulnerability, pollution risk and protection strategy. TNO Committee for Hydrological Research. Proceedings and Information, 38: 36 – 86.

Golder Associates, 2008. http://www.consim.co.uk/ Accessed 04/04/2008

Graham, J.D., and J.B. Weiner, eds. 1995. Risk versus risk: Tradeoffs in protecting health and the environment. Cambridge: Harvard University Press.

GRASS site, accessed 10/10/2003. http//grass.itc.it.

Green, W. H. & Ampt, G. A., 1911. Studies on soil physics 1: The flow of air and water through soils. J. Agric.Sci., Vol. 4, No. 1, pp. 1-24.

Grover, I.S., and Kaur S., 1999. Genotoxicity of wastewater samples from sewage and industrial effluent detected by the Allium root anaphase aberration and micronucleus assays. Mutation Research; 426: 183–188.

Gustafson, D. I. 1989. Groundwater Uniquity Score: A simple method for assessing pesticide leachability. Environmental Toxicology and Chemistry; 8: 339 – 357.

Haimes Y. Y., 2006. On the Definition of Vulnerabilities in Measuring Risks to Infrastructures. Risk Analysis, Vol. 26, Issue 2, Pp 293–296.

Harbaugh, A.W., and McDonald, M.G., 1996, User's documentation for MODFLOW-96, an update to the U.S. Geological Survey modular finite-difference ground-water flow model: U.S. Geological Survey Open-File Report 96-485, 56 p

Harbaugh, A.W., Banta, E.R., Hill, M.C., and MacDonald, M.G., 2000. MODFLOW – 2000, The U.S. Geological Survey modular groundwater model: U.S. Geological Survey open – file report 00 – 92.

Hill, M.C., 1990. Preconditioned conjugate-gradient 2 (PCG2), a computer program for solving ground-water flow equations: U.S. Geological Survey Water-Resources Investigations Report 90-4048; 43 p

Hill, M.C., Banta, E.R., Harbaugh, A.W., and Anderman, E.R., 2000. MODFLOW – 2000. The U.S. Geological Survey modular groundwater model – User guide to the observation, sensitivity, and parameter – estimation processes and three post – processing programs. *U.S. Geological Survey open – file report 00 – 184*.

Hough, M. N. and Jones, R. J. A., 1997. The United Kingdom Meteorological Office rainfall and evaporation calculation system: MORECS version 2.0 – an overview. Hydrology and Earth System Sciences, 1(2), 227-239.

Hu, Y., Liao, X., Wong, K., Zhou, Q., 2009. A true random number generator based on mouse movement and chaotic cryptography. Chaos, Solitons & Fractals, Volume 40, Issue 5, Pp. 2286-2293.

Hydrology and Statistical software website (HSSW), Accessed 2008. http://www.spatialhydrology.com/software_hydrostat.html

International Organization for Standardization (ISO), 2002. Risk management vocabulary. ISO/IEC Guide 73. Geneva: ISO.

International Risk Governance Council (IRGC), 2005. White paper on risk governance. Towards an integrative approach. Geneva: IRGC.

Jackson, D. and Llooyd, J.W. 1983. Groundwater chemistry of the Birmingham Triassic sandstone aquifer and its relation to structure. Quarterly Journal of Engineering Geology London. 16: 135-142.

Jeong, C.H., 2001. Effect of land use and urbanization on hydrochemistry and contamination of groundwater from Taejon area, Korea. Journal of Hydrology. 253: 194-210

Jones, H.K., Morris, B.L., Cheney, C.S., Brewerton, L.J., Merrin, P.D., Lewis, M.A. MacDonald, A.M., Coleby, L.M., Talbot, J.C., Mckenzie, A.A., Bird, M.J., Cunningham, J. and Robinson, V.K., 2000. The physical properties of minor aquifers in England and Wales. British Geological Survey Technical Report WD/00/4. 234pp. Environment Agency R & D Publication 68.

Kaplan, S. 1991. Risk assessment and risk management – basic concepts and terminology. In Aven, T. and Renn, O., 2009. On risk defined as an event where the outcome is uncertain. Journal of Risk Research, 12: 1, 1 — 11.

Khan, M.A., and Liang, T., 1989. Mapping pesticide contamination potential. Environment Management. 13: 233 – 242.

Knipe, C.V., Lloyd, J.W., Lerner, D.N., and Greswell, R. 1993. Rising groundwater levels in Birmingham and the engineering implications. CIRIA Special Publication 92, 116p.

Konikwo, L.F., Goode, D.J., and Hornberger, G.Z., 1996. A three – dimensional method – of – characteristics solute transport model (MOC3D) : *U.S. Geological Survey Water – Resources Investigations Report 96 – 4267*; 87p

Kumar,C.P., accessed 10/10/2005. Technical notes on Groundwater flow models. National Institute of Hydrology; Roorkee-247667 (Uttaranchal) http://www.angelfire.com/nh/cpkumar/publication/flowmodels.pdf

Kurt, U., Apaydin, O. and Gonullu, M. T. 2006. Reduction of COD in wastewater from an organized tannery industrial region by Electro-Fenton process. Journal of Hazardous Materials. 143 (1-2); 33 – 40.

Land, D.H., 1966. Hydrogeology of the Triassic sandstones in the Birmingham-Lichfield district. Water Supply Papers of the Geological Survey of Great Britain. Natural Environment Research Council, Hydrogeology Report No. 2

Leal, J. and Castillo, R., 2003. Aquifer vulnerability mapping in the Turbio river valley, Mexico: A validation study. Geofisica Internacional, 42 (1): 141 – 156.

Lee, L.J., Chan, C., Chung, C., Ma, Y. and Wang, J., 2002. Health risk assessment on residents exposed to chlorinated hydrocarbons contaminated in groundwater of a hazardous waste site. Journal of Toxicology and Environmental Health. 65: 219 – 235

Li, G., Huang W., Lerner, D. N., and Zhang, X., 2000. Enrichment of degrading microbes and bioremediation of petrochemical contaminants in polluted soil. Water Resources 34 (15): 3845 – 3853.

Lowrance, W.W. 1976. Of Acceptable Risk: Science and the Determination of Safety. Los Altos, CA: W. Kaufmann.

Mackay, R., and Morakinyo, J.A., 2006. A stochastic model of surface contaminant releases to support assessment of site contaminant at a former industrial site. Stochastic Environmental Research and Risk Assessment. Vol. 20 Pp 213 – 222.

Maidment, D.R. 1993. GIS and hydrologic modelling. Environmental modelling with geographic information systems. Oxford University Press, Oxford.

Margat, J., 1968. Groundwater vulnerability to contamination. In: Vrba, J., and Zoporozec A., (eds.) 1994. Guidebook on mapping groundwater vulnerability. International Association of Hydrogeologists. International contributions to Hydrogeology Volume 16, Verlag Heinz Heise, Hannover, germany, 131p.

Marilyn, B., 2001. The Lancet. 358.

McDonald M.G., and Harbaugh, A.W. 1988. A modular three-dimensional finite-difference groundwater flow model. Techniques of Water Resources Investigations of the United States Geological Survey Open file Report 83 – 875.

Neteler, M. and Mitasova, H., 2003. Open source GIS: A GRASS GIS Approach. Kluwer Academic Publishers. 434p.

Nisan, N. 1996. Extracting randomness: How and why. In Proceedings of the 11th IEEE Conference on Computational Complexity (1996). Pp. 44–58.

Old, R.A., Hamblin, R.O., Ambrose, K., and Warrington, G. 1991. Geology of the country around Reddish. Memoir of the British Geological Survey. Sheet 183 (England and Wales)

Olmer, M., and Rezac, B., 1974. Methodological principles of maps for protection of groundwater in Bohemia and Moravia. In: Vrba, J., and Zoporozec A., (eds.) 1994. Guidebook on mapping groundwater vulnerability. International Association of Hydrogeologists. International contributions to Hydrogeology Volume 16, Verlag Heinz Heise, Hannover, germany, 131p.

Olokesusi, F., 2005. An overview of pollution in Nigeria and the input of legislated standards on its abatement. The Environmentalist. 8 (1): 31 – 37.

Ormsby, T., Napoleon, E., Burke,R., Groessl, C., and Feaster, L.; 2001. Getting to know ArcGIS desktop: Basics of Arcview, ArcEditor and ArcInfo. ESRI Press. Redlands, Califonia. 541p.

Pallasade 2008. http://www.palisade.com/risk/?gclid=CL3R4pXl9pUCFQ6T1 QodPWRk4g; Accessed 1/8/2008

Palmquist, R.C., 1991. Groundwater vulnerability: a DRASTIC approach. In: Vrba, J., and Zoporozec A., (eds.) 1994. Guidebook on mapping groundwater vulnerability. International Association of Hydrogeologists. International contributions to Hydrogeology Volume 16, Verlag Heinz Heise, Hannover, germany, 131p.

Parsons, E.C., 1998. Trace metal pollution in Hong Kong: Implications for the health of Hong Kong's Indo-Pacific hump-backed dolphins (Sousa chinensis). The Science of the Total Environment; 214: 175-184.

Piscopo, G. 2001. Groundwater vulnerability map, explanatory notes. In: Al-Adamat, R. A., Foster I. D., and Baban, S. M. 2003. Groundwater vulnerability and risk mapping for the Basaltic aquifer of the Azraq basin of Jordan using GIS, Remote sensing and DRASTIC. Applied Geography; 23 (4): 303-324.

Pinder, G. F. and Gray, W. G., 1977. Finite element simulation in surface and subsurface hydrology. Academic Press, New York. Pp 295

Powell, J.H., Glover, B.W., and Waters, C.N., 2000. Geology of the Birmingham area. Memoir of the British Geological Survey. Sheet 168 (Englang and Wales).

Project Management Institute (PMI), 2000. A Guide to the Project Management Body of Knowledge (PMBOK® Guide) - Third Edition, Pp 388.

Rao, P.S.C., Hornsby, A.G., Jessup, R.E., 1985. Indices for ranking the potential for pesticide contamination of groundwater. Soil and Crop Science Society of Florida Proceedings; 44: 1 – 4.

Rivett, M.O., Lerner, D.N., Lloyd, J.W. and Lewis C., 1990. Organic contamination of the Birmingham aquifer, UK. Journal of Hydrology. 113: 307 – 323.

Rosa, E.A. 1998. Metatheoretical foundations for post-normal risk. Journal of Risk Research 1: 15–44.

Rushton, K.R., and Salmon, S. 1993. Significance of vertical flow through low conductivity zones in the Bromsgrove sandstone aquifer. Journal of Hydrology. 152, 131 – 152.

Seconda, E., 2001. Water shortages and environmental degradation. In: Al-Adamat, R. A., Foster I. D., and Baban, S. M. 2003. Groundwater vulnerability and risk mapping for the Basaltic aquifer of the Azraq basin of Jordan using GIS, Remote sensing and DRASTIC. Applied Geography; 23 (4): 303-324

Shepherd, K.A., Ellis, P.A. and Rivett, M.O. 2005. Integrated understanding of urban land, groundwater, baseflow and surface-water quality- The City of Birmingham,UK. Science of the Environment. (In-press).

Sotornikova, R., and Vrba, J., 1987. Some remarks on the concept of vulnerability maps. In: Vrba, J., and Zoporozec A., (eds.) 1994. Guidebook on mapping groundwater vulnerability. International Association of Hydrogeologists. International contributions to Hydrogeology Volume 16, Verlag Heinz Heise, Hannover, germany, 131p.

South Staffs Water, 2000. St George's Barracks Pumping Test. In: Buss, S.R., Streetly, M.J., and Shepley, M.G., (Ed); 2008. Lichfield Permo-Triassic sandstone Aquifer Investigation (Final Report). Environment Agency (Midlands Region)

Suciu, D.F., and Wikoff, P.M., 1982. An evaluation of materials for systems using cooled, treated geothermal or high saline brines. United State Department of Energy, Idaho Operation Office. Contract No.: DE-AC07-761D01570 50p.

Swain, E.D. and Wexler, E.J. (1996). A coupled surface water and groundwater flow model (MODBRANCH) for simulation of stream-aquifer interaction. *Techniques of Water Resources Investigations of U.S.Geological Survey*. Book 6. Chapter A6.

Szczepanski, J., Wajnryb, E., Amigó, J., Sanchez-Vives, M., Slater, M. 2004. Biometric random number generators; Computers & Security, Volume 23, Issue 1, Pp. 77-84.

Thirumalaivasan, D. and Karmegam, M. 2001. Aquifer vulnerability assessment using analytic hierarchy process and GIS for upper Palar watershed. 22nd Asian Conference on Remote Sensing, Singapore.

Tim, U.S. and Jolly, R., 1994. Evaluating agricultural non-point source pollution using integrated Geographic Information System and hydrologic/water quality model. Journal of Environmental Quality; 23: 25–35.

UK National Statistics (accessed 25/08/2006). http://www.statistics.gov.uk/census2001/pyramids/pages/00cn.asp

Usaid (U.S. Agency for International Development) accessed 13/07/2004 http://www.usaid.gov/our_work/environment/water/urbanization.html

U.S. EPA. 1996a. U.S. Environmental Protection Agency. Exposure Models Library and Integrated Model Evaluation System. Revise. EPA/600/C-92. Washington, D.C.: Office of Research and Development.

U.S. National Research Council 1993 In: Vrba, J., and Zoporozec A., (eds.) 1994. Guidebook on mapping groundwater vulnerability. International Association of Hydrogeologists. International contributions to Hydrogeology Volume 16, Verlag Heinz Heise, Hannover, germany, 131p.

United State Environmental Protection Agency (USEPA), 1989. Risk assessment guidance for superfund. Volume I : Human Health Evaluation Manual (Part A). Technical Report EPA/540/1-89/002.

United State Environmental Protection Agency; 1988. Ambient water quality criteria for chloride - 1988. EPA 440/5-88-001. Office of the Water Regulations and standard criteria and standard division. Washington DC 20460 39p.

United State Geological Survey- Groundwater Software, accessed 2004. http://water.usgs.gov/nrp/gwsoftware/mf2k_gwt/mf2k_gwt.html

United States Environmental Protection Agency, 1996b. Compilation of Saturated and Unsaturated Zone Modeling Software EPA/600/SR-96/009. National Risk Management Research Laboratory Ada, OK 74820

Van Stempvoort, D., Ewert, L., and Wassenaar, L. 1992. AVI: A method for groundwater protection mapping in the Praire Province of Canada. PPWB Report, No.114, National Hydrology Research Institute, Saskatoon, Saskatchewan, Canada.

Vereecken, H., Binley, A., Cassiani, G., Revil, A. and Titov, K. 2006. Applied Hydrogeophysics, Springer, Pp 75 – 116.

Villumsen, A., Jacobsen, O.S., and Sonderskov, C., 1983. Mapping the vulnerability of groundwater reservoirs with regard to surface pollution. In: Vrba, J., and Zoporozec A., (eds.) 1994. Guidebook on mapping groundwater vulnerability. International Association of Hydrogeologists. International contributions to Hydrogeology Volume 16, Verlag Heinz Heise, Hannover, germany, 131p.

Vrba, J., and Zoporozec, A., (eds.) 1994. Guidebook on mapping groundwater vulnerability. International Association of Hydrogeologists. International contributions to Hydrogeology Volume 16, Verlag Heinz Heise, Hannover, germany, 129p.

Watkins D.W., McKinney D.C. and Maidment D.R., 1996. Use of geographic information systems in groundwater flow modeling, Journal of Water Resources Planning and Management; 122 (2): 88–96.

Wegenkittl, S., 2001. Gambling tests for pseudorandom number generators; Mathematics and Computers in Simulation, Volume 55, Issues 1-3, Pp 281-288.

World Health Organization (WHO), 2011. Guidelines for drinking-water quality - 4th Ed. Pp 541.

Worthington, S.R.H. and Smart C. C., 2005. Empirical determination of tracer mass for sink to spring tests in karst; Sinkholes and the Engineering and Environmental Impacts of Karst (Geotechnical Special Publication) Ed. B.F. Beck, Geotechnical Special Publication No. 122, American Society of Civil Engineers, pp. 287-295.

Wichmann, H., Kolb, M., Jopke, P., Schmidt, C., Alawi M., and Bahadir, M., 2006. Analysis package applied to groundwater flow and contaminant transport modelling assessment of the environmental impact of landfill sites with open combustion located in arid regions by combined chemical and ecotoxicological studies. Chemosphere; 65: 1778–1783.

Zheng, C. and Wang, P.P., 1999. MT3DMS: A Modular Three-Dimensional Multispecies Transport Model for Simulation of Advection, Dispersion and Chemical Reactions of Contaminants in Groundwater Systems; Documentation and User's Guide, Contract Report SERDP-99-1, U.S. Army Engineer Research and Development Center, Vicksburg, MS.

APPENDICES

A1: Utilities

A1.1: Commonly available groundwater and transport models.doc

A1.2: Risk Assessment Method control file.dat

A1.3: FORTRAN code for RAM execution.

A2: Hypothetical risk model input files for scenarios 4 and 5

A2.1a: Risk model input file: ram1_input_file (Scenario 4 -Approach 1).dat

A2.1b: Risk model input file: ram1_input_file (Scenario 5 -Approach 2).dat

A2.2: advance_flag.dat

A2.3: ram1_files.dat

A3: Hypothetical risk model output files for scenarios 4 and 5

A3.1a: Risk Model Output file: ram1_output_file (Scenario 4 -Approach 1).dat

A3.1b: Risk Model Output file: ram1_output_file (Scenario 5 -Approach 2).dat

A3.2a: Generated daily source term: ram1_distribution (Scenario 4 -Approach 1).dat)

A3.2b: Generated daily source term: ram1_distribution (Scenario 5 -Approach 2).dat)

A3.3a: Generated source terms for transport model (Scenario 4 -Approach 1).ssm

A3.3b: Generated source terms for transport model (Scenario 5 -Approach 2).ssm

A4: Flow and transport model input files for scenario 5

A4.1: Named file for flow model (fram5.nam).dat

A4.2: Basic Flow Package (ram5.ba6).dat

A4.3: Well Package (ram5.wel).dat

A4.4: Recharge Package (ram5.rch).dat

A4.5: Layer Property Flow Package (ram5.lpf).dat

A4.6: Output control file (ram5.oc).dat

A4.7: Preconditioned Conjugate Gradient Package (ram5.pcg).dat

A4.8: Link MT3D Package (ram5.lmt).dat

A4.9: Discretization file (ram5.dis).dat

A4.10: Named file for transport model (ram5.nam).dat

A4.11: Basic Transport Package (ram5.btn).dat

A4.12: Advection Package (ram5.adv).dat

A4.13: Dispersion Package (ram5.dsp).dat

A4.14: Generalised Conjugate Gradient Solver Package (ram5.gcg).dat

A4.15: Initial water level (ram5.wl).dat

A4.16: ibound.dat

A5: Hypothetical risk model output files for scenario 6

A5.1: Risk Model Output file (ram6_output_file.dat) for scenario 6.dat

A5.2: Generated daily source term (ram6_distribution.dat) for scenario 6.dat

A5.3: Generated source terms for transport model (ram6.ssm) for scenario 6.dat

A6: Hypothetical risk model output files for scenario 7

A6.1: Risk Model Output file (ram7_output_file.dat) for scenario 7.dat

A6.2: Generated daily source term (ram7_distribution.dat) for scenario 7.dat

A6.3: Generated source terms for transport model (ram7.ssm) for scenario 7.dat

A7: Hypothetical risk model output files for scenario 8

A7.1: Risk Model Output file (ram8_output_file.dat) for scenario 8.dat

A7.2: Generated daily source term (ram8_distribution.dat) for scenario 8.dat

A7.3: Generated source terms for transport model (ram8.ssm) for scenario 8.dat

A8: Borehole logs records and Monte Carlo sensitivity analysis

A8.1: Records of the borehole logs

A8.2: Monte Carlo sensitivity analysis

A.9: The risk model input files (field data)

A9.1: ram_input_file.dat Input file (field data)

A9.2: advance_flag.dat Input file (field data)

A9.3: ram_files.dat.Input file (field data)

A9.4: Raw Pollution data (field data).xls

A.10: The risk model output files (field data)

A10.1: Risk Model Output file (ram_output_file.dat) using field data

A10.2: Generated daily source term (ram_distribution.dat) using field data

A10.3: Generated source terms for transport model (ram.ssm) using field data

A11: Input files (field data) for calibrated flow model

A11.1: Named file for flow model (field.nam).dat

A11.2: Basic Flow Package (field.ba6).dat

A11.3: Well Package (field.wel).dat

A11.4: Recharge Package (field.rch).dat

A11.5: Layer Property Flow Package (field.lpf).dat

A11.6: Output control file (field.oc).dat

A11.7: Preconditioned Conjugate Gradient Package (field.pcg).dat

A11.8: Discretization file (field.dis).dat

A11.9: Initial groundwater level for layer 1 (initial_wl_1).dat

A11.10:Boundary conditions for layer 1 (ibound_1).dat

A11.11:Base of Bromsgrove layer(layer 1).dat

A11.12:Base of Wildmoor layer (layer 2).dat

A11.13:Base of Kidderminster layer (layer 3).dat

A11.14:Surface elevation.dat

A11.15:Observation Package (field.obs).dat

A11.16:Head observation Package (field.hob).dat

A11.17:River Package (field.riv).dat

A11.18:Recharge multiplier (rech_mult.dat).dat

A11.19:Horizontal flow barrier Package (field.hfb).dat

A11.20:Multiplier file (field.mult).dat

A.12: Additional Input files for Predictive coupled flow and transport model

A12.1:Named file for transport model (ram.nam).dat

A12.2:Well Package (ram.wel).dat

A12.3:Recharge Package (ram.rch).dat

A12.4:Link MT3D Package (ram.lmt).dat

A12.5: Basic Transport Package (ram.btn).dat

A12.6: Advection Package (ram.adv).dat

A12.7: Dispersion Package (ram.dsp).dat

A12.8: Generalised Conjugate Gradient Solver Package (ram.gcg).dat

A12.9: Initial groundwater level for layer 1 (initial_wl_1).dat

A12.10:Head observation Package (ram.hob).dat

A13: FORTRAN code for Risk Assessment module